UNIVERSITÉ DU QUÉBEC À RIMOUSKI

PERSPECTIVES PHYLO-EVO-DEVO DE LA DIVERSIFICATION DES VERTEBRES PALEOZOIQUES

THÈSE
PRÉSENTÉE
COMME EXIGENCE PARTIELLE
DU DOCTORAT EN BIOLOGIE

PAR
MARION CHEVRINAIS

SEPTEMBRE 2016

Composition du jury :

Béatrix Beisner, présidente du jury, Université du Québec à Montréal (Canada)

Richard Cloutier, directeur de recherche, Université du Québec à Rimouski (Canada)

Jean-Yves Sire, codirecteur de recherche, Université Pierre et Marie Curie (France)

Dominique Berteaux, examinateur interne, Université du Québec à Rimouski (Canada)

Mark V.H. Wilson, examinateur externe, Loyola University of Chicago (USA)

Dépôt initial le 15 juin 2016 Dépôt final le 8 septembre 2016

REMERCIEMENTS

Je remercie très vivement Richard. Merci de m'avoir proposé ce sujet de thèse, merci de m'avoir permis de découvrir les merveilles que renferme Miguasha. Je te remercie aussi car malgré mon impatience, mes capacités n'ont fait que s'améliorer durant ces quatre années et ma motivation n'a pas diminué d'un iota (hum sauf ces derniers jours peut être). J'ai aimé nos séances de « brainstorming » et j'espère que notre collaboration perdurera dans les années à venir. Jean-Yves, je vous remercie pour les conseils avisés et l'expérience que vous avez partagé avec moi. Merci de m'avoir accueillie dans votre laboratoire à Paris et d'avoir partagé cette aventure avec moi durant quatre ans.

Merci à vous, Béatrix et Dominique d'avoir accepté d'être membres de mon jury et de vous réunir à cette occasion. J'en suis vraiment flattée. I would like to thank Mark Wilson to be part of my committee, it makes me very proud.

Je tiens aussi à remercier le CRSNG, le laboratoire de recherche de Paléontologie et Biologie Evolutive ainsi que le CSBQ, EnviroNord, l'UQAR et Boréas pour le soutien financier.

Je suis très reconnaissante, bien sûr, aux membres du laboratoire de Paléontologie et Biologie Evolutive de l'UQAR, qui ont été présents à mes côtés durant ces quatre années. Merci Cyrena, Catherine, Caroline, Daniel, Olivier, Elodie, François, Roxanne, Vincent, Isabelle et Laurence pour le soutien intellectuel et moral, mais aussi pour les soirées nous permettant de décompresser, oh oui ! Je remercie Claude Belzile, à l'ISMER, pour la réalisation des manipulations de microscopie électronique.

A Paris, je suis très reconnaissante à l'équipe de l'UPMC : Barbara, Amandine, Jérémie,

Marie-Claire, Sidney, Tiphaine et Hayat. Vous m'avez aidé tout au long de mon doctorat, en étant présents lors de mes séjours à Paris, tant scientifiquement qu'humainement et ça a été un plaisir de partager ces moments de thèse autour d'un bagel ou d'une bière (une ?). Je remercie aussi les membres du Muséum et de l'UPMC qui m'ont accueillie et ont toujours répondu à mes interrogations, Philippe Janvier, Gaël Clément, Daniel Goujet, Alan Pradel, Vivian de Buffrénil, François Meunier, Louise Zylberberg, Armand de Ricqlès, Pierre-Yves Gagnier, Etienne Balan et Virginie Bazin. Puis, il y a l'équipe nocturne du Muséum, celle que j'ai plutôt fréquentée aux Korrigans pour les verre-dredis que dans les collections. Merci Eli, Donald, Pierre, Malcolm, Ninon, Damien et Jorge pour votre bonne humeur (et la bière) partagée.

I would like to thank Ieva Upeniece and Ivars Zupins for their warm welcome at the museum in Latvia. I learnt a lot relative to scientific condition in Latvia and also about the history of the place (thanks Ieva). In UK, I am grateful to Zerina Johanson, Emma Bernard and Stig Walsh because they allowed me to work quietly and efficiently in NHM and NMS collections respectively. Zerina, special thanks for your support during these four years and also for your interest relative to the post-doctoral project. I also would like to thank John Long, Kate Trinajstic and Claude B. Renaud for their collaboration.

Un grand merci à toute l'équipe de fouilles en Belgique, tout d'abord à Gaël car tu m'as permis de participer à ces fouilles et même mieux puisque tu m'as très chaleureusement accueillie. Paup' et Club Med (obligée, désolée maître Vin'Du) pour l'apport d'une culture placodermique (eh oui du fin fond de mon université Québecoise il est dur de trouver des publis chinoises) et early vertebriste. Et aussi Paup', parce qu'on s'est bien marré tous les deux sur le terrain, à Strud ou en Australie. Vincent P. parce que personne n'est plus aimant de la nature humaine que toi (la meilleure blague que j'ai

jamais faite) et Falcon, parce qu'on a bien ri. Et merci à Pierre, bien sûr, pour le soutien inconditionnel des débuts !

Je tiens à remercier aussi toute l'équipe de fouilles et du musée de Miguasha, merci pour ces étés de fouilles ben l'fun et pour les discussions pal en dehors du cadre universitaire (et le plus souvent autour d'une bière). Merci spécial à Oli, Jo, Jason, Benoit, Norman et France et à cet illustre inconnu, qui nous a permis de croire une dernière fois que l'on achetait du Tyrannosaure au marché Richelieu !

Thank you very much to Kate and Tet, my fieldwork friends. Fieldwork with you in Gaspésie was a pure pleasure, ok I confess that seals played a major rôle ! Tet, I'll never forget your GPS, your sleeping toy. Kate, I will always remember our discussions on the wonderful road between Percé and Gaspé.

Mes amis à Rimouski, un grand merci, sans vous ces années auraient été tellement plates ! Mathoche, Hedvig, Idaline, Claire, Chevallier, Cazelles t'es belle, Cazelles t'es belle, Cazelles t'es belle (oui je te remercie plus de fois que Steve Zissou !), Legagneux t'es joyeux, Casajus et Steve Zissou pour les soirées improvisées et spontanées (mais toujours réussies – pas comme la musique, n'est ce pas Claire et Amaël ?). Olivier M., Tas, Louis, Robin, Aurore, Quentin D., Thomas, Jacinthe, Greg, Antoine, Maude et Mélinda pour les bons moments partagés et le soutien que vous m'avez apporté. Quentin B., Guillaume et Amaël pour le partage autour de notre lopin de terre.

Merci à mes amis de Master 2 de Montpellier, mes premiers amis paléontologues et les soirées distinguées heu déglinguées pardon qui vont avec, n'est ce pas Sébastien. Je voudrais remercier aussi ceux sans qui le Master 1 à Moncton n'aurait pas ressemblé à une aquarelle de Marie Laurencin, merci pour cette année Branly et Cha ! Et Branly, tu

vois ça se finit un doc finalement !

Les amis de Licence à Poitiers, vous êtes toujours là, moins souvent certes mais toujours aussi intensément. Durand, Rolando, Robyns, Hattry et Pelard pour ne citer que les « pires », vous m'avez permis d'endurcir mon caractère avant tout, mais aussi de passer de très bons moments et de me fournir le cadre – peut être que je l'ai cherché pour m'éloigner de vous au premier abord – me permettant de choisir une orientation qui me convienne. Aller assez parlé des amis, je ne vais pas remercier jusqu'à la première personne que j'ai rencontré en maternelle, et bien si en fait. Merci Clairette, 24 ans que l'on se côtoie, que l'on s'apprécie et que l'on se soutient, c'est beau, je suis fière. Merci aussi Laurie, pour ces années partagées.

Et bien sûr, ceux sans qui rien ne serait arrivé, la famille, parce qu'on ne la choisit pas mais qu'est ce que je suis contente d'être tombée sur celle-ci ! Je suis reconnaissante pour tout le soutien que vous m'avez apporté durant ces quatre années et plus largement durant les 26 dernières années. Jpich, tu m'as donné le gout d'apprendre encore et toujours, d'avoir une curiosité pour toute chose, merci, cependant je n'ai pas tout retenu de ta sagesse et ton fameux "faut pas s'énerver pour si peu" me fait encore pogner les nerfs (en bon québecois). Chandaltouch, avec ta coupe de Playmobil ou de Bernard Thibault, tu me fais bien rire, je te remercie car tu m'as apporté assez d'amour et de tendresse pendant mes 20 premières années pour que je n'en manque pas même si je suis à 6000 km de toi depuis six ans. Ma tête de iench adorée, je n'aurais pu rêver meilleur grand frère pour me soutenir et me remonter le moral sans condition, et aussi pour me forger un caractère un peu tête de mule parfois. Merci aussi à Julie, Jer, Del, Elina et Salomé, Cricri d'amour, Flux et Alain (parce que vous avez de la Valda), Charlène, Françoise et Ludivine pour les discussions autour des pénis fossilisés et à Jérôme un merci spécial pour le magnifique dessin (« Les poissons du Dévonien pissaient sur les murs »). Merci

Mico et Jean-Noël pour le support continu.

Finalement, je te remercie Florian, parce que ces derniers mois n'ont pas toujours été faciles mais tu as su braver, affronter, apaiser tout en laissant s'exprimer la tempête, même lorsque celle-ci n'était que peu justifiée. Tu as même fait mieux puisque tu l'as calmée avec beaucoup de talent, c'est grand ! Je n'aurais pu être mieux accompagnée, merci !

A mon père, ma mère et Julo

AVANT-PROPOS

Certains auteurs m'ont marquée et ont su résumer l'idée que je peux me faire de la Science et l'état d'esprit dans lequel je suis après quatre années de thèse ...

« Je doute parfois si j'aime la biologie parce qu'elle est science de la vie, ou si j'aime la vie parce qu'elle sert à la biologie. » Jean Rostand, Carnet d'un biologiste, 1959

« La complexité ahurissante de la science : les radiations, les ondes, les électrons, les hormones, le système sympathique, [...], la psychanalyse ... On s'étonne que les gens gardent leur tête. Au fait, ils ne la gardent pas. » Jean Rostand, Carnet d'un biologiste, 1959

« Un chercheur doit avoir conscience du peu de ce qu'il a trouvé : mais il a le droit d'estimer que ce peu est immense. » Jean Rostand, Inquiétudes d'un biologiste, 1967

... ainsi que l'enjeu existant qui m'a attirée à étudier les vertébrés primitifs.

« Gnathostome traits must have evolved along the gnathostome stem lineage, but without fossils it is impossible to determine the order in which – or when – they arose. » Brazeau and Friedman (2015)

TABLE DES MATIÈRES

LISTE DES FIGURES

LISTE DES TABLEAUX

LISTE DES ABRÉVIATIONS

a Arcualium

An Anal spine

an.f Anal fin

b Acellular bone

bb Bony base

Br. r Branchiostegal rays

c Centrum

Carbonif Carbonifère/Carboniferous

cau.f Caudal fin

cb Cellular bone

cc Canal cavity

Cir. or Scl. Sclerotic bones

Cryo Cryogénien/Cryogenian

D Dorsal spine

dmr Dorsomedian rod

dor.f Dorsal fin

Dent. Paired fins denticles

dt.t Dentine ascending canals and canaliculi

ee Elastica externa

en Enamel/enameloid

end Posterior extremity of the body

fr Fin ray

g Ganoine layer

g. c Gut contents

GZ Growth zones

ha Haemal arch

hs Haemal spine

h. l Hypochordal lobe

h. sc Head scales

int Intermediate spine

IO Intromittent organs

le Lepidotrichium

l.l Lateral line canal

m mesodentine

mde Mediodorsal elements

Mk Meckel's cartilage

n Notochord

na Neural arch

na. bones Nasal bones

nc Notochordal cartilage

ne Scale neck

Ng Néogène/Neogene

ns Notochordal sheath

nsp Neural spine

nt Neural tube

orb Orbit

Ord Ordovicien/Ordovician

odont. Odontoblast cavities

ot Otolith

pec.f Pectoral fin

Pect Pectoral spines

Pelv Pelvic spines

pel.f Pelvic fin

Pg Paléogène/Paleogene

Pq Palatoquadrate

rb Rib

ri Superficial ridge

sc Scales

Sca Scapula

Sh Sharpey's fibers

Sil Silurien/Silurian

Sl Superficial layer

ns Notochordal sheath

va Ventral arch

vc Vascular canal cavity

vert. Vertebral element

vmr Ventromedian rod

RÉSUMÉ

Une partie importante de l'histoire évolutive des vertébrés est inscrite dans le registre fossile. La compréhension de cette histoire passe par l'étude de l'évolution des traits anatomiques et des relations de parenté (*i.e.* phylogénie) entre les différents taxons de vertébrés. Actuellement, la résolution imparfaite de la phylogénie des vertébrés soulève la question de l'optimisation des caractères utilisés dans les matrices de phylogénie.

Pour répondre à cette problématique, cette thèse utilise une approche Evo-Dévo afin de comprendre l'histoire évolutive des vertébrés et les interrelations au sein des vertébrés. La croissance de deux espèces de vertébrés paléozoïques retrouvées dans le *Lagerstätte* du Dévonien supérieur de Miguasha (Québec, Canada) (380 millions d'années) est étudiée : l'anaspide *Euphanerops longaevus* (*i.e.* vertébré sans mâchoire ou agnathe) et l'acanthodien *Triazeugacanthus affinis* (*i.e.* vertébré à mâchoires ou gnathostome). La préservation exceptionnelle des fossiles du *Lagerstätte* de Miguasha en fait de bons candidats pour améliorer la résolution de la phylogénie des vertébrés et comprendre les grandes modifications évolutives ayant eues lieu à la période de transition entre les agnathes et les gnathostomes. Des techniques d'histologie, de microscopie électronique, de spectrométrie à rayons X ainsi que des dessins de précision et des analyses phylogénétiques sont utilisés afin d'exploiter au maximum le potentiel de ces fossiles. En effet, l'ajout de caractères développementaux aux caractères morphologiques déjà existants dans la littérature (rassemblés à partir de spécimens adultes le plus souvent), représente une solution pour une meilleure résolution de la phylogénie des vertébrés.

L'attribution historique de *Scaumenella mesacanthi* à des stades de décomposition de l'acanthodien *Triazeugacanthus affinis* a été réfutée : *Scaumenella* représente des stades immatures de *Triazeugacanthus* et d'*Euphanerops*. Les résultats apportés par l'étude des ontogénies d'*Euphanerops* et de *Triazeugacanthus* sont inédits. D'une part, la nouvelle description d'*Eu-phanerops*, à partir de spécimens juvéniles et adultes, indique que le squelette interne de cet agnathe est composé d'une colonne vertébrale régionalisée, de longues nageoires paires ventrales s'étendant de la partie postérieure de la bouche à la partie antérieure de l'anus, de ceintures pelviennes ainsi que d'une paire d'organes d'intromission. Avant cette découverte, la présence d'un squelette axial et d'un squelette appendiculaire complexes n'était connue que chez les gnathostomes. D'autre part, la croissance de *Triazeugacanthus*, décrite à partir d'une série de taille de 178 individus, est continue et composée de trois stades ontogénétiques (larvaire, juvénile et adulte). Ces stades sont définis à partir 1) de l'étendue de l'écaillure (*i.e.* les écailles sont absentes chez les larves, elles sont en formation chez les juvéniles et

l'écaillure est totale chez les adultes), et 2) de périodes de transitions déterminées par les alternances de paliers et de seuils de la trajectoire développementale. La progression de la minéralisation du squelette interne renseigne sur l'ossification d'éléments squelettiques cartilagineux (neurocrâne et éléments vertébraux) au cours de la croissance. En plus de l'ontogénie des spécimens complets, le développement d'éléments isolés a été étudié. Les taux de croissance des épines des nageoires diffèrent entre les larves, juvéniles et adultes, ce qui indique que la croissance chez *Triazeugacanthus* est allométrique. La relation entre 1) la croissance des écailles et le patron de développement de l'écaillure, et 2) la croissance des spécimens complets indique que les écailles sont une bonne approximation de la croissance des individus et de l'espèce. Ce résultat est primordial étant donné que les séries de croissance sont rares dans le registre fossile (dû à la faible minéralisation du squelette des stades précoces) alors que les écailles sont abondantes.

Concernant *Euphanerops*, ces découvertes impliquent que les mécanismes développementaux et génétiques, permettant la mise en place des appendices pairs et de la régiona-lisation du squelette axial, étaient présents bien avant l'émergence des gnathostomes. Quant à *Triazeugacanthus*, la préservation exceptionnelle, la large étendue de taille ainsi que l'abondance des spécimens complets font de la série de croissance de cette espèce une des ontogénies fossiles de gnathostomes les mieux connues. L'étude comparée des patrons et des processus de croissance de cet acanthodien au sein des gnathostomes informe sur une condition commune pour les gnathostomes retrouvée chez *Triazeugacanthus*. Malgré la présence de similitudes entre *Triazeugacanthus* et les ostéichtyens primitifs, la nouvelle analyse phylogénétique des gnathostomes indique que les acanthodiens sont à la base du groupe total des chondrichtyens soutenant ainsi l'hypothèse de la paraphylie des acanthodiens. En conclusion, cette thèse améliore la compréhension de l'évolution du système squelettique chez les vertébrés ainsi que la phylogénie des grands groupes de gnathostomes ; ces résultats permettent maintenant de poser la question des interrelations au sein du groupe total des vertébrés.

Mots clés : Développement, Phylogénie, Evolution, Dévonien, Acanthodien, Taphonomie, Anaspide, Miguasha

ABSTRACT

Most of the evolutionary history of vertebrates is written in the fossil record. The understanding of this evolutionary history is studied through the evolution of anatomical traits and the interrelationships between vertebrate taxa (*i.e.* phylogeny). Today, the unresolved phylogeny of vertebrates questions the optimisation of characters used in phylogenetic matrices.

To answer this research question, this thesis uses an Evo-Devo approach to understand vertebrate evolutionary history and interrelationships among vertebrate groups. The growth of two Paleozoic vertebrate species from the Late Devonian Miguasha *Lagerstätte* (Quebec, Canada) (380 million years ago) is studied : the anaspid *Euphanerops longaevus* (*i.e*. jawless fish or agnathan) and the acanthodian *Triazeugacanthus affinis* (*i.e*. jawed vertebrate or gnathostome). The exceptional preservation of fossils from the Miguasha *Lagerstätte* makes them good candidates to clarify vertebrate phylogeny and understand the major evolutionary modifications occurring at the transition between jawless and jawed vertebrates. Histological techniques, scanning electron microscopy, X-ray spectrometry, *camera lucida* drawing and phylogenetic analyses are used to maximize the information from these fossils. Indeed, the addition of supplementary characters to the morphological characters already used in the literature (gathered mostly from adult specimens), represents a potential for a better resolution of vertebrate phylogeny.

The historical assignment of *Scaumenella mesacanthi* as decomposition stages of the acanthodian *Triazeugacanthus* is rejected. Instead, *Scaumenella* is recognised as immature stages of *Triazeugacanthus* and *Euphanerops*. Results from the developmental study of *Euphanerops* and *Triazeugacanthus* are new. On one hand, the new description of *Euphanerops*, from juvenile and adult specimens, indicates that the endoskeleton of this agnathan is composed of a regionalized vertebral column, ventral paired fins extending posterior to the mouth to anterior to the anus, pelvic girdles and paired intromittent organs. Before this discovery, complex axial and appendicular skeletons were only known in gnathostomes. On the other hand, *Triazeugacanthus* growth, described from a size series of 178 specimens, is direct and composed of three ontogenetic stages (larval, juvenile and adult). These stages are defined from 1) the extent of squamation (i.e. the larvae show no scales, the squamation starts in juveniles and is completed in adults), and 2) periods of transitions in the developmental trajectory established by the alternation of steps and thresholds. The progressive mineralization of the endoskeleton indicates the progressive ossification of chondrified elements (vertebral elements and

scapula) during growth. Added to the ontogeny of complete specimens, the development of individual skeletal elements has been studied. The growth rates of fin spines differ between larvae, juveniles and adults, this indicates that *Triazeugacanthus* growth is allometric. The relationships between 1) scale growth and squamation, and 2) the growth of complete specimens indicates that scale growth is a reliable proxy for individual and species growth. This result is important given that growth series of complete specimens are rare in the fossil record (owing to the poor mineralisation of immature specimens) whereas isolated remains such as scales are abundant.

Concerning *Euphanerops*, these discoveries imply that developmental and genetic mechanisms responsible of the formation of paired appendages and the regionalisation of the axial skeleton, were present before the rise of gnathostomes. The exceptional preservation, the large size range and the abundance of specimens position *Triazeugacanthus* ontogeny as one of the best known fossilised early vertebrate ontogeny. The comparative study of growth patterns and processes of this acanthodian within gnathostomes informs relative to a common condition for gnathostomes found in *Triazeugacanthus*. Despite the presence of anatomical similarities between *Triazeugacanthus* and early osteichthyans, the new phylogenetic hypothesis of gnathostomes indicates that acanthodians are stem chondrichthyan, resolving acanthodians as paraphyletic. In conclusion, this thesis refines the understanding of vertebrate skeletal system evolution and gnathostome phylogeny, questioning the early vertebrates phylogeny.

Keywords : Development, Phylogeny, Evolution, Devonian, Acanthodian, Taphonomy, Anaspida, Miguasha

INTRODUCTION GÉNÉRALE

La problématique de cette thèse intitulée “Perspectives phylo-évo-dévo de la diversification des vertébrés paléozoïques” fait référence à l’intégration de trois disciplines dans un champ de recherche, soit la phylogénie, l’évolution et le développement (“phylo-évo-dévo”) (Minelli, 2009). Ce terme s’applique ici à un groupe d’organismes spécifique, les vertébrés paléozoïques communément appelés “poissons”. La problématique de cette thèse s’inscrit dans la compréhension de l’histoire évolutive des vertébrés, donc des interrelations entre les grands groupes [à ce jour mal connues (Zhu et al., 2013; Janvier, 2015; Burrow et al., 2016)] par l’étude du développement d’espèces fossiles (Figure 1).

Dans cette introduction, une définition de ce que contient le terme “phylo-évo-dévo” sera donnée, pour ensuite décrire les grands groupes de vertébrés paléozoïques. Leur âge géologique (Annexe I), leur anatomie générale, et les relations de ces groupes entre eux seront passés en revue. Deux groupes seront définis plus en détail car ils représentent le matériel d’étude de cette thèse (les anaspides et plus exhaustivement les acanthodiens). Après cet état de l’art, l’accent sera mis sur les séquences de développement fossiles ainsi que sur la description du squelette dermique, deux aspects majeurs de l’optimisation de la description des interrelations entre les grands groupes. Dans une dernière partie, la problématique de recherche sera développée ainsi que le matériel utilisé et les principaux objectifs abordés dans chacun des cinq chapitres de cette thèse.

Le concept de phylo-évo-dévo

Le terme Phylo-Evo-Dévo exprime l'intégration d'un champ de recherche préalablement développé – l'Evo-Dévo ou la biologie évolutive du développement – comme un nouveau niveau de caractères permettant d'analyser les relations évolutives des espèces entre elles (*i.e.*, analyse phylogénétique). L'Evo-dévo est définie comme étant l'étude des modalités d'évolution du développement et comment ces modifications affectent les transitions évolutives (Hall, 2002, p.647) (Figure 1). Tandis que la reproduction et le développement d'organismes actuels sont observables dans la nature et en laboratoire, les fossiles occupent une place différente dans ces études puisque chaque fossile traduit en fait un instantané de vie. Les séries de croissance représentent des séries d'instantanés. Cependant les fossiles sont utiles dans ces études grâce à l'apparition de nouvelles méthodes permettant des analyses précises dépassant le niveau des traits anatomiques (Hall, 2002; Wilson, 2013). L'Evo-Dévo est considérée comme une contribution essentielle de la théorie étendue de l'évolution (Gould, 1977; Mayr, 1993; Pigliucci, 2007; de Ricqlès and Padian, 2009). Afin de comprendre l'évolution des caractères et la présence d'homologies [*i.e.*, caractères communs hérités d'un ancêtre commun (Simpson, 1961)] au sein des espèces à travers le temps, l'analyse phylogénétique permet de mettre en lumière quels traits ont évolué une ou plusieurs fois et si ces traits complexes peuvent évoluer à nouveau dans des lignées qui les ont perdus. Cependant, les caractères développementaux sont difficiles à intégrer dans les phylogénies, notamment en raison de la difficulté d'identifier les homologies (Baguna and Garcia-Fernandez, 2003).

En effet, derrière la question de la reconnaissance des homologies, la résolution des phylogénies dépend de l'identification de deux types d'homologies *i.e.*, homologies évolutives profondes et les homologies latentes (Cracraft, 2005). Les ho-

mologies évolutives profondes concernent des espèces partageant le même appareil génétique régulateur, utilisé pour cons-truire des éléments morphologiquement et phylogénétiquement différents mais fonctionnellement identiques (Shubin and Tabin, 1997; Rutishauser and Moline, 2005). L'évolution des caractères au sein des espèces peut être expliquée par les variations des homologies profondes, comme dans le cas des membres des tétrapodes par exemple (Shubin et al., 2009; Scotland, 2010). Les homologies profondes réfèrent donc à l'intégration génétique et à la dépendance d'éléments morphologiquement distincts mais aussi à l'intégration développementale [*i.e.*, interdépendance entre les structures morphologiques souvent due à des origines développementales communes (Willmore et al., 2007)]. L'homologie latente est définie comme la présence d'un élément morphologiquement différent chez un ancêtre en comparaison d'un élément nouvellement présent chez un descendant [*e.g.*, os articulaire de la mâchoire inférieure des amniotes non mammifères qui est homologue à un osselet de l'oreille moyenne (le malleus) chez les mammifères]. Ces éléments sont homologues lorsque l'on considère le niveau des processus développementaux partagés (Hall, 2007). Cependant dans le cas de l'homologie latente, l'ancêtre et le descendant partagent les mêmes trajectoires de développement mais sans posséder des caractères morphologiques homologues (Rutishauser and Moline, 2005).

Une des difficultés majeures dans la reconstruction phylogénétique est donc de discriminer les homoplasies (*i.e.*, similitudes morphologiques chez différentes espèces ne provenant pas d'un ancêtre commun) des homologies. L'analyse phylogénétique fondée sur le principe de parcimonie (*i.e.*, utilisation du minimum de causes élémentaires pour expliquer la distribution des caractères) permet la reconnaissance de ces deux types. La principale différence entre l'homoplasie et l'homologie est le niveau phylogénétique ; en d'autres mots, la récence de l'ancêtre commun le plus proche et la présence ou l'absence continue versus interrompue d'un caractère (Hall, 2007). Les homoplasies

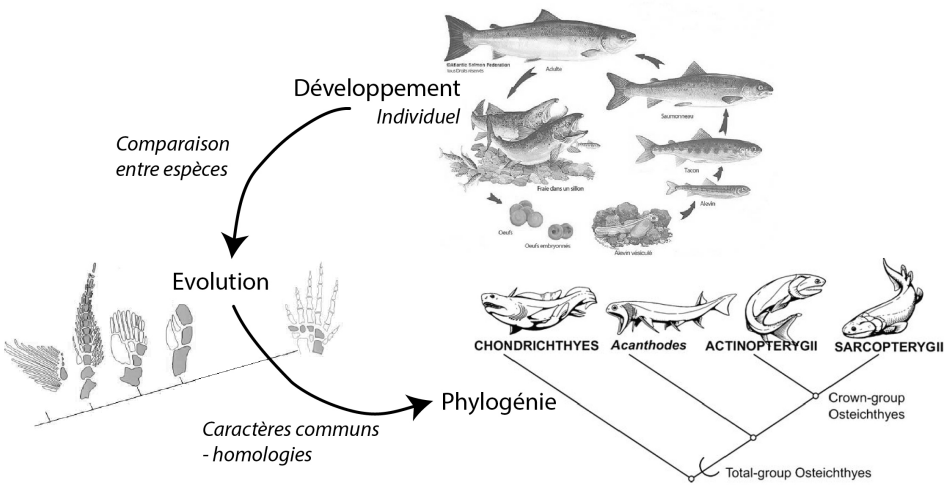

Figure 1: **Représentation schématique du concept de Phylo-Evo-Dévo.** Illustrations de Shubin and Tabin (1997); Friedman and Brazeau (2010) et the Atlantic Salmon Federation.

peuvent être vues comme des parallélismes chez les organismes qui ne partagent pas d'ancêtre commun récent (Scotland, 2010).

Afin d'affiner la résolution de la phylogénie des vertébrés paléozoïques, et ainsi des groupes de vertébrés actuels, l'étude du développement chez des fossiles peut aider à discriminer les homoplasies, les homologies profondes et les homologies latentes. Dans ce sens, l'étude phylo-évo-dévo des séquences développementales de vertébrés paléozoïques permet de décrire les processus et patrons partagés par le groupe total des vertébrés [*e.g.*, la direction proximo-distale de formation des éléments du squelette interne des nageoires paires (Freitas et al., 2007)] et leur évolution.

Les vertébrés paléozoïques : Morphologie et phylogénie

Étant donnée que la diversité des grands groupes de vertébrés est principalement représentée au Paléozoïque (541-242 millions d'années) et que les dernières analyses phylogéné-tiques des vertébrés sont controversées, ces groupes fossiles sont le modèle d'étude choisi dans cette thèse. Nous verrons que la position et le statut phylogénétiques de certains taxons ne font pas encore consensus. Cependant, une hypothèse largement admise des relations phylogénétiques entre vertébrés est représentée sur la Figure 2.

Les gnathostomes (*i.e.*, placodermes, acanthodiens, chondrichtyens et ostéichtyens, Figure 2) sont notamment différenciés des agnathes (*e.g.*, myxines, lamproies) par la présence de mâchoires, de nageoires paires pectorales et pelviennes possédant des ceintures endosquelettiques, d'organes d'intromission pour la fécondation interne, d'os périchondral ainsi que d'une nageoire caudale épicerque (Forey and Janvier, 1993; Forey, 1995; Janvier, 2001; Gai et al., 2011). Il n'existe cependant pas beaucoup de phylogénies prenant en compte à la fois les gnathostomes et les agnathes fossiles et actuels. Les caractères définissant les espèces de chaque groupe étant très dérivés, ils sont difficilement informatifs au niveau de la résolution des interrelations entre les grands groupes. Par exemple, une des grandes distinctions au niveau des structures crâniennes est la présence, chez les cyclostomes (*i.e.*, myxines et lamproies), et contrairement aux gnathostomes, d'un conduit médian simple, ou « narine », menant à l'organe hypophysaire, qui se développe à partir d'une placode nasohypophysaire médiane (Gai et al., 2011). Chez le galéaspide *Shuyu* (qui est pourtant un agnathe), le conduit nasohypophysaire débouche cependant dans le plafond de la cavité orale (Gai et al., 2011). Cet exemple met en lumière la difficulté de décrire des caractères communs définissant uniquement les agnathes ou les gnathostomes.

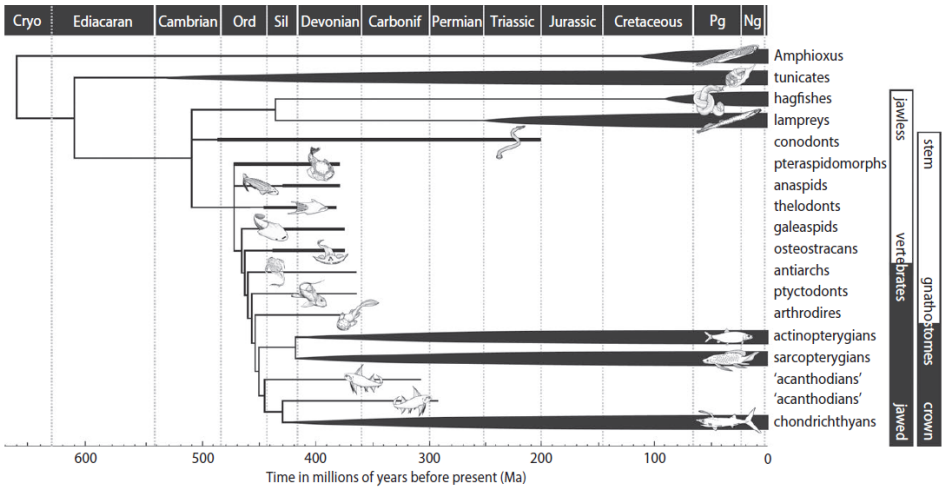

Figure 2: **Phylogénie des chordés et sélection représentative des vertébrés éteints en fonction des temps géologiques.** Les relations sont fondées sur les études de Donoghue et al. (2000); Heimberg et al. (2010); Sansom et al. (2010); Zhu et al. (2013). Figure tirée de Donoghue and Keating (2014).

Dans cette perspective phylogénétique et afin de mieux cerner les différents groupes appartenant aux agnathes et aux gnathostomes, une description succincte des différents groupes de vertébrés primitifs sera donnée dans les deux prochaines sections. L'emphase sera mise sur leurs différences morphologiques et les différentes hypothèses phylogénétiques en résultant. Ces sections permettent d'établir les connaissances nécessaires à la compréhension de la morphologie, du développement et des relations phylogénétiques des espèces d'agnathes et de gnathostomes.

Les agnathes

Les vertébrés sans mâchoire, aussi appelés agnathes (Figure 3), sont actuellement repré-sentés par deux groupes, les myxines et les lamproies [regroupées dans le groupe controversé des cyclostomes (Forey, 1995; Mallatt, 1996; Janvier, 2001)].

Dans le registre fossile, les agnathes sont très diversifiés puisque pas moins de huit groupes, comptant plusieurs genres et espèces chacun, ont été répertoriés (*i.e.*, conodontes, hétérostacés, arandaspides, astraspides, anaspides, thélodontes, galéaspides et ostéostracés). Ceux-ci présentent des morphologies diversifiées, notamment si l'on considère la présence ou l'absence de plaques osseuses recouvrant le corps. Cela peut aller jusqu'à des morphologies très extrêmes comme le "Tully monster" *Tullimonstrum gregarium* retrouvé dans un gisement du Carbonifère des États-Unis (Figure 4) (McCoy et al., 2016).

Les Petromyzontiformes (*i.e.*, lamproies) et les Myxiniformes (*i.e.*, myxines) sont les seuls représentants actuels des agnathes (Figure 3 A, B). Ils sont retrouvés dans le registre fossile depuis le Dévonien supérieur (370 millions d'années) pour les lamproies (Gess et al., 2006) et le Carbonifère (320-300 millions d'années) pour les myxines (Bardack, 1991) ; ces deux taxons ne possèdent pas de squelette minéralisé (*e.g.*, écailles) ni de canaux et de sillons sensoriels. Les myxines ont longtemps été classées comme des crâniates, qui regroupent des organismes plus basaux que les vertébrés, mais la mention récente d'éléments vertébraux ventraux dans la région caudale de la myxine *Eptatretus burgeri* (Ota et al., 2011) ainsi que d'un neurocrâne caractéristique des cyclostomes (Kuratani et al., 2016), confirme une appartenance aux vertébrés. Les lamproies possèdent une nageoire dorsale, des éléments de squelette axial (*i.e.*, arcualia), mais n'ont pas de nageoires paires [*i.e.*, nageoires dont la base, étroite, est constituée d'un squelette interne (*i.e.*, endosquelette) qui supporte la nageoire (rayons, radiaux, pièces basales), lui-même supporté par une ceinture] (Tulenko et al., 2013). Les lamproies sont notamment caractérisées par la présence d'une métamorphose lors de leur développement (Marinelli and Strenger, 1954; Chang et al., 2014). L'anatomie des lamproies immatures (ammocoètes) étant très différente de celle des lamproies adultes, ces animaux sont de bons modèles pour l'étude du développement chez les vertébrés (Ri-

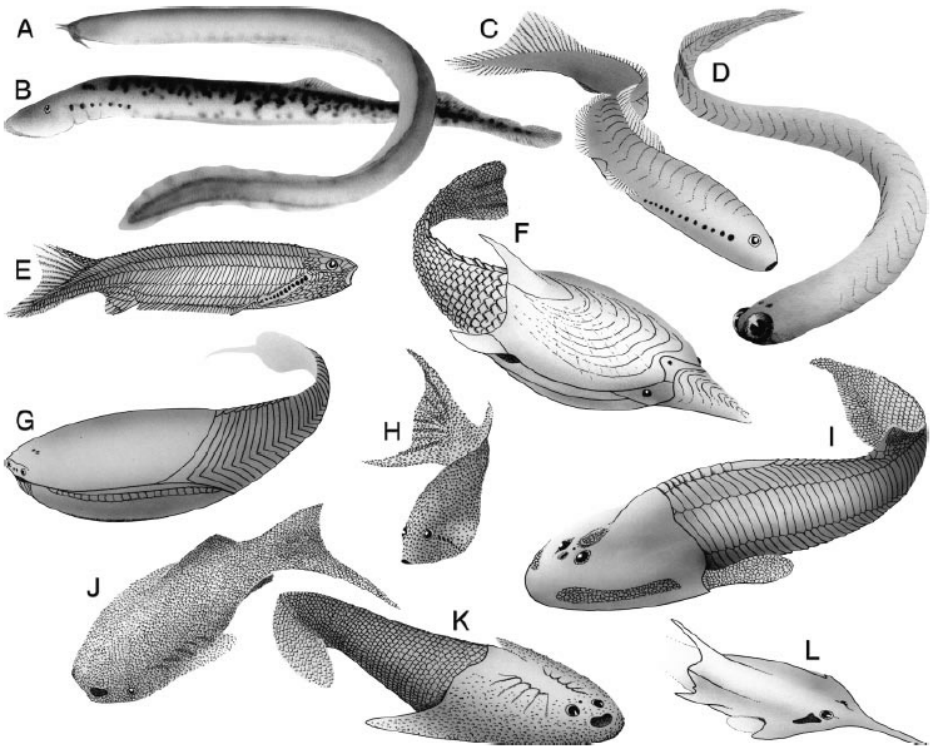

Figure 3: **Représentations de taxons d'agnathes** à partir de Donoghue et al. (2000). A. La myxine *Eptatretus stoutii* (60 cm). B. La lamproie *Petromyzon marinus* (80 cm). C. L'anaspide *Jamoytius kerwoodi* (130 mm). D. Le conodonte *Clydagnathus windsorensis* (60 mm). E. L'anaspide *Pharyngolepis oblongus* (15 cm). F. L'hétérostracé *Errivaspis wayensis* (15 cm). G. L'arandaspide *Sacabambaspis janvieri* (30 cm). H. Le thélodonte *Furcacauda heintzae* (35 mm). I. L'ostéostracé *Hemicyclaspis murchisoni* (15 cm). J. Le thélodonte *Loganellia scotica* (12 cm). K. Le galéaspide *Geraspis rara* (15 cm). L. Le pituriaspide *Pituriasps doylei* (bouclier céphalique : 45 mm).

Figure 4: **Reconstruction de la morphologie de *Tullimonstrum***. Tirée de McCoy et al. (2016).

chardson et al., 2010; Green and Bronner, 2014).

Les conodontes (Figure 3D) sont retrouvés de la fin du Cambrien à la fin du Trias (environ 480 à 200 millions d'années). Ce sont des animaux anguilliformes avec des éléments phosphatiques constituant un appareil d'alimentation complexe (Briggs et al., 1983; Mikulic et al., 1985; Aldridge et al., 1993; Gabbott et al., 1995). Aucune nageoire n'a été décrite chez ces organismes dont les restes complets sont très rares, ce qui explique que la position et le statut phylogénétique de ces animaux restent controversés (Donoghue et al., 2000; Turner et al., 2010).

Les ostracodermes regroupent un ensemble d'agnathes du Paléozoïque, caractérisés par la présence de plaques dermiques recouvrant la tête (Cope, 1889; Stensiö, 1964). Ce groupe paraphylétique (*i.e.*, groupe possédant une partie des descendants d'un ancêtre commun) comprend plusieurs grands clades succinctement décrits ci-dessous.

Les anaspides (Figure 3 C, E) sont connus du Silurien supérieur au Dévonien supérieur (420 à 360 millions d'années), ils possédent une épine triradiée située postérieurement à leurs fentes branchiales, une paire de structures ressemblant à des nageoires (aucun squelette n'est encore connu) postérieures à l'épine triradiée et antérieures à l'anus et

une nageoire caudale hypocerque (Janvier, 1996b). Le groupe des anaspides est particulièrement intéressant au niveau phylogénétique, car sa position et son statut monophylétique (*i.e.*, se dit d'un groupe contenant un ancêtre commun et tous les descendants de cet ancêtre) sont très controversés (Shu et al., 2003; Gess et al., 2006; Sansom et al., 2010). Cependant, deux grandes catégories se retrouvent dans le registre fossile : les espèces possédant un squelette dermique bien développé et celles qui n'en possèdent pas, les "anaspides-nus". Des analyses phylogénétiques récentes en font un groupe polyphylétique (*i.e.*, groupe incluant les descendants d'un ancêtre commun et ceux d'autres organismes) avec les "anaspides-nus" plutôt groupés au sein ou à la base des Petromyzontiformes (Gess et al., 2006; Blom, 2012) ou en groupe frère des autres anaspides et agnathes (Forey, 1995; Janvier, 1996a; Donoghue et al., 2000; Shu et al., 2003; Sansom et al., 2010) et les anaspides à écailles à la base des autres groupes de vertébrés sans mâchoire (Forey, 1995; Janvier, 1996a; Donoghue et al., 2000; Shu et al., 2003; Blom, 2012) (Figure 5). Cette problématique quant à la classification des anaspides a été récemment résumée par Janvier (2015) qui propose de séparer les anaspides en Euphaneropides, *Jamoytius* et anaspides ; cependant la position des "Euphaneropides" (incluant notamment *Euphanerops longaevus* du Dévonien supérieur de Miguasha, Canada) n'est pas résolue (Figure 5). Contrairement à cette proposition, Keating and Donoghue (2016), après avoir récemment décrit le squelette dermique de certains anaspides, et notamment la croissance de celui-ci, ont proposé de nouvelles hypothèses phylogénétiques : les Euphaneropides forment un groupe monophylétique avec les autres anaspides, lui-même groupe frère des [thélodontes + [galéaspides + [ostéostracés + gnathostomes]]] (Janvier, 2015).

Le groupe des hétérostracés (Figure 3G), présent de l'Ordovicien supérieur au Dévonien supérieur (environ 450 à 370 millions d'années), est caractérisé par la présence de globes oculaires placés antérieurement, ainsi que par une longue série oblique de

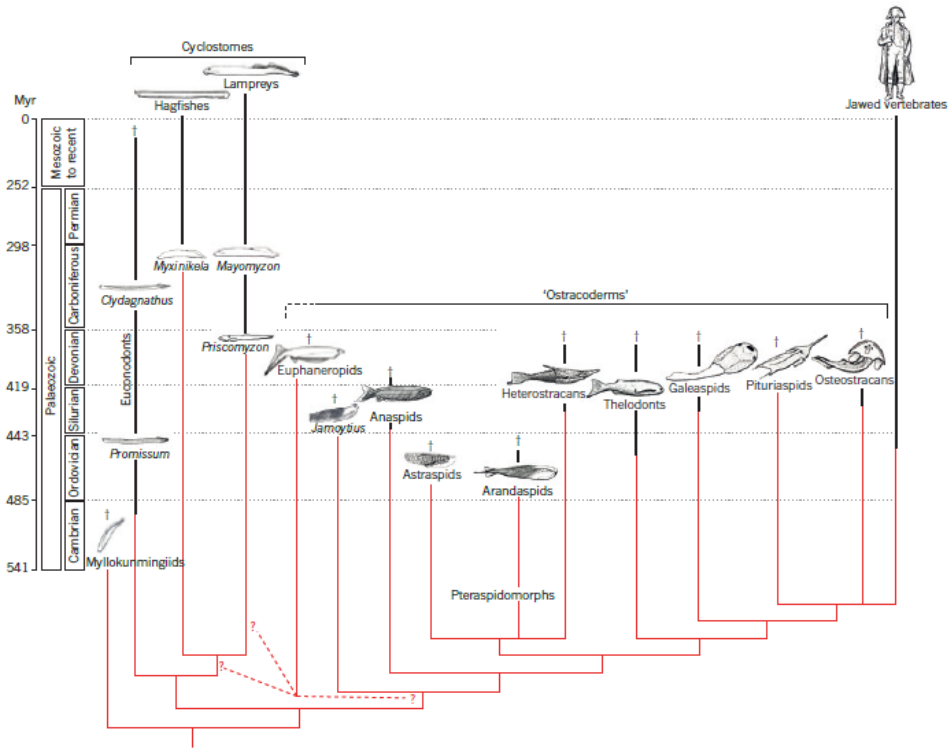

Figure 5: **Distribution des principaux groupes de vertébrés sans mâchoire paléozoïques (dague) et leurs représentants actuels à travers les temps géologiques (barres noires) et relations de parenté entre ces groupes (en rouge)**. Ces dernières sont adaptées de Sansom et al. (2010) excepté pour la position des Euphaneropides. Échelle non respectée. Figure tirée de Janvier (2015).

plaques dermiques en forme de diamant, séparant la partie dorsale de la partie ventrale du bouclier (Ritchie and Gilbert-Tomlinson, 1977). De petites ouvertures externes, correspondant à l'emplacement de branchies, sont placées entre ces plaques (Soehn and Wilson, 1990). Les hétérostracés ont parfois été considérés comme des précurseurs possibles des gnathostomes car ils possèdent un patron de canaux sensoriels similaire à celui des gnathostomes ainsi que des capsules olfactives paires (Janvier, 2001). Les hétérostracés ne possèdent pas de nageoires paires, seule la nageoire caudale assure la locomotion (Blieck and Heintz, 1983; Blieck, 1984). Cependant, les astraspides, arandaspides et hétérostracés forment un clade qui est groupe-frère de la souche des gnathostomes (Janvier, 2015) (Figure 5).

Les thélodontes, connus de l'Ordovicien supérieur au Dévonien supérieur (environ 450 à 370 millions d'années), possèdent des structures de type nageoire localisées au niveau de la région branchiale (Figure 3J), une nageoire caudale hypocerque et des petites écailles sur tout le corps (Turner, 1992; Donoghue and Smith, 2001). Les Furcacaudiformes possèdent un corps compressé latéralement (Figure 3H), en forme de tonneau, avec des yeux larges et positionnés latéralement immédiatement devant les ouvertures branchiales. Le pédoncule caudal est haut, la nageoire caudale a un lobe dorsal et un lobe ventral avec de multiples lobes intermédiaires (Wilson and Caldwell, 1998). Les thélodontes sont considérés comme le groupe frère des [galéaspides + [pituriaspides + [ostéostracés + [gnathostomes]]]] (Janvier, 2015).

Les galéaspides (Figure 3K), connus du Silurien moyen au Dévonien supérieur (environ 430 à 360 millions d'années), présentent une mosaïque de caractères de cyclostomes (comme *Shuyu* qui possède des capsules nasales localisées juste derrière l'avant de la tête et s'ouvrant au niveau d'un conduit commun nasohypophysaire) ainsi que des caractéristiques de gnathostomes dérivés (large séparation des capsules nasales) (Gai

et al., 2011). Cependant, ceux-ci ne possèdent pas de nageoires paires. Leur position phylogénétique est assez stable, en groupe frère des [pituriaspides + [ostéostracés + [gnathostomes]]] (Janvier, 2015).

Les pituriaspides (Figure 3L) sont connus principalement à partir de leur bouclier céphalique, ils sont peu informatifs en ce qui concerne leur anatomie interne (*e.g.*, squelettes axial et appendiculaire) (Janvier, 2008). Ce manque d'information est un biais ne permettant pas de répondre de façon exhaustive à la problématique de ce travail de thèse ; ce groupe ne sera donc pas traité.

Finalement, chez les ostéostracés (Figure 3I), connus du Silurien inférieur au Dévonien supérieur (environ 440 à 360 millions d'années), les nageoires paires sont uniquement repré-sentées par des nageoires pectorales bien développées associées à des ceintures, une nageoire caudale épicerque et une ossification endochondrale et périchondrale (Janvier, 1996b). La présence de squelette interne au niveau des nageoires pectorales a été décrite chez *Escuminaspis laticeps* (Belles-Isles, 1989; Janvier et al., 2004) et une ceinture pectorale a été identifiée chez *Norselaspis* (Coates, 2003). A ce jour, ces découvertes représentent les seules mentions de squelette interne de nageoires chez des agnathes. Ces caractères en font le plus souvent le groupe frère des gnathostomes (Figure 5) (Forey, 1995; Janvier, 1996a; Donoghue et al., 2000; Shu et al., 2003; Sansom et al., 2010; Janvier, 2015).

Les gnathostomes

Les vertébrés à mâchoires articulées, ou gnathostomes, représentent actuellement la plus grande diversité d'espèces de vertébrés, comptant les chondrichtyens ou poissons cartilagineux (*i.e.*, chimères, raies et requins) et les ostéichtyens ou poissons osseux (*i.e*,

actinoptérygiens et sarcoptérygiens dont les tétrapodes font partie). A titre d'exemple, les téléo-stéens à eux seuls comptent plus de 28 000 espèces actuelles (Barton and Bond, 2007).

Outre la présence de mâchoires, ce qui différentie notamment les gnathostomes des agnathes est la présence d'un squelette appendiculaire (*e.g.*, appendices pairs et ceintures) formé de nageoires pelviennes, de ceintures comprenant un squelette interne ainsi que des organes pairs d'intromission (Brazeau and Friedman, 2014). Les gnathostomes possèdent aussi une ou plusieurs nageoires dorsales, une nageoire anale et une nageoire caudale (Tableau 1, Figure 6). Leur squelette axial (*i.e.*, formant l'axe du corps) est composé de vertèbres, le plus souvent minéralisées et/ou ossifiées. Une régionalisation morphologique de la colonne vertébrale est observée tout au long du corps (Sallan, 2012). Les représentants fossiles de gnathostomes comptent moins d'espèces mais plus de classes (*i.e*, placodermes, acanthodiens, chondrichtyens et ostéichtyens) que les représentants actuels. Leur diversité morphologique et fonctionnelle est donc très importante.

Les premiers placodermes (Figure 6 A, B, D) sont datés du Silurien inférieur (440 millions d'années) et les derniers fossiles sont retrouvés au Dévonien supérieur (360 millions d'années) (Young, 2010). De manière générale, les placodermes sont caractérisés par la présence de plaques dermiques recouvrant la tête et le tronc, et possèdent des nageoires paires pectorales et pelviennes avec ou sans squelette dermique et dont l'endosquelette est peu connu (Trinajstic et al., 2015; Long et al., 2015), ainsi qu'une nageoire dorsale et anale et une nageoire caudale le plus souvent hétérocerque (Figure 6). Plusieurs groupes de placodermes ont des capsules nasales séparées du reste de la boîte crânienne par une fissure optique ; cette condition est plésiomorphe (*i.e.*, condition ancestrale) chez les vertébrés (Goujet, 2001; Young, 2010, Fig. 5e). Récemment,

Tableau 1: **Liste des caractères de gnathostomes potentiellement préservés dans le registre fossile**. Tirée de Maisey (1986); Janvier (2001); Goujet (2001); Brazeau and Friedman (2014)

1	Mâchoires, comprenant un palato-carré supérieur et une mandibule inférieure (cartilage de Meckel)
2	Squelette viscéral (squelette branchial et hyoïdien) indépendant du neurocrâne
3	Squelette branchial en position médiane par rapport aux branchies, chaque arc branchial étant composé de cinq éléments au maximum
4	Neurocrâne avec un processus post-orbitaire
5	Capsules nasales paires s'ouvrant séparément par des narines paires, et non connectées à un conduit nasohypophysaire ou à un sinus prénasal
6	Anneau sclérotique
7	Insertion antérodorsale du muscle oblique supérieur de l'orbite
8	Conduits endolymphatiques avec ouverture extérieure
9	Canal semicirculaire horizontal et renfoncement utriculaire ; statoconies ou otolithes composés de carbonate de calcium
10	Partie antérieure du cerveau large (mise en évidence par la forme de la cavité cérébrale)
11	Nageoires pectorales et pelviennes paires avec support endosquelettique interne (ceinture et radiaux)
12	Éléments ventraux de la colonne vertébrale (basiventraux et interventraux)
13	Système de la ligne latérale passant dans des canaux
14	Système de la ligne latérale largement distribué sur le corps et la nageoire caudale
15	Contenu stomacal permettant de définir les limites de l'estomac
16	Rayons de nageoires fait de collagène (actinotriches, cératotriches)
17	Un ou plusieurs arcs occipitaux incorporés dans le neurocrâne
18	Fissure occipitale latérale à travers laquelle les nerfs glossopharyngiens quittent le crâne
19	Os dermique et dentine
20	Ossification périchondrale ou calcification de l'endosquelette
21	Nageoire caudale épicerque (lobe chordal postéro-dorsal)
22	Nageoire anale
23	Veine jugulaire dorsale large
24	Processus postorbital

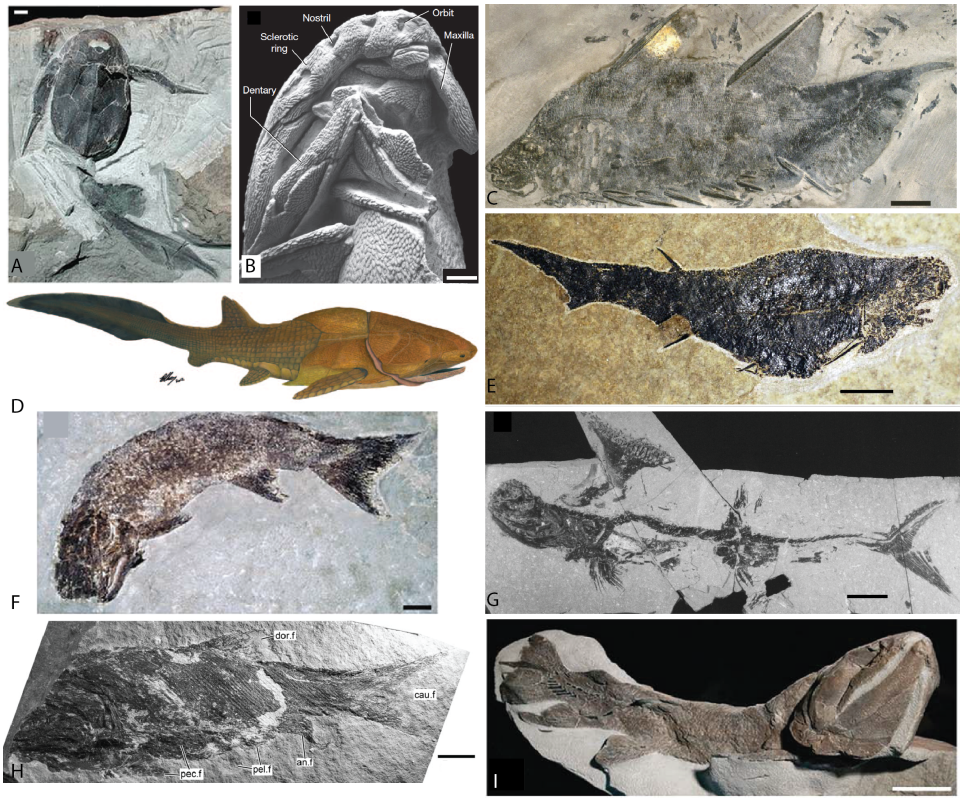

Figure 6: **Représentants des grands groupes de gnathostomes illustrés dans la Figure 7**. A. Le placoderme *Bothriolepis canadensis* (Cloutier, 2013). B. et D. Le placoderme *Entelognathus primordialis* (Zhu et al., 2013). C. L'acanthodien *Brochoadmones milesi* (Hanke and Wilson, 2006). E. L'acanthodien *Triazeugacanthus affinis*. F. L'actinopterygien *Cheirolepis* (Cloutier, 2013). G. Le chondrichtyen *Akmonistion zangerli* (Coates and Sequeira, 2001). H. L'actinoptérygien *Moythomasia lineata* (Choo, 2015). I. Le sarcoptérygien *Eusthenopteron foordi* (Cloutier, 2013). Échelles = 10 mm en A-C ; 10 cm en F ; 5 mm en E et H ; 5 cm en I ; et 40 mm en G.

Long et al. (2015) ont montré la présence d'organes d'intromission, non homologues aux ptérygopodes des chondrichtyens, placés postérieurement à la ceinture pelvienne. La position phylogénétique des placodermes ainsi que leur statut demeurent controversés (Goujet, 2001; Dupret, 2004; Goujet and Young, 2004; Young, 2010; Zhu et al., 2013; Brazeau and Friedman, 2014; Long et al., 2015). Les placodermes ont longtemps été considérés comme le groupe-frère des [ostéichtyens + chondrichtyens] (Young, 2010). Cette position phylogénétique implique que le squelette dermique macromérique (*i.e.*, composé de larges plaques osseuses), présent chez les placodermes et certains ostéichtyens, a évolué indépendamment chez ces deux groupes à partir d'un ancêtre commun avec un squelette dermique micromérique (*e.g.*, composé de petits denticules uniques) (Reif, 1982). Une hypothèse alternative est proposée, à partir de la comparaison de placodermes nouvellement découverts en Chine et datant du Silurien et d'ostéichtyens primitifs nouvellement décrits (*i.e.*, *Psarolepis*, *Meemania*, *Guiyu*) (Young, 2010; Friedman and Brazeau, 2013; Qu et al., 2013; Zhu et al., 2013). Les ostéichtyens et les placodermes peuvent avoir évolué à partir d'un ancêtre commun possédant un squelette dermique macromérique. Cependant, cette condition plésiomorphe implique une évolution indépendante des dents et de la lame dentaire chez les ostéichtyens et les chondrichtyens et une perte secondaire du squelette macromérique chez les chondrichtyens (Young, 2010). Cette nouvelle hypothèse phylogénétique propose les chondrichtyens comme le groupe-frère des [ostéichtyens + placodermes]. Cependant, Zhu et al. (2012b) ont montré la présence d'une ceinture pelvienne dermique chez l'antiarche *Parayunnanolepis xintunensis* du Dévonien inférieur ainsi que la présence d'os dermiques de type ostéichtyen au niveau des mâchoires du placoderme primitif *Entelognathus* (Figure 6 B) (Zhu et al., 2013). Ces chercheurs ont donc proposé les placodermes comme groupe-frère des [[chondrichtyens + "acanthodiens"] + ["acanthodiens" + ostéichtyens]].

Les plus vieux microrestes (*e.g.*, dents, écailles) avérés de chondrichtyens (Figure 6 G) sont datés de l'Ordovicien supérieur (455 millions d'années) mais le plus vieux spécimen articulé a été découvert dans des sédiments du Dévonien inférieur (environ 410 millions d'années) (Miller et al., 2003). Étant donné que le squelette interne des chondrichtyens n'est que peu ou pas minéralisé (Dean and Summers, 2006), les restes fossiles sont surtout des écailles, dents et denticules. Certaines caractéristiques des écailles sont notamment utilisées pour identifier les supposés chondrichtyens : (1) écailles non-croissantes, monodontode, écailles "placoïdes" avec une cavité pulpaire plus large que longue ; (2) écailles polyodontodes croissant par l'accrétion aréolaire d'odontodes, non attachées à une plaque dermique ; et (3) présence de canaux vasculaires au niveau du col de l'écaille et/ou la rétention de cavités vasculaires ouvertes ou de canaux dans chaque écaille (Hanke and Wilson, 2010). Les chondrichtyens actuels et certains groupes fossiles comme *Emsolepis hanspeteri* du Dévonien inférieur (environ 410 millions d'années) (Turner, 2004) possèdent un squelette dermique micromérique (Zangerl, 1981). L'identification des chondrichtyens paléozoïques est donc principalement basée sur les microrestes. Cependant, la description du squelette complet permet une meilleure résolution de la position phylogénétique, Maisey (2001) a décrit le crâne du chondrichtyen *Pucapampella* du Dévonien moyen et l'a classé comme un chondrichtyen primitif parce qu'il possède notamment des éléments de gnathostomes primitifs (*e.g.*, des fissures otique ventrale et otico-occipitale persistantes, un long canal notochordal entre les parachordaux) (Brazeau, 2009; Davis et al., 2012) (Figure 7). Cependant, Davis (2002) a montré que le groupe chondrichtyen-acanthodien est peu soutenu en raison du manque de synapomorphies (*e.g.*, caractères communs permettant de déterminer qu'un groupe est monophylétique) partagées par les deux groupes.

Les plus vieux restes d'ostéichtyens (Figure 6 F, H, I) ont été retrouvés dans des roches du Silurien supérieur (environ 420 millions d'années) (Zhu et al., 2009). Les

ostéichtyens possèdent un squelette dermique largement minéralisé et une ossification endochondrale au niveau du squelette interne. Les formes primitives ont des plaques dermiques très développées, localisées au niveau du crâne (Figure 6 I). Les ostéichtyens sont différentiés en deux grands groupes : les actinoptérygiens qui possèdent des nageoires paires à rayons (Figure 6 F, H) et les sarcoptérygiens qui ont des nageoires paires charnues (Figure 6 I). Les sarcoptérygiens, dont *Eusthenopteron* fait partie, possèdent un humérus, un radius et un ulna, présents aussi chez les tétrapodes, descendants de cette lignée (Coates et al., 2002). Les espèces du Silurien supérieur *Lophosteus superbus* et *Andreolepis hedei* sont placées à la base des ostéichtyens parce qu'elles possèdent des os dentaires et maxillaires mais elles différent des ostéichtyens plus dérivés par l'organisation de leurs denticules dermiques ressemblant à des dents (Botella et al., 2007). *L. superbus* partage des caractères avec les acanthodiens (*e.g.*, présence d'épines aux nageoires) et les placodermes (similarités au niveau du dermosquelette) et *A. hedei* avec le groupe total des ostéichtyens (*e.g.*, possible cléithrum et fulcres) ce qui ajoute de la confusion à leur position phylogénétique déjà controversée. Ces taxons, aux squelettes encore incomplets dans le registre fossile, ont tout d'abord été décrits sur la base de microrestes (Märss, 2001). Cette pauvreté de caractères phylogénétiques n'a pas permis à Cloutier and Arratia (2004) de les inclure dans une analyse phylogénétique des actinoptérygiens. Plus tard, Cunningham et al. (2012) décrivent à nouveau les maxillaires et les dentaires de *L. superbus* et *A. hedei* et montrent les caractères mosaïques de leurs os et denticules dermiques. Récemment, la description de l'espèce *Guiyu oneiros* du Silurien inférieur a apporté de nouvelles informations, notamment sur la présence d'une ceinture pelvienne dermique chez les ostéichtyens (Zhu et al., 2012a). Ce caractère est partagé avec des acanthodiens et les placodermes, et semble être un caractère primitif des gnathostomes. Cela implique cependant une perte secondaire chez les chondrichtyens (Zhu et al., 2012a, Figure 7).

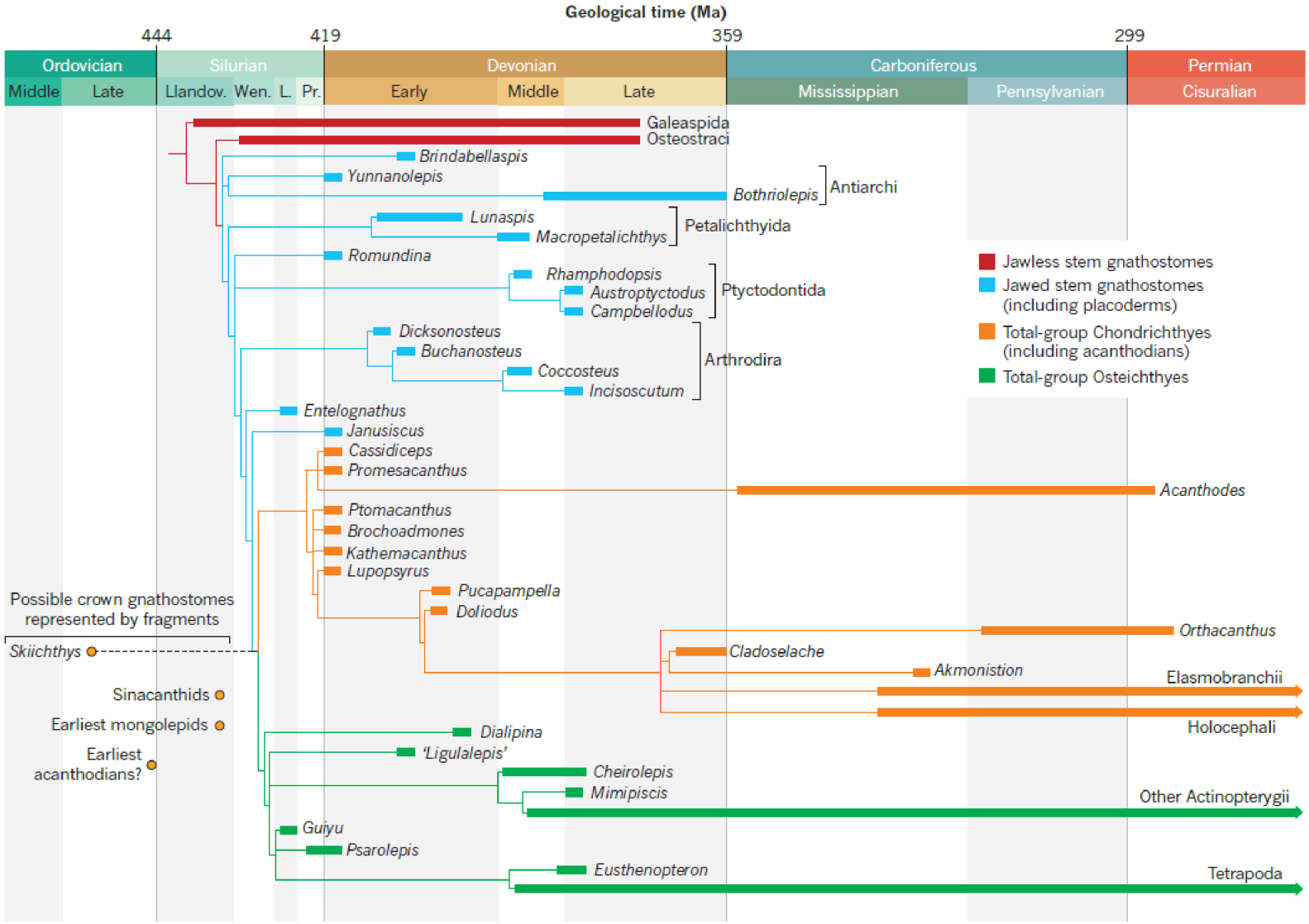

Figure 7: **Phylogénie des gnathostomes du Paléozoïque. Les temps de divergence minimums sont estimés à partir des fossiles**. Tirée de Giles et al. (2015b); Brazeau and Friedman (2015).

Les acanthodiens, enfin, partagent comme caractéristique la présence d'une épine dermique à la base de chaque nageoire à l'exception de la nageoire caudale (Figure 6 C, E). Les acanthodiens sont retrouvés dans le registre fossile depuis le Silurien inférieur (Karatajute-Talimaa and Predtechenskyj, 1995) jusqu'au Permien moyen-supérieur (Mütter and Richter, 2007) (environ 444 à 260 millions d'années). Ce groupe possède des nageoires paires pectorales et pelviennes, une ou deux nageoires dorsales, une nageoire anale et une nageoire caudale épicerque (Denison, 1979). A ces structures classiques, s'ajoutent, chez plusieurs ordres des séries d'épines paires à l'avant des nageoires pectorales et pelviennes (Figure 6 C). Les acanthodiens sont particulièrement intéressants car depuis Watson (1937) jusqu'à Burrow et al. (2016), leur position phylogénétique au sein des gnathostomes n'a cessée d'être revue. Tout d'abord, dans sa révision des acanthodiens, Watson (1937) les a classés dans le groupe des Aphetohyoidea avec plusieurs ordres de placodermes (*i.e.*, Arthrodira, Antiarchi, Petalichthyida et Rhenanida), considéré comme un intermédiaire entre les Cyclostomata et les Pisces (*i.e.*, vertébrés à mâchoires non tétrapodes). Cette classification était fondée sur la théorie de l'aphétohyoidie chez les acanthodiens : l'arc hyoïde est similaire aux arcs branchiaux suivants et une fente branchiale complète est positionnée derrière l'arc mandibulaire. Plus tard, se basant sur la description d'*Acanthodes*, Holmgren (1942) a révisé les arguments de Watson (1937) et a suggéré une proximité phylétique avec les élasmobranches (*i.e.*, raies et requins).

Miles (1965) a proposé que les acanthodiens et les élasmobranches ne soient pas si proches phylogénétiquement, et que les actinoptérygiens et les sarcoptérygiens (*i.e.*, les crossoptérygiens et les dipneustes) soient plus proches entre eux que des acanthodiens. Il a placé les acanthodiens dans le groupe des Teleostomi avec les Crossopterygii, les Actinopterygii et les Dipnoi par opposition aux Elasmobranchiomorphi (*i.e.*, Elasmobranchii, Placodermi et Holocephali). Apportant de nouvelles données

sur la colonne vertébrale et la nageoire caudale d'*Acanthodes*, Miles (1970) a mis en lumière des similarités avec des Teleostomi (*e.g.*, radiaux hypochordaux courts et non-segmentés comme chez les sarcoptérygiens, rangées d'écailles sur les nageoires similaires à la condition plésiomorphe des lépidotriches d'ostéi-chtyens) mais aussi avec les élasmobranches et les ostéichtyens primitifs (*e.g.*, notochorde non contrainte, arcs neuraux et haemaux séparés). Contrairement à Watson (1937), Miles (1973b) considère les acanthodiens comme de "vrais poissons" notamment par la présence de protections au niveau des branchies et de leur mode de suspension amphistylique des mâchoires. Des similarités au niveau du squelette crânien ont été démontrées entre l'acanthodien *Acanthodes bronni* du Permien inférieur (environ 290 millions d'années) et les ostéichtyens, comme la présence d'un éthmoïde minéralisé avec le sphénoïde et des capsules nasales complètement closes (Miles, 1973b). Ces similarités renforcent selon lui l'hypothèse que les acanthodiens appartiennent aux Teleostomi. Cependant, Miles (1973a) a aussi relevé la présence de caractères problématiques comme la présence d'une ceinture pectorale dermique proéminente caractérisant les placodermes et les ostéichtyens, alors que les acanthodiens et les chondrichtyens possèdent plutôt une ceinture endosquelettique très développée. Finalement, Miles (1973b) a proposé la monophylie des acanthodiens et a formulé trois hypothèses alternatives concernant leur position phylogénétique : (1) les acanthodiens partagent un ancêtre commun avec l'ancêtre commun des chondrichtyens et des ostéichtyens ; (2) les acanthodiens sont plus proches des chondrichtyens que des ostéichtyens ; et (3) les acanthodiens sont plus proches des ostéichtyens que des chondrichtyens.

Jarvik (1977) a étudié les relations phylogénétiques des gnathostomes entre eux, en se basant sur des caractères du crâne, des nageoires et du couvert branchial. En suivant Holmgren (1942), il a proposé que les acanthodiens (basé sur le modèle d'*Acanthodes*) appartiennent aux élasmobranchiomorphes. Selon Jarvik (1977), les

acanthodiens partagent des caractères avec les élasmobranches, en particulier les requins actuels (*e.g.*, commissure au niveau du palato-carré, double articulation des mâchoires) mais diffèrent des placodermes et des holocéphales. A partir de ces observations, une nouvelle hypothèse phylogénétique est proposée montrant les acanthodiens comme le groupe-frère des Selachii [*i.e.*, Palaoselachii + Euselachii [Squalimorphii + Galeomorphii]], et tous ces taxons sont regroupés dans les Elasmobranchii avec les Bathoidei.

Dans les années suivantes, les acanthodiens ont été considérés comme le groupe frère des chondrichtyens (Jarvik, 1980), ou des ostéichtyens (Denison, 1979; Maisey, 1986; Schultze, 1990), ou plus rarement à la base des gnathostomes (Rosen et al., 1981). Comme la position des acanthodiens au sein des gnathostomes est débattue, les recherches se sont concentrées jusqu'à la fin de la première décennie du XXI^{ème} siècle sur les interrelations au sein des acanthodiens (Denison, 1979; Long, 1986; Maisey, 1986; Hanke and Wilson, 2004; Burrow and Turner, 2010) (voir section "Les interrelations au sein des acanthodiens").

En 2009, de nouveaux caractères relatifs au crâne, jusqu'alors très peu connus chez les acanthodiens sont définis grâce à la re-description du crâne du climatiiforme *Ptomacanthus anglicus* du Dévonien inférieur (Brazeau, 2009). La courte région ethmosphénoïde, observée chez *Ptomacanthus*, ressemble plus à ce que l'on retrouve chez les placodermes et chondrichtyens qu'à ce qui est observé chez *Acanthodes* et les ostéichtyens. *Ptomacanthus* est placé à la base du clade regroupant les chondrichtyens et les ostéichtyens, alors que les acanthodiformes sont placés à la base des ostéichtyens seulement (Brazeau, 2009, Figure 3). Brazeau (2009) a conclu que *Ptomacanthus* présente des traits plésiomorphes des gnathostomes en partageant des caractères avec les chondrichtyens (*i.e.*, la partie mésiale de la rangée de dents est

supportée par l'ethmoïde). A cause du placement différent de *Ptomacanthus* et des autres acanthodiens, cette étude propose une hypothèse paraphylétique pour le groupe des acanthodiens. De même, Davis et al. (2012) ont révisé la description du crâne d'*Acanthodes* et ont fait une nouvelle analyse phylogénétique. Ils ont montré que les crânes d'*Acanthodes* et des chondrichtyens partageaient des caractères similaires : l'articulation paire de la mâchoire supérieure est positionnée derrière le processus postorbital et un plateau otique proéminent traverse la surface externe de la capsule otique. Une analyse morphométrique en coordonnées principales a montré (1) une disparité significative entre les placodermes et les autres gnathostomes ; (2) que les acanthodiens forment un groupe cohérent ; et (3) *Acanthodes* et les autres acanthodiens en général semblent plus similaires aux chondrichtyens qu'aux ostéichtyens (Davis et al., 2012, Figure 3). Finalement, l'analyse de Davis et al. (2012) renforce la précédente étude menée par Brazeau (2009) sur plusieurs points : (1) les placodermes sont paraphylétiques ; (2) les acanthodiens sont paraphylétiques ; (3) les acanthodiens sont inclus dans le groupe dérivé des gnathostomes ; (4) tous les acanthodiens sont plus proches des groupes de gnathostomes actuels que des placodermes.

Ces dix dernières années, le nombre toujours croissant de descriptions, de redescriptions et de nouvelles analyses phylogénétiques de gnathostomes basaux prouve que la phylogénie des vertébrés inférieurs n'est pas résolue (la Figure 7 ne représentant pas un consensus) (Brazeau and Friedman, 2014). Les descriptions de fossiles montrant des caractères mosaïques sont légions. Parmi celles-ci, la découverte d'un fossile de placoderme possédant des os marginaux de la mâchoire, caractéristique des ostéichtyens, a remis l'emphase sur une paraphylie des placodermes, plaçant ceux-ci à la base des gnathostomes (Zhu et al., 2013). De même la présence d'organes d'intromission chez les placodermes, non homologues à ceux qui sont connus chez les chondrichtyens, en font un groupe primitif par rapport aux autres gnathostomes (Long

et al., 2015). Récemment, seuls Dupret et al. (2014) ont proposé la monophylie des acanthodiens tandis que Brazeau and Friedman (2014) reconnaissent la paraphylie des placodermes, placés à la base des gnathostomes et proposent deux positions pour les acanthodiens paraphylétiques : exclusivement à la base des chondrichtyens [supportée par Burrow et al. (2016)] ou distribués à la base des chondrichtyens et à la base des ostéichtyens. Finalement, deux hypothèses sont avancées quant à la condition morphologique de l'ancêtre commun des gnathostomes : une condition regroupant des caractères de chondrichtyens (Figure 7) (Miles, 1973b; Brazeau, 2009; Davis et al., 2012) ou des caractères d'ostéichtyens (Zhu et al., 2013; Dupret et al., 2014). Cependant, derrière ces relations phylogénétiques controversées au sein des gnathostomes, les interrelations au sein des acanthodiens sont, elles aussi, débattues.

Les interrelations au sein des acanthodiens

Woodward (1891) fut le premier à définir trois familles d'acanthodiens – Acanthodidae, Ischnacanthidae et Diplacanthidae – auxquelles il ajouta en 1906, la famille des Gyracanthidae. Miles (1966) a fait de ces familles des ordres, qu'il a ensuite subdivisés (sauf pour les Ischnacanthiformes) : Acanthodiformes en Mesacanthidae, Acanthodidae et Cheiracanthidae ; Climatiiformes en Diplacanthidae et Climatiidae (Brazeau, 2008, Figure 10). Miles (1965, 1973a) a défini des tendances dans l'évolution des caractères anatomiques des Acanthodiformes et a conclu que les Acanthodiformes et les Ischnacanthiformes semblent partager un ancêtre commun plus récent qu'avec celui des Climatiiformes (Figure 8 B). Les Climatiiformes sont séparés en deux sous-ordres, les Climatioidei et les Diplacanthoidei, différant par l'absence d'épines pré-pectorales, la réduction totale des plaques loricales, la réduction de la série pinale de la plaque postérieure (*i.e.*, plaques dermiques situées en partie ventrale de la ceinture pectorale), et l'hypertrophie de la première épine intermédiaire chez les Diplacanthoidei. Denison

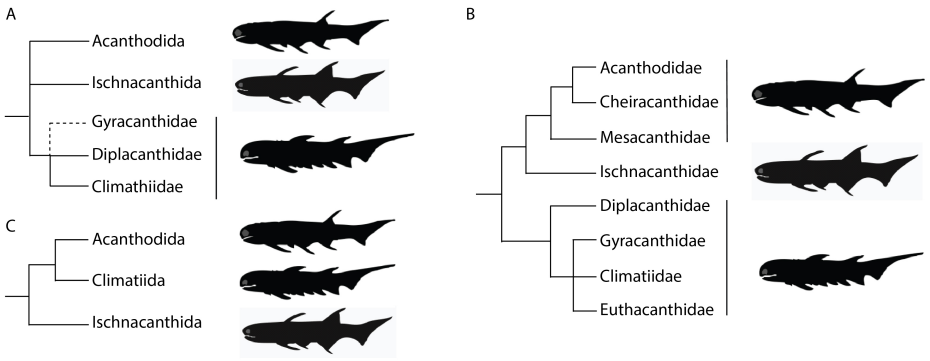

Figure 8: **Cladogrammes montrant les différentes hypothèses proposées sur les interrelations au sein des acanthodiens**. A. Selon Denison (1979) ; B. Selon Miles (1973a) ; C. Selon Long (1986). Modifié de Long (1986).

(1979) a renommé les sous-ordres Diplacanthoidei et Climatioidei en familles en se basant sur des caractéristiques communes (*i.e.*, présence de tessères sur la tête et d'une ceinture pectorale bien développée). Il valide l'hypothèse de Miles (1973b), suggérant que les caractéristiques ancestrales des acanthodiens sont présentes chez les Climatiidae (Denison, 1979, p. 20). Les Gyracanthidae et les Climatiidae possèdent des plaques dermiques pectorales portant des épines prépectorales. Finalement, Denison (1979) a montré qu'il n'y a pas d'évidences claires pour conclure sur les interrelations au sein des acanthodiens et a donc représenté ces relations par une trichotomie (Figure 8 A).

Long (1986) a revu la description des caractères des acanthodiens à partir de Denison (1979) et a précisé trois caractères : 1) les dents sont absentes chez les Euthacanthidae, Climatiidae et les Acanthodiformes, mais l'absence de dents semble être un caractère dérivé étant donné que des dents isolées et des plaques de dents sont connues chez les chondrichtyens, les Ischnacanthiformes et certains Climatiiformes ; 2) chez certains acanthodiens, on retrouve des épines de nageoires avec une simple ornementation linéaire, plus ou moins profondément insérées, les épines pectorales sont libres et l'armure de la ceinture pectorale est peu développée chez certains Ischnacanthiformes

et Acanthodiformes ; et, 3) la présence de nombreuses épines intermédiaires peut être une synapomorphie des Climatiidae. La révision du diagnostic des caractères ancestraux des acanthodiens suggère, à l'opposé de Miles (1973a) que les Diplacanthiformes et Climatiiformes sont primitifs aux Ischnacanthiformes et Acanthodiformes (Figure 8 C) ; les Acanthodiformes et Climatiiformes étant considérés cependant comme des groupes dérivés car ils possèdent une double articulation mandibulaire, aussi connue chez les chondrichtyens, et de possibles os multiples recouvrant les branchies. Aucun consensus n'a pu être établi sur les interrelations des acanthodiens. Les nouvelles diagnoses permettent d'établir de nouveaux groupes ; Gagnier and Goujet (1997) ont proposé un ordre de Subclimatiiformes, les Diplacanthiformes, alors que Karatajute-Talimaa and Smith (2002) ont décrit un quatrième ordre, les Tchunacanthida, fondé sur l'histologie des écailles.

Au-delà des relations entre les ordres, l'étude des relations entre les espèces peut résoudre de façon plus précise la phylogénie et donner de l'information supplémentaire sur le statut phylogénétique. La monophylie des acanthodiens a été remise en cause pour la première fois dans les années 1990 (Gagnier and Wilson, 1996; Janvier, 1996b). Hanke and Wilson (2004) ont décrit des espèces du Dévonien inférieur de la localité de MOTH (Canada) ; ces spécimens ont été attribués à *Obtusacanthus corroconis* et à *Lupopsyroides macracanthus*. La description de ces deux espèces leur a permis de proposer une nouvelle phylogénie avec des groupes externes clairement définis et de donner un argument supplémentaire à la paraphylie des acanthodiens et des Climatiiformes. Ces espèces partagent des caractères avec les chondrichtyens comme la présence d'écailles "placoïdes" (*i.e.*, denticules dermiques ou odontodes) mais aussi avec les acanthodiens puisqu'elles possèdent des épines de type acanthodien. La présence d'une écaillure simple chez *L. macracanthus*, *O. corroconis* et l'acanthodien *Lupopsyrus pygmaeus* du Dévonien inférieur supporte l'hypothèse que les premiers gnathostomes de-

vaient posséder des écailles monodontodes simples (*i.e.*, composées d'un seul odontode, voir plus bas), ressemblant à des écailles placoïdes. *L. pygmaeus* possède un scapulocoracoïde avec une ossification typique, des procoracoïdes ossifiés, des protections de type "plaques" au niveau des branchies, et des écailles monodontodes avec des cavités. A partir de ces caractères, Hanke and Davis (2012) considèrent cette espèce comme un acanthodien basal mais ne lui attribuent pas d'ordre, alors que Denison (1979) considérait *L. pygmaeus* comme faisant partie des Climatiidae tandis que Long (1986) plaçait cette espèce comme groupe frère des Diplacanthidae et des Ischnacanthidae. La position phylogénétique de cette espèce est non résolue à cause d'un manque de synapomorphies des différents ordres d'acanthodiens. Comme pour le groupe en entier, le statut phylogénétique des ordres demeure incertain.

Récemment, Brazeau (2009) a suggéré que les caractères partagés par les "Climatiiformes" sont (1) la présence d'une armure pectorale dermique et ventrale ; (2) trois épines pré-pelviennes (ou intermédiaires) ; (3) une tête couverte par des tessères polygonales montrant une ornementation stellaire ; et, (4) des épines de nageoires avec des rainures prononcées portant des noeuds. Cependant, la paraphylie des Climatiiformes est suggérée notamment en raison de l'absence de synapomorphies entre *Climatius reticulatus* et les autres Climatidae (Hanke and Wilson, 2004). De plus, la position de *Brochoadmones milesi* au sein des Climatiiformes (Gagnier and Wilson, 1996) a été révisée, montrant que celui-ci serait plus proche des Ischnacanthidae et des Acanthodiformes en raison de l'absence de plaques au niveau de l'armure pectorale, de la présence d'épines pré-pectorales, de l'ornementation des épines médianes ainsi que de la structure des écailles recouvrant la tête (Hanke and Wilson, 2006). Les Ischnacanthiformes, ordre le plus proche des ostéichtyens selon Davis et al. (2012) (incluant les Actinopterygii, Sarcopterygii, *Lingulalepis* et *Dialipina*), possèdent des plaques dentaires non-symphysaires, une rainure oblique au niveau mésial du palato-carré (Bra-

zeau, 2009), et des os des mâchoires portant des dents (Young and Burrow, 2004). Les espèces du genre *Diplacanthus* et *Uraniacanthus probaton* forment le groupe-frère du clade contenant les espèces du genre *Tetanopsyrus* notamment en raison de la spécialisation de la région pectorale de *Diplacanthus* (Hanke and Wilson, 2004) : la famille des Gladiobranchidae, à laquelle appartiennent les espèces du genre *Uraniacanthus* avait été précédemment placée dans l'ordre des Ischnacanthiformes (Miles, 1973b,a). La diagnose révisée des Gladiobranchidae regroupe plutôt ces espèces dans les Diplacanthiformes (Newman et al., 2012). Cependant, il y a peu d'évidence pour unir les Diplacanthidae, les Gladiobranchidae, les Culmacanthidae et les Tetanopsyridae dans un seul et même ordre (Young and Burrow, 2004). Le clade le plus dérivé des acanthodiens est l'ordre des Acanthodiformes qui comprend les familles Acanthodidae (*e.g.*, *Acanthodes*), Mesacanthidae (*e.g.*, *Mesacanthus mitchelli* et *Triazeugacanthus affinis*) et Cheiracanthidae (*e.g.*, *Homalacanthus concinnus* et *Cheiracanthus latus*). Les Mesacanthidae sont cependant considérés comme primitifs au sein des Acanthodiformes en raison de la présence d'épines pré-pelviennes paires, d'écailles élargies sur la tête et d'épines robustes (Cumbaa and Schultze, 2002).

En résumé, à ce jour, les synapomorphies des acanthodiens (et notamment la présence d'épines pectorales paires) sont souvent remises en question et cette incertitude est au cœur de la question initiale de ce travail de thèse. La présence d'épines pectorales paires comme synapomorphie des acanthodiens est mise à mal depuis la description d'épines pectorales paires chez les chondrichtyens *Doliodus problematicus* du Dévonien inférieur (Miller et al., 2003) et *Wellerodus priscus* du Dévonien moyen (Potvin-Leduc et al., 2011). Une nouvelle interprétation a été proposée pour les épines du chondrichtyen *Antarctilamna prisca* comme étant des épines pectorales (Miller et al., 2003). D'autre part, le supposé acanthodien *Yealepis douglasi* du Silurien supérieur possède de larges écailles ornementées à la place des épines pectorales et in-

termédiaires, aucune épine pectorale n'a été décrite chez le Diplacanthiforme *Culmacanthus* sp. du Dévonien supérieur (Burrow and Young, 2012) alors que le supposé acanthodiforme *Paucicanthus vanelsti* du Dévonien inférieur ne possède pas du tout d'épines paires (Hanke, 2002). Ceci implique donc que si les épines pectorales paires sont considérées comme une synapomorphie, celle-ci est soumise à une grande disparité morphologique au sein du groupe Acanthodii.

Les analyses phylogénétiques les plus récentes montrent que les Diplacanthidae (*e.g.*, *Tetanopsyrus*, *Culmacanthus*, *Diplacanthus*, *Uraniacanthus*, *Rhadinacanthus*) sont le groupe-frère monophylétique de tous les autres acanthodiens ainsi que des chondrichtyens et des ostéichtyens (Davis et al., 2012). Les Climatidae (*i.e.*, *Ptomacanthus*, *Climatius*, *Brachyacanthus* et *Parexus*) sont regroupés en groupe-frère des gnathostomes dérivés tandis que les autres taxons de Climatiiformes sont répartis à la base des ostéichtyens (*i.e.*, *Euthacanthus*) ou à la base des chondrichtyens (*i.e.*, *Brochoadmones*). Les Acanthodiformes (*i.e.*, *Mesacanthus*, *Promesacanthus*, *Cheiracanthus*, *Acanthodes* et *Homalacanthus*) et *Cassidiceps* sont considérés comme le groupe-frère des Ischnacanthiformes (i.e, *Ischnacanthus* et *Poracanthodes*) et des ostéichtyens. Tout récemment, les dernières analyses phylogénétiques, fondées sur la re-description d'écailles d'acanthodiens du Dévonien inférieur à moyen d'Écosse, placent les Diplacanthiformes au sein d'un clade contenant des acanthodiens, eux-mêmes placés comme groupe paraphylétique à la base des chondrichtyens. Ici, l'hypothèse d'un groupe monophylétique [acanthodiens + chondrichtyens] est supportée (Burrow et al., 2016). Cette remise en question mène certains chercheurs à conclure que la diversité morphologique des acanthodiens est finalement plus grande que ce que les précédentes études ont suggéré (Burrow and Young, 1999; Hanke and Wilson, 2004).

Derrière la morphologie : Le développement et l'histologie

Les statuts et positions phylogénétiques non résolus des anaspides entre eux et au sein des agnathes d'une part et des acanthodiens entre eux et au sein des gnathostomes d'autre part montrent les limites des analyses phylogénétiques basées essentiellement sur les caractères morphologiques définis à partir des spécimens les mieux préservés (*i.e.*, des adultes avec un squelette minéralisé permettant une fossilisation optimale). Néanmoins, les améliorations technologiques (*e.g.*, micro et nano CT-scan, synchrotron) rendent possibles des études morphologiques plus fines. Cependant, au delà des seuls caractères morphologiques, l'étude de potentiels caractères histologiques et développementaux ouvre une voie prometteuse pour une meilleure identification des caractères homologues et plésiomorphes au niveau des grands groupes, et ainsi pour une résolution plus réaliste de la phylogénie. L'étude du développement des vertébrés (*i.e.*, ontogénies fossiles et actuelles) ainsi que l'étude de leurs micro restes (*e.g.*, écailles et dents) peuvent apporter des informations essentielles sur l'évolution des premiers groupes de vertébrés.

Les ontogénies fossiles

Les ontogénies fossiles sont rares parce que la préservation des éléments faiblement minéralisés des spécimens immatures requiert des conditions de fossilisation exceptionnelles. Chez les taxons éteints, comme les acanthodiens et les placodermes, cette faible préservation est problématique car seules les ontogénies ont le potentiel d'informer sur les processus et patrons développementaux du passé. Bien qu'elles soient difficiles à caractériser, les ontogénies fossiles ont été décrites pour quelques groupes de vertébrés non tétrapodes fossiles [Cloutier (2010) a référencé les ontogénies fossiles

de quelques 90 espèces] (Figure 9). Des patrons caractérisant les ontogénies fossiles sont reconnaissables (Cloutier, 2010) : (1) des yeux proportionnellement plus larges chez les juvéniles que chez les adultes, (2) un ratio longueur de tête-longueur du corps diminuant avec la croissance, (3) la position relative des nageoires le long de l'axe horizontal du corps se modifiant avec la croissance, (4) les écailles apparaissent graduellement le long du corps, et (5) le nombre de rayons aux nageoires est fixé de façon précoce. Les données obtenues à partir des taxons existant montrent que les séquences de chondrification/minéralisation peuvent être décrites en termes de temps de première apparition d'un élément, temps relatif au sein des unités morphologiques, et direction de formation entre des éléments sériés au sein des unités morphologiques. A partir des ontogénies fossiles, des stades ontogénétiques (*i.e.*, embryon, larve, juvénile, adulte, sénescent), correspondant à des caractéristiques morphologiques et anatomiques des spécimens, peuvent être définis suivant certains critères que Cloutier (2010) a regroupé ainsi : (1) la période embryonnaire finit avec l'éclosion ou le début de l'alimentation externe ; (2) la période larvaire est caractérisée par la présence d'un sac vitellin et d'un repli natatoire ainsi que l'absence d'écailles sur le corps et la différentiation incomplète des rayons des nageoires ; (3) la phase juvénile est reconnaissable à l'absence de sac vitellin et de repli natatoire, à une écaillure incomplète sur le corps, et à des proportions du corps qui tendent à ressembler à celles de l'adulte ; et (4) le stade adulte est caractérisé par une écaillure complète et par la complétion de l'ossification du squelette.

Chez les agnathes, des ontogénies partielles à partir de fossiles d'individus en connexion (*i.e.*, articulés) ou de restes isolées ont été mentionnées chez l'anaspide *Euphanerops longaevus* du Dévonien supérieur (Janvier, 2007) ; les hétérostracés *Woodfjordaspis felixi* (Pernegre, 2006), *Panamintaspis snowi* et *Blieckaspis priscillae* (Elliott and Ilyes, 1996), *Pteraspis carmani* (Denison and Lillian, 1960), *Dinaspidella elizabethae* et *Nahanniaspis mackenziei* (Greeniaus and Wilson, 2003) du Dévonien inférieur ;

Figure 9: **Ontogénie fossile du placoderme du Dévonien supérieur *Bothriolepis canadensis***. Le bouclier céphalique du plus petit spécimen (à gauche) mesure 8 mm, tandis que le plus grand (à droite) mesure 20 cm. Échelle = 1 cm. Tirée de Cloutier (2010).

les ostéostracés *Superciliaspis gabrielsi* (Hawthorn et al., 2008) du Dévonien inférieur et *Escuminaspis laticeps* du Dévonien supérieur (Arsenault and Janvier, 1995) et probablement chez le thélodonte *Lanarkia* du Dévonien inférieur (Turner, 1992).

Chez les gnathostomes, des ontogénies fossiles basées sur des spécimens complets ont été identifiées chez tous les grands groupes : placodermes, acanthodiens, chondrichtyens et ostéichtyens (Cloutier, 2010; Johanson and Trinajstic, 2014). Des séquences ontogénétiques ont été identifiées chez 14 taxons d'acanthodiens (Zidek, 1976; Cloutier, 2010) : le possible Ischnacanthiformes *Nerepisacanthus denisoni* (Burrow and Rudkin, 2014), les deux Diplacanthiformes *Diplacanthus horridus* (Cloutier et al., 2009) et *Uraniacanthus curtus* (Newman et al., 2012), le Climatiiformes *Tetanopsyrus breviacanthias* (Hanke et al., 2001), les deux espèces d'ordre incertain *Machaeracanthus goujeti* (Botella et al., 2012) et *Lupopsyrus pygmaeus* (Hanke and Davis, 2012), et chez les huit Acanthodiformes *Lodeacanthus gaujicus* (Upeniece, 1996, 2001; Upe-

niece and Beznosov, 2002), *Homalacanthus concinnus* (Cloutier et al., 2009), *Acanthodes bridgei* (Zidek, 1985), *A. bronni* (Heidtke, 1990), *A. gracilis* (Zajic, 2005), *A. lopatini* (Beznosov, 2009), *A. ovensi* (Forey and Young, 1985), et une espèce d'acanthodiforme indéterminée (Coates, 1993).

A ce jour, une des ontogénies les mieux décrites est celle du Mesacanthidae *L. gaujicus* (Upeniece, 2011). Cette espèce est retrouvée dans la Formation de Lode datée du Dévonien supérieur de Lettonie. Les trois stades ontogénétiques de cet acanthodien ont été décrits à partir du patron de mise en place des écailles. Des différences anatomiques ont été décrites notamment entre le stade juvénile et le stade adulte : la morphologie des écailles et l'étendue de l'écaillure, la forme des os nasaux, le nombre d'os autour de l'orbite [identifiés comme des os circulaires par (Upeniece, 2011) mais qui sont probablement des os sclérotiques selon Burrow et al. (2011)], et la variation de taille des épines des nageoires.

Les ontogénies des acanthodiens et des vertébrés fossiles en général apportent des informations relatives aux patrons et processus développementaux ayant lieu durant la croissance. Ces caractères développementaux peuvent être identifiés comme des homologies évolutives latentes et leur inclusion dans des analyses phylogénétiques peuvent en ce sens aider à affiner les phylogénies. Bien que les spécimens complets et articulés soient rares dans le registre fossile, l'ontogénie des espèces peut être inférée en utilisant les micro restes isolés qui sont abondants.

Squelette dermique : variations morphologiques et ontogénie

Dans le registre fossile, et spécialement durant le Paléozoïque, les micro restes de vertébrés représentent une grande majorité des éléments retrouvés et sont très diver-

sifiés. Parmi les éléments du squelette dermique, les écailles enregistrent l'ontogénie des individus (de façon analogue à la détermination de l'âge chez les saumons actuels) et fournissent donc une opportunité unique pour décrire l'ontogénie des espèces possédant ces structures. Les micro restes peuvent donc être une source de nouveaux caractères phylogénétiques, notamment chez les espèces fossiles où les informations relatives à l'ontogénie sont limitées.

Les odontodes sont les premiers éléments du squelette dermique à se développer lors de l'ontogénie. Le terme "odontode" fut proposé pour la première fois par Ørvig (1967) (p.47) où il définit tous les éléments isolés, durs et localisés dans la peau formés à partir d'une papille "dentaire" unique et composés d'une cavité centrale "pulpaire" entourée de dentine, ou de tissus ressemblant à la dentine, qui peut être recouvert ou non d'une couche hyperminéralisée d'émail ou d'émailloïde. Subséquemment, Sire (2001) proposa d'utiliser ce terme d'odontode pour tous les denticules dermiques de lignées partageant un ancêtre commun. Deux hypothèses majeures ont été proposées pour expliquer les processus par lesquels les odontodes croissent ou s'agrègent pour former des éléments plus complexes comme les écailles et les plaques dermiques. La première hypothèse, appelée la "théorie lépidomoriale" propose que les éléments plus complexes sont formés par la fusion d'odontodes au niveau du stade papillaire de développement (Stensiö, 1962). La seconde hypothèse, "la régulation des odontodes", a été suggérée par Ørvig (1967). S'appuyant sur cette hypothèse, Reif (1982) considère qu'il n'y pas de fusion des odontodes durant le développement mais que l'accrétion et l'attachement des odontodes à l'os dermique sous-jacent est l'explication de la formation des éléments complexes. Cette théorie semble avoir reçu une large reconnaissance et être favorisée (Karatajute-Talimaa, 1998).

L'origine du squelette dermique est complexe. Dès le Paléozoïque, il existe une diver-

sité importante d'écailles, tant au point de vue morphologique qu'histologique, chez les différents groupes d'agnathes et de gnathostomes. Cependant, à des fins de clarté, l'accent sera mis sur cinq groupes, les thélodontes, les placodermes, les acanthodiens, les chondrichtyens et les actinoptérygiens.

Les écailles de thélodontes (Figure 10 A) sont petites, morphologiquement simples et superficiellement comparables aux denticules dermiques (*i.e.*, écailles "placoïdes") des chondrichtyens (Gross, 1947; Reif, 1982; Karatajute-Talimaa, 1998). Généralement, un denticule dermique de thélodonte est composé d'une couche épaisse d'orthodentine entourant une cavité pulpaire et est supporté par de l'os acellulaire (Sire et al., 2009). Chaque élément peut être couvert superficiellement par une fine couche d'émailloïde ou d'émail (Sire et al., 2009).

Les écailles de placodermes sont petites et se chevauchent (Figure 10) (Denison, 1978; Burrow and Turner, 1999). Chez les antiarches, phyllolepides et certains arthrodires, les écailles sont composées de deux régions sans dentine : une couche superficielle formée d'os lamellaire cellulaire et une couche centrale caractérisée par de complexes canaux vasculaires (parfois cette couche est organisée en deux niveaux différents). Chez les arthrodires, les écailles sont composées d'os cellulaire ornementé avec des tubercules de semi-dentine de type odontode (Burrow and Turner, 1999; Sire et al., 2009). Parce que les fossiles de placodermes consistent le plus souvent en la préservation des plaques dermiques de la tête et du thorax, le mode de croissance de leurs écailles n'est pas connu.

Les denticules dermiques des chondrichtyens actuels (*i.e.*, écailles "placoïdes") sont caractérisés par la présence d'une couche superficielle d'émailloïde recouvrant l'orthodentine (Figure 10) (*i.e.*, tissu acellulaire avec une matrice riche en collagène et

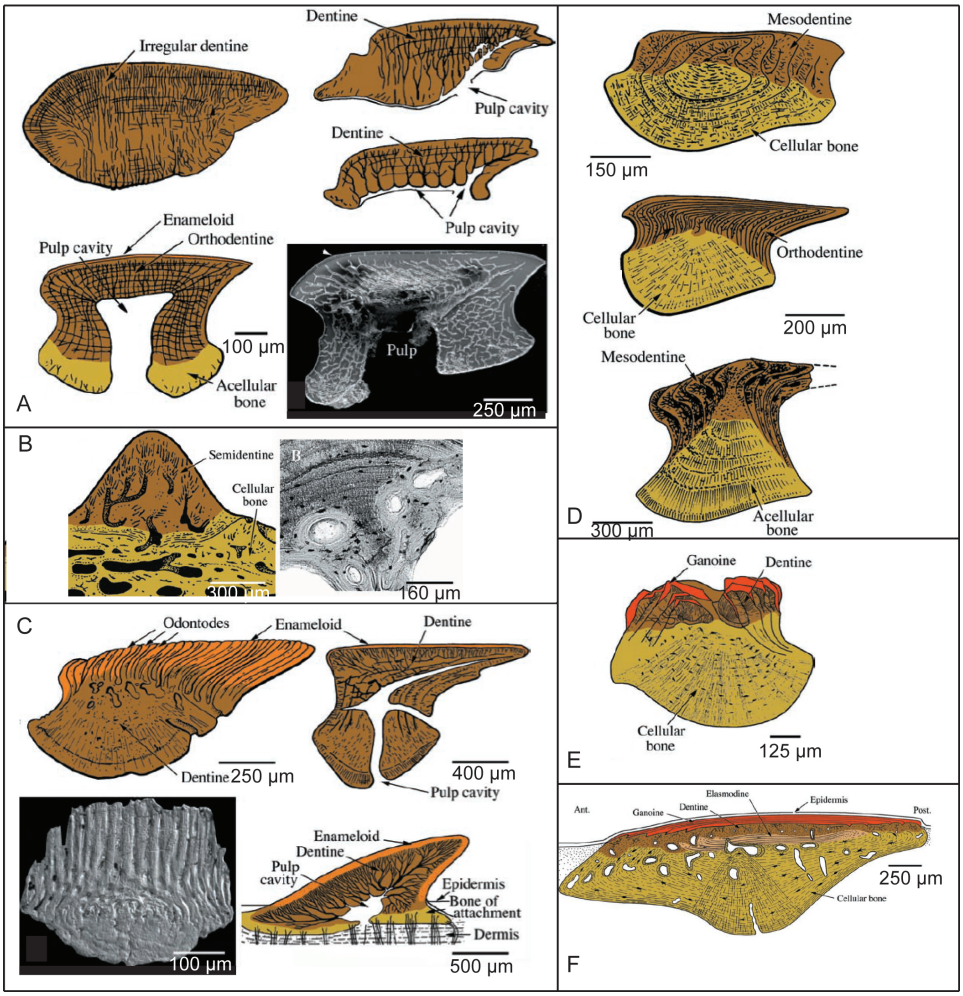

Figure 10: **Structure schématique des écailles**. A. Écaille de thélodonte. B. Écaille de placoderme. C. Écailles de chondrichtyens. D. Écailles d'acanthodiens. E. Écaille de paléoniscoïde. F. Écaille de *Polypterus*. Tirée de Janvier (1996b); Sire et al. (2009).

un arrangement des tubules caractéristique). Au centre, une cavité pulpaire permet la vascularisation et l'innervation du denticule (Sire et al., 2009). Chez les taxons du groupe souche des chondrichtyens, les denticules sont fixés à la surface d'un os dermique, comme chez les ostéichtyens. Les denticules et les écailles polyodontodes (*i.e.*, élément avec ou sans croissance) sont caractérisés par la présence de canaux vasculaires (avec un branchement latéral au niveau de la cavité pulpaire) (Zangerl, 1981; Karatajute-Talimaa, 1992). En ce basant sur les travaux de Karatajute-Talimaa (1992), Hanke and Wilson (2010) ont défini huit types d'écailles sur la base de caractères de croissance ou non. Chaque type est aussi défini par des traits histologiques qui sont utilisés dans les analyses phylogénétiques. Les denticules ne grandissent pas une fois qu'ils sont définitivement formés (comme les dents), mais leur nombre sur le corps du spécimen augmente au cours de la croissance, alors que chez certains chondrichtyens paléozoïques les écailles s'accroissent de manière aréolaire, appositionelle ou aréolaire et appositionelle (Karatajute-Talimaa, 1992).

Deux régions composent les petites écailles, souvent qualifiées de rhombiques, des acanthodiens (Figure 10) : une région basale composée d'os cellulaire ou acellulaire et une région superficielle composée de plusieurs couches de mésodentine ou d'orthodentine (Gross, 1971; Valiukevičius and Burrow, 2005; Sire et al., 2009). Les études histologiques ont révélé des disparités de la structure des écailles d'acanthodiens (Gross, 1957; Valiukevičius, 1995; Valiukevičius and Burrow, 2005; Burrow et al., 2016). De façon générale, quatre types d'écail-les ont été décrits (Valiukevičius, 1995) : (1) le type *Nostolepis*, caractéristique des Climatiiformes, présente une base d'os cellulaire et de couronnes composées de mésodentine simple ou orientée ; (2) le type *Diplacanthus*, observé chez les Diplacanthiformes, est caractérisé par la présence d'une base d'os acellulaire contenant des canaux vasculaires et une couronne composée de mésodentine ; (3) le type *Acanthodes*, retrouvé chez les Acanthodiformes, est caractérisé par la présence

d'une base d'os acellulaire avec des canaux vasculaires étroits, et une couronne composée de dentine ; et (4) le type *Poracanthodes*, typique des Ischnacanthiformes, composé d'une base cellulaire ou acellulaire et d'une couronne de dentine, de mésodentine simple ou des deux types avec les pores des canaux s'ouvrant sur la surface ou le côté de l'écaille. Parmi les écailles du type *Nostolepis*, Valiukevičius and Burrow (2005) ont décrit cinq groupes structuraux, fondés sur la présence ou l'absence de « Stranggewebes » (*i.e.*, tubules de mésodentine larges et orientés avec de rares interconnections) et de réseaux de mésodentine odontocytique (avec des lacunes de cellules) et syncitial (sans lacunes cellulaires). La séquence ontogénétique des écailles d'acanthodiens diffère de celle des écailles de chondrichtyens par la composition de l'écaille primordiale (*i.e.*, la première à se former) ; celle-ci est constituée, chez les acanthodiens, d'une base (cellulaire ou acellulaire) et d'une couronne de type dentinaire [*i.e.*, un odontodium, une écaille composée d'un odontode ou un groupe d'odontodes situés sur une plaque osseuse (Karatajute-Talimaa, 1998)]. La croissance a lieu par l'enveloppement de l'écaille primordiale par l'odontode de deuxième génération. Les couronnes croissent alors soit de manière concentrique, aréolaire, appositionelle ou aréolaire et appositionnelle (Valiukevičius and Burrow, 2005) et la hauteur et le nombre d'écailles n'augmentent pas durant l'ontogénie de l'individu (Zidek, 1985; Karatajute-Talimaa, 1998).

Chez les actinoptérygiens (Figure 10), deux types d'écailles sont décrits : les écailles ganoïdes et élasmoïdes. Les écailles ganoïdes, et particulièrement les écailles palaeoniscoïdes (*e.g.*, retrouvées chez *Dialipina*, *Andreolepis*, *Cheirolepis*), sont formées d'une région basale d'os cellulaire vascularisé, d'une région centrale de dentine et d'une région superficielle composée de plusieurs couches de ganoïne (Sire and Huysseune, 2003; Sire et al., 2009) (Figure 10). Les écailles d'actinoptérygiens paléozoïques croissent le plus souvent de façon concentrique ("box-in-box" ou en "pelure d'oi-

gnons") (Sire et al., 2009). Les écailles élasmoïdes sont fines et imbriquées, elles sont composées de trois couches : une couche superficielle fine et ornementée composée d'un tissu hyperminéralisé, d'une couche d'élasmodine (Meunier et al., 1978; Meunier, 1981) et d'un tissu limitant déposé sur la surface externe mais dont la distribution est restreinte à la partie postérieure de l'écaille. Les écailles élasmoïdes sont présentes chez les téléostéens et chez des représentants non-tétrapodes des sarcoptérygiens.

Récemment, Burrow and Turner (2012) ont fourni plus d'informations à propos de la condition plésiomorphe des écailles chez les gnathostomes, en décrivant le supposé requin *Gladbachus adentatus* du Dévonien moyen. Les écailles de *Gladbachus* possèdent une mosaïque de caractères présentant des similarités à la fois avec les écailles de placodermes du Dévonien inférieur et celles de la tête de certains acanthodiens. De plus, les plateaux denticulés de la mâchoire ressemblent aux plaques denticulées oropharyngiennes du thélodonte *Loganellia*, et la mésodentine est comparable à celle qui a été trouvée chez les ostéostracés et les acanthodiens. De même que les caractères morphologiques sont souvent répartis de façon mosaïque chez les groupes primitifs, les caractères histologiques de ces mêmes groupes le sont également.

Problématiques et objectifs de recherche

La problématique de cette thèse s'inscrit donc dans le *triumvirate* phylogénie, évolution et développement, autrement dit dans l'implication phylogénétique que peut avoir l'étude comparée du développement d'individus de différentes espèces, dans ce cas d'une espèce d'anaspide et d'une espèce d'acanthodien. Ces données sont la matière première utilisée pour la création de matrices de phylogénie afin de connaître la position des espèces entre elles. Des espèces proches vont partager plus de caractères communs, ce qui implique que les caractères se trouvant à certains nœuds phylogénétiques

nous en apprennent davantage au niveau de la macroévolution des différentes structures squelettiques.

Le site fossilifère à préservation et concentration exceptionnelles (*Konservat und Konzentrat Lagerstätte*) de Miguasha est daté du Dévonien supérieur (380 millions d'années) (Prichonnet et al., 1996) (Figure 11). Ce site se trouve dans l'est du Canada, plus précisément au niveau de la péninsule gaspésienne (Québec), dans les limites de la municipalité de la ville de Nouvelle. A partir des spécimens fossiles découverts sur ce site, des séquences ontogénétiques ont été décrites chez au moins quatre espèces (*i.e.*, le placoderme *Bothriolepis canadensis*, l'actinistien *Miguashaia bureaui*, le dipnoiforme *Scaumenacia curta*, et l'ostéolépiforme *Eusthenopteron foordi*) et probablement chez neuf autres espèces incluant l'anaspide *Euphanerops longaevus* et l'acanthodien *Triazeugacanthus affinis* (Cloutier et al., 2009). La préservation et la concentration exceptionnelles de ce site ainsi que le riche matériel ontogénétique déjà décrit en font un site idéal pour répondre à la problématique de cette thèse qui consiste à identifier et à décrire des séquences développementales de vertébrés paléozoïques dans le but de trouver de nouveaux caractères pouvant être intégrés dans une analyse phylogénétique de ces groupes.

Les organismes fossiles modèles, pour lesquels des éléments individuels isolés et des spécimens complets sont connus, sont nécessaires pour décrire les relations entre la croissance individuelle des éléments isolés et l'ontogénie de l'espèce (Cloutier, 2010). La conservation exceptionnelle du *Lagerstätte* de Miguasha permet la préservation de nombreux spé-cimens de très petite taille, appelés communément "scauménelles" (Figure 12). Le terme "scauménelle" provient du nom de genre (*Scaumenella*) dont ces spécimens furent affublés lors de leur première description (Graham-Smith, 1935). L'interprétation des scauménelles demeure cependant problématique. L'hypothèse la

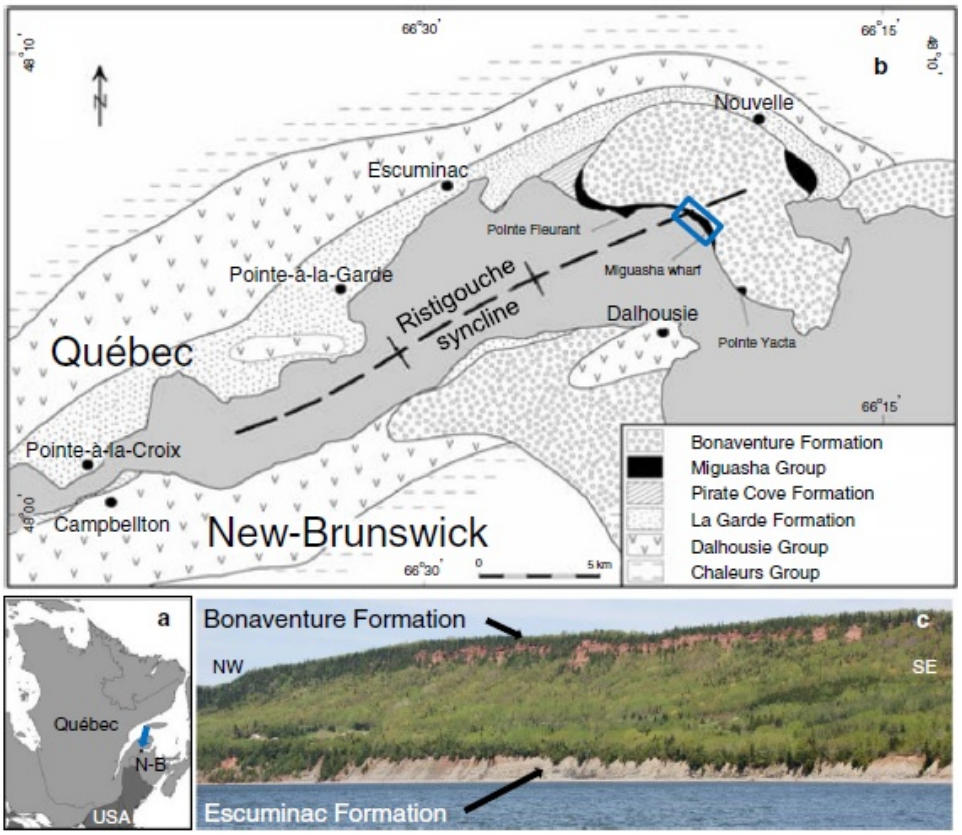

Figure 11: **Cartes géologique et géographique de la Formation d'Escuminac, Québec, Canada.** a. Localisation de Miguasha, Québec. b. Carte géologique de la zone de Miguasha ; le Groupe de Miguasha inclue les Formations de Fleurant et d'Escuminac. c. Vue générale de la partie Est du synclinal de la Formation d'Escuminac représentant la partie principale de la section de Miguasha. Tirée de Cloutier et al. (2011b).

Figure 12: **Lectotype de *Scaumenella mesacanthi*, Graham-Smith (1935) NMS 2002.59.17 spécimen 6 reconnu et mentionné pour la première fois depuis la description de Graham-Smith (1935) dans la littérature**. Échelle = 1 mm.

plus admise considère les scauménelles comme des stades de décomposition de l'acanthodien *Triazeugacanthus affinis* mais il a aussi été suggéré que ces spécimens pouvaient représenter des stades larvaires (Béland and Arsenault, 1985; Cloutier et al., 2009; Cloutier, 2010). Cette espèce représente alors le principal matériel d'étude de cette thèse, étant donnée sa position et son statut phylogénétique non résolus au sein des acanthodiens, l'abondance de spécimens (4278 sur les 18 059 que compte la formation fossilifère) (Cloutier et al., 2011b) ainsi que la présence d'un squelette dermique partiellement décrit (Gagnier, 1996) mais potentiellement informatif par rapport à la croissance. Cependant, en plus de cette première espèce, l'identification d'une deuxième espèce parmi les scauménelles, l'anaspide *Euphanerops longeavus* permet de décrire une série de croissance pour un anaspide du Paléozoïque sur la base de plus de 2000 spécimens immatures. Suite à cette découverte, le matériel de cette thèse, permet de documenter une transition évolutive majeure, celle des agnathes aux gnathostomes.

La problématique de cette thèse liant phylogénie, évolution et développement, à la lumière de ce qui est actuellement connu des vertébrés primitifs et du matériel d'étude, soulève les questions suivantes. Quels sont les patrons et processus décrivant la croissance chez *Triazeugacanthus* ? Ces patrons et processus sont-ils communs à ce qui est

connu chez d'autres acanthodiens, gnathostomes ou vertébrés ? La croissance observée à partir du squelette entier est-elle retrouvée dans des éléments isolés (écailles) chez *Triazeugacanthus* ? Quelles sont les informations développementales apportées par la re-description de l'anaspide *Euphanerops* ? L'étude comparée de la croissance chez différentes espèces renseigne-t-elle sur l'évolution au cours du temps d'éléments squelettiques spécifiques ? Les données développementales permettent-elles de définir des caractères informatifs au niveau phylo-génétique ?

Les quatre premiers chapitres de cette thèse traitent de la croissance chez l'acanthodien *Triazeugacanthus affinis*. Le premier chapitre consiste à la confrontation de deux hypothèses : l'hypothèse de décomposition et l'hypothèse de croissance afin d'expliquer les variations de taille observées dans la série de taille de *Triazeugacanthus*. En somme, les scauménelles seront ici ré-interprétées. Dans le deuxième chapitre, la description de la croissance de *Triazeugacanthus* en termes de progression de la minéralisation est effectuée grâce à l'utilisation de méthodes d'imagerie rayons X permettant de fournir des données chimiques et minéralogiques sur des structures anatomiques. De plus, cette analyse apporte une information sur les processus de fossilisation à Miguasha. Dans un troisième chapitre, afin de pouvoir la comparer à celle d'autres espèces, nous décrirons la croissance de structures individuelles (écailles). En effet, les séries de croissance étant très rares dans le registre fossile, il est important de pouvoir inférer celle-ci à partir de structures individuelles. Cette inférence est justifiée ici par la présence d'une série de croissance décrite ainsi que l'abondance de micro restes, permettant leur analyse histologique. A la lumière de ces données, une nouvelle analyse phylogénétique des gnathostomes sera proposée. Le dernier chapitre traitera de la croissance de *Triazeugacanthus*, avec principalement la description de la mise en place des éléments squelettiques au cours de la croissance fondée sur une série de taille de 178 individus. La précision de cette information en fait la série de croissance la plus complète du re-

gistre fossile étudiée à ce jour. Dans tous ces articles l'accent est mis sur les caractères développementaux et leur implication dans la résolution de la phylogénie.

Dans un cinquième et dernier chapitre, une nouvelle analyse de l'anatomie des squelettes axial et appendiculaire de l'anaspide *Euphanerops longaevus* du Dévonien supérieur de Miguasha est proposée suite à l'attribution de la plupart des scauménelles à des stades immatures de cette espèce. Cette description propose des résultats inédits, tant du point vue morphologique que pour l'implication de ces caractères morphologiques dans l'étude évolutive et phylogénétique des premiers vertébrés. En effet, pour la première fois dans le registre fossile, la présence d'organes d'intromission, d'une ceinture pelvienne, et de nageoires ventrales paires sans ceinture (absence de nageoires pectorales) est décrite chez un agnathe. Cette nouvelle information développementale et évolutive sera intégrée dans la compréhension de l'histoire évolutive des vertébrés.

ARTICLE 1

LA RENAISSANCE D'UN POISSON SOI-DISANT DÉCOMPOSÉ : L'ONTOGÉNIE DE L'ACANTHODIEN DÉVONIEN *TRIAZEUGACANTHUS*

1.1 Résumé en français du premier article

Depuis sa description originale comme un chordé, l'espèce du Dévonien supérieur *Scaumenella mesacanthi* a été interprétée alternativement comme un prochordé, une larve d'ostracoderme et un acanthodien immature. Depuis les 30 dernières années, ces petits spécimens furent généralement considérés comme des acanthodiens en décomposition, la plupart appartenant à l'espèce *Triazeugacanthus affinis*. Parmi le matériel abondant de *"Scaume-nella"*, nous avons identifié une série de taille de 188 spécimens de *Triazeugacanthus* basée sur des caractéristiques des otolithes. Malgré l'altération taphonomique, nous décrivons une croissance proportionnelle et une apparition progressive des éléments squelettiques avec l'augmentation de taille. Trois stades ontogénétiques sont identifiés basés sur l'étendue de l'écaillure, l'achèvement de l'ossification et la croissance allométrique. Nous démontrons que ce qui a précédemment été interprété comme différents degrés de décomposition correspond en fait à des changements ontogénétiques.

Ce premier article, intitulé « *The revival of a so-called rotten fish: The ontogeny of the Devonian acanthodian* Triazeugacanthus », fut corédigé par moi-même ainsi que par Richard Cloutier et Jean-Yves Sire. Il fut accepté pour publication dans sa version finale en 2015 par les éditeurs de la revue *Biology Letters*. En tant que premier

auteur, ma contribution à ce travail fut l'essentiel de la recherche sur l'état de l'art, la réalisation des observations et l'analyse de données ainsi que la production des figures et du matériel supplémentaire avec les contributions de Richard Cloutier et Jean-Yves Sire. J'ai écrit la première version et tous les auteurs ont contribué à la version finale. Une version abrégée de cet article a été présentée à la rencontre annuelle de la Palaeontological Association à Zurich (Suisse) à l'automne 2013.

Nous remercions O. Matton, F. Charest et J. Kerr (MHNM) et S. Walsh (NMS) pour l'accès aux collections, ainsi que Z. Johanson et deux arbitres anonymes pour l'apport de commentaires constructifs. Cette recherche fut supportée par NSERC 238612 (Richard Clou-tier) et par le Centre pour la Science de la Biodiversité du Québec (Richard Cloutier et Marion Chevrinais).

1.2 The revival of a so-called rotten fish: The ontogeny of the Devonian acanthodian *Triazeugacanthus*

Summary

Since its original description as a chordate, the Late Devonian *Scaumenella mesacanthi* has been interpreted alternately as a prochordate, a larval ostracoderm and an immature acanthodian. For the past 30 years, these minute specimens were generally considered as decayed acanthodians, most of them belonging to *Triazeugacanthus affinis*. Among the abundant material of "*Scaumenella*," we identified a size series of 188 specimens of *Triazeugacanthus* based on otolith characteristics. Despite taphonomic alteration, we describe proportional growth and progressive appearance of skeletal elements through size increase. Three ontogenetic stages are identified based on squamation extent, ossification completion and allometric growth. We demonstrate that what has been interpreted previously as various degrees of decomposition corresponds to ontogenetic changes.

Keywords: Acanthodii; Devonian; fossilised ontogeny; palaeontology; taphonomy

1.3 Introduction

In 1935, Graham-Smith (1935) described *Scaumenella mesacanthi* based on 560 specimens from the Upper Devonian (380 Ma) Escuminac Formation (Miguasha, Canada) as a "chordate, and probably a vertebrate" because of the presence of a head, an abdomen with branchial arches, a notochordal or vertebral region, and a hypocercal tail. Subsequently, *Scaumenella* was frequently considered when dealing with vertebrate

origin (Lehman, 1957; Tarlo, 1960; Piveteau et al., 1978). Lehman (1957) and Piveteau et al. (1978) reinterpreted *Scaumenella* as a prochordate closer to cephalochordates than ascidians, whereas Tarlo (1960) proposed that *Scaumenella* was most similar to an ammocoete (his "larval ostracoderm").

In the early 1980s, the Quebec ichthyologist Vianney Legendre made detailed observations on more than 900 specimens of *Scaumenella* from the Miguasha museum (MHNM). Among other things, Legendre identified nasal bones on some of the *Scaumenella* diagnostic to those of the acanthodian *Triazeugacanthus affinis* (Figure 13 *d*) which he used to associate these two taxa. Therefore, Béland and Arsenault (1985) turned upside down Graham-Smith's (1935) reconstruction of *Scaumenella* and proposed that these specimens correspond to partially decomposed *Triazeugacanthus* (Gagnier, 1996, fig. 11). They referred to "scaumenellization," the taphonomical alteration leading to an ultimate state of degradation being the "scaumenelle." This interpretation was based on the so-called progressive disappearance of fin spines, scales, cranial and girdle bony elements (Béland and Arsenault, 1985) and used subsequently as a classical example of decaying effect on the anatomical and taxonomic interpretation of a vertebrate (Gagnier, 1996). Since then, various fossil fish specimens were said to be scaumenellized (Béland and Arsenault, 1985; Newman, 2002; Janvier and Arsenault, 2007).

Besides scaumenellization, Béland and Arsenault (1985) mentioned that some of the small *Scaumenella* could correspond to immature *Triazeugacanthus*. Recently, Cloutier et al. (2009) and Cloutier (2010) agreed with this interpretation based on shape morphometry and squamation pattern. However, this ontogenetic interpretation has to be quantitatively tested on a large number of specimens.

Our main objective was to describe a size series of *Scaumenella-Triazeugacanthus* in

order to recognise if the primary source of variation corresponds to ontogenetic changes or taphonomic alteration. In favor of the ontogenetic changes, we expect to observe, despite taphonomic alterations, (1) linear relationships among the size of individual skeletal structures and body size and (2) progressive appearance of skeletal elements correlated to body size. Concerning the taphonomic alteration, we expect (1) non proportional relationships among the size of individual skeletal structures and body size and (2) progressive disappearance of skeletal structures not correlated to body size. The large sample size provided the opportunity to quantify the variation along the size series.

1.4 Material and methods

Triazeugacanthus specimens come from the middle Frasnian Escuminac Formation (Miguasha, Canada) that is an UNESCO World Heritage site (Cloutier, 2013). *Triazeugacanthus* and the so-called 'scaumenellized' *Triazeugacanthus* are housed in the MHNM (1620 specimens) and NMS (National Museums of Scotland) (2015 specimens) collections. A subsample of 188 specimens was selected based on (1) the presence of diagnostic *Triazeugacanthus* features (Annexe II), (2) the integrity of the specimens (*e.g.*, specimens without preparation artefacts), and (3) the presence of representatives along an optimised size range. Specimens have been observed under water immersion (Leica MZ9.5), drawn using a *camera lucida*, and photographed (Nikon D300).

Morphotypes were recognised based on squamation: morphotype 1 (morph-1) shows no body scales, morphotype 2 (morph-2) displays a partial body squamation, and morphotype 3 (morph-3) shows complete body squamation (Figure 13). Continuous [length

of skeletal elements and distances among them (Annexe III)] and discrete data [presence/absence of skeletal structures (Annexe IV)] were collected. Linear regressions between $\log_{10}$-transformed measurements and total length (TL) have been calculated by morphotypes and for combined morphotypes. The cumulative number of 23 skeletal elements (Annexes IV-V) was calculated in relation to TL. The squamation extent (maximum length of scaled area/TL*100; the maximum length of scaled area is used as a proxy for the scaled area) is given in relation to TL. A von Bertalanffy growth model is used on squamation data.

Three principal component analyses (PCA) on variance-covariance matrices of five log10-transformed measurements were performed for morph-2, morph-3 and the combined dataset (Annexe VI). Morph-1 was excluded from the PCA because most landmarks are absent. Multivariate normality is accepted (Mardia's test: $p < 0.05$). Multivariate coefficients of allometry were calculated from PC1 loadings (Kowalewski et al., 1997) for morph-2 and morph-3. PCA, multivariate normality and allometric coefficients were calculated with PAST 2.17, whereas all remaining statistics were performed with R 3.0.2.

1.5 Results

The size series includes 188 specimens of *Triazeugacanthus* ranging from 4.51 to 52.72 mm in TL. There is a significant linear relationship between the length and height of the lens (n = 142, $R^2 = 0.79$; F = 110.4, $p < 2.2e^{-16}$) (Figure 14 *a*) suggesting a proportional size change. The length of the pectoral spine (Figure 14 *b*) shows a significant linear relationship with TL (n = 117, $R^2 = 0.77$; F = 396.1, $p < 2.2e^{-16}$).

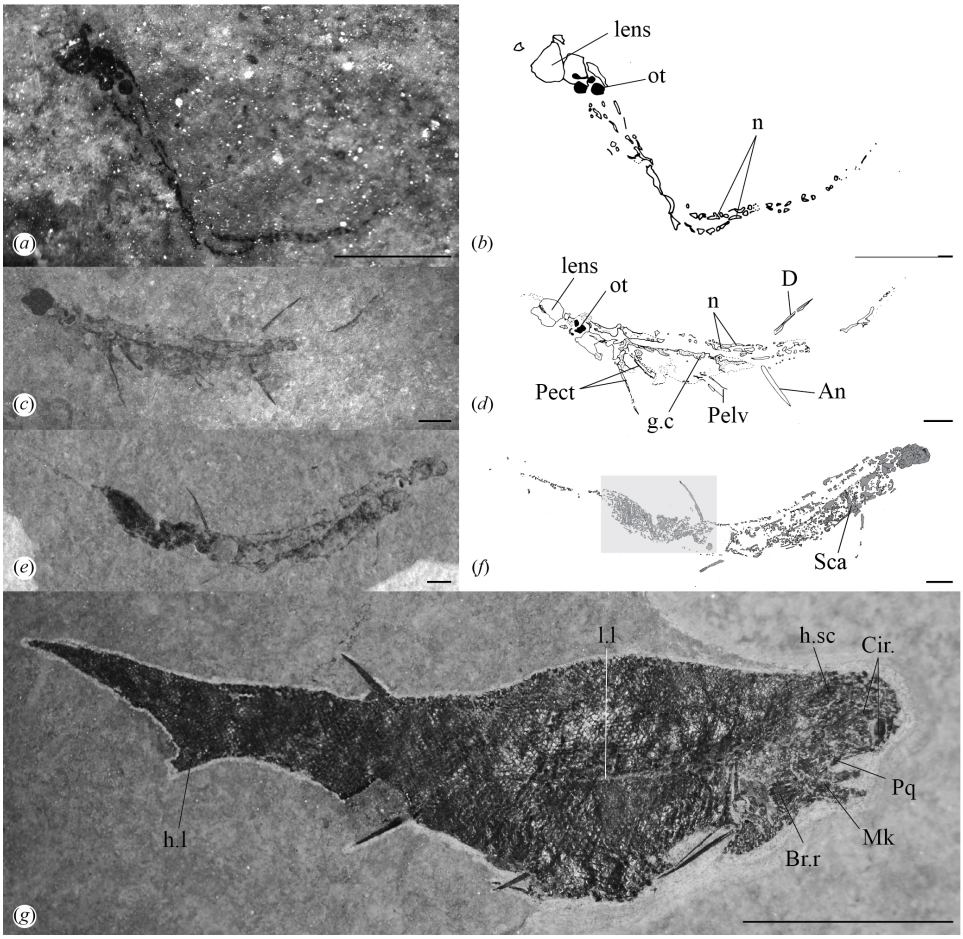

Figure 13: ***Triazeugacanthus*** **growth series**. (*a-b*) Smallest larval specimen showing no squamation (MHNM 03-403). Juvenile specimens showing (*c-d*) fin spines (MHNM 03-316) and (*e-f*) the initiation of squamation (grey area) (MHNM 03-2015). (*g*) Adult specimen (MHNM 03-1497) with full body squamation. Scale bars = (*a-f*) 1 mm, (*g*) 10 mm.

In the smallest specimen (4.51-mm TL; Figure 13 *a*-*b*), eye lenses, otoliths and traces of the notochord are present. Pectoral, pelvic, anal and dorsal spines are present in slightly larger specimens (13.58-mm TL; Figure 13 *c*-*d*). Squamation is recorded in larger specimens (19.2-mm TL; Figure 13 *e*-*f*) at the level of the dorsal fin and extends towards the skull and the caudal fin in larger specimens. The squamation is total around 25-mm TL (Figures 13 *d*-14 *c*); while palatoquadrates, Meckel's cartilages, circumorbital bones, branchiostegal rays, head scales and the hypochordal lobe of caudal fin are recorded. The cumulative number of skeletal elements and the squamation extent are correlated to TL (rs = 0.99, $p < 2.2e^{-16}$ and rs = 0.67, $p < 2.2e^{-16}$, respectively) (Figure 14 *c*). All skeletal structures are present around 40-mm TL (Figure 14 *c*).

In our sample, 81.5% of the specimens show signs of taphonomic alterations. The most recurrent signs are: a dorsal curvature of the body [owing to post-mortem tetany (Parent and Cloutier, 1996); 73%], a rupture of the abdominal cavity [owing to bacterial activity or fermentation (Cloutier, 2010); 33%], and a scattering of scales (owing to decaying; 33%). Most detached scales are localised ventrally in mid-trunk region and are associated to the rupture of the abdominal cavity; these two conditions are not observable in morph-1 because scales are absent. Most detached scales are not loss on the tip of the caudal fin thus not affecting specimen TL. Specimens showing the greatest deviation from the means in terms of squamation and cumulative number of skeletal elements display evidence of abdominal rupture (Annexe V).

We observe that the size of each morphotype increases although there are some overlaps among morphotypes (Figure 13 *d*). Comparison among morphotypes shows significant differences in linear regression slopes for both eye lenses (morph-1: 0.81; morph-2: 0.77; morph-3: 0.91; Figure 14 *a*) and pectoral spines (morph-1: 0.95; morph-2: 1.1; morph-3: 0.74; Figure 14 *b*). These changes are suggestive of allometry. Multivari-

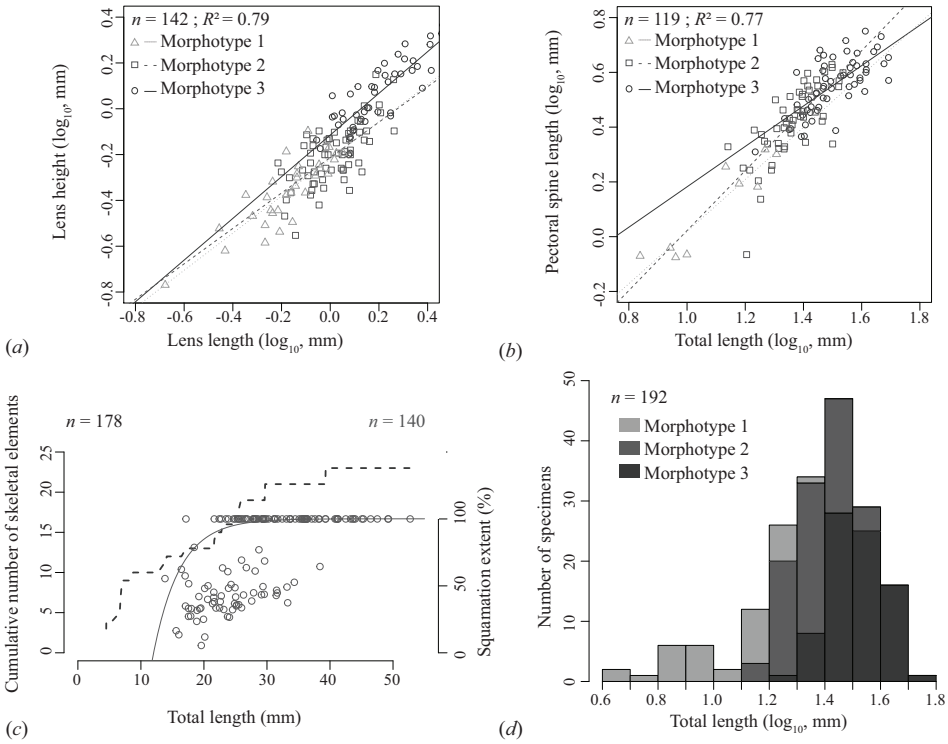

Figure 14: **Metrics of *Triazeugacanthus* growth**. (*a*) Linear regressions showing the relationship between eye lens length and height. (*b*) Linear regressions showing the relationship between pectoral spine length and TL. (*c*) Cumulative number of skeletal elements (Annexe IV) (left, dotted line) and squamation extent (right, grey points and von Bertalanffy curve) in relation to TL. (*d*) Distribution of three ontogenetic stages (morphotypes) of *Triazeugacanthus*.

ate allometric coefficients on PC1 of the separated PCAs (morph-2 PCA and morph-3 PCA) show a trend (allometric coefficients are non-significant most likely because of small sample size) towards allometry in the distance between the anal and dorsal fins (morph-2: 4.47; morph-3: 2.16) with respect to the remaining four variables. Morph-2 specimens have a greater propensity to allometric changes. Morph-2 and morph-3 specimens cluster into two groups in the combined PCA (Annexe VI) corroborating their morphotypic assignation.

1.6 Discussion

We have shown clearly that (1) the size of individual anatomical structures, (2) the number of skeletal elements and (3) the squamation extent increase with TL. Based on the squamation extent and pattern, ossification completion and allometry, the three morphotypes are best interpreted as three ontogenetic stages making this growth series one of the best documented early gnathostome fossilised ontogenies (Cloutier et al., 2009; Cloutier, 2010). Morph-1 showing no body squamation corresponds to a larval stage (Urho, 2002; Cloutier et al., 2009; Cloutier, 2010); morph-2 starts with the initiation of squamation and shows allometry which is characteristic of a juvenile stage (Balon, 1981; Cloutier et al., 2009; Cloutier, 2010); and the completion of squamation and ossification characterising morph-3 corresponds to an adult stage (Cloutier, 2010). The evidence for ontogeny in *Triazeugacanthus* that we have presented does not rule out taphonomic alteration but shows that the main trend of variation is explained by ontogenetic changes.

In the smallest *Triazeugacanthus*, we recorded the presence of eye lenses ("optic plates" (Béland and Arsenault, 1985), "orbits" (Gagnier, 1996)), otoliths and notochordal el-

ements (“rotten scaly skin” (Béland and Arsenault, 1985), “elements of the vertebral axis” (Gagnier, 1996)). If only taphonomic alterations occurred in *Triazeugacanthus*, the smallest specimens would represent the most rotten specimens; accordingly some of these observed structures are among the last elements to decay or to be lost during decomposition of a vertebrate in an aquatic environment (Sansom et al., 2011, 2013a). These elements are also among the first anatomical structures to form in early ontogeny that have a great potential to be fossilised. In numerous living osteichthyans, post-hatching larvae show distinctive features including a head with limited chondrified elements, large eyes, a notochordal axial support, a finfold without differentiated fins, scaleless skin, and simplified muscular and digestive systems. The absence of finfold and yolk sac are most likely owing to taphonomic loss of soft tissues. There is no indication that the length of an individual would reduce slowly during decomposition other than by the losses of the anteriormost and posteriormost elements (Sansom et al., 2013a). What was considered as the progressive disappearance of fin spines, scales, cranial and girdle bony elements corresponds in fact to the sequential appearance of these elements, primarily as a sequence of skeletal formation. The shape of the cumulative curve of elements is similar to “maturity curves” or “ontogenetic trajectories” in living (Grünbaum et al., 2012) and extinct fishes (Cloutier et al., 2011a). The postero-anterior direction of squamation development in *Triazeugacanthus* is also congruent with that observed for other acanthodians and some actinopterygians (Zidek, 1985; Cloutier et al., 2011a); it would be unlikely for scales or patches of scales to be lost in a non-random pattern (detached scales were found in the abdominal region as a result of decay).

Thus, what has been interpreted specifically as evidence for the decomposition of *Triazeugacanthus* (Béland and Arsenault, 1985; Gagnier, 1996; Janvier and Arsenault, 2007; Donoghue and Purnell, 2009) is reinterpreted as evidence of ontogenetic changes.

Interpretation of qualitative decay in fossils would benefit from being combined with quantitative analysis. Some fossil vertebrate taxa, such as the Middle Devonian *Achanarella* (Newman, 2002), should be reanalysed with such an approach because of their anatomical and taphonomic similarities with "*Scaumenella*."

ARTICLE 2

NOUVELLES PERSPECTIVES SUR L'ONTOGÉNIE ET LA TAPHONOMIE DE L'ACANTHODIEN DU DÉVONIEN *TRIAZEUGACANTHUS AFFINIS* DU *LAGERSTÄTTE* FOSSILE DE MIGUASHA, EST DU CANADA

2.1 Résumé

La minéralisation progressive du squelette a lieu durant l'ontogénie chez la plupart des animaux. Chez les poissons, les larves sont faiblement minéralisées, alors que les juvéniles et les adultes montrent une biominéralisation progressive de leur squelette. Les restes fossiles sont constitués principalement de spécimens adultes parce que la fossilisation de larves et juvéniles faiblement minéralisés nécessite des conditions exceptionnelles. Le *Lagerstätte* fossile de Miguasha est reconnu pour sa faune de vertébrés du Dévonien supérieur, révélant la préservation exceptionnelle d'ontogénies fossiles chez 14 des 20 espèces de poissons de cette localité. La minéralisation des structures anatomiques de l'acanthodien *Triazeugacanthus affinis* de Miguasha est comparée entre spécimens larvaires, juvéniles et adultes par l'utilisation de spéctrométrie en énergie dispersive des rayons X. La composition chimique des structures anatomiques de *Triazeugacanthus* révèle des différences entre le cartilage et l'os. Bien que l'histologie et l'anatomie sont bien préservées, la spéctrométrie infrarouge en transformée de Fourier montre que la composition chimique originale de l'os est altérée par la diagénèse ; la phase minérale de l'os (*i.e.*, hydroxyapatite) est chimiquement modifiée pour former une fluorapatite carbonée, plus stable. La fluorination, survenant dans les structures squelettiques minéralisées des *Triazeugacanthus* adultes, indique des échanges entre

les eaux du sol et le squelette au moment de l'enfouissement, alors que la préservation des tissus mous des larves est probablement due à un enfouissement rapide en conditions anoxiques. L'état de préservation exceptionnel d'une ontogénie fossile permet de caractériser chimiquement la minéralisation progressive du squelette chez un vertébré primitif du Dévonien.

Ce deuxième article, intitulé « *New insights in the ontogeny and taphonomy of the Devonian acanthodian Triazeugacanthus affinis from the Miguasha Fossil-Lagerstätte, Eastern Canada* », fut corédigé par moi-même ainsi que par Etienne Balan et Richard Cloutier. Il fut accepté pour publication dans sa version finale en 2015 par les éditeurs de la revue *Minerals*. Tous les auteurs ont conçu les expériences. En tant que premier auteur, ma contribution à ce travail fut l'essentiel de la recherche sur l'état de l'art, la réalisation des observations et l'analyse de données ainsi que la production des figures et du matériel supplémentaire avec les contributions de Richard Cloutier et Etienne Balan. J'ai écrit la première version et tous les auteurs ont contribué à la version finale. Une version abrégée de cet article a été présentée à la rencontre annuelle de la *Canadian Society of Vertebrate Paleontogy* à Montreal (Canada) à l'été 2014 ainsi que lors du cours intensif de Biominéralisation à Paris (France) à l'automne 2014.

Nous remercions J. Kerr, O. Matton et F. Charest (MHNM) pour l'accès aux collections. Nous avons apprécié l'aide de Claude Belzile (UQAR) concernant les analyses de microscopie et de spectométrie. Nous sommes reconnaissant envers le personnel de l'Institut Maurice Lamontagne (DFO-MPO) pour nous avoir fourni les spécimens juvéniles d'organismes actuels. Cyrena Riley (UQAR) a aidé à la préparation de l'aiguillat noir. François Grégoire (UQAR) a fourni les maquereaux juvéniles. Nous remercions Maxime Guillaumet (IMPMC), Benoit Baptiste (IMPMC) et Guillaume Morin (IMPMC) pour leur aide dans les mesures de FTIR et XRD. Ce projet fut supporté fi-

nancièrement par NSERC Discovery grant (RC), EnviroNorth mobility grant (MC), et l'équipe "Evolution et développement du squelette" (CNRS, IPBS Paris). Nous remercions aussi le Labex Matisse pour avoir organisé le cours intensif de Biominéralisation et proposé ce numéro spécial.

2.2 New insights in the ontogeny and taphonomy of the Devonian acanthodian *Triazeugacanthus affinis* from the Miguasha *Fossil-Lagerstätte*, Eastern Canada

Summary

Progressive biomineralization of a skeleton occurs during ontogeny in most animals. In fishes, larvae are poorly mineralized, whereas juveniles and adults display a progressively more biomineralized skeleton. Fossil remains primarily consist of adult specimens because the fossilization of poorly-mineralized larvae and juveniles necessitates exceptional conditions. The Miguasha *Fossil-Lagerstätte* is renowned for its Late Devonian vertebrate fauna revealing the exceptional preservation of fossilized ontogenies for 14 of the 20 fish species from this locality. The mineralization of anatomical structures of the acanthodian *Triazeugacanthus affinis* from Miguasha are compared among larval, juvenile and adult specimens using Energy Dispersive X-ray Spectrometry. Chemical composition of anatomical structures of *Triazeugacanthus* reveals differences between cartilage and bone. Although the histology and anatomy is well-preserved, Fourier transform infrared spectrometry shows that the original chemical composition of bone is altered by diagenesis; the mineral phase of the bone (*i.e.*, hydroxyapatite) is modified chemically to form more stable carbonate-fluorapatite. Fluorination occurring in mineralized skeletal structures of adult *Triazeugacanthus* is indicative of exchanges between groundwater and skeleton at burial whereas the preservation of larval soft tissues is likely owing to a rapid burial under anoxic conditions. The exceptional state of preservation of a fossilized ontogeny allowed us to characterize chemically the progressive mineralization of the skeleton in a Devonian early vertebrate.

Keywords: Acanthodii; biomineralization; fossilized ontogeny; paleontology; Devo-

nian

2.3 Introduction

Fossilized fish ontogenies are rare, especially in the Paleozoic (Cloutier, 2010) because the mineralization of an animal's skeleton progresses during ontogeny and the preservation of poorly mineralized or ossified structures of immature (larval and juvenile) specimens requires exceptional fossilization conditions. Biomineralization of the skeleton during ontogeny is a condition shared by most vertebrates (Donoghue and Sansom, 2002). Extant jawless fish (hagfishes and lampreys) lack biomineralized tissues which differs from their extinct relatives (Donoghue and Sansom, 2002; Cloutier, 2010). In extant cartilaginous fishes (Chondrichthyes; chimaera, sharks, skates and rays), the skeleton mineralizes as ontogeny progresses, at least superficially by means of tesserate calcified cartilage (Kemp and Westrin, 1979; Dean and Summers, 2006). In extant bony fishes (piscine Osteichthyes; ray-finned fishes, coelacanths and dipnoans), young individuals show an unmineralized or poorly mineralized skeleton whereas older ones are highly mineralized (Gavaia et al., 2000; Faustino and Power, 2001; Grünbaum et al., 2012). In extinct jawed vertebrates, such as acanthodians and placoderms, this progressive biomineralization is assumed, rather than observed, because of the rarity of ontogenetic material but also because fossilization processes tend to favor the preservation of hard tissues, thus frequently leaving an information gap during early ontogenetic stages. Since ontogenies have the potential to elucidate evolutionary developmental patterns and processes from the deep past (Cloutier, 2010; Johanson and Trinajstic, 2014), it is crucial to detect if fossilization biased our understanding of the early phase of biomineralization and how it could modify the preservation of the original tissues in fossils.

Vertebrate fossils predominantly consist of remains of mineralized skeletal structures (Trueman et al., 2008), while soft tissues are only preserved exceptionally (Arsenault et al., 2004; Trinajstic et al., 2007; Morris and Caron, 2012; Cloutier, 2013). The quality and fidelity of tissue preservation depend, among other things, on the nature of the tissues in the organism, the amount of decay that precedes mineralization, and the availability of mineral-forming ions. It is however often difficult to determine whether the minerals observed in the fossils correspond to the original biomineralization of the tissues or result from diagenetic transformations of the fossils (Kolodny et al., 1996). The comparison of chemical and mineralogical composition of anatomical structures during the ontogeny of an organism allows one to discriminate between these two mineralization processes. Indeed, as the biomineralization of skeletal structures progresses during ontogeny, or in relation to the size of an individual, the chemical and mineralogical signatures of skeletal structures change (*e.g.*, carbon or calcium phosphate composition for cartilage or bone, respectively) (Mahamid et al., 2008; Cambra-Moo et al., 2015). On the other hand, an increase in exogenous ions (*e.g.*, F ions) and modifications of the internal structure of skeletal tissues are expected with diagenetic mineralization, because it likely depends on local fossilization conditions.

The rapidity of consumption (*i.e.*, mechanical degradation by predators or scavengers) and decay (*i.e.*, degradation by bacteria) of an animal under oxic conditions is negatively correlated with the preservation of soft tissues in an aquatic environment (Allison and Briggs, 1991). The decomposition process of organic carbon by aerobic respiration roughly corresponds to the transformation of organic and dioxygen molecules into carbon dioxide and water molecules. Thus, anoxic conditions can be reached when the amount of organic carbon exceeds the oxygen supply. Specifically, the deposition of a large number of individuals (mass mortality) during a short period of time can locally reduce the level of dissolved oxygen which could create anoxic condition at the

water/sediment boundary, decreasing scavenging and bioturbation (Allison and Briggs, 1991). These sporadic mass mortality events are characterized by a large number of fossil specimens in a given horizon. Fossiliferous sites and horizons yielding assemblages of mass mortalities are qualified as *Konzentrat-Lagerstätten*. Furthermore, when these fossiliferous environments present exceptionally well-preserved specimens, they are qualified of *Konservat-Lagerstätten*. It is likely that both, *Konzentrat-* and *Konservat-Lagerstätten*, favor soft tissues preservation.

Skeletal tissues showing early phases of biomineralization are prompt to be affected by two fossilization processes: the permineralization and the authigenic mineralization. Permineralization results from the early infiltration and permeation of tissues by mineralizing aqueous solutions (Schopf, 1975). In contrast, authigenic mineralization is often a product of biological tissues decay by bacterial activity; therefore, the types of minerals depend on the chemical composition of the sediment and the environmental conditions when bacterial decay occurred (Briggs, 2003).

The Late Devonian Miguasha *Fossil-Lagerstätte* (Québec, Canada), a UNESCO world heritage site, yielded fossilized ontogenies for 14 out of the 20 fish species (Cloutier et al., 2009). Among these 14 species, larval and juvenile specimens of the acanthodian *Triazeugacanthus affinis* have been reinterpreted recently (Chevrinais et al., 2015b). The exceptional preservation of a large number of *Triazeugacanthus* within a large size range allowed the description of ontogenetic changes. This ontogenetic series is characterized by the simultaneous increase in the number of skeletal structures and the progressive extension of the squamation as a function of animal size (Chevrinais et al., 2015b); thus, endoskeletal as well as exoskeletal mineralization proceed simultaneously.

In the present study, our main objectives are (1) to compare the chemical and mineralogical composition of larval, juvenile and adult specimens of *Triazeugacanthus*, and (2) to provide new information about the diagenesis of *Triazeugacanthus* from the Miguasha *Fossil-Lagerstätte*.

2.4 Experimental section

2.4.1 Material

The acanthodian *Triazeugacanthus affinis* Whiteaves (1887) is common (more than 300 complete or almost complete specimens) in the middle Frasnian Escuminac Formation (Miguasha, Quebec, Canada) (Cloutier et al., 2011b). The distribution of *Triazeugacanthus* is uneven lithologically and stratigraphically. *Triazeugacanthus* is found predominantly in the laminites (Cloutier et al., 2011b) and occurs primarily in two stratigraphic zones of the Escuminac Formation [*i.e.*, from 5 to 17 m and from 83 to 90 m from the base of the Escuminac Formation (R. Cloutier, pers. observ.)].

Three ontogenetic stages (larval, juvenile and adult) have been recognized in *Triazeugacanthus* based on the degree of squamation, the progression of the ossification and the size of the specimens (Chevrinais et al., 2015b). Six complete or almost complete specimens, two larvae (Figure 15 a-f), two juveniles (Figures 15 j-o, and 15 a-f) and two adults (Figure 15 h-s) and one thin section of the dermal skeleton of a juvenile (Figure 15 g-i) *Triazeugacanthus* preserved in laminites, have been used for the non-destructive scanning electron microscopy (SEM) coupled to the energy dispersive X-ray spectrometry (EDX) (Figures 15 and 16). One partial adult specimen of *Triazeugacanthus* allowing destructive analysis has been used for Fourier transform infrared spectrometry

(FTIR) and X-ray diffraction (XRD) (Annexe VII). Specimens are curated in the Musée d'Histoire naturelle de Miguasha (MHNM).

2.4.2 SEM observation and EDX analysis

SEM microscopy has been performed using an environmental JEOL 6460LV SEM. The surface of samples was observed without conductive coating. Elemental composition analysis was performed using an INCA X-sight (Oxford Instruments) energy dispersive X-ray spectrometer; this analysis permits to identify the presence of chemical elements in the skeletal structures (Gupta et al., 2008; Schweitzer et al., 2008). Each spectrum was acquired with a 10 μm spot size, for 100 seconds of lifetime (process time 5, spectrum range 0–20 keV, 2000 channels) at an accelerating voltage of 20 kV. The detection limits of chemical elements are about 1000 ppm or 0.1 wt%. System quantitative optimization was done using Cu as a standard.

2.4.3 Fourier transform infrared spectrometry

The surface of one adult specimen of *Triazeugacanthus* (MHNM 03-1699; Annexe VII) was scraped using a needle in order to obtain powder for Fourier transform infrared spectrometry (FTIR). Pellets for FTIR measurements were obtained by pressing a mixture of 1.0 mg of gently ground sample diluted in 210 mg of dried KBr. Transmission IR spectra were recorded between 400 and 4000 cm^{-1}, by averaging 150 scans with a resolution of 1 cm^{-1}, using a Nicolet 6700 FTIR spectrometer. The spectrometer was equipped with an Ever-Glo source, KBr beamsplitter and DTGS-KBr detector. The usual crystallinity index was calculated as the infrared splitting factor (IRSF): IRSF =

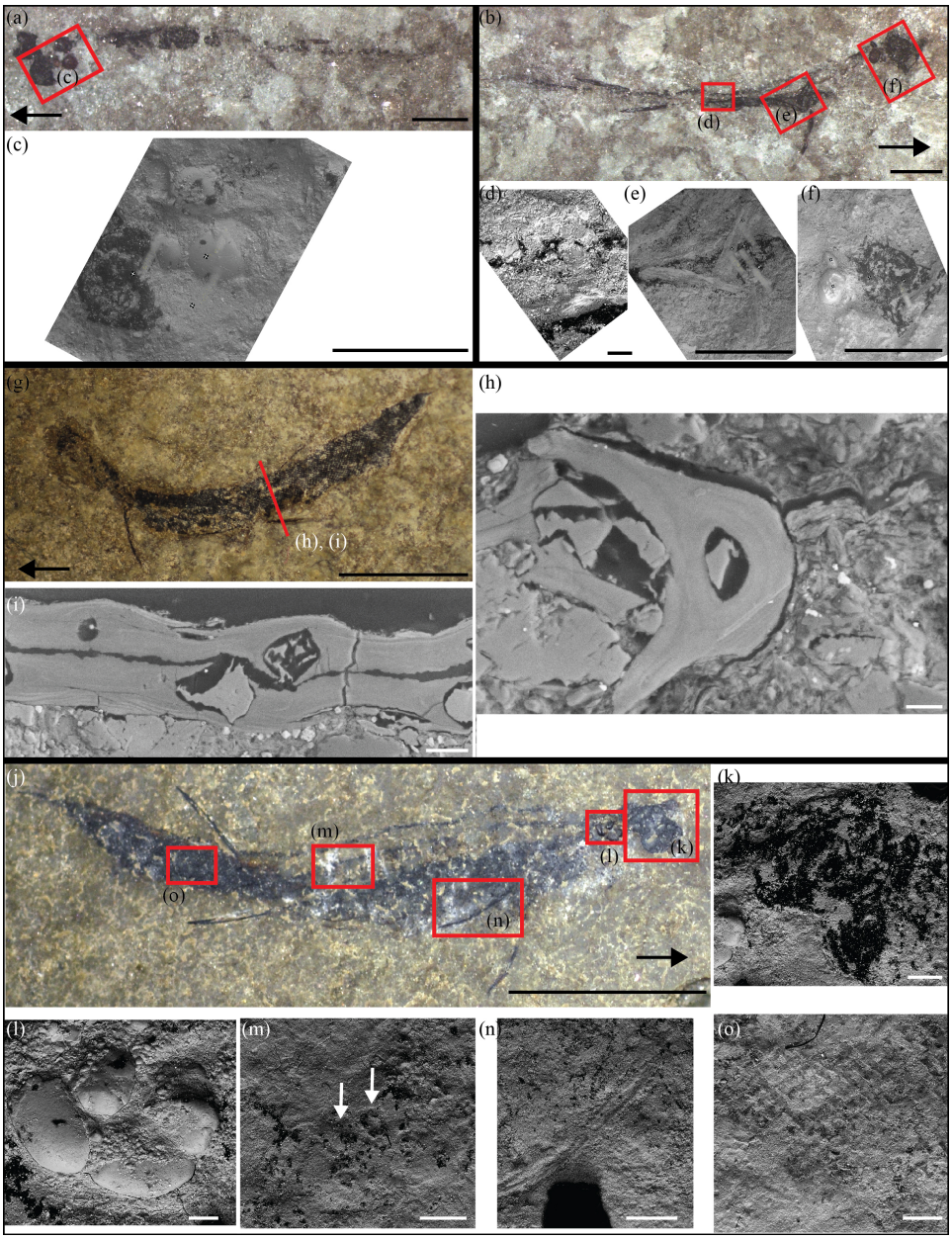

Figure 15: ***Triazeugacanthus affinis* anatomical structures for EDX analyses**. (a) Larval specimen MHNM 03-440 1 and SEM close-ups of the (c) head region. (b) Larval specimen MHNM 01-440 2 and SEM close-up of the (d) notochordal elements, (e) scapulocoracoid and pectoral fin spine, and (f) head region. (g) Juvenile specimen MHNM 03-398, red line shows the position of the histological section (h) of the anal spine and (i) the two lateral coverings of body scales in cross-sections. (j) Juvenile specimen MHNM 03-1252 and SEM close-ups of the (k) eye lenses, (l) otoliths, (m) notochordal elements (white arrows), (n) pectoral fin spine, (o) scales. Red squares show SEM close-up areas. Arrows point forward. Scale bars = 1 mm in (a), (b); 600 μm in (c); 500 μm in (d); 800 μm in (e) and (f); 5 mm in (g) and (j); 10 μm in (h); 20 μm in (i); 200 μm in (k), (m), and (o); 100 μm in (l); and 500 μm in (n).

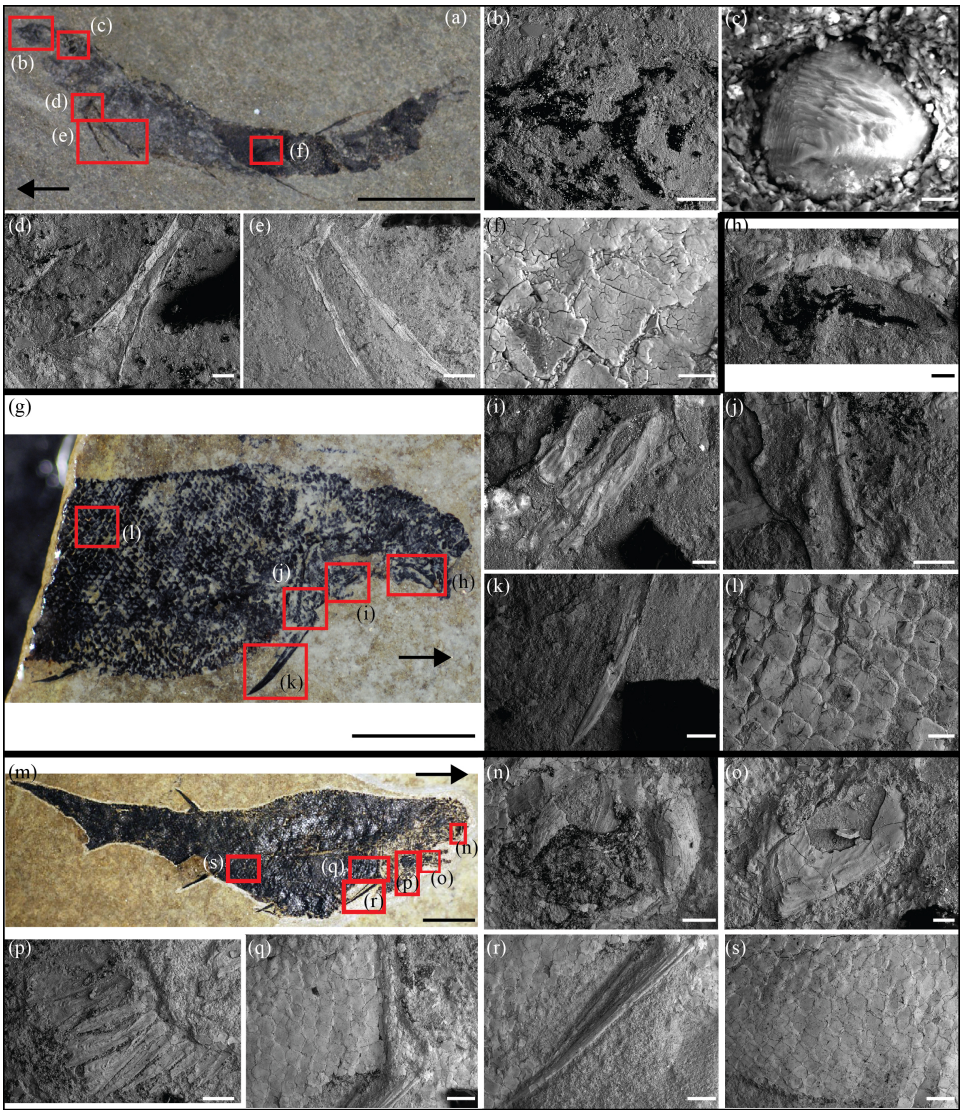

Figure 16: ***Triazeugacanthus affinis*** **anatomical structures for EDX analyses**. (a) Juvenile specimen MHNM 03-2684 and SEM close-ups of the (b) eye lenses, (c) otolith, (d) scapulocoracoid, (e) pectoral spines, and (f) scales. (g) Adult specimen MHNM 03-2669 and SEM close-ups of the (h) eye lenses and sclerotic plates, (i) branchiostegal rays, (j) scapulocoracoid, (k) pectoral fin spine and (l) scales. (m) Adult specimen MHNM 03-1497 and SEM close-ups of the (n) sclerotic plates, (o) palatoquadrate process, (p) branchiostegal rays, (q) scapulocoracoid, (r) pectoral fin spine and (s) scales. Red squares show SEM close-up areas. Arrows point forward. Scale bars = 5 mm in (a), (g) and (m); 200 μm in (b) and (h), 10 μm in (c), 100 μm in (d), (i), (o); 500 μm in (e), (j), (k), (n), (p), (q), (r), (s); 50 μm in (f).

(A605 + A565)/A590, where Ax is the measured absorbance at wavenumber x, assuming a straight baseline between 450 and 750 cm^{-1} (Weiner and Bar-Yosef, 1990; Shemesh, 1990).

2.4.4 X-ray diffraction

The mineralogical composition of the sedimentary rock was determined by powder X-ray diffraction (XRD) using few mg of a sample obtained from the laminated matrix of *Triazeugacanthus* specimen MHNM 03-1699 (Annexe VII). The powder sample was deposited on a Si spinning sample holder. Analyses were performed using a PANALYTICAL Expert Pro apparatus using the Co Kradiation. Measurements were performed from 2 to 90° in 1000 sec with a fixed slit size of 1°.

2.5 Results

2.5.1 SEM observations and EDX analyses of skeletal tissues

2.5.1.1 Fossilized tissues of *Triazeugacanthus affinis*

Chemical analyses of non-bony (eye lenses, otoliths), endochondral (palatoquadrate, scapulocoracoid, notochordal elements) and dermal elements (sclerotic plates, branchiostegal rays, pectoral spines, scales) have been performed for each ontogenetic stage [larval (Figure 17), juvenile (Figure 18) and adult (Figure 19)]. Irrespective to the ontogenetic stages, (1) C and O are recorded in each skeletal element, (2) Ca and P are

recorded in all dermal elements, and (3) the simultaneous presence of Ca and P is associated with F (with the exception of analyses performed on the internal structure of bones). Minor Al and Si contributions are detected and are likely related to the presence of aluminous clay minerals in the surrounding matrix (*i.e.*, illite and chlorite; Figures 17, 18 and 19).

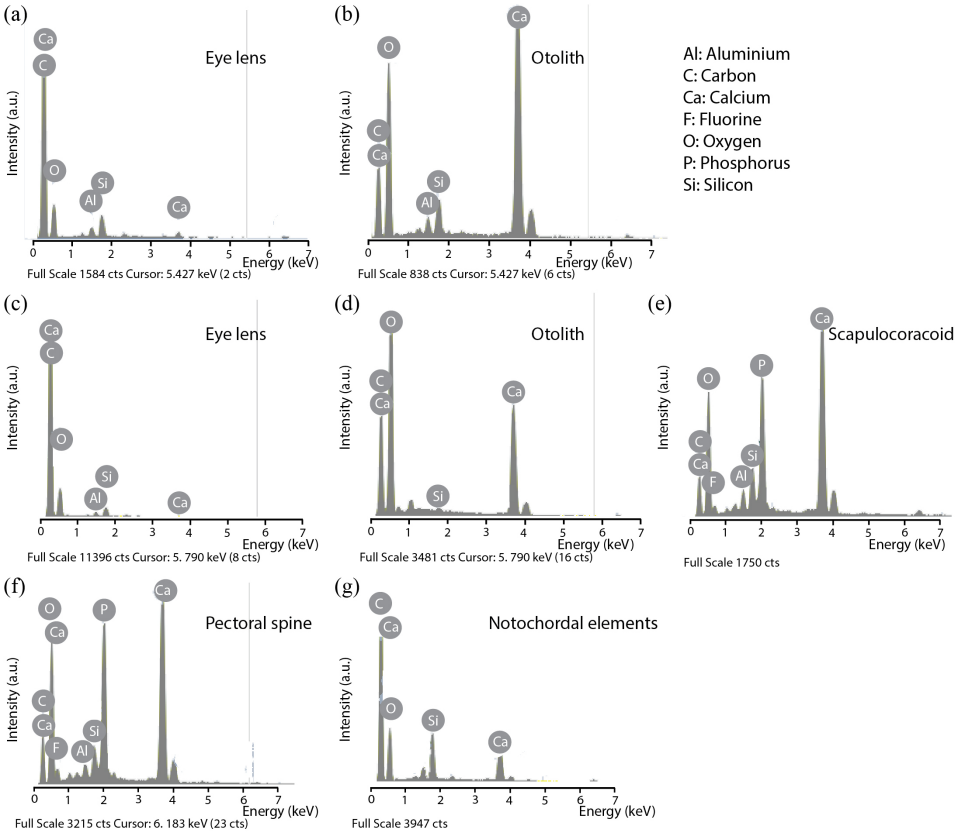

Figure 17: **Representative spectra of larval *Triazeugacanthus* samples using EDX punctual microanalyses**. (a) and (b) MHNM 03-440 1. (c)-(g) MHNM 03-440 2. Note that the intensity of the oxygen peak is non-significant and depends essentially on the vacuum level in the chamber of the environmental SEM.

In larval *Triazeugacanthus* (Figure 17 a and b), notochordal elements and eye lenses are among the first elements to develop (Chevrinais et al., 2015b, suppl.mat.). Notochordal

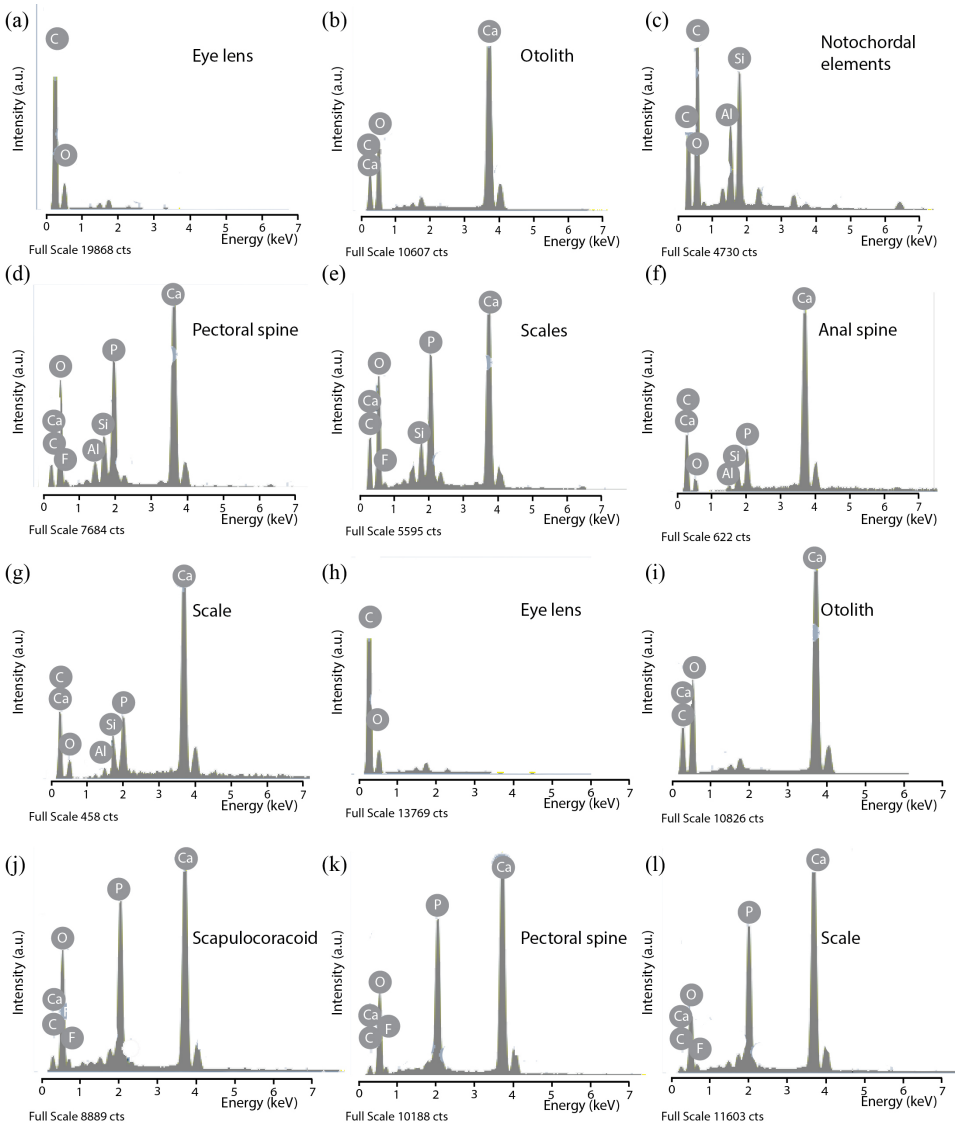

Figure 18: **Representative spectra of juvenile *Triazeugacanthus* samples using EDX punctual microanalyses**. (a)-(e) MHNM 03-1252. (f), (g) MHNM 03-398. (h)-(l) MHNM 03-2684. Note that the intensity of the oxygen peak is non-significant and depends essentially on the vacuum level in the chamber of the environmental SEM. See Figure 17 for chemical elements legend.

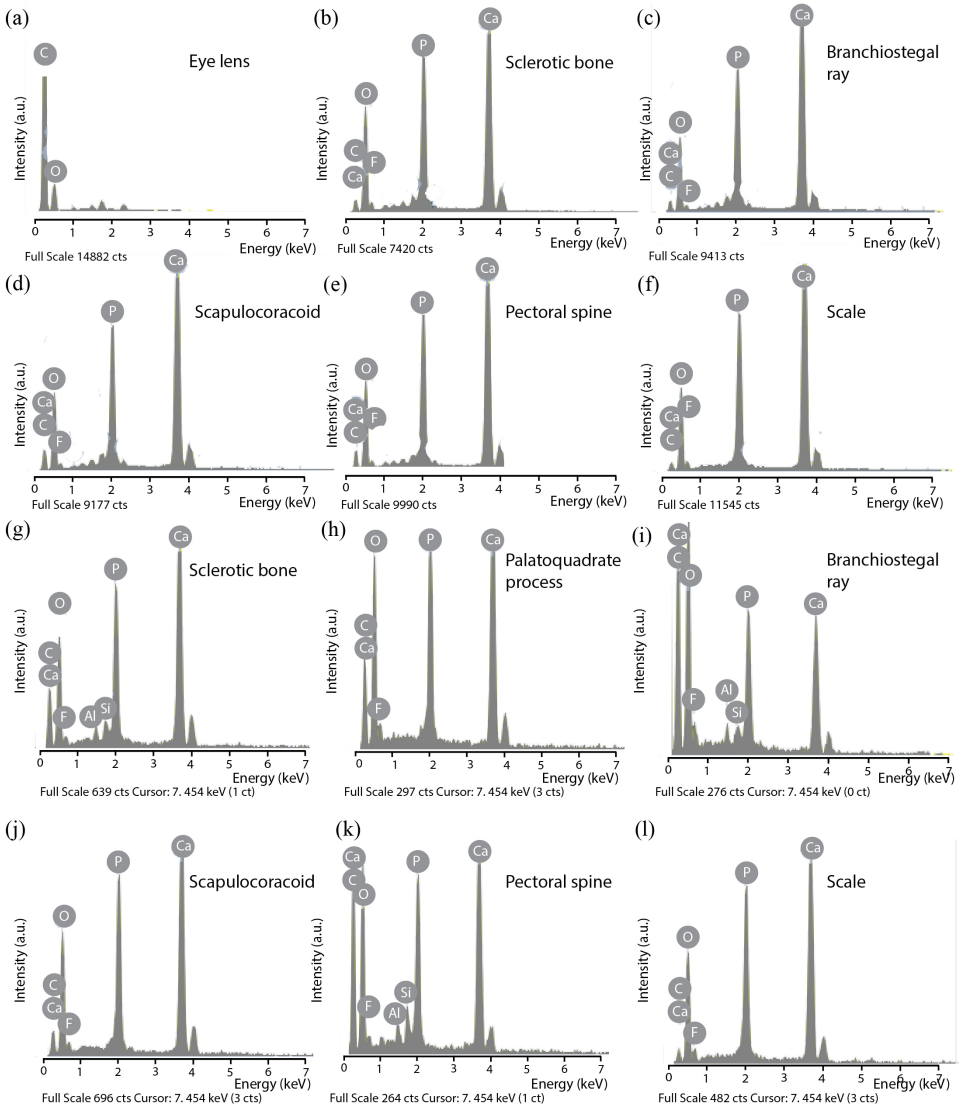

Figure 19: **Representative spectra of adult *Triazeugacanthus* samples using EDX punctual microanalyses**. (a)-(f) MHNM 03-2669. (g)-(l) MHNM 03-1497. Note that the intensity of the oxygen peak is non-significant and depends essentially on the vacuum level in the chamber of the environmental SEM. See Figure 17 for chemical elements legend.

elements and eye lenses display C and O peaks with a minor contribution of Ca, Al and Si in the EDX spectrum (Figure 17 a, c and g). The notochordal elements (visible only in rare specimens) show no sign of mineralization (Figure 17 g). During the larval stage, otoliths form shortly after the previous elements (Chevrinais et al., 2015b, Annexe IV). These non-bony elements display a strong Ca peak and lack P; these results are consistent with the expected calcium carbonate composition (Schultze, 1990) (Figures 15 c, f, 16 c). Among the first appendicular elements to form (Chevrinais et al., 2015b, Annexe IV), the scapulocoracoid and the pectoral spine display clear Ca and P peaks associated to a F peak (Figures 15 e, 16 d and e). Even in the youngest occurrence of the scapulocoracoid (Chevrinais et al., 2015b, Annexe IV, MHNM 03-440 2), there is already a clear mineralized signature (Figure 17 e); the pre-mineralized state of this endochondral element has not been sampled.

Juvenile *Triazeugacanthus* specimens (Figures 15 j and 16 a), characterized by the appearance and progression of the squamation (Chevrinais et al., 2015b), show dermal elements (scales: Figure 18 e, g and l; spines: Figure 18 d, f and k) with clear signatures of mineralization (Ca and P peaks). Elemental composition on the internal structure of dermal scales and spine (thin section; Figure 15 h-i) also reveals the presence of Ca and minor P (Figure 18 f and g), but the absence of F. Chemical composition of the eye lenses (Figure 18 a and h), notochordal elements (Figure 18 c), scapulocoracoid (Figure 18 j) and otoliths (Figure 18 b and i) remain similar to the larval condition.

In adult *Triazeugacanthus* specimens (Figure 16 g and m), the chemical composition of previously formed skeletal structures remains similar to that of the immatures (Figure 19). The newly developed palatoquadrate (Figure 19 h) is already mineralized. The dermal sclerotic plates (Figure 19 b and g) and branchiostegal rays (Figure 19 c and i) are also mineralized as suggested by the presence of strong Ca and P peaks (with similar

relative intensities) associated with a F peak. Notochordal elements and otoliths are not observed in adults because they are overlaid by body and head scales, respectively.

2.5.1.2 Living models: *Centroscyllium fabricii* and *Scomber scombrus*

The elemental composition analysis of the juvenile *C. fabricii* mostly consists in C, O and N, consistent with the absence of mineralization on the surface of the neurocranium, the eye lenses and the vertebral centra (Annexe X). Tesserate mineralization indicated by the presence of P and Ca occurs in the mandibular and hyoid arches (Annexe X). The skeletal structures of the juvenile *S. scombrus* display mainly the presence of C, O and N in the eye lenses and Ca and P signatures in the exoccipital, the dentary and the basihyal (Annexe XI).

2.5.2 Mineralogical analysis of *Triazeugacanthus* skeleton

The FTIR spectrum of *Triazeugacanthus* skeletal structures displays the characteristic absorption bands of apatite (Figure 20 a-c) (Yi et al., 2014). These bands are related to the internal vibrational modes of PO_4 groups. The phosphate groups lead to intense bands at 565-576 and 605 cm^{-1} (PO_4 bending modes), and 1041 and 1096 cm^{-1} (PO_4 anti-symmetric stretching modes).

A weaker band related to the PO_4 symmetric stretching mode is observed at 965 cm^{-1}. The wavenumber of this band is correlated with F concentration and ranges between 960 in modern fish bone (Pucéat et al., 2004) to 965.6 cm^{-1} in a sedimentary carbonate-fluorapatite (Yi et al., 2014). Its position in the present study thus corroborates the

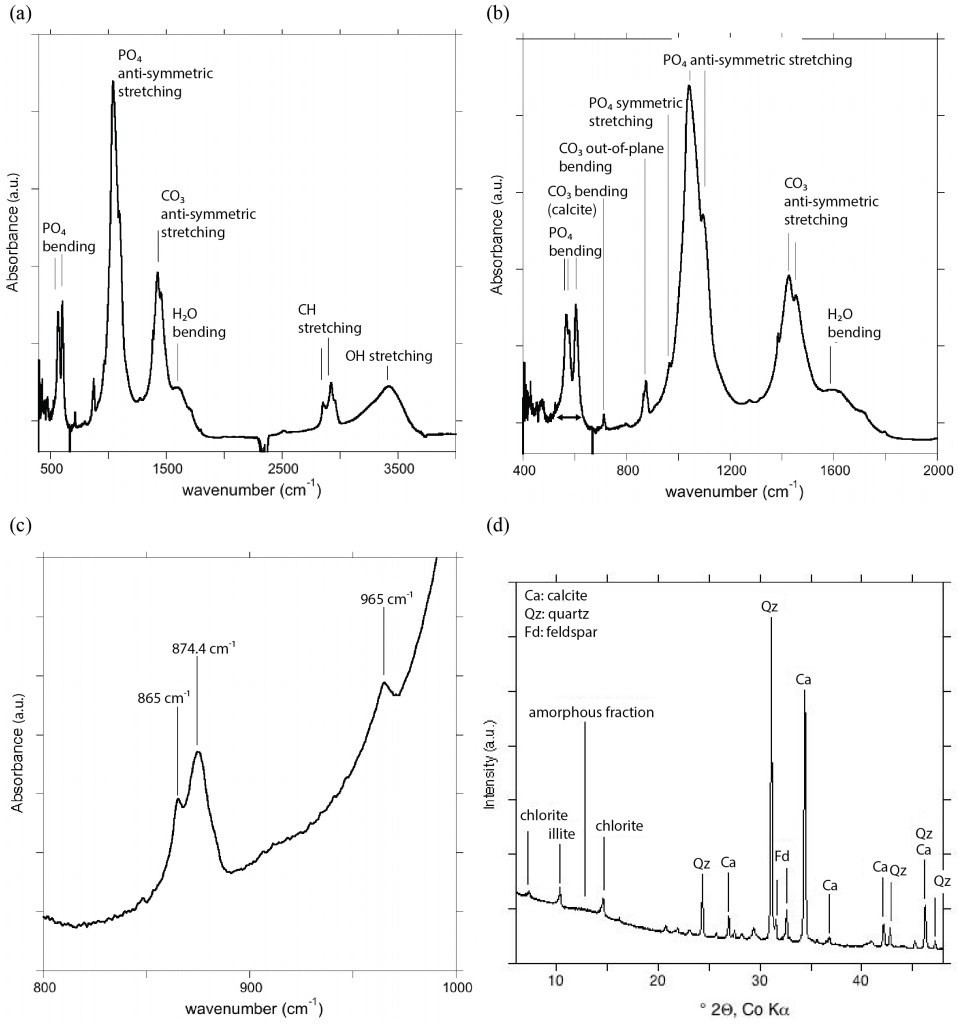

Figure 20: **Powder transmission infrared spectrum of *Triazeugacanthus* and XRD pattern of surrounding sedimentary matrix.** (a) Powder transmission infrared spectrum of *Triazeugacanthus* (MHNM 03-1699) showing PO_4, CO_3, OH, CH and H_2O bands and close-up (b) focusing on major CO_3 and PO_4 bands. Horizontal arrow points the line splitting of PO_4 bending modes. (c) Close-up of the FTIR spectrum focusing on the $\nu 2$ CO_3 and $\nu 1$ PO_4 signals. The band at 865 cm^{-1} is diagnostic of the presence of a francolite-type carbonate environment. (d) XRD pattern of sedimentary matrix surrounding the specimen of *Triazeugacanthus*.

presence of a F concentration in apatite, consistent with the EDX measurements performed on specific skeletal structures of *Triazeugacanthus* (Figure 16 i-n). The width of this band is dominated by the atomic-scale distortions of the apatite-structure (Balan et al., 2011) but overlapping with the strong PO_4 anti-symmetric stretching bands affects accurate analysis.

The splitting factor (IRSF) determined from the relative intensity of PO_4 bending bands is a practical way to assess the width of these bands, which is expected to reflect the apatite crystalline order but may also depend on the shape of apatite particles (Figure 20 b). However, for samples with ordinary particle shapes, the full width at half maximum (FWMH) of the splitting factor (IRSF) determined from the relative intensity of PO_4 symmetric stretching band and the infrared splitting factor (IRSF) parameter lead to similar information about apatite crystalline order (Yi et al., 2014). In the present sample, the IRSF is 5.17, notably higher than that previously reported for bioapatite and slightly smaller than that reported for a sedimentary carbonate-fluorapatite sample (Yi et al., 2014). For example, an IRSF of around 2.8 has been reported for vertebral centra of modern shark and ranging between 3.41 and 5.39 for Cenozoic fossil sharks (MacFadden et al., 2004; Labs-Hochstein and MacFadden, 2006). Values of 2.6 and 3.2 have been reported for newly formed bones (fin rays) in the extant zebrafish *Danio rerio* (Mahamid et al., 2008). Recent marine apatites also display low IRSF indices (3.0-3.6) whereas those of inland ancient apatites are higher (4.5-7.8) (Shemesh, 1990). The IRSF of extant mammal bones exposed on tropical savannah grasslands varies from 2.7 to 3.5 and was found to be correlated to the mean length of apatite particles (Trueman et al., 2004). IRSF values increase to approximately 3.9 in Pleistocene bird and mammal bones (Trueman et al., 2008). The enamel of modern mammals displays a relatively high IRSF (Schweitzer et al., 2008, *e.g.*, 4.3). The comparatively high IRSF of *Triazeugacanthus* skeletal structures suggests that diagenetic transformations

increased the apatite crystalline order with respect to that observed in extant and extinct biological materials.

Several bands related to vibrational modes of carbonate groups are also observed. Carbonate groups are responsible for the set of absorption bands at 1426 and 1453 cm^{-1} (anti-symmetric stretching) and the two overlapping signals at 865 and 874.4 cm^{-1} (out-of-plane bending modes). An additional band at 712 cm^{-1} indicates the presence of calcite.

Based on the signal related to out-of-plane bending modes, two main environments of carbonate groups occur in the sample. The band at 875 cm^{-1} can be mostly ascribed to calcite. The band at 865 cm^{-1} is related to carbonate groups incorporated in the apatite structure with a "francolite"-type environment (Yi et al., 2013). This peculiar environment corresponds to an isovalent coupled substitution of the phosphate groups by clumped carbonate and F ions. Note that this type of environment does not imply any bonded interaction between the carbonate and the F ions but corresponds to a geometrical association, which ensures a local electrostatic charge neutrality.

The absorption bands related to the two anti-symmetric stretching modes of CO_3 groups, split by the site distortion, are observed at 1409-1440 cm^{-1} and 1450-1455 cm^{-1} (Figure 20 b). These frequencies are consistent with the above interpretation. The absence of a marked absorption band at higher frequency (1550 cm^{-1}) rules out a major occurrence of carbonate groups in the structural channels of apatite (A-type carbonates). However, an uncertainty remains about the occurrence of carbonate groups in the usual B-type environment of hydroxyapatite because of its potential overlap with the calcite and "francolite"-type carbonate bands. The peculiar "francolite"-type substitution at the B-site of fluorapatite differs from ordinary B-type carbonate substitution. In biological

apatite, the B-type carbonate substitution corresponds to the replacement of PO_4^{3-} by CO_3^{2-}, along with the substitution of Ca^{2+} by Na^{+} or K^{+} to preserve the electroneutrality.

Broad absorption features between 1560 and 1800 cm^{-1} are related to the presence of organic matter (carbonyl and amide functions) and water molecules (H_2O bending mode). Water molecules are also responsible for the broad OH-stretching band at 3420 cm^{-1}. In contrast, no stretching band related to OH groups in the structural channels of hydroxyapatite (at 3572 cm^{-1}) is observed.

Taken together, these results indicate that the mineral composition of the fossilized *Triazeugacanthus* skeleton mostly consists of carbonate-fluorapatite and calcite. As bioapatite usually consists in poorly ordered carbonate-bearing hydroxyapatite, the occurrence of carbonate-fluorapatite strongly suggests a post-depositional recrystallisation of the bioapatite (Shemesh, 1990).

Finally, the sedimentary matrix surrounding the fossil sample was analyzed by X-ray diffraction to better infer the conditions of preservation of *Triazeugacanthus* fossils (Annexe VII). The observed minerals are dominantly calcite and quartz with feldspar, chlorite and illite in lower abundance (Figure 20 d). Note that the clay fraction could also contain smectite but its identification would require further physical separation and chemical treatments because of the overlap of the smectite with the chlorite (001) peak. The presence of an amorphous fraction is suggested by a weak broad band at 12° in the diffraction pattern (Figure 20 d). Overall, these results are consistent with previously published data (El Albani et al., 2002; Matton et al., 2012) showing the occurrence of quartz, calcite and smaller proportions of illite, muscovite, chlorite, plagioclase and amorphous organic matter. This mineralogical composition has been interpreted as

resulting from shallow burial diagenesis and early formation of diagenetic calcite(El Albani et al., 2002; Matton et al., 2012).

2.6 Discussion

Here, we have shown that (1) both unmineralized (carbon signature) and mineralized anatomical elements (calcium and phosphorus signatures) are preserved depending on the ontogenetic stages of *Triazeugacanthus*, and (2) the carbonate-fluorapatite is the main mineralogical structure of *Triazeugacanthus* fossil skeleton.

2.6.1 Chemical composition of *Triazeugacanthus* biomineralized tissues depends on ontogenetic stages

Published spectrometry on *Triazeugacanthus* reported the dominant presence of Si with traces of Al, K, Mg, Ca and Fe for various skeletal elements (scales, "vertebral column" and "adjacent plates") (Béland and Arsenault, 1985). Our observations do not confirm this previous report, which may correspond to an analytical artifact. It is unlikely that the specimen used for that study (Béland and Arsenault, 1985) would be indicative of silicification, while none of our specimens show such a chemical signature.

Our results indicate that both unmineralized (C signature) and mineralized anatomical remains (Ca and P signatures) are preserved differentially according to the ontogenetic stages of *Triazeugacanthus* and the histological origin of the elements. With the exception of the notochordal elements for which a non-mineralized signature has been found in the immatures, the pre-mineralized (cartilaginous) state of endochondral elements

has not been observed in our coarse sampling of the ontogenetic series of *Triazeugacanthus*. The notochordal elements correspond either to the cartilaginous precursors of vertebral elements or to the notochord itself. The appearance and growth of dermal elements is always characterized by the presence of both Ca and P peaks. However, a difference has been noticed between the elemental composition at the surface of the bone and the internal structure of the bone; F has been recorded at the exposed surface (scales and spines), while it is not recorded internally.

While the larval individuals show the preservation of soft tissues (*e.g.*, eye lenses, notochordal elements), juveniles and adults display notable concentrations of Ca and P which are characteristic of bone chemical composition (Young and Brown, 1982). However, in the juveniles, the relative P/Ca content in the scales and fin spines is smaller than in the adults. Therefore, we interpret this progressive mineralization of skeletal elements as reflecting an ontogenetic transformation of the bony material.

EDX analyses and anatomical comparisons allowed us to identify properly the rounded anteriormost elements observed in the head of *Triazeugacanthus* (Figure 15 a, b) (Graham-Smith, 1935; Béland and Arsenault, 1985; Gagnier, 1996). These elements have been alternately interpreted as (1) optic plates (Béland and Arsenault, 1985), (2) orbits (Gagnier, 1996), and (3) eye lenses (Chevrinais et al., 2015b). The use of the term "optic plates" was not justified in the original paper (Béland and Arsenault, 1985), as this term does not correspond to any anatomical element. The term "orbit" [="orbital cavity" (Franz-Odendaal and Vickaryous, 2006)] corresponds either to the cavity that structurally supports the eyeball, or the bones (*e.g.*, circumorbitals) forming the margin of the eye socket (Burrow et al., 2011). None of the known acanthodian neurocrania (Brazeau, 2009; Davis et al., 2012) display paired rounded elements as those seen in *Triazeugacanthus*. A series of four dermal sclerotic plates forms the margin of the eye

socket of *Triazeugacanthus* (Gagnier, 1996; Burrow et al., 2011, this study). Thus, the rounded elements seen in *Triazeugacanthus* do not correspond to the orbit. Anterior paired rounded elements have been identified as the eyes of the Carboniferous acanthodian *Acanthodes bridgei* (Tanaka et al., 2014). Rods and pigments, as well as molecules common only to eumelanine were found in the dark brown fragments from these fossil eyes. EDX analyses on the eye lenses of the extant *C. fabricii* and *S. scombrus* are similar to those of the *Triazeugacanthus* elements (this study). Characteristics of the crystalline lens of aquatic vertebrates [*e.g.*, rounded-shape of the lens with low deformability (Levine, 1985)] and similarities shared with cartilage [abundance and chemical composition of crystalline proteins and collagen proteins (Tanaka et al., 2014) in the lens and the cartilage, respectively] might explain its potential for fossilization. We suggested that the rounded elements in *Triazeugacanthus* specimens could be interpreted as eye lenses. The anterior morphological position in the head region, their rounded shape, the absence of mineralized tissues (C and O peaks), and the similarities with acanthodian, chondrichthyan and osteichthyan anatomy (Tanaka et al., 2014, this study) corroborate this interpretation.

2.6.2 Preservation vs. recrystallization of *Triazeugacanthus* tissues

In the stratigraphic sequence of the Miguasha *Fossil-Lagerstätte*, larval, juvenile and adult *Triazeugacanthus* are found in the same lithologies, primarily in laminites, as well as on the same bedding plane. The characteristic "laminites" facies is composed of an alternation of fine siltstones and shales (Cloutier et al., 2011b) rich in organic matter interpreted as a tidal deposit (El Albani et al., 2002). This lithofacies is in agreement with an intertidal deposit likely in a wave-dominated estuarine environment, with periodic input of sediment by floods (El Albani et al., 2002). Miguasha *Konservat-* and

Konzentrat-Lagerstätte horizons occur mostly in the transgressive phases and primarily towards the maximum paleodepth water (El Albani et al., 2002). Sedimentological and geochemical investigations have shown that the Escuminac Formation has been subjected only to a shallow burial diagenesis (depth < 1500 m, T < 430°C) (Chidiac, 1996; El Albani et al., 2002; Matton et al., 2012). The clay mineral fraction is considered to be mostly detrital whereas calcite cement and fibrous calcite are attributed to early diagenesis of organic matter (El Albani et al., 2002). Thus, shallow burial allowing exchanges between groundwater and skeleton, and early diagenesis are required conditions for recrystallization of skeletal structures.

Despite the excellent state of preservation of bones at the microstructural (Sanchez et al., 2013; Downs and Donoghue, 2009), histological (Figure 15 h-i) and anatomical levels, our results indicate a pervasive recrystallization of bioapatite in *Triazeugacanthus* skeletal structures. Modification of the mineral composition of fossil bones (*e.g.*, presence of authigenic calcite) from the Escuminac Formation has been previously reported in the placoderm *Bothriolepis canadensis* and the osteolepiform *Eusthenopteron foordi* (Matton et al., 2012). Bioapatites usually display small particle sizes and significant carbonate contents (Nemliher et al., 2004; Mahamid et al., 2008). In addition, apatite particles in bones of living animals are coated by a poorly-ordered hydrous phosphatic phase (Wang et al., 2013) and associated with organic polymers (collagen), which transform (Kalvoda et al., 2009) or decay after an animal's death (Sansom et al., 2013a). In contrast, carbonate-fluorapatite is less soluble than bioapatite (Shemesh, 1990; Kalvoda et al., 2009) and often represents an ultimate stage of recrystallization of biomineralized anatomical structures in geological environments (Shemesh, 1990; Nemliher et al., 2004; Kalvoda et al., 2009; Pasteris and Ding, 2009; Yi et al., 2014). Carbonate-fluorapatite also occurs in sedimentary environments as an authigenic mineral, likely produced from the bacterial decay of organic matter (O'Hagan and Harper,

1999; Murphy et al., 2003; Cosmidis et al., 2013a,b).

Transformation of bioapatite to carbonate-fluorapatite can occur in low-temperature environments and has been reported in marine or continental fossil deposits (Kolodny et al., 1996; Nemliher et al., 2004; Ifrim et al., 2007; Yi et al., 2014). It however depends on the F supply. In the present case, the F source might be related to the early diagenetic transformation of carbonates. As a matter of fact, the early diagenesis of biogenic calcium carbonate minerals has been reported to be a major source of F in modern shallow sediments of the Florida Bay, USA (Rude and Aller, 1991). The transformation of bioapatite in carbonate-bearing fluroapatite is thus still consistent with the rapid burial and early diagenetic transformations under anoxic conditions. Indeed, rapid burial and early diagenetic transformations limiting the rapidity of consumption and degradation, which are the most important bias in the preservation of soft tissues, allowed the preservation of these tissues such as those observed in *Triazeugacanthus* larvae (Allison, 1988; Allison and Briggs, 1991).

Last, bioapatite to carbonate-fluorapatite transformation of mammal enamel in late Tertiary continental environments has been shown to occur through a dissolution/precipitation mechanism (Yi et al., 2014). However, such type of replacement modifies the structure of the biological material at a micrometric scale [*e.g.*, presence of carbonate-fluorapatite infillings discordant with the biogenic Retzius striae in mammalian tooth enamel (Yi et al., 2014)]. In the Miguasha *Fossil-Lagerstätte*, the preservation of the bone microstructures (Downs and Donoghue, 2009; Sanchez et al., 2013, 2014) could suggest a more subtle transformation mechanism, consistent with an early diagenetic stage, even though the formation of the ”francolite”-type environment of substituted carbonates implies a transformation of apatite down to the atomic scale. Therefore, the respective contributions of early transformation and potential slow modifications (Reynard and

Balter, 2014) in the sedimentological environment of the Escuminac Formation have still to be determined.

2.7 Concluding remarks

The preservation of fossil anatomical remains, especially the preservation of soft tissues, and pervasive chemical modification of hard tissues in the same sedimentary horizons, suggest specific conditions of burial and diagenesis. The investigation of ontogenetic changes of the Late Devonian acanthodian *Triazeugacanthus affinis*, using different methods for chemical identification, allowed us to better describe the growth in this fossil fish in documenting the progressive mineralization. The presence of soft tissues in larvae and the biomineralization of tissues in juveniles and adults throughout a growth series are described for the first time in a Paleozoic vertebrate.

ARTICLE 3

DE L'ONTOGÉNIE DE L'ÉCAILLE À L'ONTOGÉNIE DE L'ESPÈCE : ÉTUDE HISTOLOGIQUE ET MORPHOLOGIQUE DE L'ACANTHODIEN DU DÉVONIEN SUPÉRIEUR *TRIAZEUGACANTHUS AFFINIS* (MIGUASHA, CANADA)

3.1 Résumé en français du premier article

Les séries de croissance de vertébrés paléozoïques sont rares, notamment à cause de la fragilité des spécimens larvaires et juvéniles étant donné leur faible degré de minéralisation et la rareté des spécimens articulés. Cette rareté rend difficile la description exhaustive des patrons et processus de croissance des taxons éteints. Cependant, l'information disponible à partir des quelques séries de croissance d'individus complets du Paléozoïque permet la description de la croissance d'éléments dermiques isolés (*e.g.*, dents, écailles) et alors d'inférer la croissance des individus à partir de ces éléments. De plus, les écailles isolées et *in situ* sont généralement abondantes, très bien préservées, et apportent de l'information sur (1) leur morphologie et leur structure en fonction des relations phylogénétiques, et (2) les patrons et processus développementaux relatifs à l'ontogénie de l'espèce. L'acanthodien *Triazeugacanthus affinis* du Dévonien supérieur du *Lagerstätte* de Miguasha représente une des ontogénies fossiles de vertébrés primitifs les mieux connues grâce à la préservation exceptionnelle, la large étendue de taille, et l'abondance des spécimens complets. Ici, nous rassemblons des données morphologiques, histologiques et chimiques relatives aux écailles à partir d'une série de croissance consistant en juvéniles et adultes (les écailles n'étant pas formés chez les

larves). Au niveau histologique, les écailles de *Triazeugacanthus* sont composées d'une couche basale d'os acellulaire comprenant des fibres de Sharpey, une couche centrale de mésodentine, et une couche superficielle de ganoine. Au niveau développemental, les écailles grandissent premièrement par l'addition concentrique de mésodentine et d'os autour d'un primordium central et ensuite par la superposition de couches de ganoine. Au niveau ontogénétique, les écailles se forment d'abord dans la région au dessous de l'épine de la nageoire dorsale, puis l'écaillure s'étend antérieurement et postérieurement, et sur les nageoires. Au niveau phylogénétique, les écailles de *Triazeugacanthus* montrent des similarités avec les acanthodiens (*e.g.* croissance "box-in-box"), les chondrichtyens (*e.g.* patrons de squamation) et les actinoptérygiens (*e.g.* ganoine). Cependant, une nouvelle analyse phylogénétique des gnathostomes indique que les acanthodiens sont à la base des chondrichtyens.

Ce troisième article, intitulé « *From body scale ontogeny to species ontogeny: Histological and morphological assessment of the Late Devonian acanthodian* Triazeugacanthus affinis *from Miguasha, Canada* », fut corédigé par moi-même ainsi que par Jean-Yves Sire et Richard Cloutier. Il fut soumis pour publication dans la revue internationale *PlosOne* dans sa version finale en Juin 2016. Tous les auteurs ont conçu les expériences. En tant que premier auteur, ma contribution à ce travail fut l'essentiel de la recherche sur l'état de l'art, la réalisation des manipulations d'histologie (avec l'aide de Jean-Yves Sire à l'UPMC), les observations et l'analyse de données, la réalisation de l'analyse phylogénétique (avec Richard Cloutier) ainsi que la production des figures et du matériel supplémentaire avec les contributions de Richard Cloutier et Jean-Yves Sire. J'ai écrit la première version et tous les auteurs ont contribué à la version finale. Une version abrégée de cet article a été présentée à la rencontre annuelle de la *Society of Vertebrate Paleontogy* à Berlin (Allemagne) à l'automne 2014 ainsi que lors des *Rencontres de l'Ichthyologie francophone* à Paris (France) au printemps 2015.

Nous remercions J. Kerr, O. Matton et F. Charest (MHNM). Nous sommes reconnaissants envers V. Bazin (IFR 83/FRE 3595, UPMC) et C. Belzile (UQAR) pour les analyses de microscopie électroniques et de spectométrie. Nous remercions H. Lamrous (UPMC), V. de Buffrénil (MNHN), et V. Rommeveaux (MNHN) pour leur aide concernant la préparation du protocole d'histologie. Nous avons apprécié les discussions avec H.-P. Schultze (University of Kansas), L. Zylberberg (UPMC), F. Meunier (MNHN), A. de Ricqlès (UPMC), P. Andreev (University of Birmingham), et Z. Min (Chinese Academy of Sciences). Les financements de cette étude proviennent du NSERC (R. Cloutier), du CSBQ (bourse d'excellence) (Marion Chevrinais) et de l'UMR7138 (UPMC, CNRS) (J.-Y. Sire).

3.2 From body scale ontogeny to species ontogeny: Histological and morphological assessment of the Late Devonian acanthodian *Triazeugacanthus affinis* from Miguasha, Canada

Summary

Growth series of Palaeozoic fishes are rare notably because of the fragility of larval and juvenile specimens owing to their weak degree of mineralisation and the scarcity of articulated specimens. This rarity makes it difficult to describe early vertebrate growth patterns and processes in extinct taxa. Indeed, only a few growth series of complete Palaeozoic fishes are available; they allow to describe the growth of isolated elements and to infer individual growth from these isolated elements. In addition, isolated and *in situ* scales are generally abundant and well-preserved, and bring information on (1) their morphology and structure relative to phylogenetic relationships and (2) individual growth patterns and processes relative to species ontogeny. The Late Devonian acanthodian *Triazeugacanthus affinis* from the Miguasha *Fossil-Lagerstätte* is one of the best known fossilised ontogenies of early vertebrates because of the exceptional preservation, the large size range, and the abundance of complete specimens. Here, we gathered morphological, histological, and chemical data on scales from juvenile and adult specimens (scales not being formed in larvae). Histologically, *Triazeugacanthus* scales are composed of a basal layer of acellular bone housing Sharpey's fibers, a mid-layer of mesodentine, and a superficial layer of ganoine. Developmentally, scales grow first through concentric addition of mesodentine and bone around a central primordium and then through superposition of ganoine layers. Ontogenetically, scales form first in the region below the dorsal fin spine, then squamation spreads anteriorly and posteriorly, and on fin webs. Phylogenetically, *Triazeugacanthus* scales show similarities with acanthodians (*e.g.* "box-in-box" growth), chondrichthyans (*e.g.* squamation pattern),

and actinopterygians (*e.g.* ganoine). Scale histology and growth are interpreted in the light of a new phylogenetic analysis of gnathostomes supporting acanthodians as stem chondrichthyans.

Key words: Acanthodii, growth, squamation pattern, scale structure, ontogeny, stem chondrichthyans, gnathostome phylogeny

3.3 Introduction

Fish fossilised ontogenies are rare, especially in the Palaeozoic record (Cloutier, 2010) because the preservation of weakly mineralised skeletal elements of immature specimens requires exceptional conditions of fossilisation. In extinct fish taxa, such as placoderms and acanthodians, the paucity of ontogenies is problematic because only ontogenies have the potential to inform us relative to developmental patterns and processes in the past. Complete and articulated fossil fishes are rare in the Palaeozoic record, comparatively to isolated elements, which are fairly abundant. Among these isolated elements, some, such as scales, are recording the ontogeny of the individual and thus provide a unique opportunity to describe their ontogeny (Cloutier, 2010; Qu et al., 2016). Fossil model organisms, for which both abundant individual isolated elements and complete specimens are known, are indispensable to describe the relationship between individual growth of isolated elements and species ontogeny (Cloutier, 2010).

Among early vertebrates, acanthodians have been recovered both from isolated elements and complete specimens from the Upper Silurian (423-419 million years ago) (Burrow and Rudkin, 2014) to the Middle-Upper Permian (272-252 million years ago)

(Mütter and Richter, 2007). Acanthodian species known from complete specimens are relatively rare compared to the number of taxa known solely from isolated scales (Denison, 1979; Trinajstic, 2001; Burrow and Young, 2005). Furthermore, only a few acanthodian ontogenies based on complete specimens have been discovered (Zidek, 1976; Cloutier, 2010): one possible ischnacanthiform [*Nerepisacanthus denisoni* (Burrow and Rudkin, 2014)], two diplacanthiforms [*Diplacanthus horridus* (Cloutier et al., 2009) and *Uraniacanthus curtus* (Newman et al., 2012)], one climatiiform [*Tetanopsyrus breviacanthias* (Hanke et al., 2001)], two species of uncertain order [*Machaeracanthus goujeti* (Botella et al., 2012) and *Lupopsyrus pygmaeus* (Hanke and Davis, 2012)], and nine acanthodiforms [*Triazeugacanthus affinis* (Chevrinais et al., 2015a,b), *Lodeacanthus gaujicus* (Upeniece, 1996, 2001; Upeniece and Beznosov, 2002), *Homalacanthus concinnus* (Cloutier et al., 2009), *Acanthodes bridgei* (Zidek, 1985), *A. bronni* (Heidtke, 1990), *A. gracilis* (Zajic, 2005), *A. lopatini* (Beznosov, 2009), *A. ovensi* (Forey and Young, 1985)], and an acanthodiform indet. (Coates, 1993). The rarity of complete specimens of acanthodians has been associated to the micromeric nature of the dermal skeleton as well as to the poor ossification of the endoskeleton (Janvier, 1996b; Upeniece and Beznosov, 2002).

The micromeric dermal skeleton of acanthodians, composed of minute scales on the head and body, has been mainly described from adult specimens. Typically, acanthodian body scales are small, rhombic and composed of two tissue layers: a basal layer of bone and a middle layer of dentine (Gross, 1947, 1971). Some fundamental, histological differences have been reported among acanthodian groups such as the presence of osteocytes in the basal layer of the climatiiform scales, the presence of vascular canals in the dentine layer of the ischnacanthiform scales and the presence of a superficial well-mineralised layer in some climatiiform and acanthodiform scales (Gross, 1947; Denison, 1979; Valiukevičius, 1995). With regard to this disparity and based on tissue

composition, Valiukevičius (1995) defined four main types of scales characterising the four acanthodian orders; however, the phylogenetic status of these orders is questionable (Hanke and Wilson, 2004; Brazeau, 2009; Davis et al., 2012). In addition, these scale types are only defined from adult specimens and from a few species. The *Nostolepis*-type (1) characterises climatiiforms: a thick basal plate of cellular bone, a crown of mesodentine, and no well-mineralised, enamel-like tissue at the scale surface (Valiukevičius and Burrow, 2005). The *Diplacanthus*-type (2) characterises diplacanthiforms: a thick, vascularised basal plate of acellular bone, a crown of mesodentine, and no well-mineralised, enamel-like tissue at the scale surface. The *Poracanthodes*-type (3) characterises ischnacanthiforms: a basal plate of either acellular or cellular bone, a crown composed of either orthodentine, mesodentine or both, with a pore canal system opening superficially and on the neck, and no well-mineralised, enamel-like tissue at the scale surface. Finally, the *Acanthodes*-type (4) characterises the acanthodiforms: a basal plate of acellular bone housing narrow vascular canals, a crown of mesodentine, and a well-mineralised, enamel-like tissue at the scale surface.

The four types of scales share a similar growth process, mainly characterised by the periodic apposition of bone and dentine layers around a single primordium. This mode of concentric growth is known as the "box-in-box" or "onion skin" pattern (Gross, 1971; Denison, 1979). With the exception of the general recognition of this growth process, scale ontogeny is poorly known mainly due to the destructive nature of histological methods, which explains why only a few adult specimens were analysed in previous studies. Non-destructive techniques such as nano-CT scanning (Khoury et al., 2015) or synchrotron analysis (Rücklin et al., 2011; Qu et al., 2016) are promising but their availability is still limited (Cunningham et al., 2014). As a result, histological descriptions are rare and only the general structure of acanthodian scale tissues is known, meaning the presence of a basal layer of bone, a middle layer of dentine, and with or

without a superficial layer of well-mineralised enamel-like tissue. This general structure is fairly generalised among early gnathostomes but the diversity of histological and fine anatomical features and growth patterns and processes is still understudied. Therefore, ontogenetic data can potentially provide clues on the phylogenetic conditions of acanthodian scales in comparison to scales described in other early gnathostomes.

Among the well-documented fossilised ontogenies of Acanthodiformes recorded so far, the best documented one is that of the middle Frasnian mesacanthid *Triazeugacanthus affinis* from the Escuminac Formation (Chevrinais et al., 2015a,b), approximately 380 million years old. Phylogenetically, the Acanthodiformes are considered either as stem osteichthyans within polyphyletic acanthodians (Brazeau, 2009; Davis et al., 2012), stem chondrichthyans in paraphyletic acanthodians (Zhu et al., 2013), or as a paraphyletic sister-group of chondrichthyans and some acanthodians (Burrow et al., 2016). Given the debated phylogenetic position and status of the Acanthodiformes, new histological and ontogenetic information are, therefore, pertinent. Recently, the ontogeny of *Triazeugacanthus* was described from a large number of specimens [315 complete or almost complete specimens (Cloutier et al., 2011b)], ranging in size from 4.51 to 52.72 mm, bridging larval, juvenile and adult stages, and showing exceptional preservation (Chevrinais et al., 2015a,b). This ontogeny demonstrates an increasing number of skeletal elements and a progressive extension of the squamation pattern as body size increases (Chevrinais et al., 2015b). However, all previous observations on *Triazeugacanthus* ontogeny dealt with either changes in gross anatomy (Cloutier et al., 2009; Chevrinais et al., 2015b) or chemical characterisation of anatomical elements (Chevrinais et al., 2015a), leaving the histological ontogenetic changes undescribed.

Taking advantage of this exceptional growth series of *Triazeugacanthus* specimens, we decided to use this species as a model to describe histological changes during on-

togeny at the individual (within an individual) and species (among individuals) levels. The main objectives of this study were to (1) describe histological and morphological changes of scales during ontogeny, (2) investigate the relationship between these changes and the individual and species ontogenies, (3) characterise the squamation pattern during ontogeny, and (4) discuss phylogenetic implications of histological and ontogenetic changes.

Institutional abbreviations: MHNM, Musée d'Histoire naturelle de Miguasha, Parc national de Miguasha, Québec, Canada; MNHN, Muséum national d'Histoire naturelle, Paris, France; UPMC, Université Pierre et Marie Curie, Paris, France; UQAR, Université du Québec à Rimouski, Québec, Canada.

3.4 Material and methods

Triazeugacanthus affinis comes from the middle Frasnian Escuminac Formation (Miguasha, Québec, Canada) (Cloutier et al., 1996). The studied material is housed in the MHNM collections.

Gross scale morphology was observed with a binocular microscope Leica MZ9.5 under water immersion, drawn using a camera lucida, and photographed with a Nikon D300. Samples for scanning electron microscopy (SEM) observations (six juveniles and one adult: Annexe XII) were cleaned with 5% acetic acid, dried, glued on an aluminum stub and either sputter-coated with a thin layer of gold or not, according to the type of SEM analyses. Images were obtained with a Cambridge Instruments Stereoscan 260 SEM (Leica, Cambridge, UK) at UPMC. Elemental composition analysis was performed on two specimens [one juvenile (MHNM 03-398) and one adult (MHNM 03-1497);

Annexe XII] using an INCA X-sight (Oxford Instruments) energy dispersive X-ray spectrometer coupled to a JEOL 6460LV SEM at UQAR. Each spectrum was acquired for 100 seconds of lifetime (process time 5, spectrum range 0–20 keV, 2000 channels) at an accelerating voltage of 20 kV. Quantitative optimisation of the system was done using copper as a standard. Elements were automatically identified and quantified in weight by the INCA software and results were normalised to 100%.

Scale histology was analysed on 17 complete specimens: two early juveniles, in which squamation covers the region below the dorsal fin without extension to the pelvic fins (Figure 21 A, 21 B and 21 F1-2), 11 late juveniles with incomplete squamation reaching the pectoral and pelvic fins (Figure 21 C, 21 D and 21 F3), and four adults (Figure 21 E and 21 F5) (Table 3). The ontogenetic stages are defined following the criteria established by Chevrinais et al. (2015b) (Table 3 and Annexe XII). Blocks were restricted to the specimens using a BROT 380V diamond saw, embedded in stratyl resin containing 2% Luperox K1 catalyst, and sectioned into *ca.* 2-mm thick sections from the head to the caudal fin, i.e. perpendicular to the antero-posterior body axis, with a Leica 1600 saw microtome. These transverse ground sections (n = 207, with an average of 12 sections per specimens) were reduced to a final thickness of 150-200 μm using abrasive disks, and then polished on both sides using alumina powder. Sections were glued with Araldite 2020 on glass slides and mounted with cover glass (Petropoxy 154 or Araldite 2020). Thin sections were observed under natural and polarised light with a binocular microscope (either Nikon Eclipse E600 POL or Leika DM LB2) and photographed with a microscope digital camera AmScope 10MP.

The size and shape of juvenile and adult body scales of *Triazeugacanthus* (Figures 21-

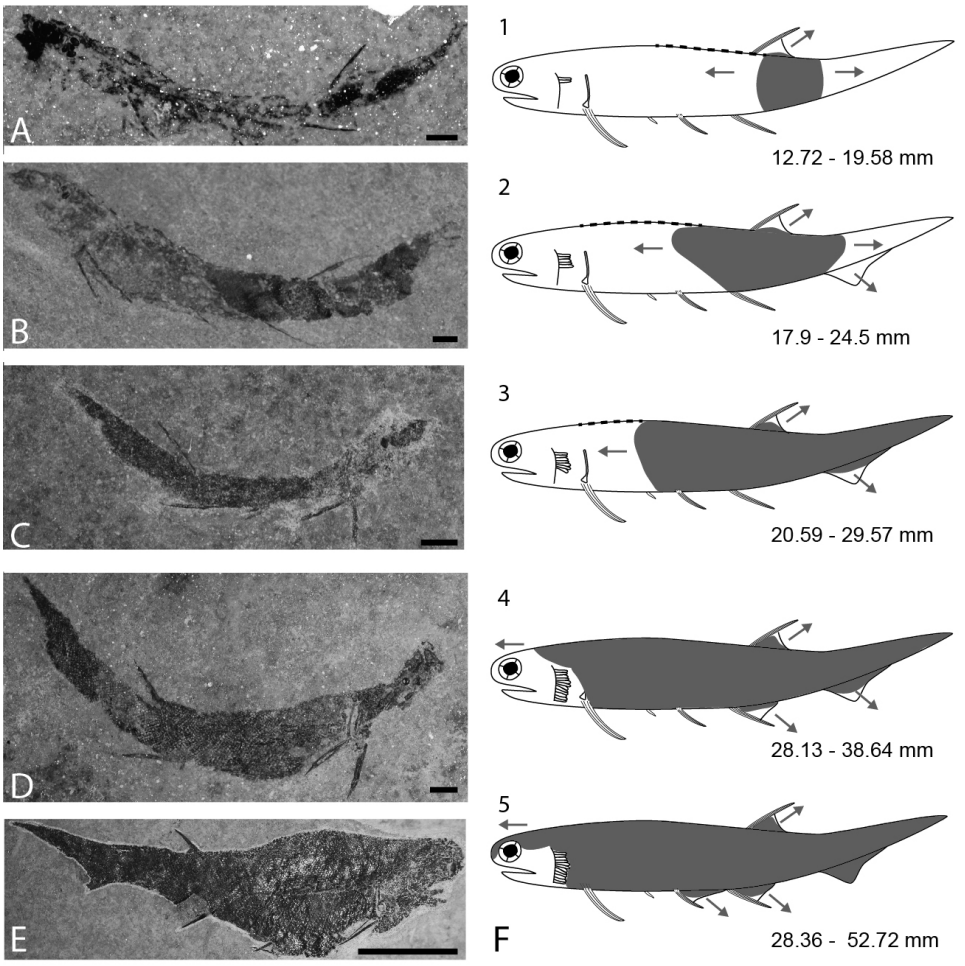

Figure 21: **Development of the squamation pattern in *Triazeugacanthus affinis***. A-E: Ontogenetic stages with the corresponding squamation pattern schematically represented in F (1 to 5), respectively. A: Early juvenile MHNM 03-401. B: Early juvenile MHNM 03-2684. C: Late juvenile MHNM 03-259. D: Late juvenile MHNM 03-435. E: Adult MHNM 03-1497. F: Development of the squamation (grey zones) in relation to size ranges (not to scale). Dashed lines indicates the presence of median ridge scales. Arrows indicate the direction of the squamation progression along the body and in the fin webs. Scale bars: A-D = 1 mm; E = 10 mm.

Table 3: **Characteristics of the ontogenetic stages of the acanthodian *Triazeugacanthus affinis* based on Chevrinais et al. (2015b).**

	Larvae	Early juvenile	Late juvenile	Adult
Total length range (mm)	4.5-20.3	12.72-24.5	20.59-38.64	28.36-52.72
Squamation cover	no scale	dorsal fin region	from pectoral fins to caudal	complete
Squamation extent (% of total length)	0	<30	30-90	90-100
Cumulative number of skeletal elements at maximum size	13	16	21	23
Number of specimens	31	26	52	79

24) were measured on SEM and ground section images using Adobe Photoshop 14.0 (Figure 25 A and Annexe XIII). Linear regressions between $\log_{10}$-transformed measurements of scale thickness and width were calculated for 74 juvenile (from two early and three late juveniles) and 144 adult scales (from three specimens). Mean thickness/width ratio of scales was compared between juveniles and adults as well as among body regions of juveniles and adults separately. Four body regions are defined based on previous descriptions of body regions in acanthodiforms (Zidek, 1985; Upeniece, 2011). In *Triazeugacanthus*, they are delimited by fin positions, which allowed similar measurements among specimens (Figure 22 A). The trunk region extends from the pectoral to the anal fins, the dorsal-anal region extends from the anterior limit of the anal fin to the posterior limit of the dorsal fin, the post-dorsal region extends from the posterior limit of the dorsal fin to the mid-length of the ventral web of the caudal fin

and the caudal region extends from there to the posterior extremity of the caudal lobe. Comparisons of scale parameters among body regions were performed using the non-parametric Kruskal-Wallis test and the Tukey's multiple comparisons test in R 3.0.2. Non-parametric tests were used because of the non-normality of the data.

The number of growth zones ["Wachstumszones" *sensu* Gross (1947)] in adult scales was recorded from images of ground sections. Data were taken in the dorsal-anal (region in which the squamation is initiated), post-dorsal and caudal regions. A Spearman correlation coefficient between the number of growth zones and the total length (TL) of specimens was calculated with R 3.0.2. The distances between two successive growth zones were measured in 16 adult scales from four adult specimens. Inter-growth zone distances have been plotted showing the growth variations among scales for "box-in-box" and superficial growth.

The data used to determine the squamation pattern (*i.e.*, progression of scale coverage during growth) were collected from 188 specimens of *Triazeugacanthus*, with no or minimal taphonomic bias (Chevrinais et al., 2015b).

3.4.1 Phylogenetic analysis

We included *Triazeugacanthus* and *Lodeacanthus* in a revised version of the data matrix recently published by Burrow et al. (2016). Burrow et al. (2016)'s data matrix included 262 characters: 253 characters from Zhu et al. (2013), two characters from Dupret et al. (2014), and six original characters (including one uninformative character). The data matrix of Zhu et al. (2013) took into account a great deal of the data from Davis et al. (2012) and Brazeau (2009). Our data matrix included the 261 characters

used by Burrow et al. (2016) plus six new characters (see Annexe XIV for the lists of characters and taxa as well as the data matrix). Twenty-nine characters and character states have either been rephrased, redefined, or repolarised (Characters 7-9, 11, 13, 18, 19, 26, 31, 51, 81, 104, 149, 160, 167, 177, 182, 190, 191, 195, 196, 209, 241, 242, 246, 252, 257, 258, and 260). Numerous modifications have been done throughout the matrix and more specifically on characters related to scales and histological features (Characters 8, 9, 11, 13, 260, 263-266); changes are given in the list of characters (Annexe XIV) and highlighted in the matrix. Coding has been validate for numerous taxa with a special emphasis on *Homalacanthus* (M.C. and R.C., pers. observ., and Annexe XV), *Cheirolepis* [M.C. and R.C., pers. observ., Annexe XVI and Giles et al. (2015a); Zylberberg et al. (2016)], *Miguashaia* (R.C., pers. observ.), *Gogonasus* (John A. Long, pers. comm.), and *Eusthenopteron* [R.C., pers. observ. and Porro et al. (2015)]. *Lodeacanthus* has been coded based on Upeniece and Beznosov (2002) and Upeniece (2011) as well as direct observation on the material in the Latvian Museum of Natural History (Riga). Unknown data ("?") represent 38.6% of the matrix, whereas not applicable codings ("-") represent 18.5% of the total characters coded.

The data matrix (79 taxa and 267 characters) was analysed with PAUP version 4.0b10 (Swofford and Sullivan, 2003). The matrix was rooted on two outgroups (Galeaspida and Osteostraci). All characters were unordered and unweighted. We used a heuristic search; the branch-and-bound search did not yielded trees. Maxtrees was set at 100,000. ACCTRAN and DELTRAN options were used. We performed 1,000 bootstrap replicates using heuristic searches. We set the maximum number of trees saved for each random sequence addition to 50,000.

3.5 Results

3.5.1 Scale morphology

Body scale width ranges from *ca.* 0.08 mm (12 scales/mm; juveniles) to 0.20 mm (5 scales/mm; adults), and scale thickness ranges from ca. 30 μm (juveniles) to 60 μm (adults). Ventral scales are broader than trunk scales (Figure 22 B).

Body scales are organised into oblique rows (Figure 22 C and 22 D) and are imbricated at one fifth of their length. The anterior region of a scale is overlapped by the elongated, posterior region of the preceding scale. The dorsal and ventral margins are anteriorly overlapped by the neighbour lateral scales, while they overlap the latter posteriorly (Figure 23 A and 23 B).

Trunk scales have a diamond-shape crown with a rounded angular anterior margin and a pointed posterior process. Such morphology is observed in juveniles and adults (Figure 22). The crown and the base, delimited by a poorly-developed neck (Figures 23, 24 A, 24 C and 25 A), are of equal depth in juveniles and adults (Figure 23 D-23 F). The base is flat in juveniles and weakly convex in adults (Figure 23). The crown surface is flat in juveniles and adults (Figure 23 D-23 H). In juvenile specimens, the upper surface is smooth and homogeneous. In some ground sections of juvenile specimens (*e.g.*, MHNM 03-210), this surface seems to be cover by a thin organic dark layer. Superficially, this layer covers scale boundaries (Figure 22 E unlike in Figure 22 F). We interpret this feature as potential remains of the epidermal cover (Figure 22 E). In adult scales, the surface is ornamented with irregularly spaced microtubercles as revealed by SEM (Figure 24 D and 24 F).

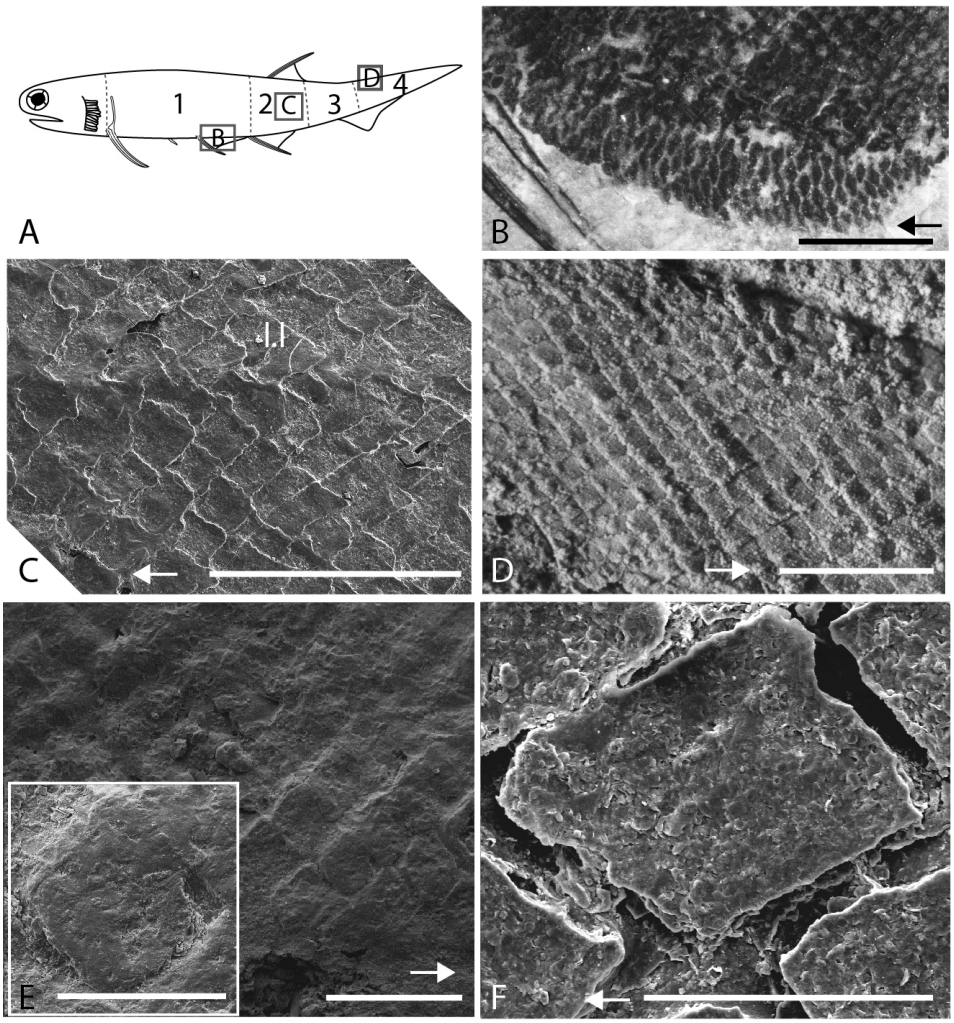

Figure 22: **Variation of squamation along the body of *Triazeugacanthus affinis*.** A: Schematic representation of an adult *Triazeugacanthus affinis* with position of the four body regions. Squared regions are detailed in B, C and D. B: MHNM 03-1550, detail of ventral scales. C: MHNM 03-1819, SEM showing scale alignment in the region below the dorsal fin (2). D: MHNM 03-1497, scale alignment in the caudal region whiten with ammonium chloride. E: juvenile MHNM 03-2631, SEM showing the organic layer ("epidermal cover") covering the trunk scale ornementation. F: juvenile MHNM 03-1819, SEM of a trunk scale. Arrows point forward. Body region 1, trunk; 2, dorsal-anal; 3, post-dorsal; 4, caudal. Scale bars: A = 5 mm; C = 500 μm; D = 1 mm; E = 250 μm; E (close-up), F = 100 μm.

3.5.2 Scale histology

In juvenile 30 μm-thick scales, ground sections reveal a homogeneous tissue composition (Figure 23 H). Cell lacuna and canaliculi were not identified in the main tissue; these features characterize either acellular bone or dentine (Figure 23 H). The upper surface is not covered with a well-mineralised tissue.

In contrast to juveniles, ground sections in adult 60 μm-thick scales reveal three distinct tissues (Figure 23 D-23 G). The following three tissues are found from the deeper to the upper surface: a fibrillar and homogeneous tissue resembling acellular bone (= type 1), a fibrillar, thick and well-mineralised tissue (= type 2), and a thin, well-mineralised homogeneous tissue, organised into several, thin, superimposed layers (= type 3) (Figure 23 D). None of the sections showed vascular canals. Type 1 tissue represents the main tissue forming the so-called basal plate. Neither osteocyte lacunae nor canaliculi are observed. This bone-like tissue is found at the base of the scale, and in the peripheral parts of the scale. In the lateral and posterior parts of the scales, longitudinal fibers oriented perpendicularly to the scale margin are similar to the Sharpey's fibers and are therefore interpreted as collagen bundles (Figure 23 D-23 F). Type 2 tissue occupies mainly the central part of the scale, above the basal plate and is less developed in the anterior and posterior regions (Figure 23 D, 23 E and 23 G). It is characterised by the presence of numerous canaliculi, often branched and running mostly perpendicular to the upper and lateral surfaces of the scales. The proximal extremity of the canaliculi exhibits cell lacuna. These canaliculi, interpreted as dentine canaliculi and cell lacunae, represent the space where odontoblast bodies were located in the scale. This tissue organisation with ascending canaliculi, putative horizontal connecting canaliculi and isolated odontoblasts is interpreted as mesodentine (Figure 23 E and 23 G). Up to three levels of mesodentine cells (*i.e.*, odontoblast cavities and canaliculi) have been

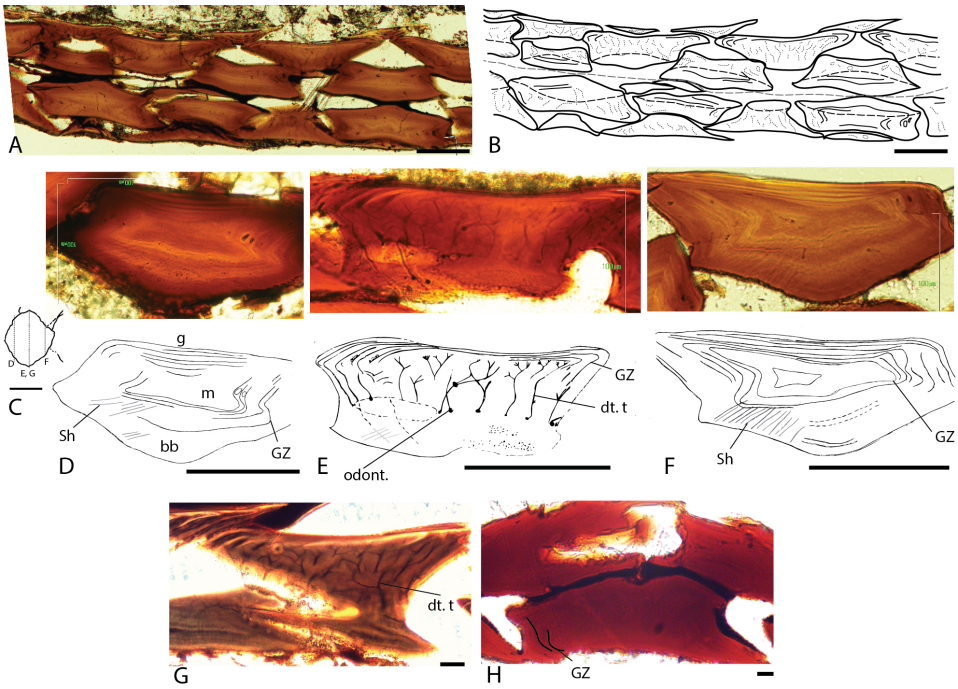

Figure 23: **Transverse ground sections of *Triazeugacanthus affinis* scales.** A-B: MHNM 03-2620, scale arrangement on both sides of the specimen showing the antero-posterior and lateral overlapping of the scales. B: MHNM 03-2620, interpretative drawing of A. The grey dashed line indicates the boundary between both sides; dark dotted lines indicate dentine tubules; dashed lines indicate the boundary between the crown and the basal plate. C: Diagram showing position of ground sections D-G in a body scale. D-F: Ground sections through the anterior, middle, and posterior levels of the scale and their interpretative drawings. D: MHNM 03-1817, the anterior region of the scale is mostly composed of acellular bone with embedded Sharpey's fibers, a small, centrally located mesodentine layer, and thin layers of well-mineralised ganoine. E: MHNM 03-2620, the central region of the scale shows a basal plate of acellular bone, a thick middle region housing numerous ascending canaliculi and branched canaliculi, characteristic of the mesodentine, and a ganoine covering best visible in lateral regions, showing the growth zones. F: MHNM 03-1817, the posterior region of the scale is organised similarly to the anterior region of the scale. G: MHNM 03-2620, central region of the scale showing three dentine layers delimited by osteocyte cavities and tubules; each layer corresponds to a growth zone. H: juvenile MHNM 03-701, transverse section through the scales of a juvenile specimen showing a homogeneous histological composition. Scale bars: A-G, I = 100 μm; G = 20 μm; H = 10 μm.

observed in some adult scales; each level corresponding to a growth zone (Figure 23 G). There is a clear boundary between Type 2 and Type 3 tissues (Figure 24 A-24 C). Type 3 tissue, covering the upper surface of the scale, is well-mineralised and organised into several, thin, superimposed layers (Figures 23 F and 24 B). This tissue is birefringent and lacks cell lacuna and canaliculi. SEM observations reveal that this superficial layer is composed of parallel crystallites oriented perpendicularly to the scale surface forming rod-like structure (Figure 24 E); this organisation suggests that collagen fibers are absent from the matrix. Microtubercles (*ca.* 2.5 μm in diameter) of various shapes are irregularly distributed on the surface of this tissue (Figure 24 D and 24 F). Individual crystallites are too small to be clearly recognisable. The mineral of the scale tissues is chemically composed of carbonate-fluorapatite (calcium, phosphorus and fluorine; Annexe XVII).

3.5.3 Scale ontogeny

Triazeugacanthus scales show two distinct growth patterns: "box-in-box" and superpositional. The "box-in-box" pattern is recognizable in the central part of the scales. It is composed of acellular bone and mesodentine, and reveals concentric addition of layers of bone and dentine matrix from the primordium towards the periphery, that are interpreted as growth zones (Figure 23 D-23 G). Growth zones appear as alternation of thin dark and thick light layers (Figure 24 B and 24 C). This incremental pattern is clearer in the periphery (Figure 23 E) than in the center of the scales. Once the "box-in-box" growth of the bony and dentine tissues is mostly achieved superficially, the deposition of a well-mineralised tissue starts at the upper surface of the scales (Figure 24 B).

The relationship between the thickness and width of scales differs between juvenile

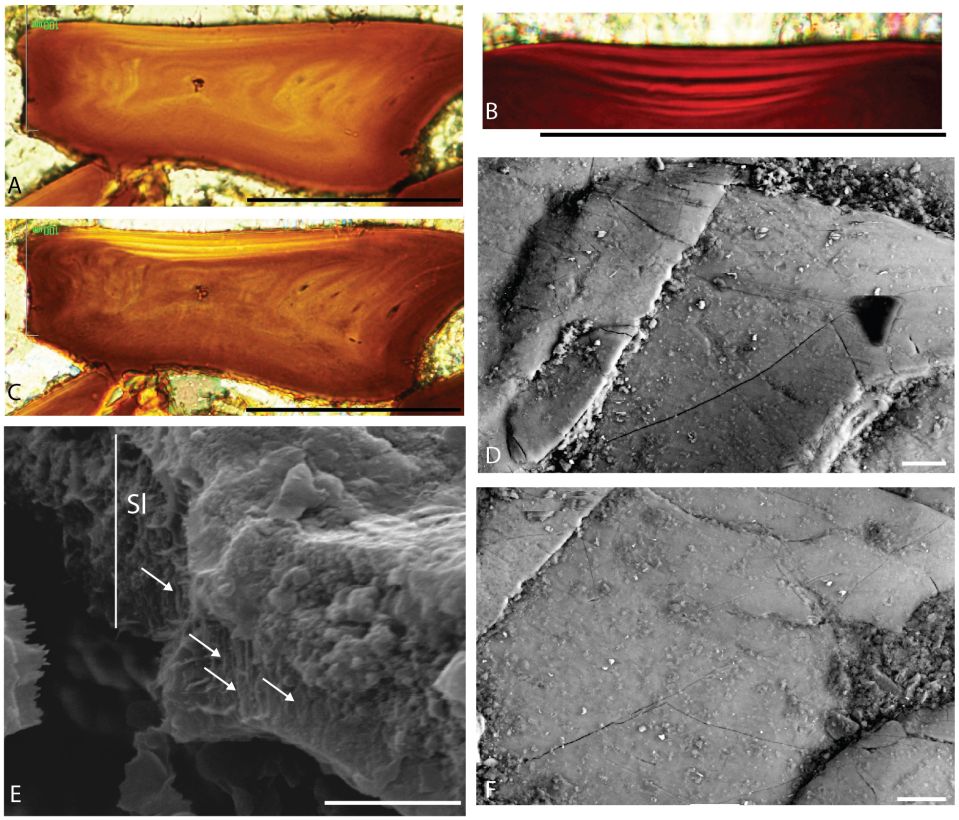

Figure 24: **Superficial hypermineralised tissue of *Trizeugacanthus affinis* scales.** A, C: MHNM 03-1817, ground section in natural (A) and polarised (C) light. B: MHNM 03-1817, close-up of the superficial multilayered ganoine. D, F: MHNM 03-1460, SEM of the microtubercles of the ganoine surface. E: MHNM 03-1699, SEM showing the ganoine crystallites (arrows). Scale bars: A-C = 100 μm; D = 2 μm; E and F = 20 μm.

and adult *Triazeugacanthus* (Figure 25 B). Linear regressions are significant but have a weak coefficient of determination (R^2 = 0.29, *p-value* = 3.489e^{-7} in juveniles; R^2 = 0.17, *p-value* = 1.93e^{-7} in adults) revealing a high degree of intra- and inter-individual variation (Figure 25 C). This difference is visible in ground sections, reflecting an ontogenetic change in the shape of the basal plate of the scales (Figures 23 and 25 A). The thickness/width ratio differs significantly between juveniles and adults (Figure 25 C: K = 49.96, *p-value* = 1.57e^{-12}) and among body regions in juveniles (Figure 25 D: K = 9.53, *p-value* = 0.02), whereas it is similar among body regions in adults (Figure 25 E: K = 1.45, *p-value* = 0.48). Pairwise comparisons of this ratio among body regions of juveniles show significant differences between the trunk and caudal regions (*p-value* = 0.007) and between the dorsal-anal and caudal regions (*p-value* = 0.04) (Figure 25 D).

3.5.4 Individual and species ontogeny

Individual ontogeny, *i.e.* the growth of a single individual, is recorded from the growth zones observed in scale sections. The bony tissues display zones with relatively fast (clear) and slow (dark) growth (Figure 23 D-23 F). Two growth zones are already present in the scales of the smallest (youngest) available juvenile specimen MHNM 03-701 (33.18 mm TL; Figure 23 H). In all adult scales studied, the number of growth zones range from three to eleven clear zones (Figure 23 D-23 F). The strong positive correlation (r_s = 0.85, *p-value* = 0.008) between the number of growth zones in scales and the total length of the adult specimens reveals a clear relationship between individual growth (number of growth zones) and species growth (body size of specimens) (Figure 25 F). Variation in the thickness of growth zones associated to the "box-in-box" growth indicates non proportional deposition of these tissues, even within individuals (Annexe XVIII). In contrast, growth of superficial layers is more constant and displays

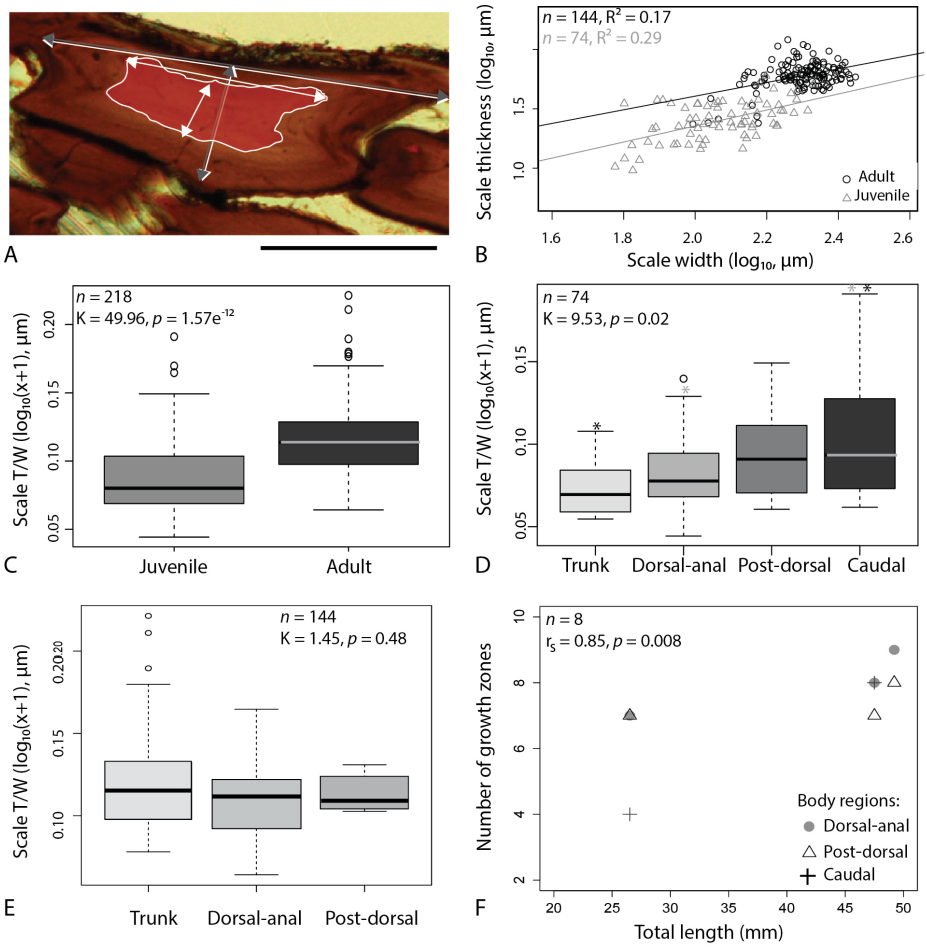

Figure 25: **Individual and species ontogeny in *Triazeugacanthus affinis*.** A: adult MHNM 03-1817, scale section of an adult specimen with superimposition (white lines) of the contours of a sectioned scale from a juvenile specimen (MHNM 03-701) [Annexe XIII for measurements (grey and white arrows)]. B: Scale thickness/width relationship in juvenile and adult specimens. C: Side-by-side boxplot showing thickness to width scale ratio in juvenile and adult specimens. D, E: Side-by-side boxplot showing thickness to width scale ratio in various body regions of juvenile D and adult E specimens. F: Number of growth zones per scale in function of the total length in various body regions of adult specimens. The regions from which measurements were taken are shown in Figure 22 A. Asterisks refer to significant differences between two groups. Scale bar: A = 100 μm.

weaker variation in the thickness of successive layers than observed in the scale thickness (Annexe XVIII).

3.5.5 Squamation pattern

Data from 188 complete *Triazeugacanthus* specimens of various sizes and ontogenetic stages allowed accurate description of the squamation pattern (Figure 21). From 12.72 to 19.58 mm TL, juvenile specimens possess a single, small patch of scales on the body, located below the dorsal fin spine, suggesting that scales initiate first in this region (Figure 21 A and 21 F1). This patch develops at the mid-height of the body, but precise position in earliest stages of squamation is difficult to assess because the body outlines are poorly defined (Figure 21 A). Simultaneously, scales of the dorsal fin web and of the caudal lobe start to develop; scales are added proximo-distally and organised in multiple rows along the base of the fins. Anteriorly to the progression of this main body squamation, there is a median row of paired small scales that developed on the dorsal edge of the body from posterior to anterior forming a dorsal mid-line. Their position clearly anterior to the anterior edge of the main squamation and their shape show that they likely develop earlier than the scales from the main squamation (Figure 21 dashed line and Annexe XIX). In juvenile individuals between 17.90 and 24.50 mm TL, scales cover most of the posterior half of the trunk, which indicates that squamation extends anteriorly and posteriorly from the initial region (Figure 21 B and 21 F2). The squamation progresses first dorsally then ventrally. In 20.59 to 29.57 mm TL specimens, the squamation has expanded anteriorly towards the head, dorsally towards the dorsal fin web and posteriorly towards the caudal lobe (Figure 21 C and 21 F3). In individuals between 28.13 and 38.64 mm TL, the caudal fin and the posterodorsal part of the head region are scaled (Figure 21 D and 21 F4). In adult specimens from 28.36

to 52.72 mm TL, the squamation is complete on the body, covers the head dorsally, and scales are present on the pelvic, anal, dorsal and caudal fin webs (Figure 21 E and 21 F5). None of the adult specimens, even the largest one (52.72 mm-TL, MHNM 03-1107), display scales associated to the pectoral and intermediate spines. Dorsal mid-line scales show a ridge at the mid-width of the scale (Annexe XIXC) suggesting that the paired small scales may have fused during development to form a dorsal mid-line of median ridge scales as observed in some basal osteichthyans (Gardiner, 1984; Jarvik, 1996; Arratia, 2009).

In adult *Triazeugacanthus*, 114 scales are counted on the longitudinal row at mid-height of the body, along the antero-posterior axis from the scapula to the posterior extremity of the caudal fin. At the deepest part of the body (*i.e.*, between the dorsal and anal fins) a total of 15, 17 and 21 scale rows are present in early juveniles (incomplete squamation), late juveniles (nearly complete squamation) and adults, respectively.

3.5.6 Phylogenetic analysis

Burrow et al. (2016) published the most recent phylogenetic analysis to investigate the phylogenetic status of acanthodians in relation to gnathostome interrelationships. Our phylogenetic analysis of the revised data matrix (see Annexe XIV) provided 100000 equally parsimonious trees at 711 steps (CI = 0.3952; RI = 0.7947; rescaled CI = 0.3141). Interrelationships among acanthodian taxa as well as the phylogenetic position of acanthodians among gnathostomes are recovered in the strict (Annexe XX), Adams (Annexe XX) and 50% majority rule consensus (Figure 26) trees; uncertainties in the topologies come primarily from placoderm and basal osteichthyan interrelationships (Figure 26 and Annexe XX).

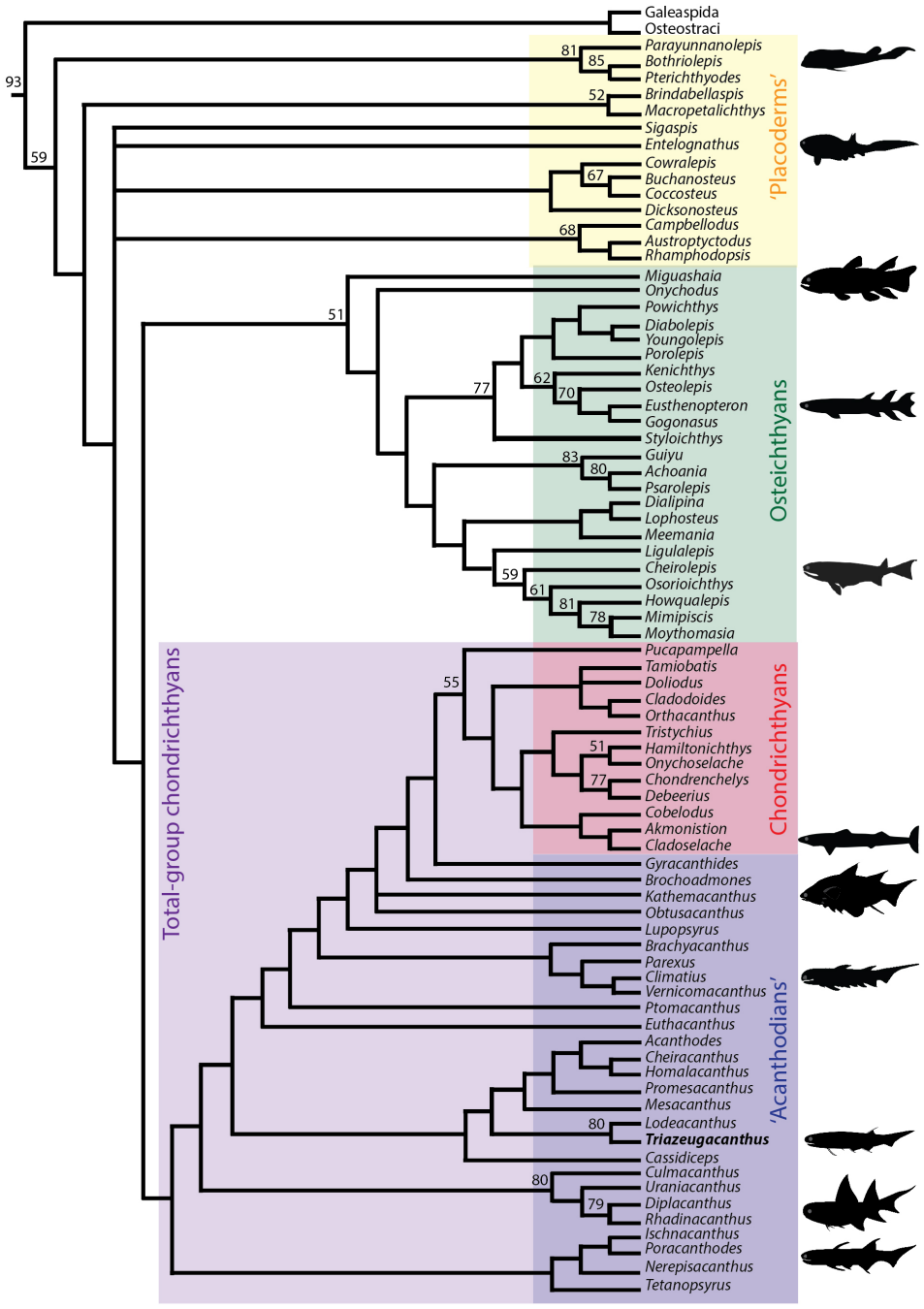

Figure 26: **Phylogenetic relationships among early gnathostomes.** 50 % majority rule consensus tree based on 100 000 trees at 711 steps (79 taxa, 267 characters). Numbers on branches show percentage bootstrap support.

As proposed by Brazeau (2009), Davis et al. (2012) and Burrow et al. (2016), the "Acanthodii" are considered to be paraphyletic with respect to the Chondrichthyes. Ischnacanthiformes and Diplacanthiformes are basal stem taxa. *Triazeugacanthus* is considered as the sister-group of *Lodeacanthus* in a monophyletic Acanthodiformes. The *incertae Euthacanthus*, the *incertae* gnathostome *Ptomacanthus*, climatiids, the Lockhovian MOTH *Lupopsyrus*, the so-called "putative" stem chondrichthyan *Obtusacanthus* and *Kathemacanthus*, the Lockhovian MOTH *Brochoadmones*, and the Early Carboniferous *Gyracanthides* are considered as stem chondrichthyans. It takes 22 supplementary steps to move the clade including acanthodiforms, ischnacanthiforms and diplacanthiforms as stem-osteichthyans in a topology similar to that proposed by Davis et al. (2012).

3.6 Discussion

Previous to this study, the scale structure of *Triazeugacanthus* was poorly known. Here, owing to the large number of *Triazeugacanthus* scales sectioned we provide accurate description of the histology and spatial organisation of the scale tissues and their changes during ontogeny. The growth series of *Triazeugacanthus affinis* shows clearly that (1) the histological composition of the scales increases in complexity during ontogeny from a single, homogeneous tissue in juveniles to three tissues in adults including the well-mineralised superficial layer, (2) the central part of the scale grows according to a "box-in-box" pattern and the superficial part grows by superposition of well-mineralised layers, (3) the shape of the scales varies among body regions and ontogenetic stages, (4) the number of growth zones in scales is positively correlated with the total length of individuals, and (5) the squamation is initiated in the mid-body region, at the level of the dorsal fin, then spreads bidirectionally. In addition, this histo-

logical investigation of *Triazeugacanthus* yielded to the reinterpretation of certain scale characteristics that have been taken into consideration in a revision of the phylogenetic analysis of gnathostomes with a special emphasis on acanthodians.

In order to discuss the histological characters observed in *Triazeugacanthus*, we will first discuss some of the major results from the phylogenetic analysis of the revised data matrix from Burrow et al. (2016). The original objective of this re-analysis was to include two new taxa in Burrow et al. (2016)'s data matrix, *Triazeugacanthus* and *Lodeacanthus* [a species suggested as closely related to *Triazeugacanthus* (Upeniece, 2011; Hanke and Davis, 2012)], in order to discuss the histological observations in a phylogenetic context. However, in the process of completing the data matrix, some characters were redefined, some characters were added, the polarity of certain characters changed, and the coding of acanthodian and non-acanthodian taxa were revised and completed. As a result of these modifications, the new consensus topology differs slightly from Burrow et al. (2016) but agrees with the overwhelming tendency to consider acanthodians as paraphyletic.

Only four recent phylogenetic analyses addressed specifically the phylogenetic status of acanthodians (Brazeau, 2009; Hanke and Davis, 2012; Davis et al., 2012; Burrow et al., 2016). In three of these analyses, acanthodians are recognised paraphyletic; the acanthodian paraphyly is also recognised in studies focusing on gnathostome interrelationships with a special emphasis on placoderms (Zhu et al., 2013; Long et al., 2015). In both Brazeau (2009) and Davis et al. (2012), some acanthodians are considered as stem gnathostomes and stem chondrichthyans and while acanthodiforms are stem osteichthyans. Burrow et al. (2016) proposed that acanthodians are solely stem chondrichthyans; this conclusion had already been reached in part prior to the phylogenetic analysis in Burrow and Rudkin (2014). Burrow and Rudkin (2014) had sug-

gested that acanthodians were either stem chondrichthyans or the monophyletic sister-group of chondrichthyans. Chondrichthyan affinities were also suggested by Brazeau and Friedman (2015) and Giles et al. (2015b). On the other hand, Hanke and Davis (2012) suggested a monophyletic Acanthodii sister-group to osteichthyans and Dupret et al. (2014) suggested a monophyletic Acanthodii sister-group to chondrichthyans; the monophyly had repeatedly been suggested for more than 40 years [e.g. (Miles, 1973b; Long, 1986; Janvier, 1996b; Hanke and Wilson, 2004)].

As in most analyses using large data matrix for fossil taxa, the high proportion of unavailable coding (both "?" and "-") is most likely a major source of phylogenetic ambiguities: 48.3% [47 taxa and 134 characters; (Brazeau, 2009)], 49.6% [60 taxa and 138 characters; (Davis et al., 2012)], 57.1% [79 taxa and 267 characters; this study], 60.1% [77 taxa and 262 characters; (Burrow et al., 2016)], 61.5% [75 taxa and 253 characters; (Zhu et al., 2013)]. Although we are dealing with more than 50% of missing data, we recovered a phylogenetic signal showing that acanthodians are stem chondrichthyans. The main differences between our topology and that reported by Burrow et al. (2016) come from the order of "acanthodian" taxa along the stem. In our topology, climatiids are closer to putative chondrichthyans (*i.e. Brochoadmones*, *Kathemacanthus*, *Obtusacanthus*, *Lypopsyrus*) rather than being at the base of the clade (Burrow et al., 2016). Furthermore, as suggested by Brazeau and Friedman (2015), *Ptomacanthus* is closer to the chondrichthyans than the main acanthodian clade.

Considering the large size of the data matrices, very few characters were dealing with the morphology, histology, growth and organisation of the scales. Brazeau (2009) used 12 characters (4-6, 8-16) out of 134 characters, Davis et al. (2012) used 11 characters (4-6, 8-15) out of 138 characters, and Burrow et al. (2016) used 16 characters (4-6, 8-15, 139, 143, 144, 260 and 262) out of 262 characters. We used 20 characters (rel-

ative to scales) out of 267. Scale histology characters 8 (condition of scale growth pattern with polyodontode or monodontode), 9 (concentric growth pattern), 260 (areal growth pattern) were redefined (see List of characters Annexe XIV). Polarity of scale characters 8 (polyodontode or monodontode), 11 (body scale profile), and 13 (flatten base of body scales) were changed. Characters 263 (appositional growth pattern), 264 (hypermineralized superficial layer of scale), 265 (type of hypermineralized tissue), and 266 (single- or multi-layered enamel) were added. Fourteen out of the 20 scale characters are relevant for acanthodians. The deletion of anyone of these 14 characters has a significant impact on the resulting topology (Annexe XXI). The deletion of 12 of these 14 characters [5 (dentine types), 8 (poly-/monodontode), 9 (box-in-box growth), 11 (profile), 12 (bulging base), 13 (flat base), 14 (flank scale alignment), 160 (areal growth), 263 (appositional growth), 264 (superficial hypermineralized tissue), 265 (enamel/enameloid), and 266 (single/multi-layered enamel)] makes the acanthodians and putative chondrichthyans as a monophyletic group closely related to chondrichthyans (Annexe XXII). The number of steps to obtain the monophyly of the acanthodians plus putative chondrichthyans varies between 700 and 710 (Annexe XXII), which is a minor difference from the 711 steps of the complete analysis. The deletion of two of the fin spines characters [character 127 (anal fin spine) and character 128 (paired pectoral fin spines)] also led to the monophyly of the acanthodians, with trees being only one and four steps shorter, respectively.

In addition to these phylogenetic characters, we compiled the Annexe XXIII from previously described scales in 43 acanthodians (including putative chondrichthyans), four early chondrichthyans and four early osteichthyans.

3.6.1 Morphology and histology of scales

Typically, acanthodian scales are rhombic with little or no overlapping, and organized in oblique rows [character 14(1)], each scale being attached to the neighbour scales and to the underlying dermis by Sharpey's fibers (Denison, 1979). Their crown surface is often ornamented and their neck is clearly constricted (Denison, 1979) [character 11(1)]. In contrast to the general condition, the scales of *Triazeugacanthus* are diamond-shaped, they only slightly overlap, the crown surface is smooth with subtle microtubercles, the neck is poorly developed and the base is convex [in contrast to the flat base reported by Burrow and Young (2005)] [characters 12(1), 13(0)]. The number of flank scales per millimetre in *Triazeugacanthus* fits within the acanthodiform range (2-16 scales/mm) which is higher than in most other acanthodians (Annexe XXIII).

Acanthodian scales are commonly described as composed of two tissues: a deep basal plate formed either by acellular or cellular bone and a crown region composed of multiple layers of dentine (Annexe XXIII) (Sire et al., 2009) (character 4). In most acanthodians, the basal plate is primarily acellular or occasionally cellular, whereas the crown is composed of mesodentine with a few exceptions in which it is composed of orthodentine (Annexe XXIII). In previous descriptions (Annexe XXIII), the composition of the crown was frequently referred simply as dentine. The distinction between the two types of dentine found in acanthodians (orthodentine and mesodentine; the semidentine being restricted to placoderms; character 5) takes into account the relative position of the cell bodies or odontoblasts. Mesodentine is characterized by cell bodies embedded within the dentine matrix, whereas in orthodentine all cell bodies are located at the matrix surface, along the walls of vascular canals or pulp cavities (Sire et al., 2009). The crown of *Triazeugacanthus* scales is clearly composed of mesodentine. Narrow vascular canals, even if they are absent in the crown, could be present in the basal plate

of some acanthodiforms. In *Acanthodes bronni*, the scale structure is characterised by the presence of dentine canaliculi in both the crown and the basal plate, with a clear boundary between the two zones (Gross, 1947). However, in acanthodiforms (in which scales are small in comparison to other acanthodians), the canal network at the base is reduced to thin tubules where remnants of a vascular plexus are present in the center of the scale (such as in *Halimacanthodes*) (Burrow et al., 2012). This absence of nutrient supply through vascularisation could explain the presence of mesodentine, with a rich network of long canaliculi. *Triazeugacanthus* shows the typical *Acanthodes*-type defined by Valiukevičius (1995); this condition could be considered derived among acanthodians.

Based on the topology, there seems to be no strong phylogenetic signal associated to the presence of the different types of dentine among acanthodian taxa. This is in contrast to Davis et al. (2012) who suggested that mesodentine was found at the base of a large clade [“acanthodians” + [[“acanthodians” + chondrichthyans] + [“acanthodians” + osteichthyans]]], and also Brazeau (2009), who suggested that mesodentine was only characteristic of the clade [“acanthodians” + osteichthyans]. The type of dentine might be phylogenetically informative at a higher phylogenetic level, but the coding of this character is certainly in need of revision.

Among acanthodians, the scale surface is either smooth (unornamented) or ornamented with longitudinal or radiating ridges, which cover either the complete surface of the scales or are limited to the anterior edge. At the base of the total-group chondrichthyan, scales have primarily a ridged crown surface as the main condition in ischnacanthiforms (some species do have a smooth surface Annexe XXIII) and diplacanthiforms. Based on our topology, the smooth surface is most likely independently derived in acanthodiforms and *Lupopsyrus*; the smooth surface also occurs in some climatiids and early

ischnacanthids (Richter et al., 1999). With the exception of *Lupopsyrus*, so-called putative chondrichthyans and *Gyracanthides* have an ornamented scale surface owing to their polyodontode condition [character 8(0)].

The smooth scales of acanthodians are occasionally covered by minute superficial microtubercles (Burrow, 1995; Märss, 2006; Burrow et al., 2012). Such microtubercles are also present on the scale surface of some osteichthyans (*e.g.* *Polypterus* and *Lepisosteus*) (Sire, 1989; Richter and Smith, 1995; Märss, 2006). In adult *Triazeugacanthus*, the crown surface is ornamented with microtubercles, similar to those described on the crown surface of the scales in three acanthodiform taxa [*i.e.* *Acanthodes* sp., acanthodiform indet. (Derycke and Chancogne-Weber, 1995) and *Halimacanthodes ahlbergi* (Burrow et al., 2012)] (Annexe XXIII). The presence of these microtubercles has been considered as characteristic of ganoine (Schultze, 1966; Ørvig, 1967; Gross, 1971; Schultze, 1977; Richter and Smith, 1995; Märss, 2006; Schultze, 2015). However, in order to conclude to the presence of ganoine in *Triazeugacanthus* histological and SEM investigations were necessary.

The crown surface of acanthodian scales is generally covered by a hypermineralised tissue (Annexe XXIII) (characters 264, 265, and 266). The identification of this hypermineralised tissue is still controversial since it was interpreted either as enamel, enameloid or ganoine (Richter and Smith, 1995; Friedman and Brazeau, 2010; Schultze, 2015). Enamel is a homogeneous tissue that does not include collagen fibrils nor cells during its development (Schultze, 2015). The mature enameloid differs from the enamel by the presence of a loose network of collagen fibres resulting in less ordered mineral crystals (Sire et al., 2009). The mature ganoine is a non-collagenous tissue and differs from dental enamel by the presence of multiple layers (Sire et al., 2009; Schultze, 2015); single-layered ganoine is accepted by some authors (Richter and Smith, 1995).

Ganoine is considered as homologous to enamel by some others (Sire et al., 1987; Sire, 1995; Zylberberg et al., 2016). Ganoine is known unambiguously in early actinopterygians (Burrow, 1994; Richter and Smith, 1995; Zylberberg et al., 2016) as well as extinct and extant polypterids and lepisosteids (Richter and Smith, 1995; Sire et al., 2009). As a result, the presence of ganoine has been frequently considered as an actinopterygian synapomorphy (Schultze, 1977; Patterson, 1982; Cloutier and Arratia, 2004; Schultze, 2015). However, the identification of ganoine in acanthodians has been suggested to invalidate this character as an actinopterygian synapomorphy (Richter and Smith, 1995; Friedman and Brazeau, 2010). Only few reports have suggested the presence of ganoine in acanthodians, and its proper identification remains questionable. In one species of acanthodians, referred to *Acanthodes* sp. 4 (Derycke and Chancogne-Weber, 1995), ganoine was identified solely on the presence of superficial microtubercules. Burrow et al. (2012) identified the presence of ganoine in the scales of *Halimacanthodes ahlbergi* based on both the presence of superficial microtubercules and the multi-layered nature of the tissue. Richter and Smith (1995) suggested the presence of enamel-like ganoine in a scale identified as "*Cheiracanthoides*" sp. based on the multi-layered superficial tissue which lacked the microtubercules. In adult *Triazeugacanthus* scales, the superficial layer consists of crystallites organised perpendicularly to the scale surface. However, these crystallites were too small to be clearly recognisable, a condition similar to that observed in the Late Silurian "*Cheiracanthoides*" sp. (Richter and Smith, 1995). Richter et al. (1999) mentioned that an unclear or non-existent boundary between the dentine and the superficial hypermineralized layer seems to be the commonest condition in acanthodian scales. This unclear boundary is an additional argument that these authors used to question the clear identification of ganoine in acanthodians. However, the boundary between the mesodentine and the hypermineralised tissue in the scales of *Triazeugacanthus* is clear and distinct. Therefore, we interpret the superficial hypermineralised tissue on the body scales of *Triazeuga-*

canthus as ganoine based on the presence of microtubercles at the crown surface, the multi-layered structure, the perpendicular orientation of the mineral crystallites to the scale surface suggesting that collagen fibers are not present in the matrix (Qu et al., 2013), and the clear boundary with the mesodentine. As far as we know, this makes it the first unambiguous identification of ganoine in an acanthodian.

As proposed by Valiukevičius (1995) and Valiukevičius and Burrow (2005), various groups of acanthodians shared histological similarities of their scales. These similarities led to the recognition of four types of scales: the *Nostolepis*-type (1) (in climatiiforms), the *Diplacanthus*-type (2) (in diplacanthiforms), the *Poracanthodes*-type (3) (in ischnacanthiforms), and the *Acanthodes*-type (4) (in acanthodiforms). Based on our topology, a sequence of *Poracanthodes*-type – *Diplacanthus*-type – *Acanthodes*-type – *Nostolepis*-type would form a transformation series precursor to the polyodontode scales found in putative chondrichthyans *Gyracanthides* and chondrichthyans. However, the phylogenetic distribution of some of the different characteristics (acellular or cellular base, vascularised or avascularised base, orthodentine or mesodentine, presence or absence of enamel-like tissue) defining these four types is not congruent with our topology. The distribution of dentine and hypermineralized tissue types is homoplastic; thus suggesting that these scale types might be informative to identify acanthodian groups but poorly informative phylogenetically.

One would expect that closely related species are more likely to share similar histological composition. *Triazeugacanthus* is considered as the sister-group of *Lodeacanthus* (Upeniece, 1996, 2011; Hanke and Davis, 2012, this study) which is reflected in part by some histological similarities (*e.g.* mesodentine and acellular bony base) (Annexe XXIII) (Upeniece, 2011). However, major histological differences are also observed: *Lodeacanthus* scales show the presence of vascular canals and a mono-layered hyper-

mineralised superficial tissue, while *Triazeugacanthus* scales lack vascular canals but have multi-layered ganoine.

At a higher phylogenetic level, a few histological scale characters are suggestive of phylogenetic affinities. For example, the presence of ganoine in *Triazeugacanthus* would suggest a phylogenetic affinity with actinopterygians. However, as we have demonstrated it would require minimally 22 steps to place the acanthodiforms [and related taxa as suggested by Brazeau (2009) and Davis et al. (2012)] as the sister-group to osteichthyans, while it would require either 26 or 39 additional steps to place *Triazeugacanthus* alone as the sister-group of actinopterygians or basal osteichthyans, respectively. The presence of ganoine alone cannot support a close relationship between some acanthodians and actinopterygians. An additional character shared by *Triazeugacanthus* (Béland and Arsenault, 1985; Chevrinais et al., 2015b), numerous acanthodiforms, and osteichthyans is the presence of three pairs of otoliths (Schultze, 1988, 1990). Schultze (1988, 1990) considered the presence of three pairs of otoliths as a synapomorphy shared by acanthodians (acanthodiforms) and osteichthyans. However, the rarity of information concerning the presence of this character would not have an impact on the resolution of the tree. For instance, none of the osteichthyan taxa used in this phylogenetic analysis could be coded for the presence of otoliths while *Triazeugacanthus*, *Homalacanthus*, *Mesacanthus*, and *Acanthodes* would have been coded as sharing three pairs of otoliths (Schultze, 1990). Similarly the paucity of endochondral information for acanthodian taxa limits potentially our phylogenetic resolution of this group (Brazeau and Friedman, 2014).

3.6.2 Assessment of individual and species ontogeny from scale growth pattern

The abundant material of *Triazeugacanthus* alowed us to evaluate both ontogenetic changes within a single individual by looking at scale growth, and ontogenetic changes among individuals by comparing morphology and histology along a size series. Individual growth of *Triazeugacanthus* had already been alluded by Gagnier (1996) who mentioned two distinct orders of growth lines in a saccular otolith. On the other hand, *Triazeugacanthus* ontogeny had already been evaluated among individuals by looking at body shape changes (Cloutier et al., 2009), size changes (Chevrinais et al., 2015b), squamation pattern (Chevrinais et al., 2015b), and mineralisation pattern (Chevrinais et al., 2015a). In the present investigation, we intended to combine both levels of ontogenetic information.

Scale growth process varies among acanthodians. Most acanthodian scales grow by addition of concentric layers of mesodentine (or orthodentine) forming growth zones which results in the classical "box-in-box" (or concentric "onion skin") pattern (Denison, 1979) [character 9 (1)]. This "box-in-box" pattern has been reported in the acanthodid *Acanthodes bridgei*, *A. lopatini*, and *A. lundi* , the cheiracanthid *Homalacanthus concinnus* (Annexe XV), all mesacanthids, some Diplacanthiformes, Climatiiformes and Ischnacanthiformes (Denison, 1979; Zidek, 1985) (Annexe XXIII). In addition to this "box-in-box" growth, the superficial region of the scale might thicken by the superimposition of ganoine layers as described in *Triazeugacanthus*. In living polypterid and lepisosteid actinopterygians, the first layer of ganoine matrix is deposited on the scale surface only when the basal layer cells of the epidermis become in close contact with the upper layer of either the dentine (polypterids) or bone (lepisosteids) matrix (Sire et al., 1987; Sire, 1994, 1995). In lepisosteids and polypterids, the epidermal cells partially retract periodically from the scale surface allowing the mesenchymal cells to

invade the space left free between the epidermal basal cells and the scale, in particular in the lateral parts. We observed the same growth pattern at the surface of *Triazeugacanthus* scales. Therefore, *Triazeugacanthus* scales show two growth modes: (1) the "box-in-box" growth for mesodentine and basal bone and (2) the superpositional growth for ganoine.

The "box-in-box" growth pattern has frequently been considered as an acanthodian synapomorphy (Denison, 1979; Janvier, 1996b; Miller et al., 2003) or defining a sub-inclusive acanthodian clade (Brazeau and Friedman, 2014). Although the "box-in-box" pattern is recognised by most authors as a generalised condition among acanthodians, there are some disagreements in terms of recognising this growth pattern as either characteristic of monodontode (monoodontode) or polyodontode scales. Monodontode scales represent scales composed of a single unit, the odontode (vascular supply takes place through basal canals and/or neck canals) (Ørvig, 1977); they either grow, or not, by concentric addition of dentine and bone layer. On the other hand, polyodontode scales correspond to a complex of fused or apposed odontodes (*i.e.* single units) lying on a bony basal plate and showing areal or appositional growth (Ørvig, 1977; Reif, 1979, 1982; Karatajute-Talimaa, 1992; Johanson, 2010; Andreev et al., 2015; Qu et al., 2016). Considering the "box-in-box" of acanthodians, Ørvig (1977) referred to these scales as odontocomplex without mentioning if they were either monodontode or polyodontode. Therefore, the "box-in-box" scales of acanthodians and early actinopterygians (*e.g.* *Cheirolepis canadensis* Annexe XVI) are considered as monodontode [*contra* Brazeau (2009); Davis et al. (2012); Burrow et al. (2016)] because of the presence of a single primordium per scale and the non-independence of individual growth layers. We suggest that each layer does not represent a single, separate unit (*i.e.* each layer is not a separate odontode) but rather an accretion around an initial unit; however, 3D microanatomical and histological data would be necessary to clarify this

issue [see Qu et al. (2016)]. Based on our topology, the "box-in-box" growth pattern, occurring at the base of the total-group chondrichthyan, was replaced by polyodontode scales growing through appositional and areal growth in putative chondrichthyans (Gagnier and Wilson, 1996; Warren et al., 2000; Hanke and Wilson, 2004; Hanke and Davis, 2012) and chondrichthyans (Karatajute-Talimaa, 1992, 1998). However, the polyodontode growth was already present prior to the origin of the total-group chondrichthyans since it is present in osteostracans (Hawthorn et al., 2008; Qu et al., 2015) and also in basal osteichthyans (Qu et al., 2016). Furthermore, even in basal stem chondrichthyans, such as the Silurian ischnacanthiform *Nerepisacanthus denisoni*, "box-in-box" scales are present on the body and areal-growth polyodontode scales are present on the cheek region (Annexe XXIII) (Burrow and Rudkin, 2014). Such polyodontode-type tesserae and *Nostolepis*-type scales are also found in the Early Devonian climatiiform *Acritolepis ushakovi* (Valiukevičius, 2003). Therefore, the "box-in-box" growth represents an evolutionary novelty at the base of the total-group chondrichthyans, but the presence of polyodontode scales (or the potential of forming polyodontode scales) remained present.

It is also likely that the so-called polyodontode condition regroups different similar but non-homologous growth patterns. We agree with Qu et al. (2016) who concluded that a complete revision of paleohistology of early vertebrates is needed.

Scale ontogeny is described from a single element, and then individual ontogeny is inferred. We showed that scale ontogeny reflects the individual ontogeny in *Triazeugacanthus*. For example, ganoine has not been observed in ground sections of juvenile *Triazeugacanthus*, whereas it was unambiguously present in adults. This ontogenetic difference suggests that ganoine develops later in ontogeny when mesodentine and bone are well formed. One could suggest that the ganoine layer could have been abraded

during the fossilisation process, however, the outer surface of juvenile scales is covered with tissues interpreted as skin remnants (epidermis and mesenchyme) (Figure 22 E) and the abrasion of this well-mineralised would have produce the destruction of the scale material. Thus, this difference reflects a true ontogenetic change rather than a taphonomic bias. The condition observed in *Triazeugacanthus* shows similarities with that is found in the living *Polypterus senegalus*. In this basal actinopterygian, the scales extend first in surface then in thickness and subsequently the ganoine layer is deposited only when the upper dentine layer is well developed in late juveniles (Sire et al., 1987; Sire, 1989, 1995). Therefore, the late ontogenetic formation of ganoine in *Triazeugacanthus* is similar to what is described for the ganoine deposition in lepisosteid and polypterid scales (Thomson and McCune, 1984; Sire, 1995).

Different scale shapes have been reported along the body (and head) of acanthodians (Young, 1995; Beznosov, 2000; Trinajstic, 2001; Burrow and Young, 2005; Upeniece, 2011; Brazeau, 2012; Burrow et al., 2016). One of these changes reported in various acanthodians (*e.g.* *Climatius*, *Ptomacanthus*, *Lodeacanthus*) is the presence of flat-based scales anteriorly and bulging-based scales posteriorly (Upeniece, 2011; Brazeau, 2012). In *Lodeacanthus*, Upeniece (2011) described two types of scale bases in juveniles: fully-developed conical (or bulging) bases (type 1) and incompletely-developed flat bases with a deep ventral pit (type 2) from the ventral and dorso-lateral areas of the prepectoral region. Based on our findings on the bidirectional pattern of squamation from a relatively posterior origin in *Triazeugacanthus*, anterior scales would develop later in ontogeny than posterior scales, and thus would exhibit a younger phenotype. We suggest that type 2 (flat base) of *Lodeacanthus* corrresponds to younger scales (as in juvenile *Triazeugacanthus*), whereas type 1 (convex base) of *Lodeacanthus* corresponds to older scales (as in adult *Triazeugacanthus*). The allometry of the thickness/width ratio in *Triazeugacanthus* scales indicates that body scales grow first

in area then in thickness (as already mentioned for *Polypterus*). This thickness change is reflected morphologically by the change in the shape of the basal layer from a flat surface in juveniles to a convex surface in adults. Retention of flat-based scales in the anterior part of body in adults (such as in *Ptomacanthus*) could suggest a heterochronic shift showing a juvenile feature in the last scales to develop. This presence of anterior flat-base scales has also been mentioned for scales attributed to chondrichthyans (Brazeau, 2012).

Growth zones are recognised in extant fish scales and are generally related to periodic changes of environmental conditions (seasonal or annual cycles) promoting the intake of nutritive elements (Ottaway, 1978; Schlosser, 1991; Fisher and Pearcy, 2005). Such variations, revealed by the alternation of short dark zones (rest zones) and large light zones (growth zones), occurred also during *Triazeugacanthus* life (Figure 23). Based on the growth of complete *Triazeugacanthus* specimens and that of isolated elements, we showed that the individual growth of scales is correlated to species ontogeny as suggested by Zidek (1985) and Karatajute-Talimaa (1998); this is in contrast to Valiukevičius and Burrow (2005) who mentioned that the number of growth lamellae do not reflect the developmental stage of the animal. "Box-in-box" growing scales are reliable proxies of species growth.

3.6.3 Squamation pattern

In acanthodians, the squamation pattern has only been described in some acanthodiforms (Annexe XXIII). Based on the literature, the general acanthodiform pattern of squamation is characterised by an initiation in the caudal region and an anterior progression following initially the lateral line trajectory (Watson, 1937; Zidek, 1985; Upe-

niece, 2011) (Figure 27). Such pattern was described in various species [*i.e.* *Acanthodes bridgei* (Zidek, 1976), *A. bronni* (Heidtke, 1990), *A. gracilis* (Zajic, 2005), *A. ovensi* (Forey and Young, 1985), *Lodeacanthus gaujicus* (Upeniece, 2011)] and is shared with some early actinopterygians (Hutchinson, 1973; Cloutier, 2010) and many extant teleost fish (Sire and Arnulf, 1990; Sire et al., 1997) (Figure 27). This observed caudal-rostral progression differs from the hypothesized direction suggested by Hanke and Wilson (2004). In their phylogenetic analysis of acanthodians, Hanke and Wilson (2004) coded for a character (their character 21) that takes into account the scale growth origin (or initiation). The 20 acanthodian taxa, with the exception of *Obtusacanthus* and *Lupopsyroides* (which they used as out-groups), were coded as having the first scales develop below the second dorsal fin (assuming that dorsal fin of the single-dorsal-fin taxa correspond to the second dorsal fin). They used the larger size of the scales as a proxy of the first formed scales.

In *Triazeugacanthus*, we found a pattern of squamation similar to that suggested by Hanke and Wilson (2004) rather than that described from growth series in the literature. Based on the progression of the squamation from the size series and scale proportions, the squamation of *Triazeugacanthus* is initiated in the posterior region of the body, below the dorsal fin and progresses bidirectionally; the postero-anterior direction is predominant over the antero-posterior direction because of the relatively posterior position of the site of initiation. As a result the number of rows as well as the number of scales per row increases during the ontogeny of *Triazeugacanthus*. This information refutes the hypothesis suggested by Karatajute-Talimaa (1998) that the number of scales remained stable during the ontogeny of acanthodians.

General conditions of squamation have already been described in different taxonomic groups. The squamation of the heterostracan *Dinaspidella elizabethae* developed first

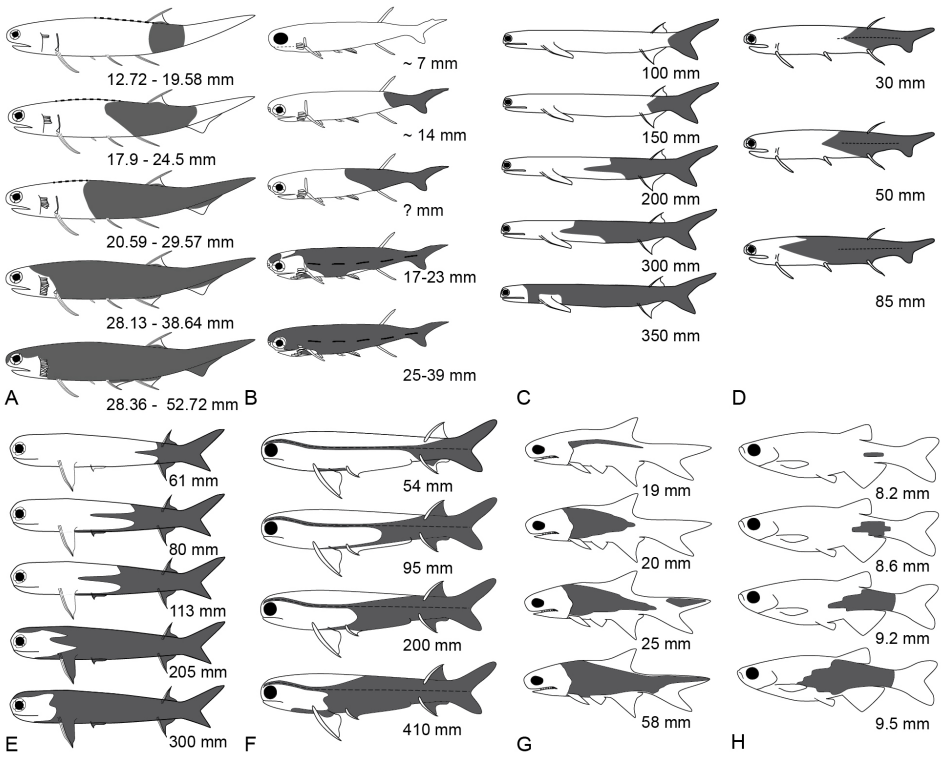

Figure 27: **Development of the squamation pattern in various acanthodiforms (A-F) compared to that in actinopterygians (G-H).** A: *Triazeugacanthus affinis*. B: *Lodeacanthus gaujicus* [modified from Upeniece (2011)]. C: *Acanthodes bronni* [modified from Heidtke (1990)]. D: *Acanthodes ovensi* [modified from Forey and Young (1985)]. E: *Acanthodes gracilis* [modified from Zajic (2005). F: *Acanthodes bridgei* [modified from Zidek (1976)]. G: *Elonichthys peltigerus* [modified from Cloutier (2010)]. H: *Danio rerio* [modified from Sire and Akimenko (2004)]. Estimated total length is given in A to G whereas standard length is given in H.

ventrally and dorsally following an antero-posterior direction (Greeniaus and Wilson, 2003). Such an antero-posterior pattern is also described for the thelodont *Lanarkia horrida* (Turner, 1992), *Loganellia scotica* (Märss and Ritchie, 1997) and *Thelodus laevis* (Märss, 2011). There is no information relative to the direction of squamation for placoderms. Although the information is sparse for jawless vertebrates and early gnathostomes (and not necessarily representative of the complete phylogenetic diversity), an antero-posterior patterning of body scales is suggested to be plesiomorphic for vertebrates.

The scarce information available in Palaeozoic chondrichthyans indicates that scales are present first along the lateral line (Zangerl, 1981; Lund, 1985; Donoghue, 2002). In extant chondrichthyans, scale development is generally considered to differ from other gnathostomes because head and body scales do not form sequentially but rather simultaneously and in a non-regular pattern (Reif, 1985; Sire and Akimenko, 2004; Johanson et al., 2007, 2008). However, Johanson et al. (2007, 2008) described an initiation of primary scale (or patterned tail scales) development on the extremity of the caudal fin progressing anteriorly along the caudal peduncle, then followed by a more irregular origin and arrangement of body scales, from anterior to posterior, to cover the ventral and dorsal lobes of the caudal fin; the initial sequential caudal scales are subsequently lost during ontogeny. Johanson et al. (2007, 2008) suggested that this regulated and sequential development of the caudal primary scales retained in early ontogeny may represent the plesiomorphic condition for chondrichthyans.

In the living basal actinopterygian *Polypterus senegalus*, there are two sites of squamation initiation which start almost simultaneously (Bartsch et al., 1997): an anterior site located just behind the pectoral girdle, and a second site in the caudal region. In both sites, scales form close to the lateral line. Thus, in *Polypterus*, scales develop

antero-posteriorly from the anterior site and bidirectionally from the caudal site. In the Carboniferous actinopterygian *Elonichthys peltigerus* (Schultze and Bardack, 1987; Cloutier, 2010) and the Triassic *Brookvalia gracilis* (Donoghue, 2002), scales initiate in the anterior region of the body near the lateral line and progress posteriorly (Figure 27 G).

This antero-posterior patterning is also conserved in the living *Amia calva*, where the first scales form on the lateral line just behind the pectoral girdle than the squamation extends posteriorly along the lateral line (Jollie, 1984b; Grande and Bemis, 1998). In the living *Lepisosteus oculatus* and *L. osseus*, the first scales appear along the lateral line in the tail region, then the squamation spreads anteriorly (Jollie, 1984a; Grande, 2010). Sire and Akimenko (2004) reported that the main generalised condition of scale development in teleosts (Figure 27 H) is the initiation of the first scales along the mid-line row at the level of the caudal peduncle, followed by a rapid progression of the squamation anteriorly and posteriorly along this row, while new rows are added ventrally and dorsally. Although further information relative to the squamation patterning in actinopterygians are needed, it seems that the plesiomorphic condition for the group is the antero-posterior direction, and that a postero-anterior direction (similar to the acanthodian pattern) would have occurred near the base of the neopterygians; however, as reported in *Polypterus*, both patterns are present in some species.

Independently of the direction of progression, Johanson et al. (2007) considered that the presence of scale patterning maintained through ontogeny might be a synapomorphy of crown group gnathostomes. Our data on acanthodian scale patterning through ontogeny corroborates this hypothesis. The bidirectional pattern of squamation in juvenile *Triazeugacanthus* is similar to the pattern reported in most acanthodian (Hanke and Wilson, 2004) and teleost fish (Sire and Arnulf, 1990), while a unidirectional de-

velopment seems to be restricted to some acanthodiforms and living chondrichthyans during early ontogeny solely. The difference between the pattern described for *Triazeugacanthus* and that reported for acanthodiforms might be biased by the greater number of specimens observed, the availability of younger developmental stages and the exceptional state of preservation allowing the fossilisation of soft and weakly mineralised tissues such as developing scales. The squamation pattern observed in acanthodians might well represent a precursor condition to that of chondrichthyans which would also corroborate the stem-group position of acanthodians.

Three hypotheses, mainly based on scale development in teleost fish, are given concerning the region of first scale development: (1) gene expression patterns, (2) lateral line induction, and (3) mechanical constraints imposed to the fish skin during swimming (Sire and Arnulf, 1990). The first hypothesis suggests a role of *Shh* and/or *ScShh* which is known to be involved in the positional specification along the antero-posterior axis in vertebrates (Yang and Niswander, 1995; Johanson et al., 2008). *Shh* expression is involved in the control of epidermal-dermal interactions but seems not essential for scale initiation and patterning of squamation (Sire and Akimenko, 2004). The second hypothesis proposes that the development of the lateral line neuromasts during the embryonic phase of fish ontogeny could induce the formation of the first scales notably because whatever the portion of the body from which the scale initiate (anterior or posterior), their development follows the lateral line in several actinopterygians (Neave, 1936; McCrimmon and Swee, 1967; White, 1977). However, Wada et al. (2008) have shown that the final position of each terminal neuromast coincided with the position of a scale in the proximal region of the caudal fin in zebrafish. They suggested that the prospective scale region may emit chemoattractive factors that regulate neuromast migration. Thus, scale patterning would in part regulate lateral line patterning rather than the opposite. The third hypothesis is suggested by the flexibility of the body in the

mobile posterior region, which has been proposed as a possible factor triggering early scale formation in this region (Sire and Arnulf, 1990; Sire et al., 1997); however, the anterior site of initiation would not be subject to special mechanical epigenetic constraint. In extant teleosts, opposite directions of squamation development are observed in closely related species such as in two cyprinids (posterior-anterior in *Danio rerio versus* anterior-posterior in *Cyprinus carpio*) and were related to swimming mode in juveniles prior to scale formation (Sire and Arnulf, 1990; Sire et al., 1997). Our data on *Triazeugacanthus* squamation do not allow us to choose among the three hypotheses. However, the progression seems to be following grossly the trajectory of the lateral line system and most likely the body shape of *Triazeugacanthus* would suggest some type of undulatory locomotion with greater amplitude of movement in the dorsal-caudal region. On the other hand, the conservatism of patterning among acanthodians as well as the relative conservatism in other groups would rather suggest the importance of fundamental developmental pattern under the control of gene expression.

3.7 Conclusions

The fossilised ontogeny of the Late Devonian acanthodian *Triazeugacanthus* allowed us to describe a scale structure similar to the *Acanthodes*-type scale and to define a bidirectional pattern of squamation. We identified three tissues composing the scales (*i.e.* a basal layer of acellular bone, a middle layer of mesodentine and a superficial layer of ganoine). Ontogenetic data (thickness/width ratio, growth zone distances, and squamation pattern) allowed us to recognize two types of growth (*i.e.* the "box-in-box" growth of mesodentine and basal bone and the subsequent superimpositional growth of the well-mineralised ganoine layer). *Triazeugacanthus* scales show similarities with acanthodians (*e.g.* "box-in-box" growth), chondrichthyans (*e.g.* squamation pattern),

and actinopterygians (*e.g.* ganoine), which phylogenetically are interpreted considering acanthodians as stem chondrichthyans. The usage of scales as proxies to study developmental patterns and processes in extinct groups (Cloutier, 2010; Qu et al., 2016), such as acanthodians, opens the possibility to not only determine phylogenetic relationships but infer developmental novelties important during the evolutionary history of early vertebrates.

ARTICLE 4

DÉCRYPTAGE DE L'ONTOGÉNIE DES CHONDRICHTYENS SOUCHES : CROISSANCE DE L'ACANTHODIEN DU DÉVONIEN SUPÉRIEUR *TRIAZEUGACANTHUS AFFINIS*, CANADA

4.1 Résumé

L'étude comparée des ontogénies a le potentiel de nous informer sur le partage des patrons et processus dévelop-pementaux entre les espèces. Cependant, les ontogénies fossiles de vertébrés primitifs sont extrêmement rares au Paléozoïque. La série de taille de l'acanthodien *Triazeugacanthus affinis* du Dévonien supérieur du *Lagerstätte* de Miguasha, a récemment été identifiée comme une des ontogénies fossiles de vertébrés primitifs les mieux connues étant donné sa préservation exceptionnelle, sa large étendue de taille, et l'abondance de ses spécimens. Des données morphologiques, morphométriques, histologiques et chimiques sont extraites à partir de la série de croissance de *Triazeugacanthus* comprenant des spécimens de 4 à 52 mm. La trajectoire développementale de ce chondrichtyen souche du Dévonien est caractéristique des poissons montrant un développement direct avec une alternance de seuils et de plateaux. Les larves ne possèdent pas d'écailles mais un développement progressif des vertèbres et du neurocrâne cartilagineux, alors que l'ossification et l'écaillure progresse chez les juvéniles. La présence de tissus cartilagineux et osseux, discriminés à partir de leur signature chimique et histologique, montre une minéralisation progressive des éléments vertébraux et du neurocrâne. La comparaison des différentes proportions du corps entre les larves, les juvéniles et les adultes suggère une croissance allométrique chez les juvéniles. A

cause de la position phylogénétique des acanthodiens, *Triazeugacanthus* nous informe sur les conditions développementales primitives des chondrichtyens souches.

Ce quatrième article, intitulé «*Unravelling stem chondrichthyan ontogeny: Growth of the Late Devonian acanthodian* Triazeugacanthus affinis *(Eastern Canada)*», fut corédigé par moi-même ainsi que par Jean-Yves Sire et Richard Cloutier. Il est en préparation pour publication dans la revue internationale *Proceedings of the Royal Society B*. Tous les auteurs ont conçu les expériences. En tant que premier auteur, ma contribution à ce travail fut l'essentiel de la recherche sur l'état de l'art, la réalisation de la prise de données, les observations et l'analyse de données, la production des figures et du matériel supplémentaire avec les contributions de Richard Cloutier et Jean-Yves Sire. J'ai écrit la première version et tous les auteurs ont contribué à la version finale. Une version abrégée de cet article a été présentée à la rencontre annuelle de la *Society of Vertebrate Paleontogy* à Berlin (Allemagne) à l'automne 2014 ainsi que lors des *Rencontres de l'Ichthyologie francophone* à Paris (France) au printemps 2015.

Nous remercions J. Kerr, O. Matton et F. Charest (MHNM) pour l'accès aux collections du Musée d'Histoire Naturelle de Miguasha. Nous sommes reconnaissants envers E. Bernard, Z. Johanson et S. Walsh pour l'accès aux collections du NHM et du NMS respectivement. Nous remercions C. Belzile (UQAR) pour les analyses de microscopie électronique et de spectométrie et B. Crighton (NMS) pour son aide avec les photographies. Les financements proviennent du NSERC (R. Cloutier) et du CSBQ (M. Chevrinais).

4.2 Unravelling stem chondrichthyan ontogeny: Growth of the Late Devonian acanthodian *Triazeugacanthus affinis* (Eastern Canada)

Summary

The study of ontogenies has the potential to inform us on shared developmental patterns and processes among vertebrates. However, early vertebrate fossilised ontogenies are extremely rare in the Palaeozoic Era. The size series of the Late Devonian acanthodian *Triazeugacanthus affinis*, from the Miguasha-*Fossil-Fish Lagerstätte*, has been recently identified as one of the best known early vertebrate fossilised ontogenies given the exceptional preservation, the large size range, and the abundance of specimens. Morphological, morphometric, histological and chemical data are gathered on a growth series of *Triazeugacanthus* ranging from 4 to 52 mm in total length. The developmental trajectory of this Devonian stem-chondrichthyan is characteristic of fishes showing a direct development alternating steps and thresholds. Larvae show no squamation but a progressive appearance of cartilaginous neurocranial and vertebral elements, and appendicular elements, whereas juveniles progress in terms of ossification and squamation. The presence of cartilaginous and bony tissues, discriminated on histological and chemical signature, shows a progressive mineralisation of neurocranial and vertebral elements. Comparison among different body proportions for larvae, juveniles and adults suggest allometric growth in juveniles. Because of the phylogenetic position of acanthodians, *Triazeugacanthus* ontogeny informs us about deep time developmental conditions in stem chondrichthyans.

Keywords: Gnathostomata, Acanthodii, mineralization, developmental trajectory, ossification sequence

4.3 Introduction

Historically, the identification of vertebrate fossilised ontogenies has been overseen because distinct morphologies have been assigned to different species rather than different ontogenetic stages of a same species (Cloutier et al., 2009; Donoghue and Purnell, 2009; Horner and Goodwin, 2009; Cloutier, 2010; Delfino and Sánchez-Villagra, 2010; Sánchez-Villagra, 2010). Although the recognition of developmental stages (*i.e.*, embryonic, larval, juvenile and adult) is difficult, Palaeozoic fossilised ontogenies have been recorded in most major clades of early vertebrates (Cloutier, 2010). Descriptions of fossilised ontogenies necessitate the recognition of key patterns and processes in well-preserved fossils; even when organisms are weakly mineralised during early stages of life.

Paleozoic early gnathostomes are represented by four major groups, namely the "placoderms" (Early Silurian to Late Devonian), "acanthodians" (Early Silurian to Middle-Late Permian), chondrichthyans (Late Ordovician to Recent), and osteichthyans (Late Silurian to Recent). The phylogenetic position and status of both placoderms and acanthodians is problematical (Brazeau, 2009; Davis et al., 2012; Zhu et al., 2013; Brazeau and Friedman, 2015; Burrow et al., 2016; Qu et al., 2016; Chevrinais et al., submitted). The placoderms are either considered as a paraphyletic group at the base of other gnathostomes (Young, 2010; Zhu et al., 2013; Dupret et al., 2014; Long et al., 2015) or a monophyletic sister-group of either chondrichthyans or osteichthyans (Young, 2010). Acanthodians are either considered as stem chondrichthyans (Zhu et al., 2013; Long et al., 2015; Burrow et al., 2016; Chevrinais et al., submitted), or stem gnathostomes, stem chondrichthyans, and stem osteichthyans (Brazeau, 2009; Davis et al., 2012), or as the monophyletic sister-group to chondrichthyans (Dupret et al., 2014) or osteichthyans (Schultze, 1990; Hanke and Davis, 2012). Ontogenetic data on "placoderms" and

"acanthodians," provided by the description and understanding of their early stages of development, is of paramount importance for resolving the early vertebrate phylogeny because developmental data represent an underused source of phylogenetic data.

For more than 30 years, acanthodian growth series have been recognised but they are frequently based on limited size series including already large individuals (Zidek, 1985; Heidtke, 1990; Beznosov, 2009). Nevertheless, more than 15 ontogenies have been documented: one possible Ischnacanthiformes [*Nerepisacanthus denisoni* (Burrow and Rudkin, 2014), two Diplacanthiformes [*Diplacanthus horridus* (Cloutier et al., 2009) and *Uraniacanthus curtus* (Newman et al., 2012)], one Climatiiformes [*Tetanopsyrus breviacanthias* (Hanke et al., 2001)], two species of uncertain order [*Machaeracanthus goujeti* (Botella et al., 2012) and *Lupopsyrus pygmaeus* (Hanke and Davis, 2012)], and nine Acanthodiformes [*Triazeugacanthus affinis* (Chevrinais et al., 2015a,b), *Lodeacanthus gaujicus* (Upeniece, 1996, 2001; Upeniece and Beznosov, 2002), *Homalacanthus concinnus* (Cloutier et al., 2009), *Acanthodes bridgei* (Zidek, 1985), *A. bronni* (Heidtke, 1990), *A. gracilis* (Zajic, 2005), *A. lopatini* (Beznosov, 2009), *A. ovensi* (Forey and Young, 1985)], and an acanthodiform indet. (Coates, 1993). Three acanthodian growth series (*i.e.*, *Diplacanthus horridus*, *Triazeugacanthus affinis*, and *Homalacanthus concinnus*) come from the middle Frasnian (*ca.* 380 Ma) Escuminac Formation (Miguasha, Quebec, Canada) which shows fossilised ontogenies for 14 out of the 20 Escuminac vertebrate species (Cloutier et al., 2009). Recently, the ontogeny of *Triazeugacanthus* has been reinvestigated (Chevrinais et al., 2015a,b, submitted) showing significant increases of (1) the size of individual anatomical elements, (2) the number of skeletal elements, and (3) the squamation extent with the total length, and (4) the progressive mineralisation of skeletal elements with growth.

Our aims are (1) to describe the ontogeny of *Triazeugacanthus* in terms of sequence

of ossification and morphometric changes and (2) to compare the developmental sequence and trajectory of *Triazeugacanthus* to that reported in other acanthodians, chondrichthyans and osteichthyans. Because of the stem-chondrichthyan phylogenetic position of *Triazeugacanthus* we expect to identify patterns of development shared by several gnathostomes.

4.4 Material and methods

4.4.1 Material

Specimens of *Triazeugacanthus affinis* (MHNM and NMS collections) were observed under water immersion (Leica MZ9.5), drawn using a camera lucida, and photographed (Nikon D300). *Triazeugacanthus* ontogenetic stages were recognised originally based on distinctive characteristics (Cloutier, 2010): (1) larvae are identified by the absence of body scales (Urho, 2002; Cloutier et al., 2009; Cloutier, 2010), (2) juveniles are characterised by a partial body squamation (Balon, 1981; Cloutier et al., 2009; Cloutier, 2010), and (3) adults show complete body squamation (Cloutier, 2010). Histological data were gathered from transverse ground sections of complete specimens on two "early" juveniles, 10 "late" juveniles, and five adults (Chevrinais et al., submitted, see protocol). Elemental composition analyses were performed on two larvae, one juvenile thin ground sections and one adult (Chevrinais et al., 2015a, see protocol).

4.4.2 Spectrometry

Skeletal structures were considered as mineralised when calcium and phosphorus were recorded in proportion close to the hydroxyapatite composition (P-Ca%wt ratio around 1:2) (Dorozhkin and Epple, 2002). A small amount of calcium coupled with a high amount of carbon and no phosphorus was interpreted as calcified cartilage (Chevrinais et al., 2015a). When a structure was mainly composed of carbon, it was interpreted as largely composed of collagen and identified as non-calcified cartilage.

4.4.3 Developmental sequence and trajectory

Continuous [length of skeletal elements and distances among elements (Annexe XXIV)] and discrete data [presence/absence of anatomical structures (Annexe XXV)] were collected on 178 specimens belonging to a growth series (29 larvae: 4.5-17.49 mm; 71 juveniles: 12.71-33.29 mm; 78 adults: 21.64-52.72 mm) (Chevrinais et al., 2015b). The developmental (chondrification and ossification) sequences [*i.e.*, the relative timing and order of skeletal events through ontogeny (Grünbaum et al., 2012)] of *Triazeugacanthus* were reconstructed for 34 elements using 178 specimens. A developmental (ossified) trajectory [*i.e.*, the cumulative addition of elements through ontogeny (Grünbaum et al., 2012); also known as maturity curve or bone maturity (Cloutier, 2010)] for *Triazeugacanthus* was reconstructed based on the ossification sequence.

Inter-individual variation in developmental sequence has been reported in developmental sequences of living organisms (Colbert and Rowe, 2008; Maxwell, 2008; de Jong et al., 2009; Fischer-Rousseau et al., 2009). Here, we developed a reliability estimate (RE) (Annexe XXVI) calculated for each structure by dividing the actual number of

specimens having an anatomical structure by the number of specimens expected to have this structure [*i.e.*, number of specimens longer (in terms of TL) than the smallest specimen that displays the structure]. The RE is calculated for each event because non-developmental sources of variation (*e.g.* taphonomic alteration, preservational position of the specimen) have the potential to alter differentially certain anatomical structures in fossilized ontogenies.

4.4.4 Statistical analyses

To characterize the growth of individual skeletal elements and shape changes during ontogeny, linear regressions between $\log_{10}$-transformed measurements and $\log_{10}$-transformed total length ($\log_{10}$TL) have been calculated for individual ontogenetic stages and for combined stages. Principal component analyses (PCA) on variance–covariance matrices of five $\log_{10}$-transformed measurements were performed for juveniles, adults and the combined dataset (Chevrinais et al., 2015b). To measure continuous global body shape changes during growth, an elongation ratio was also calculated as a ratio of total length to body depth (Katz and Hale, 2016). Body depth was measured at the level of the dorsal fin spine, an anatomical element that could be identified in larval, juvenile and adult specimens (Figure 28). A high elongation ratio means that the body is very elongated. Comparison of elongation ratios among groups was performed using the non-parametric Kruskal-Wallis test and the Tukey's multiple comparisons test. Non-parametric tests were used because of the non-normality of the data. All statistical analyses were done with R 3.0.2.

4.4.5 Institutional abbreviations

LDM: Latvijas Dabas muzejs (Latvia), MHNM: Musée d'Histoire Naturelle de Miguasha (Canada), NHM: National History Museum (United Kingdom), NMS: National Museums of Scotland (Scotland), UPMC: Université Pierre et Marie Curie (France), UQAR: Université du Québec à Rimouski (Canada).

4.5 Results

The sequence of cumulative appearances of skeletal elements (based on 178 specimens of *Triazeugacanthus*) shows a developmental trajectory with periods of gradual or rapid changes (*i.e.* thresholds) intercalated with periods of slow anatomical changes (*i.e.* steps) (Figure 28).

Endoskeletal elements are poorly represented in the sequence, especially because the scale coverage starts in early juveniles hiding internal elements (Figure 29). Early in the larval period, a threshold occurs at 7 mm TL (*i.e.* development of neurocranial and vertebral elements, and pectoral, anal and dorsal fin spines). This threshold is followed by a step of slower development between 8 and 13 mm TL (Figure 28). The transition between the larval and juvenile periods is characterized by a threshold at 13 mm TL synchronously with the initiation of squamation. The juvenile period is characterised by extensive gradual addition of elements (more than 10 events developed over a period of 18 mm of growth) followed by a threshold at 29 mm TL. This threshold, coupled with the completion of the squamation, determines the transition between juveniles and adults. Adult stage shows a long step from 30-mm TL onward.

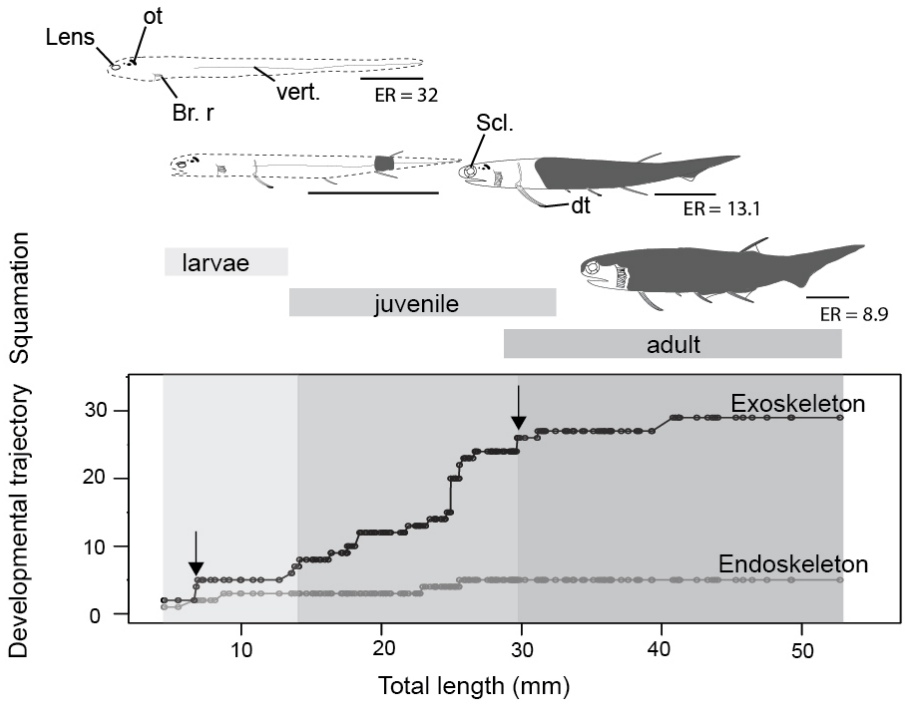

Figure 28: **Developmental trajectory of endo- and exoskeletal ossification of *Triazeugacanthus***. Light grey background: larvae; medium grey background: juveniles; dark grey background: adults. ER is for the elongation ratio (see Figure 29). Scale bars = 1 mm in larvae and 5 mm in juvenile and adults.

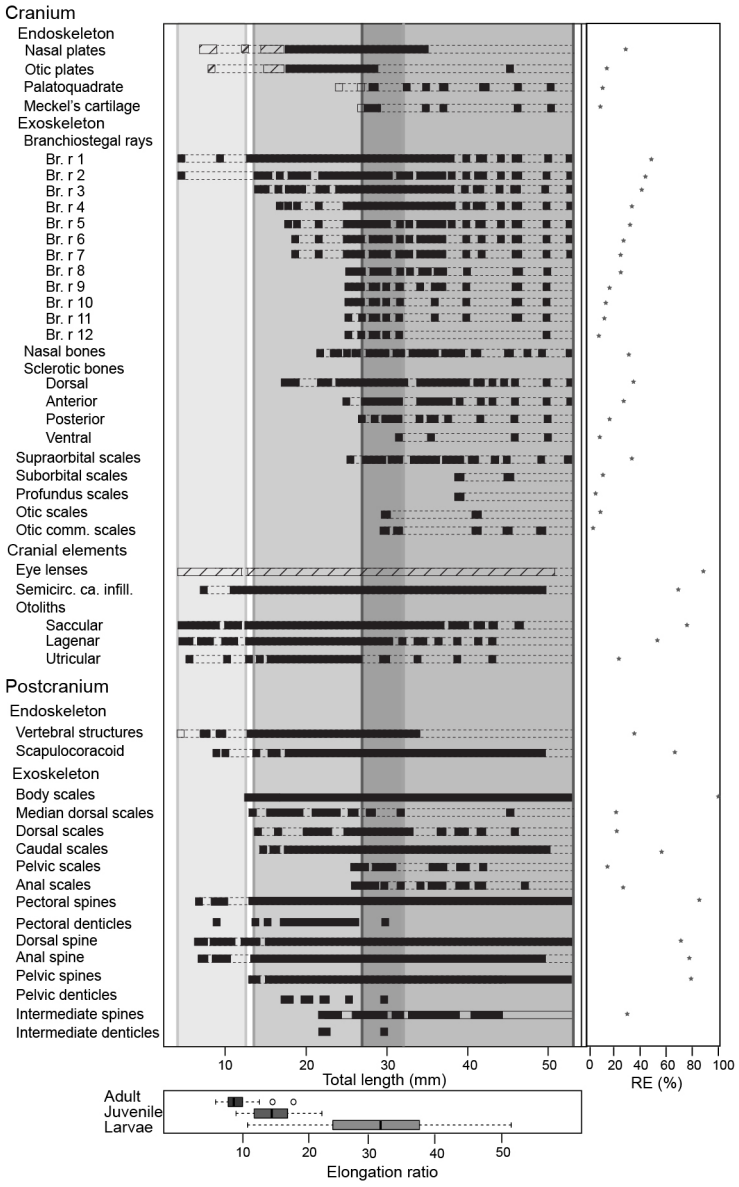

Figure 29: ***Triazeugacanthus*** **developmental sequence.** Ontogenetic stage: light grey background, larvae; medium grey background, juveniles; dark grey background, adults. Chemical composition: empty boxes, presence of a structure without information on the chemical composition; dashed boxes, presence of a chondrified structure; horizontal dashed lines, putative presence of a structure; full boxes, presence of a mineralised structure. Reliabilitiy: stars, reliability index (x axis). Elongation ratios are given at the bottom of the figure for larvae, juvenile and adult specimens.

4.5.1 Larvae (4.5-17.5 mm TL)

The first developmental stage available for *Triazeugacanthus* is the larval period; no embryonic specimens have been identified yet. The general body shape is relatively filiform; the average larval elongation ratio is 32 (Figure 29). Larval specimens are preserved dorso-ventrally. Paired eye lenses (RE = 88.2%), four otoliths [two hemispherical bean-shaped saccular otoliths and two ovoid intermediate lagenar otoliths (RE > 50%)], branchiostegal rays 1 and 2 and a series of vertebral elements (RE = 35%) are developed even in the smallest larvae (4.5 mm TL, MHNM 03-94). The successive crescent-shaped elements of carbonaceous composition (Figure 30 A) represent most likely vertebral elements rather than the notochord. These vertebral elements are first recognized at the level of the dorsal and anal fin spines. Amorphous organic matter from the digestive tract obliterates their presence anterior to the dorsal fin. Cartilaginous neurocranial elements develop at 5.5 mm TL (nasal plates, RE = 28%) and at 6.5 mm TL (otic plates, RE = 11%). The two smallest spherical, utricular otoliths are formed subsequently at 5.5 mm TL (RE = 23%). Associated to the presence of otoliths, granular semicircular canal infillings are recorded at 7 mm TL (RE = 69.2%) (Figure 29).

The appearance of fin spines is coupled with a lateral preservation of the specimens. Fin spines formed sequentially during the larval stage (Figures 28 and 29): pectoral (RE = 85.1%) and dorsal (6.8 mm TL; RE = 70.1%), anal (6.9 mm TL; RE = 76.9%), and pelvic spines (14 mm TL; RE = 78.9%). The early development of the pectoral spines is accomplished by the addition of denticles at the distal extremity of the anterior ridge of the spines (9 mm TL) (Figures 29 and 31 A-F). However, the precise number of denticles is difficult to determine in larval stage because of the fragile nature of these elements. The mineralised scapulocoracoid (8.8 mm TL; RE = 66.8%) and fin spines

display amounts of calcium and phosphorus superior to 19% wt and 8% wt, respectively (Figure 30 A and B, Annexe XXVII). Still at 8.8 mm TL, vertebral structures show the presence of calcium (Figure 30, Annexe XXV). Despite the fact that axial and appendicular endoskeletal elements are already mineralised, neurocranial elements mineralised only at about 17 mm TL (Figure 29).

4.5.2 Juveniles (12.7-33.3 mm TL)

The juvenile period is primarily characterized by the development of the dermal skeleton. Body shape is becoming slightly stockier; the average juvenile elongation ratio is 14.6 (Figure 29). Body squamation appears at 12.7 mm TL (RE = 100%), as a single small patch of primordium scales develop below the dorsal fin spine. Median dorsal scales develop anteriorly to the patch of body squamation at 13.8 mm TL (Annexe XXVIII). Their anterior position and their morphology suggest that median dorsal scales develop faster than body scales. The first scales associated to the fin webs are recorded almost simultaneously at the base of the dorsal fin (13.8 mm TL; RE = 21.4%) and at the base of the hypochordal lobe of the caudal fin (14.1 mm TL; RE = 55.7%). Body scales extend posteriorly to caudal extremity and anteriorly reaching the region of pectoral fins at 21 mm TL, which shows the transition between early and late juveniles. Subsequently, fin web scales develop proximo-distally in the pelvic (25.6 mm TL; RE = 14.8%) and anal fins (25.6 mm TL; RE = 26.1%) (Figure 29, Annexe XXIX). Within each web, scales are organized in adjacent rows in which the smallest scales are found distally. There is no indication of ceratotrichia in the fin webs. Cranial sensory line scales develop first at 25.9 mm TL with the supraorbital scales (RE = 33.3%), followed at 29.7 mm TL by the otic commissure and otic sensory line scales (RE = 3.6% and 9.1%, respectively).

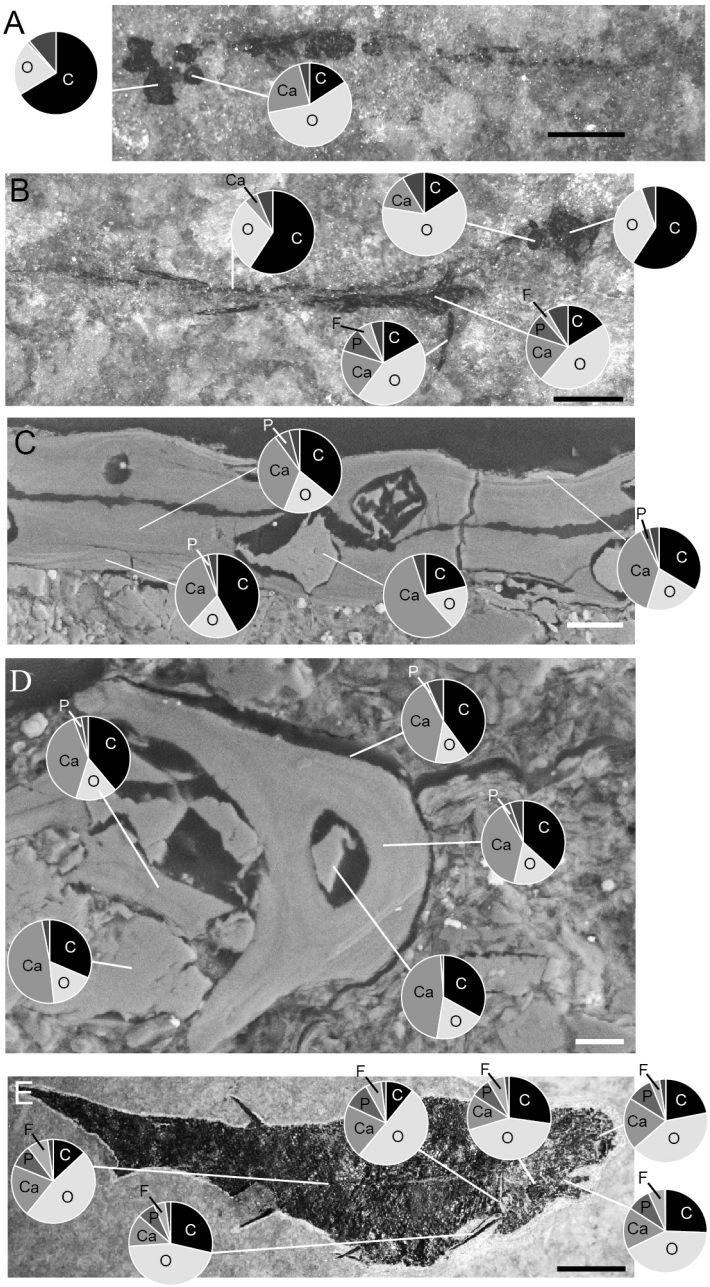

Figure 30: ***Triazeugacanthus*** **EDS X-ray punctual microanalyses.** Pie charts represent the relative percentage of main chemical elements. (a) MHNM 03-440 2. Eye lenses, otoliths, scapula, pectoral spine and vertebral structures. (b) MHNM 03-440 1. Eye lenses and otoliths. (c) MHNM 03-398. Juvenile endoskeleton and scale inner and outer layers from transverse sections. (d) MHNM 03-398. Juvenile endoskeleton and anal spine inner and outer layers. (e) MHNM 03-1497. Adult circumorbital bone, palatoquadrate, branchiostegal rays, scapula, pectoral spine and scales. Scale bars = 1 mm in (a, b); 20 μm in (c), 10 μm in (d) and 5 mm in (e).

Among the four sclerotic bones, the dorsal and anterior ones develop at 17.2 mm TL (RE = 34%) and 24.7 mm TL (RE = 27%), respectively. Branchiostegal rays 3 to 12 develop successively, from dorsal to ventral, through the juvenile period from 14 to 24.9 mm TL (Figure 2). Nasal bones form at 23.5 mm TL (RE = 33%). The last endocranial elements to develop are the mandibular elements. The palatoquadrate (23 mm TL; RE = 10.1%) forms slightly before the Meckel's cartilage (25.6 mm TL; RE = 9.1%) (Figure 29); this bias is likely owing to the weak prismatic mineralization of these two pairs of elements.

The intermediate fin spines are the last spines to develop at 22 mm TL (RE = 30%). However, the presence of these spines is rare even in well-preserved adult specimens (Figure 29). Three denticles are recorded on the intermediate fin spines at 22 mm TL. Denticles are still observed on the pectoral (six to ten denticles from 18 to 25 mm TL specimens) and are recorded for the first time in pelvic (four to seven denticles from 17 to 22 mm TL specimens) fin spines. These denticles are also visible in ground sections of juvenile spines (Figure 31 G, top). Tissues composing the spines are difficult to observe in juveniles likely due to a poorly differentiated early stage of development (Figure 31 G); however, it is highly mineralised and contains a few cell cavities and canaliculi.

4.5.3 Adults

The adult stage shows the completion of skeletogenesis (39 mm TL) and of the mineralisation (at least at 45 mm TL). The adult body shape is stocky; the average adult elongation ratio is 8.9 (Figure 29). The squamation is completed through the formation of the scales in the dorsal region of the head at around 26 mm TL. Cranial sensory line

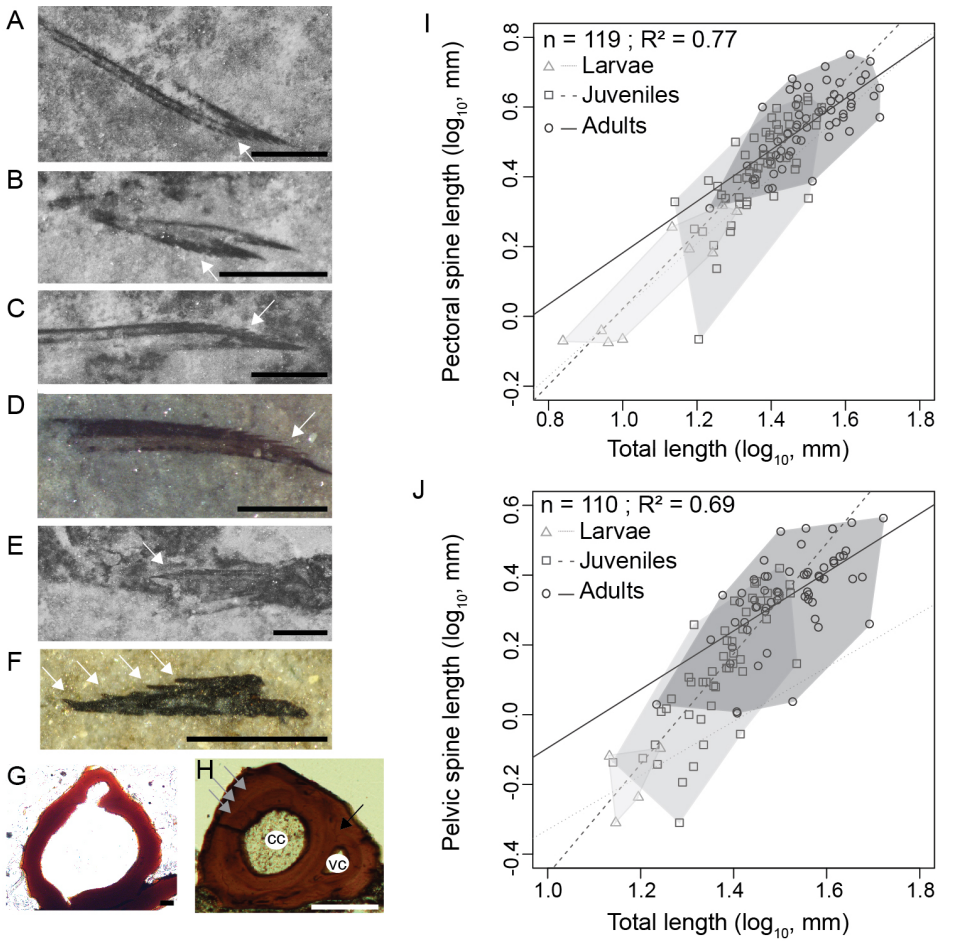

Figure 31: ***Triazeugacanthus*** **paired fin spines.** (A) MHNM 03-740. Left pectoral fin spine. (B) MHNM 03-740. Pelvic fin spines. (C) MHNM 03-740. Right pectoral fin spine. (d) MHNM 03-1985. Pectoral fin spine. (e) MHNM 03-210. Pelvic fin spines. (f) NMS 2002.59.15. Pectoral fin spine. (g) MHNM 03-701. Juvenile anal fin spine transverse section. (h) MHNM 03-2620. Adult anal fin spine transverse section. (i) MHNM 03-259. SEM detail of the central cavity wall (arrowhead) of the anal fin spine. (j) Pectoral fin spine length and TL relationship. (k) Pelvic fin spine and TL relationship. (a-h) White arrows indicate denticles, grey arrows indicate growth lines and black arrow indicates osteocyte cavities. Scale bars = 0.5 mm in (a-f), 20 μm in (g, i), 100 μm in (h).

scales continue to develop with the profundus sensory line and the suborbital sensory line scales at 39.1 mm TL (RE = 5.6% and 11.1%, respectively). The development of the cranial sensory lines is similar to the main postero-anterior direction of the body squamation and also shows a dorso-ventral direction of progression. The lateral line canal is visible along the flank as a small space between two rows of scales, at mid-height, in the anterior part of the body (at least at 45 mm TL). In the posterior part of the body, the lateral-line canal is less visible than anteriorly and the scales seem to be closer to each other (Annexe XXVIII). The development of skeletal elements is completed by the formation of branchiostegal rays 8 to 12 (25 mm TL) and the ventral sclerotic bones (31 mm TL) (Figure 29, Annexe XXVII).

Scales continue to develop proximo-distally on the pelvic and anal fin webs. Consequently, fin spines are associated to scaled fin webs in the pelvic, anal and dorsal fins (Annexe XXIX). Spine denticles are recorded until the late juvenile/early adult stages; up to ten denticles have been counted on a 0.84 mm long pectoral spine (MHNM 03-740, Figure 31 C). As the spine tissues get thicker, the individual denticles become merged to the spine and therefore are not visible in adults. The histology of adult spines reveals mesodentine with odontocyte cavities surrounding a large central vascular cavity that most likely housed the primary vascularization (Figure 31 H). A smaller vascular cavity, located dorsally to the central vascular cavity, is also present including a highly calcified tissue (Figure 30 D). The smallest vascular cavity seems to form later in spine ontogeny, after the formation of the central cavity (Figure 31 G). The tissue forming the boundary between the two cavities seems to develop secondarily (Figure 31 G and H). At least five growth zones are present in the ground section of the largest sectioned specimens.

4.5.4 Ontogenetic trends

Shape variation is recorded through ontogenetic stages (Figures 28 and 29). Comparison of elongation ratios in larvae, juveniles and adults indicates a decrease in the elongation ratio from larvae to adults (Figure 29). The anterior part of the body is more elongated in early ontogeny (Figure 28 see reconstructions). Furthermore, the range of values and the standard deviation (sd) are higher for larvae (10.5 to 51; sd = 14.5) than for juveniles (8.7 to 22; sd = 3.7) and adults (5.5 to 17; sd = 2) (Figure 29). Body shape is thicker and less elongated than described previously (Gagnier, 1996).

The relationships between the length of skeletal elements and TL display different growth rates among ontogenetic stages (Figure 31 I and J). Linear regressions between lengths of fin spines and TL are significant (Figure 31 I and J; pectoral fin spines: $R^2 = 0.77$, $p < 2.2e^{-16}$; pelvic fin spines: $R^2 = 0.69$, $p = 2.2e^{-16}$). Slopes of the linear regressions between the growth of the pectoral spine and the TL and the pelvic spine and the TL increase from larvae (pectoral: slope = 0.92, $R^2 = 0.81$, $p = 2.1e^{-10}$) to juveniles (pectoral: slope = 1.04, $R^2 = 0.55$, $p = 1.6e^{-10}$; pelvic: slope = 1.64, $R^2 = 0.64$, $p = 2.4e^{-11}$) and decrease in adults (pectoral: slope = 0.76, $R^2 = 0.53$, $p = 3.2{=}3e^{-4}$; pelvic: slope = 0.72, $R^2 = 0.32$, $p = 9.3e^{-8}$) showing that most of the differential growth occurred during the juvenile period. Those results coupled with individual skeletal elements growth (Figure 31 I, J) suggest that an allometric tendency is observed in juvenile pectoral and pelvic spines growth.

PCA loadings show that the principal source of body shape variation (65% of the variation) remains in pelvic to anal spines distance in juveniles (allometric coefficient = 4.5) and in anal to dorsal spines distance in adults (allometric coefficient = 2.2) arguing for positive allometry of the region between the pelvic fins and the dorsal fins. Those

results coupled with individual skeletal elements growth (Figure 31 I and J) suggest that an allometric tendency characterized the juvenile period.

4.6 Discussion

Based on 178 specimens, morphological, histological, and chemical changes during the ontogeny of *Triazeugacanthus affinis* were extensively analysed for the first time in a Palaeozoic vertebrate species showing that: (1) the sequence of appearance of endoskeletal and exoskeletal elements follow a developmental trajectory with an alternation of thresholds and steps, (2) skeletal systems have specific directions of formation, (3) skeletal elements mineralize progressively during the larval and juvenile stages to be completed during the adult stage, (4) positive allometry is recorded during the juvenile stage, (5) the elongation ratio decreases during ontogeny, and (6) the variation of body shape decreases from larvae to adults during ontogeny. Besides body size, we used four [(1) the degree and timing of ossification, (2) the degree of squamation, (3) the allometric growth of individual skeletal elements, and (4) body proportions] out of the six criteria proposed by Cloutier (2010) to characterize immature specimens.

4.6.1 Developmental trajectory

Developmental trajectory provides an overview of the critical periods during ontogeny. A succession of thresholds (periods with the apparition of numerous elements within a short period of time) and steps (periods of slower development) during the skeletogenesis has already been documented during the ontogeny of extinct osteolepiform (Cloutier, 2010) and living actinopterygians (Balon, 2002; Belanger et al., 2010). In

living fish, a saltatory pattern of development displays an alternation of thresholds and steps, where thresholds are associated with major physiological (*e.g.* endogenous to exogenous feeding), behavioural (*e.g.* passive to active movements), and ecological (*e.g.* passive to active predation, habitat changes) changes (Balon, 2001, 2002). We used the thresholds to delimit the three periods in *Triazeugacanthus*. Our delimitation of the three periods slightly differs from our previous interpretation based mainly on the squamation extent (Chevrinais et al., 2015a,b). The main difference between these two hypotheses pertains to the overlapping between stages. The gradual period in *Triazeugacanthus* seems to concur with the squamation progression. The gradual change could either reflects (1) the "noise" of individual variation (as suggested also by the presence of the overlap between ontogenetic stages, Figures 28 and 29) (Balon, 2001), (2) an underestimation of the threshold due to the low number of skeletal elements (34 elements at maturity), or (3) a true ontogenetic compensation where the energy is focused on a global exoskeletal development rather than the formation of specific structures. Since saltatory ontogeny has been recognized in living actinopterygians, extinct sarcopterygians and acanthodians, it is suggested that it might represent a generalised gnathostome patterns inherited at least from the Ordovician time (Donoghue and Keating, 2014).

During the ontogeny, some internal structures were hidden by the development of external structures (*e.g.* scales) which potentially could bias the developmental trajectory. Structures showing a good reliability (RE > 50%) reflect adequately the growth in *Triazeugacanthus*, whereas endoskeletal elements (*e.g.* neurocranium, vertebral structures), elements covered by scales (*e.g.* otoliths), or kinetic structures (*e.g.* branchiostegal rays, lower jaw) submitted to loss more easily than structures ankylosed or having complex sutures show a relatively low reliability in both *Triazeugacanthus* and *Lodeacanthus* (Upeniece, 1996; Hanke and Davis, 2012; Chevrinais et al., submitted) (An-

nexe XXVII and XXXI).

Body proportions changed during ontogeny mainly during the juvenile period (Cloutier, 2010). *Triazeugacanthus* is more elongate at the larval stage than at the adult stage as reflected by the elongation ratio. Such a shape variation is also present in chondrichthyans (Annexe XXX) and the majority of actinopterygians (Katz and Hale, 2016). Changes in body proportion through ontogeny is one of the criteria to recognize fossil ontogenies (Cloutier, 2010), such as in the early actinopterygian '*Elonichthys*' *peltigerus* (Schultze and Bardack, 1987). *Triazeugacanthus* has a direct development; no metamorphosis occurs as shown by the continuity in the growth of individual elements as well as the progressive shape variation among ontogenetic stages do not indicate the presence of a metamorphosis (Figure 31).

4.6.2 Cranium

Among the anatomical features to differentiate early during the ontogeny of living vertebrates, cranial systems (*i.e.* vision, breathing, feeding, and equilibrium or balance) develop first allowing the fish larvae to perceive and interact with the environment (Osse et al., 1997; Wyffels, 2009); evidently postcranial support will also be necessary to react to these initial stimuli. The smallest larval specimen of *Triazeugacanthus* (TL = 4.5 mm) already displays eye lenses, otoliths (two saccular and one lagenar), two branchiostegal rays and vertebral structures. The early appearance of the eye lenses (Figure 29) is congruent with that observed in acanthodians (Heidtke, 1990; Upeniece, 2011), extinct and living chondrichthyans (Wyffels, 2009; Sallan and Coates, 2014), and osteichthyans including tetrapods (Schoch, 2006; Hall, 2008; Cloutier et al., 2011a). In terms of body proportions, the eyes being proportionally larger in immature than adult

specimens is considered as a recurrent growth pattern in osteichthyans (Schultze, 1984; Schultze and Bardack, 1987; Cloutier, 2010). *Triazeugacanthus* eye lenses show significant differences in growth during ontogeny (Chevrinais et al., 2015b, Fig. 2a, the slope of linear regressions are different between larvae, juveniles and adults).

Associated to the eyes of teleosts, the anterior and posterior ossicles ossified from a cartilage ring surrounding the ocular globe (Franz-Odendaal and Vickaryous, 2006). In amniotes, sclera ossicles (homologous or not to those of fish) form either in a clockwork manner starting ventrally or in an alternate manner (posterior, anterior, dorsal and ventral) (Zhang et al., 2012). The four sclerotic bones (sclera ossicles) of *Triazeugacanthus* develop sequentially (dorsal, posterior, anterior and ventral) in juveniles and early adults. Sequential development of sclerotic bones is known in other acanthodians (Heidtke, 1990; Upeniece, 2011). The variable number of sclerotic bones (even in closely related species of acanthodians) and the variation in their developmental pattern indicate a high disparity among gnathostomes which necessitates further comparative studies.

Saccular and lagenar otoliths develop during the embryonic stage in *Danio rerio* (Riley and Moorman, 2000) and *Polypterus senegalus* (Bartsch et al., 1997). As in the zebrafish (Haddon and Lewis, 1996; Riley and Moorman, 2000), the saccular and lagenar otoliths of *Triazeugacanthus* develop first followed by the utricular. In the zebrafish, and most likely in *Triazeugacanthus*, the saccular and lagenar otoliths develop early during the embryonic stage. Three pairs of otoliths are known in acanthodiform acanthodians (Schultze, 1990). The record of growth lines in the otoliths in *Triazeugacanthus* (Chevrinais et al., 2015b, Annexe II) is congruent with observations already made by Gagnier (1996), who reported the presence of concentric growth zones enclosing minor secondary order zones. Three pairs of otoliths are recorded early in

the ontogeny of *Acanthodes lopatini* (Beznosov, 2009) and *A. bronni* (Heidtke, 1990) (in which statoconia are followed by three otoliths in ontogeny) and osteichthyans, whereas they are absent in chondrichthyans (Schultze, 1990). Schultze (1990) considered the presence of three pairs of otoliths as a synapomorphy shared by acanthodians and osteichthyans. Recent phylogenetic analyses of gnathostomes did not use otolith characters (Brazeau, 2009; Davis et al., 2012; Burrow et al., 2016; Chevrinais et al., submitted) and show acanthodians as stem chondrichthyans (Chevrinais et al., submitted), thus otoliths could represent a condition shared by some acanthodians, some chondrichhtyans and some osteichthyans with statoconia considered plesimorphic for gnathostomes (Schultze, 1990).

Branchiostegal rays develop relatively early in *Triazeugacanthus* considering they belong to the exoskeleton which develops later; early development of branchiostegal rays has been also documented in *Lodeacanthus* (Upeniece, 2011, Annexe XXXI) and *Acanthodes* (Zajic, 2005). The presence of elements covering externally the hyoid and branchial apparatus suggests that branchial respiration (versus skin respiration) is already acquired and efficient early in ontogeny. External gills have not been reported in acanthodians either because these structures (1) have a weak potential for fossilisation, (2) are absent or (3) are only present in very early larval stages. Wyffels (2009) considered the presence of external gill filaments as plesiomorphic for chondrichthyans, while these structures are also present in basal actinopterygians (Bartsch et al., 1997), lungfishes and amphibians (Fritzsch, 1990).

Jaws development occurs early in ontogeny of chondrichthyans and osteichthyans (Bemis and Grande, 1992; Grande and Bemis, 1998; Summers et al., 2004; Wyffels, 2009; Cloutier et al., 2011a). Jaws are attached to the neurocranium early in ontogeny (Wagemans et al., 1998) and show a mineralisation allowing a good preservation (Grande and

Bemis, 1998). In both *Triazeugacanthus* and *Lodeacanthus*, the presence of jaws is recorded relatively late and is poorly reliable (Upeniece, 2011, Annexe XXXI). In contrast, the mineralisation of the jaws in *Acanthodes* is completed early in the ontogeny (Zidek, 1985). The poor preservation of jaws in *Triazeugacanthus* and *Lodeacanthus* and the relatively large time range of formation and mineralization observed in other acanthodiforms suggest that jaw bones are weakly attached to the neurocranium in acanthodiforms in general.

In addition to the eye lenses, the larval neurocranium included the otic and nasal plates; chemical analyses revealed that they first chondrify before their mineralization. A general postero-anterior direction of formation has been suggested in the neurocranium of chondrichthyans (Summers et al., 2004; Johanson et al., 2013), in extinct and living actinopterygian (Schultze and Bardack, 1987; Grande and Bemis, 1998). This general postero-anterior direction of ossification was also found for the ossification of dermal cranial structures in *Triazeugacanthus* and *Lodeacanthus*.

4.6.3 Postcranium

Axial skeleton

The notochordal and vertebral elements develop early in fish (Hall, 2008). Axial skeletal elements are rarely preserved in acanthodians and developmental pattern is unknown. Only one specimen of *Acanthodes sulcatus* (Lower Carboniferous) shows neural and haemal arches forming a vertebral column observed from the pectoral to the dorsal fin regions (Miles, 1970). Although there is no indication of well-developed vertebral elements in adult *Triazeugacanthus*, cartilaginous precursors were documented

in early larvae before their mineralization in later stages. The poor record of acanthodian axial skeleton, even if arches are perichondrally ossified, is most likely due to the poor mineralization of the vertebral elements.

Paired fins

Gnathostomes are characterised by the presence of endoskeletal and/or dermal girdles supporting paired fins (Coates, 2003). Acanthodians show both endoskeletal and dermal pectoral girdles; however, acanthodiforms show only an endoskeletal pectoral girdle. In all acanthodiform ontogenies, a mineralised scapulocoracoid is the first element of the pectoral girdle to develop [*i.e.*, *Triazeugacanthus* (this study), *Lodeacanthus* (Upeniece, 2011, Annexe XXXI), *A. bronni* (Heidtke, 1990), *A. bridgei* (Zidek, 1985). However, the ontogenetic occurrence of pectoral spines before the scapulocoracoids, could be explained by the presence of an undocumented cartilaginous precursor of the scapulocoracoids.

One of the main acanthodian characters of the acanthodians is the presence of fin spines in front of each fin except the caudal fin (Denison, 1979; Miller et al., 2003; Brazeau and Friedman, 2014). *Triazeugacanthus* paired fin spines (pectoral, pelvic, and intermediate) are characterised by high RE with the exception of the intermediate spines. The late development of these intermediate spines as well as their poor occurrence (32.4% of the specimens) could be interpreted as the presence of a sexual dimorphism. In gnathostomes, pectoral fin spines are only known in acanthodians, the placoderm *Macropetalichthys* (Denison, 1978), three osteichthyans [*Achoania*, *Guiyu* and *Psarolepis* (Zhu et al., 1999; Zhu and Yu, 2009)], basal chondrichthyans [*Doliodus problematicus* (Miller et al., 2003), *Wellerodus priscus* (Potvin-Leduc et al., 2011) and also suggested in *Antarctilamna prisca* (Miller et al., 2003)]; however, none of them

show developmental sequence as in *Triazeugacanthus*. The paired fin spines of *Triazeugacanthus* grow by accretion of odontodes in the distal part of the spine. Small denticles have also been observed in other acanthodiforms: pectoral, intermediate and pelvic fin spines in juvenile *Lodeacanthus* (Upeniece, 2011), and paired fin spines of the juvenile *A. lopatini* (Beznosov, 2009). However, in the so-called "juveniles" of *Tetanopsyrus breviacanthias* (Lower Devonian), paired fin spines are completely formed, but there is no mention of small denticles (Hanke et al., 2001). Histological composition of fin spines differs among acanthodians (Denison, 1979; Burrow et al., 2016). *Triazeugacanthus* shows the presence of mesodentine with two canals (likely vascular). The small vascular cavity develops after the large central cavity. Larger acanthodians, such as *Rhadinacanthus* and *Diplacanthus*, have the presence of trabecular mesodentine and high vascularisation (accessory pulp canals) in paired fin spines (Burrow et al., 2016). In these diplacanthiforms, growth zones are registered only in the central part of the spines, close to pulp cavities (Burrow et al., 2016), which differs from *Triazeugacanthus* where growth zones are present even in periphery, close to the distal margin.

During ontogeny, the pectoral spines of *Triazeugacanthus* develop before the pelvic spines. This pattern has been repeatedly documented in osteichthyans (Bartsch et al., 1997; Joss and Longhurst, 2001; Mabee et al., 2002). This result supports the hypotheses that (1) pectoral fins appeared before pelvic fins during evolution (Coates, 1993, 1994), and (2) pelvic fins are duplicate from pectoral fins (Freitas et al., 2007).

4.6.4 Scales

The completion of the squamation is one of the criteria defining the passage from the juvenile to the adult stage in gnathostomes (Cloutier, 2010). Exhaustive comparison

of this pattern has shown that the bidirectional pattern is common in acanthodians (Chevrinais et al., submitted) and teleosts (Sire and Arnulf, 1990). This squamation pattern might well represent a precursor condition to the unidirectional development of initial scales in chondrichthyans. We agree with Johanson et al. (2007) who considered that the presence of scale patterning maintained through ontogeny might be a synapomorphy of crown group gnathostomes. *Triazeugacanthus* squamation initiates in the region below the dorsal fin spine, and extends bidirectionally to completion in adults.

Scale cover and more specifically squamation development in *Triazeugacanthus* allows us to infer lateral line canal development (Annexe XXVIII). The presence of a gap between scales in the anterior part of the body and its absence in the posterior part suggest that the development of the lateral line canal constrains the squamation development and thus, occurs before the squamation is completed (Annexe XXVIII). However, in *Acanthodes*, scales develop in front of the anal spine, following the lateral line and in direction of the dorsal side of the head (Zidek, 1976; Forey and Young, 1985; Heidtke, 1990; Zajic, 2005; Upeniece, 2011). This suggests a close relationship between lateral line and squamation development. In *Triazeugacanthus*, lateral line canal seems to develop antero-posteriorly and the squamation postero-anteriorly (Chevrinais et al., submitted) [such as in the actinopterygian *Danio rerio* (Ghysen and Dambly-Chaudière, 2004; Sire and Akimenko, 2004)]. This similarity between *Triazeugacanthus* and zebrafish could corroborate the hypothesis that lateral line canal and squamation develop independently in gnathostomes.

4.7 Conclusion

The description of the ontogeny of *Triazeugacanthus affinis* from 178 specimens ranging to 4.5 to 52 mm TL gives the opportunity to describe development of individual skeletal structures (mainly dermal ones), of fin spines and squamation. Developmental trajectory shows the alternance of steps and thresholds and is compared with other gnathostomes showing that *Triazeugacanthus* ontogeny represents the oldest model for the study of development in gnathostomes. Some developmental characteristics of *Triazeugacanthus* are shared with osteichtyans rather than chondrichthyans, and this despite the phylogenetic position of acanthodians as stem-chondrichthyans. Thus, developmental data could represent understudied source of data, having a potential to be included in further phylogenetic analyses.

ARTICLE 5

RÉGIONALISATION DU SQUELETTE AXIAL, PRÉSENCE D'UNE CEINTURE PELVIENNE ET D'ORGANES D'INTROMISSION CHEZ UN AGNATHE DU DÉVONIEN

5.1 Résumé

Un des évènements majeurs dans l'évolution des vertébrés est la transition entre les vertébrés sans mâchoire (agnathes) et les vertébrés avec mâchoires (gnathostomes). Les gnathostomes sont distingués des vertébrés sans mâchoire par une variété de nouveautés évolutives incluant les mâchoires, mais aussi les nageoires paires pectorales et pelviennes avec des ceintures endosquelettiques, et des organes d'intromission pour la fécondation interne. Des ceintures pelviennes et des organes d'intromission ont récemment été reportées chez le groupe le plus basal de gnathostomes, les placodermes (Long et al., 2015). Ici, nous décrivons pour la première fois, des ceintures pelviennes et des organes d'intromission chez l'anaspide *Euphanerops longaevus* Woodward (1900) du Dévonien supérieur du *Lagerstätte* de Miguasha, Canada. Ces éléments sont associés avec une région du squelette axial morphologiquement différente du reste de la colonne vertébrale. La différentiation morphologique de la partie antérieure du squelette axial est aussi décrite pour la première fois chez la lamproie marine *Petromyzon marinus*, une espèce des deux groupes formant les agnathes actuels. Nos nouvelles données concernant *Euphanerops* et *Petromyzon* indiquent que la modification du squelette postcranien a eue lieu plus tôt dans l'histoire évolutive des vertébrés que ce

qu'il a été précédemment estimé, et ne représente plus une synapomorphie des gnathostomes.

Ce cinquième article, intitulé « *Axial skeleton regionalization, pelvic girdle and intromittent organs in a Devonian agnathan* », fut corédigé par moi-même ainsi que par Zerina Johanson (Natural History Museum, Royaume-Uni), Kate Trinajstic (Curtin University, Australie), John Long (Flinders University, Australie), Catherine Morel (UQAR), Claude B. Renaud (Musée Canadien de la Nature, Canada) et Richard Cloutier. Il est en préparation pour être soumis pour publication dans la revue internationale *Nature*. Richard Cloutier et moi-même ont fait les observations sur *Euphanerops*. Catherine Morel, Claude B. Renaud et Richard Cloutier ont fait les observations sur *Petromyzon*. Kate Trinajstic, Zerina Johanson et John Long ont participé à la rédaction et à la comparaison avec les autres espèces de gnathostomes. En tant que premier auteur, ma contribution à ce travail fut l'essentiel de la recherche sur l'état de l'art, la réalisation des dessins d'observations et des analyses en spectrométrie ainsi que la production des figures et du matériel supplémentaire avec les contributions de tous les co-auteurs. J'ai écrit la première version et tous les auteurs ont contribué à la version finale. Une version abrégée de cet article a été présentée à la rencontre *Early Vertebrates, Lower Vertebrates* à Melbourne (Australie) à l'été 2015, un aspect Evo-Dévo a été présenté à la rencontre de l'*European Society for Evolutionary Developmental Biology* qui s'est tenue à Uppsala (Suède) fin Juillet 2016.

Nous remercions J. Kerr, O. Matton et F. Charest (MHNM) et E. Bernard (NHM) pour l'accès aux collections. Nous sommes reconnaissants envers C. Belzile (UQAR) pour les analyses de microscopie électroniques et de spectrométrie. Nous avons apprécié les discussions avec D. Potvin-Leduc (UQAR), H.-P. Schultze (University of Kansas), P. Janvier (MNHN), O. Larouche (UQAR) et R. Sansom (University of Manchester). Les

financements de cette étude proviennent du NSERC (R. Cloutier).

5.2 Axial skeleton regionalization, pelvic girdle and intromittent organs in a Devonian agnathan

One of the major events in vertebrate evolution involves the transition from jawless (agnathan) to jawed (gnathostome) vertebrates. Gnathostomes are distinguished from jawless vertebrates by a variety of evolutionary novelties including jaws, but also both pairs of pectoral and pelvic fins with endoskeletal girdles, and intromittent organs for internal fertilization. Pelvic girdles and intromittent organs have only recently been reported for the most phylogenetically basal gnathostomes, the placoderm antiarchs (Long et al., 2015). Here, we describe, for the first time, pelvic girdles and intromittent organs in the Late Devonian jawless anaspid-like fish *Euphanerops longaevus* Woodward (1900) (Miguasha *Lagerstätte*, Canada), associated with a morphologically differentiated region of the axial skeleton. Morphological differentiation of the anterior axial skeleton is also described for the first time in the Sea lamprey *Petromyzon marinus*, one species of only two groups of living jawless fish. Our new data from *Euphanerops* and *Petromyzon* indicate that modification of the postcranial skeleton occurred earlier in vertebrate evolutionary history than previously appreciated, and no longer represent jawed vertebrate synapomorphies.

5.3 Introduction

The evolutionary transition from jawless to jawed vertebrates involved a variety of cranial and postcranial innovations (Donoghue and Purnell, 2005; Janvier, 2007). The latter was said to include features described in various basal gnathostome placoderm groups, such as pelvic girdles and fins (Long and Young, 1988; Zhu et al., 2012b),

male intromittent organs independent from the pelvic girdle (Long et al., 2009; Trinajstic et al., 2015; Long et al., 2015), as well as a regionalized axial skeleton (Johanson et al., 2013). However, our re-examination of the anaspid-like *Euphanerops longaevus* demonstrates for the first time the presence of pelvic girdles and intromittent organs in jawless vertebrates. Furthermore, the position of the pelvic girdles and intromittent organs in *Euphanerops* is associated with a morphological differentiation (*i.e.*, regionalization) of the axial skeleton along the body, also documented for the first time in the lamprey *Petromyzon*, although more anteriorly. Our new observations provide a more precise understanding of how the appendicular and axial skeletons evolved within the evolutionary history of vertebrates.

5.4 Material and methods

5.4.1 *Euphanerops longaevus*

Specimens of *Euphanerops longaevus* come from the Upper Devonian *Fossil-Fish Lagerstätte* of Miguasha (Canada) (Cloutier et al., 1996). Interpretative drawings of specimens (MHNM 01-123, MHNM 01-02 and NHM P6813) under water immersion were realized using camera lucida (Figure 32 and Annexe XXXII).

Elemental composition analysis was performed on two immature specimens (Annexe XXXIII) using an INCA X-sight (Oxford Instruments) energy dispersive X-ray spectrometer coupled to a JEOL 6460LV SEM at UQAR. The surface of samples was observed without conductive coating. Each spectrum was acquired with a 10 μm spot size, for 100 seconds of lifetime (process time 5, spectrum range 0–20 keV, 2000 channels) at an accelerating voltage of 20 kV. The detection limits of chemical elements are about

1000 ppm or 0.1 wt%. Quantitative optimisation of the system was done using copper as a standard. Elements were automatically identified and quantified in weight by the INCA software and results were normalised to 100%.

5.4.2 *Petromyzon marinus*

Specimens of Sea Lamprey (*Petromyzon marinus*) used in this study are housed in the Fish Collection of the Canadian Museum of Nature (CMNFI). These were sampled from Lake Huron basin (ON, Canada) and the Sainte Anne River (Qc, Canada). In addition, ammocoetes freshly collected from the Old Woman River, Lake Superior basin (ON) in July 2012 were provided by the Bayfield Institute (Fisheries and Oceans Canada). The Maurice-Lamontagne Institute also provided a fresh adult collected from the Saint Lawrence River (Qc) during the summer of 2010. Fresh specimens were fixed in 4% buffered formaldehyde and transferred to 70% ethanol. Total length (TL), the distance between the tip of the snout and the posteriormost part of the caudal fin (Renaud, 2011), were measured with digital calipers.

Whole-mount specimens of ammocoetes (4 populations, n = 79, TL = 19-129 mm) and young adults (four populations, n = 21, TL = 119-153 mm) were cleared-and-stained (C&S) following Potthoff (1984) protocol. Alcian blue (0.3%) in acid solution was used to color cartilaginous structures. A structure was considered formed when uptaking the blue stain. Specimens were examined under a Leica MZ16A binocular microscope equipped with a Qicam digital camera with a CCD sensor (Meyer Instruments, TX).

The branchial, predorsal, second dorsal and caudal regions (Figure 33) of an ammocoete (Old Woman River, AMPMH-01, TL = 132.9 mm) and an adult (Saint Lawrence

River, ADPMH-01, TL = 270.5 mm) were selected for histological preparation. The samples were processed in a Shandon Citadel 2000 automated tissue processor. They were dehydrated in graded ethanol solutions (20–100%), transferred to xylene/ethanol and finally pure xylene. Samples were then transferred to a 50/50 xylene/paraffin solution and impregnated with melted paraffin under a vacuum. Samples were embedded in Paraplast Plus and sectioned at seven μm intervals. Sections were processed through regressive staining using standard haematoxylin and eosin (H&E). Sections were observed with a Leica DMLB microscope and images were taken with an AmScope MU1000 microscope digital camera using Toupview software (Version 3.7, AmScope, 2013).

5.5 Results

Euphanerops displays three rounded neurocranial elements, a head with calcified cartilage, an annular cartilage, a lamprey-like branchial apparatus, a series of arcualia and other cartilages surrounding the notochord, paired anteroventral and anal fins, a median dorsal fin, and a hypocercal tail (Janvier and Arsenault, 2007; Sansom et al., 2013b) (Figure 32 a and Annexes XXXII and XXXIII). The paired anteroventral fins insert directly behind the annular cartilage and extend caudally just anterior to the anus (Janvier and Arsenault, 2007; Sansom et al., 2013b) (Figure 32 a, b). Within these fins, distal cartilaginous elements are made of stacked chondrocytes (Figure 32 b, close-up and Annexe XXXIV g-h), whereas more proximal elements show packed cytoplasmic vacuoles of chondrocytes with thin extracellular matrix (comparable to the composition of axial skeletal elements, Annexe XXXIV e-f). Because of these differences in position and composition, we interpret these as two distinct skeletal elements. The distal elements, previously identified as “paired fin radials” (Janvier and Arsenault, 2007),

are reinterpreted as fin rays, whereas the proximal elements correspond to the supporting radials (Figure 32 a, b; Annexe XXXIV). The organisation of the radials and fin rays suggests that the paired anteroventral fins correspond either to a series of repeated anatomical units along the ventral flank (Annexe XXXV d, 'Unit'), or integrated elongated fins (Figure 32 and Annexe XXXII). A second set of paired fins with fin rays is located behind the anus, representing the anal fins (Sansom et al., 2013b) (Figure 32 a). An elongate median dorsal fin is supported by a series of radials, some bifurcated distally (Figure 32 a).

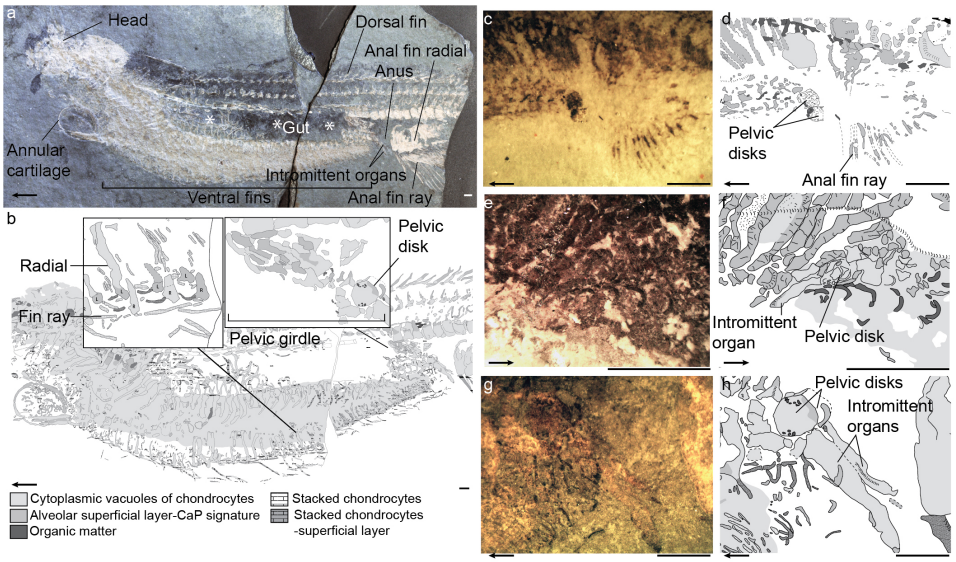

Figure 32: ***Euphanerops* pelvic region and intromittent organs.** a, MHNM 01-123 complete specimen. b, Ventral paired fin structures of MHNM 01-123 and close-up of the left (L) and right (R) body side elements (also see Annexe XXXIV and Figure 33) and of the pelvic girdle. c,d MHNM 01-02A pelvic girdles. e,f NHM P6813 pelvic girdle and intromittent organs. g, h MHNM 01-123 pelvic girdles and intromittent organs. Arrows point anteriorly. Scale bars = 3 mm.

The exceptional preservation of slightly mineralized or non-mineralized tissues (Cloutier, 2013) shows that *Euphanerops* possesses a notochord, and a series of associated dorsal and ventral cartilages. These include notochordal cartilages, left and right-side arcualia

and mediodorsal vertebral elements dorsally, and basiventrals ventrally (Figure 33 f-h). The arcualia and mediodorsal elements are comparable to those present in the anterior axial skeleton of the lamprey, *Petromyzon marinus* (Figure 33 and Annexe XXXII). The element previously identified as an elongated "white line" in *Euphanerops* (Janvier and Arsenault, 2007) is reinterpreted as a diagenetic mineralization of the notochord (Figure 33 f, g, orange). The unsegmented and longitudinal fibrous texture of the notochord of *Euphanerops* recalls the ultrastructural condition of the cephalochordate *Branchiostoma* (Welsch, 1968). Dorsolateral to the notochord, paired notochordal cartilages extend posteriorly from behind the head region to the pelvic complex (described below), and appear to have cup-shaped surfaces that would have rested against the notochord (Figure 33 f, g green). These have become disrupted anterior to the anal fins (MHNM 01-123), and shifted ventrally, possibly due to the postmortem release of decompositional gas from the gut.

Dorsal to the notochord and notochordal cartilages in *Euphanerops*, a row of paired arcualia and mediodorsal cartilages extends along the trunk; the latter much further posteriorly than in *Petromyzon*. The paired arcualia are preserved as distinct rows on MHNM 01-123 (Figures. 32 a, b, 33 f, dark blue, red), and were originally interpreted as ventral arcualia and intermuscular elements (Janvier and Arsenault, 2007). However, we suggest instead that these represent left and right dorsal arcualia that have been shifted slightly from their original positions post-mortem (although the right arcualia extend along the body, more anterior left dorsal arcualia are not preserved). Ventral arcualia are absent anteriorly, but large, rectangular elements interpreted as basiventral/haemal elements [*sensu* Arratia et al. (2001); Janvier and Arsenault (2007); Grogan and Lund (2008)] are present ventrally to the notochord; they begin just dorsal to the anal fins and extend posteriorly (Figure 33 f, purple, h) . The absence of notochordal cartilages and the presence of these morphologically distinct basiventrals in this region suggest that

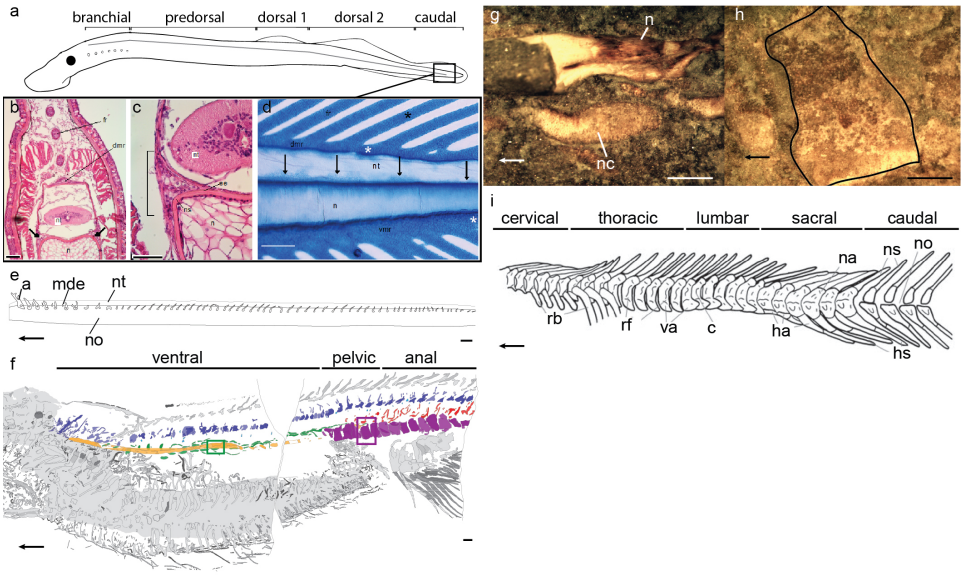

Figure 33: **Vertebrate axial skeleton.** a. *Petromyzon marinus* body sections and location of arcualia (grey bar). b, c Transverse sections of *Petromyzon marinus* ammocoete (AMPMH-01, 132.9 mm TL) of dorsal region of the caudal fin. c, chondroctytes located between the neural tube and the notochord as indicated by the arrows in b. d, Posterior region of the caudal fin of a metamorphosing ammocoete (S3-1, 125.6 mm TL). Large pentagonal cells present in the median rods of the caudal fin are shown by white asterisks. Regularly stacked cells with a rectangular shape forming the fin rays are indicated by black asterisks. Pentagonal chondrocytes lying dorsally to the notochord were also observed and are shown with black arrows. e, General morphology of the arcualia in *Petromyzon marinus*. f, *Euphanerops longaevus* MHNM 01-123 axial skeleton. Blue, right side arcualia; red, left side arcualia; orange, notochord; green, notochordal cartilages; light blue, mediodorsal vertebral elements; and purple, basiventrals (Annexe XXXII). g, notochord and notochordal cartilages MHNM 01-123. h, basiventral MHNM 01-123, with shape highlighted in black. i, Axial skeleton of *Tarrasius problematicus* from the Missisipian of Scotland showing regionalization (five regions recognized) in early actinopterygians (modified from Sallan (2012)). Horizontal bottom left arrows point anteriorly. Scale bars = 0.1 mm in b, 0.05 mm in c, 0.25 mm in d, 1 mm in e,g,h, 3 mm in f.

the axial skeleton of *Euphanerops* shows differentiation into distinct anteroposterior regions. New data from *Petromyzon* indicates that the dorsal arcualia of the lamprey axial skeleton also show regional differentiation anteroposteriorly (Figure 33 a-e and Annexe XXXVI), being larger and more complex anteriorly (bifurcated), with a foramen at the base. Between these larger arcualia are smaller mediodorsal elements. More posteriorly, the arcualia become simplified in shape, and smaller towards the caudal fin.

In *Euphanerops*, a distinct gap is present between the paired anteroventral fins (which appear to decrease in size posteriorly) and the paired anal fins. Within this gap, a pair of rod-like structures can be recognised (Figure 32 a, b, g, h), as well as a more dorsal pair of rounded, disk-like elements. The disks (Figure 32, 'Pelvic disks') were first identified as "carbonaceous imprints at the posterior end of the branchial apparatus" (Janvier and Arsenault, 2007). However, these elements are composed of calcified cartilage (Annexe XXXIV) and are not only positioned between the anteroventral and anal fins, but also at the level where the basiventrals first occur in the axial skeleton, comparable to the transition from the lumbar to sacral region in jawed vertebrates (Figure 33 i). Because of their composition and their relative position, we propose that these disks represent the pelvic girdles (Figure 32 b).

The paired, rod-like structures are associated with the distal margin of the pelvic girdles (Figure 32, 'Intromittent organs'). These show large cytoplasmic chondrocyte vacuoles covered by a mineralized areolar superficial layer (calcium phosphate; Annexe XXXIV b-d) suggesting that they are endochondral. Previously, these elements were described as "diffused mineralized matter" (Janvier and Arsenault, 2007). The calcium phosphate signature suggests the presence of mineralization at least on the surface of these endoskeletal elements, such as in perichondral ossification or in calcified cartilage with calcium phosphate crystals deposited in the extracellular matrix (Janvier and Arsenault,

2002, 2007). These elements differ from what may be expected in a pelvic fin (*i.e.*, multiple fin radials, as in the paired anal fins, rather than a pair of enlarged elements); given their shape (Long et al., 2015), composition and position relative to the pelvic girdles, we suggest these represent paired intromittent organs in *Euphanerops*.

Intromittent organs are identified in two individuals and pelvic girdles in three specimens of *Euphanerops* (Figure 32, Annexe XXXIII), from which an ontogenetic series can be described: two small complete specimens (90 and 96 mm in total length, Figure 32 c-f; Annexe XXXIII), and the large, almost complete specimen described above (distance between the anterior margin of the head to the insertion of anal fins = 170.2 mm) (Figure 32 g-h). The intromittent organs of *Euphanerops* are composed of distal components protruding ventrally from the body (Figure 32). In the smallest *Euphanerops* showing pelvic endoskeleton (90 mm in total length, Annexe XXXIII), only the pelvic disks are present, suggesting either that the intromittent organs form ontogenetically after the pelvic girdles, or, this specimen is a female (Figure 32 c, d). In a slightly larger specimen (96 mm in total length, Annexe XXXIII), a single intromittent organ and one pelvic disk are preserved (Figure 32 e, f). The presence of only one intromittent organ, rather than a pair, is likely a preservational artefact. In the largest specimen, paired intromittent organs (Figure 32 g, h) extend from the body between the paired anteroventral and anal fins. These 8.5-mm long, rod-like structures show a constricted area (neck) at two-thirds their length with the distal extremity slightly curved anteriorly (Figure 32 g, h). This shape recalls the shape observed in arthrodiran placoderms (Long et al., 2015; Trinajstic et al., 2015).

5.6 Discussion

The modification of the appendicular skeleton throughout vertebrates is a major concern in their evolutionary history. Paired appendages in vertebrates are mapped in the cladogram Figure 34 and show a diversity of shapes and positions.

Elongate anteroventral paired fins in *Euphanerops*, with proximal and distal supporting endoskeletal radials and rays, extend anteriorly along the body flank beneath the branchial arches, and could represent the pectoral fins [also in this position in certain thelodonts (Wilson et al., 2007)], although a pectoral girdle is absent. In our interpretation, the gap between these fins and the anal fins [demarcated anteriorly by the end of the digestive tract (Sansom et al., 2013b)], coupled with the differentiation and regionalization of the axial skeleton posteriorly, indicates the position of a pelvic region. Within this gap, two sets of morphologically distinct paired structures can be recognized, one more proximal and circular, representing small pelvic girdles, and one more distal, composed of two thick rod-like structures. There is some similarity to the anal fin radials (Figure 32 a), but the most anterior of these radials is clearly associated with the anteriormost of the anal fin basal supports, suggesting that none had been displaced into the pelvic region. Jawed vertebrates true pelvic fin have more radials, so alternatively, we interpret these elements as intromittent organs. The pelvic fin itself is absent.

Intromittent organs facilitate internal fertilization via transfer of sperm from males to females and are currently dated to the Middle Devonian (390 Myr) (Long et al., 2009). Both extant (lampreys and hagfishes) and extinct (heterostracans, galeaspids, osteostracans, thelodonts) jawless fishes lack intromittent organs, suggesting these first arose in jawed vertebrates (Figure 34). In extant jawed vertebrates, intromittent organs show

a range of morphologies, including modifications of the pelvic fin metapterygium in chondrichthyans (pterygopods/claspers) and the anal fin lepidotrichia in some teleost fishes (gonopodium) (Bürgin, 1990; Lombardo, 1999). Several placoderms, representing the basal phylogenetic nodes of the jawed vertebrate clade, also possess intromittent organs (Long et al., 2009, 2015; Trinajstic et al., 2015). In contrast to chondrichthyans, these appear to lack any association with the pelvic fins, instead articulating with the posterior trunkshield (Antiarchi) or lacking clear surfaces on the proximal margin of the intromittent organ for a mobile articulation to the pelvic fin and being clearly separated posteriorly from the pelvic fin/girdle (Ptyctodontida, Arthrodira) (Long et al., 2009, 2015; Trinajstic et al., 2015). In *Euphanerops*, paired intromittent organs are preserved in close association with the pelvic girdles. It is difficult to determine whether the intromittent organs articulate to the pelvic girdle, but pelvic fins are absent. This suggests that the intromittent organs develop independently from the pelvic fin, as in placoderms, and that this represents the plesiomorphic condition for jawed vertebrates.

The axial skeleton in MHNM 01-123 is well-preserved, except for some postmortem disruption as noted above, and as such, represents the best known postcranial axial skeleton among fossil jawless vertebrates. The only other descriptions of fossil jawless axial skeletons include impressions of the anterior skeleton in heterostracans (Janvier, 1993), an indeterminate portion in the osteostracan *Ateleaspis* (Ritchie, 1967) and *Escuminaspis laticeps* (Belles-Isles, 1989; Janvier et al., 2004) as well as "subunits of some form of axial skeleton" in the anaspid-like *Jamoytius* (Sansom et al., 2010). Our new observations in *Euphanerops* and *Petromyzon* allow for a more detailed comparison to the axial skeleton in these fossil taxa and extant hagfish (Ota et al., 2011, 2014). For the first time in jawless vertebrates, morphologically distinct regions can be recognised within the axial skeleton.

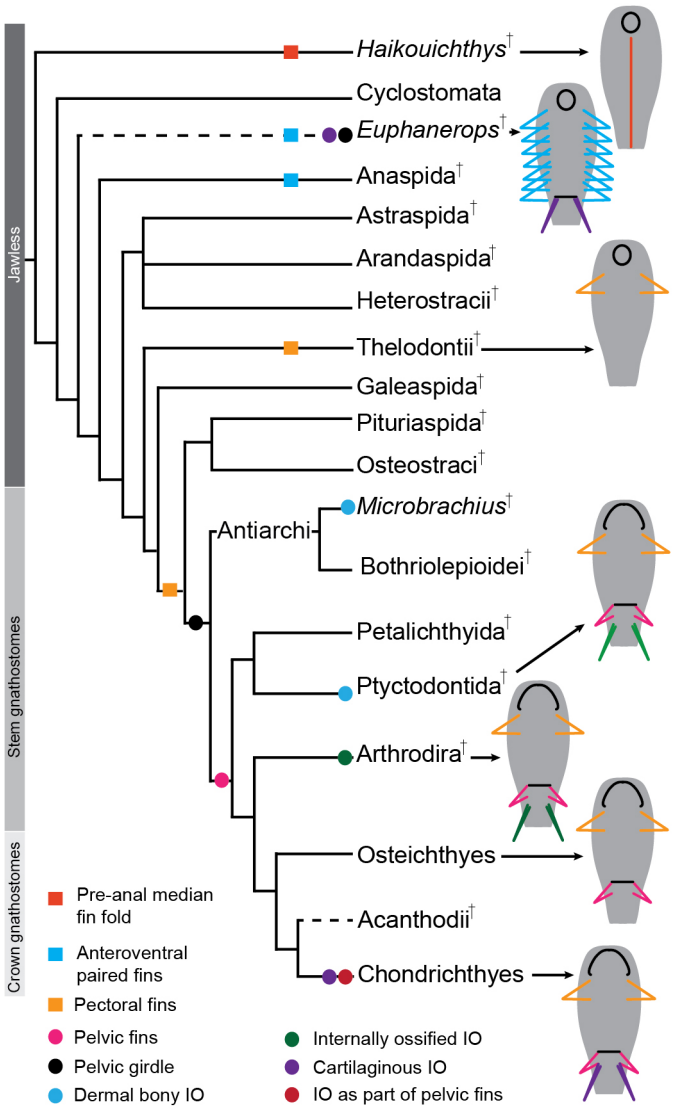

Figure 34: **Cladogram of early vertebrates with the evolution of appendicular skeleton**. Taxa are represented in ventral view. Cladogram modified from Sansom et al. (2010); Long et al. (2015).

In MHNH 01-123, differentiation of the axial skeleton is represented by the abrupt appearance of the large basiventrals (Figure 33 f), indicating an anteroposterior transition comparable to that between the lumbar and sacral regions in tetrapods, but also recognized in the placoderm *Holonema* (Trinajstic, 1999) and the fossil ray-finned fish *Tarrasius* (Figure 33 i) (Sallan, 2012). This lumbar-sacral transition in *Euphanerops* is associated with the gap between the paired anteroventral and anal fins, as well as the pelvic region including girdles and intromittent organs. By comparison, *Petromyzon* shows morphological differentiation anteriorly, involving bifid dorsal arcualia and mediodorsal cartilages. These are more complex and morphologically distinct with respect to the much simpler posterior dorsal arcualia, and there is a distinct point along the vertebral column where these arcualia change (Figure 33 a-e). Previously, lamprey and hagfish axial skeletons were said to be composed throughout of simple, dorsal and ventral arcualia, respectively (Janvier, 2003; Ota et al., 2011; Renaud, 2011). Anterior regionalization of the vertebral column is particularly well known in jawed vertebrates, including differentiation into a cervical region (Figure 33 i) (Burke et al., 1995, corresponding nested *Hox* gene expression), and fusion and modification of vertebral elements in the synarcual (Johanson et al., 2013) and Weberian apparatus (Bird and Hernandez, 2007). The caudal fin of *Petromyzon* may also represent a discrete skeletal region, with the development of cartilaginous plates and rods dorsal and ventral to the notochord (Annexe XXXII) (Ota et al., 2014, and references therein).

Postcranial regionalization in *Euphanerops* and *Petromyzon* provides important information regarding the evolution of the appendicular and axial skeletons in vertebrates. The paired appendages of the appendicular skeleton [*e.g.*, intromittent organs in placoderms (Trinajstic et al., 2015)] derive from a combination of lateral plate mesoderm forming the supporting girdles and fin skeleton, and fin musculature derived from somites. In extant lampreys, distinct regions have been established in the lat-

eral plate mesoderm, including cardiac and posterior lateral plate mesoderm (Onimaru et al., 2011). Collinear *Hox* gene expression in the lateral plate mesoderm, previously associated with positioning of the paired fins along the body (Cohn et al., 1997), has recently been identified in the lamprey posterior lateral plate mesoderm, although fins are absent. In other words, several steps in paired appendage development are already present in the lamprey. However, Tulenko et al. (2013) recently demonstrated that in lampreys, the 'persistent somatopleure' (lateral plate mesoderm + ectoderm) is absent due to a ventral migration of the somitic mesoderm and medial displacement of the lateral plate mesoderm, away from the ectoderm. The presence of radial-supported paired anteroventral fins, pelvic girdles and intromittent organs, and anal fins in *Euphanerops* (and osteostracans with a radial-supported pectoral fin (Janvier et al., 2004)) establishes the presence of this persistent somatopleure among fossil jawless vertebrates, in the stepwise acquisition of paired fins, relative to lampreys. As well, *Euphanerops* and *Petromyzon* show that regionalisation is present through the axial skeleton, both anteriorly and posteriorly, prior to the origin of jawed vertebrates.

CONCLUSION GÉNÉRALE

La problématique, le matériel, les données, les résultats et les conclusions de cette thèse s'inscrivent dans le cadre des travaux sur les vertébrés fossiles et la compréhension de leur évolution. Le contexte phylogénétique incertain concernant la position et le statut des différents groupes de vertébrés, notamment des anaspides et des acanthodiens, rend précieux le matériel fossile disponible à Miguasha, Québec, Canada. Des techniques d'histologie, de microscopie électronique, de diffraction des rayons X mais aussi des dessins de précision ainsi que des analyses phylogénétiques ont été employés afin de décrire avec une approche Evo-Dévo le matériel fossile de Miguasha.

Par l'étude de tous les systèmes anatomiques accessibles au niveau du registre fossile (squelette complet, données chimiques de minéralisation du squelette, écailles et épines qui enregistrent la croissance), l'acanthodien *Triazeugacanthus affinis* est devenu un modèle pour l'étude du développement chez les espèces fossiles. Nous connaissons maintenant une partie des patrons et processus développementaux de cette espèce qui a vécue il y 380 millions d'années bien plus que ceux de certaines espèces actuelles. Dans un deuxième temps, la redescription de l'agnathe *Euphanerops longaevus* apporte des données essentielles sur l'évolution des appendices pairs. Les nouveaux résultats développés selon cinq axes (correspondant aux cinq chapitres) ont permis une meilleure caractérisation et compréhension de l'évolution des vertébrés et de leurs liens phylogénétiques.

Le matériel de *Triazeugacanthus* a été exploité au maximum pour révéler toutes les informations que peut contenir une ontogénie fossile : 1) mise en place des éléments squelettiques, 2) minéralisation progressive du squelette et conditions de fossilisation, 3) croissance des éléments squelettiques individuels, et 4) variation de taille des éléments

squelettiques au cours du développement. Dans un premier temps, l'hypothèse, selon laquelle les individus les plus petits d'une espèce seraient des stades décomposés des spécimens adultes, qui faisait débat depuis quelques décennies, a été rejetée (Chevrinais et al., 2015b). Les variations anatomiques et morphologiques observées au niveau d'une série de taille de *Triazeugacanthus* sont mieux expliquées par la croissance que par la décomposition (Chevrinais et al., 2015b). Cette problématique résolue chez *Triazeugacanthus*, de nouvelles avenues s'ouvrent quant à l'exploitation de données d'ontogénies fossiles (Donoghue and Purnell, 2009). Dans un deuxième temps, les données morphologiques et anatomiques présentées dans Chevrinais et al. (2015b) ont été étudiées au niveau de leur composition chimique (Chevrinais et al., 2015a). Dans un troisième temps, la description de la croissance des structures individuelles retrouvées en grand nombre dans le registre fossile, permet d'inférer la croissance d'individus et donc d'espèces (Chevrinais et al., submitted). Finalement, l'ordre spécifique d'apparition des éléments squelettiques et la trajectoire ontogénétique générale de *Triazeugacanthus* permettent de reconnaitre des patrons et processus communs aux gnathostomes (article 4).

L'article 5 met en lumière une découverte remarquable permise grâce à la préservation exceptionnelle de certains spécimens d'agnathes provenant du *Lagerstätte* de Miguasha, laissant entrevoir leur squelette interne peu minéralisé. La présence chez *Euphanerops* d'une régionalisation du squelette axial, ainsi que d'une ceinture pelvienne et d'organes d'intromission couplée à une longue nageoire ventrale paire avec des éléments endosquelettiques implique que les processus développementaux permettant la mise en place des nageoires paires étaient présents chez les agnathes du Paléozoïque.

Portée de l'étude

Les quatre premiers chapitres, traitant de l'ontogénie de *Triazeugacanthus*, ont permis la résolution de questions évolutives primordiales. Que représentent les spécimens fossiles de petite taille retrouvés en grand nombre (*i.e.*, les scauménelles) à Miguasha ? Quelles sont les caractéristiques de la croissance chez *Triazeugacanthus* ? La croissance d'éléments isolés traduit-elle la croissance des individus et de l'espèce ? Qu'apporte la nouvelle description d'*Euphanerops* ? En plus d'apporter des données au niveau développemental, ces résultats sont primordiaux concernant la compréhension de l'évolution des vertébrés, étant donné que les acanthodiens et les anaspides représentent des groupes éteints.

La croissance chez les poissons est caractérisée par la présence d'une phase cartilagineuse puis d'une minéralisation partielle ou complète du squelette interne (Kemp and Westrin, 1979; Grünbaum et al., 2003; Dean and Summers, 2006). La préservation du squelette minéralisé de *Triazeugacanthus* est notamment due à sa composition en fluoroapatite carbonée (Shemesh, 1990; Kalvoda et al., 2009). Les éléments du squelette interne, comme ceux composant la structure notochordale, ne sont pas minéralisés chez les juvéniles, alors que la ceinture scapulaire est minéralisée dès sa première occurrence. Ces caractéristiques sont donc de bons indicateurs pour discriminer les séries de croissance à partir de fossiles.

Chez *Triazeugacanthus*, les premières phases de l'ontogénie sont axées sur le développement des éléments permettant la respiration, la locomotion et l'alimentation (article 4). Le dévelop-pement est direct chez *Triazeugacanthus* et la trajectoire ontogénétique est caractérisée par la présence de seuils et de plateaux, ce qui est bien connu dans les ontogénies de poissons actuels (Balon, 2001, 2002).

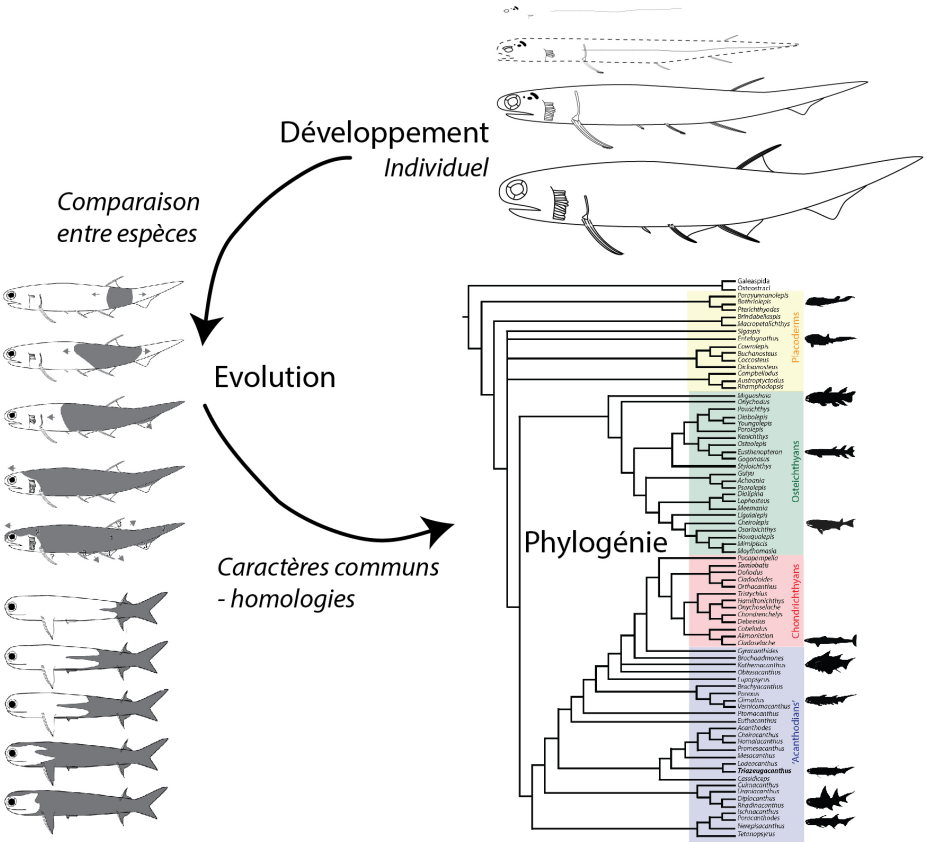

Figure 35: **Représentation schématique de l'intégration des nouvelles données concernant *Triazeugacanthus* dans le concept de Phylo-Evo-Dévo.**

L'analyse phylogénétique des gnathostomes (Chevrinais et al., submitted) permet d'établir deux grandes conclusions : 1) comme suggéré par les dernières analyses phylogénétiques (Brazeau, 2009; Davis et al., 2012; Burrow et al., 2016), les acanthodiens sont un groupe paraphylétique, dans cette étude ils font partie du groupe total des chondrichtyens mais certains ordres sont cependant monophylétiques (*e.g.*, Acanthodiformes), 2) les caractères histologiques sont sous-représentés dans les matrices de phylogénies qui demeurent instables : l'exclusion un par un de caractères provoque un changement de topologie (*e.g.*, monophylie des acanthodiens).

Les résultats qu'ont apporté ces quatre premiers chapitres s'inscrivent donc pleinement dans le *triumvirate* "phylogénie, évolution et développement" (Figure 35) et dans la reconnaissance d'homologies à deux niveaux phylogénétiques. Lors de l'étude de la croissance de *Triazeugacanthus*, la trajectoire d'ossification, l'ordre d'apparition des éléments squelettiques, la mise en place du patron d'écaillure, ainsi que le mode de croissance des écailles regroupent des caractères homologues entre les Acanthodiformes et les ostéichthyens (*e.g.*, type de croissance en "pelures d'oignons" de l'écaille) et/ou plus largement entre les Acanthodiformes et les gnathostomes (*e.g.*, développement précoce des éléments squelettiques permettant l'alimentation, la respiration et la locomotion).

Les résultats, obtenus à partir de la re-description de l'agnathe *Euphanerops*, concernent l'évolution des appendices pairs et sont d'autant plus intéressants que les agnathes actuels, ne possèdent pas de tels éléments squelettiques pairs (Tulenko et al., 2013, 2016). De plus, le fait que la régionalisation de la colonne vertébrale soit conjointe à la présence d'appendices pairs (et notamment d'une ceinture pelvienne) suggère une dépendance ou du moins une interaction entre les processus moléculaires et du développement embryonnaires nécessaires à la formation de ces deux éléments (Cohn

et al., 1997; Onimaru et al., 2011). De ce résultat, couplé à l'absence de nageoires paires chez *Euphanerops*, il découle aussi que les nageoires pectorales ne sont peut être pas les premières nageoires paires avec une ceinture endosquelettique à être apparues au cours de l'évolution des vertébrés [hypothèse soutenue par Wilson et al. (2007)]. Cette nouvelle découverte est primordiale étant donné que l'apparition et l'évolution des appendices pairs est au cœur de l'étude des innovations évolutives caractérisant les gnathostomes (Brazeau and Friedman, 2015).

Finalement, le grand nombre de scauménelles a permis la description de la série de croissance de *Triazeugacanthus*, mais celles-ci, parce que composées à 98 % de spécimens immatures d'*Euphanerops*, renferment un potentiel énorme pour la description de la série de croissance de cet agnathe.

Perspectives de recherche dans le domaine concerné

Les perspectives développées suite à ce travail de recherche résident à court terme dans la possibilité de la description de l'ontogénie d'une seconde espèce à Miguasha, le vertébré sans mâchoire *Euphanerops longaevus*.

Tout d'abord, une re-description de cette espèce a déjà permis d'identifier la présence d'organes d'intromission, d'une ceinture pelvienne ainsi que d'une régionalisation du squelette axial (article 5). Pour la première fois, des caractères que l'on croyait présents seulement chez les gnathostomes sont retrouvés chez un agnathe. Une nouvelle analyse phylogénétique permettra d'ajouter ces caractères dans une matrice avec des taxons représentatifs permettant de traiter des relations agnathes-gnathostomes. Ces caractères représentent la possibilité de lier la paléontologie et la biologie du développement d'une

manière plus que claire. Le terme Phylo-Evo-Dévo prend ici tout son sens.

Dans un second temps, la présence de plus de 2000 spécimens de scauménelles attribuables à *Euphanerops* va permettre, de la même façon que pour *Triazeugacanthus*, de décrire la croissance de cet anaspide du Dévonien, groupe pour lequel la position phylogénétique est débattue (Forey, 1995; Janvier, 1996a; Donoghue et al., 2000; Shu et al., 2003; Gess et al., 2006; Sansom et al., 2010; Blom, 2012; Janvier, 2015). Le matériel brut pour cette étude est déjà disponible, puisque les observations et prises de données ont été réalisées durant cette thèse. Ce travail va donc continuer tout naturellement et promet des résultats rapides. L'étude de la croissance chez *Euphanerops* laisse déjà entrevoir que celle-ci pourrait être indirecte, avec une phase larvaire et une métamorphose (identifiée notamment par une réduction de taille importante de la série branchiale entre les larves et les juvéniles). Ce patron de croissance présente des similarités avec la croissance des lamproies, elle aussi étant indirecte [composée d'une phase ammocoete puis d'une phase adulte suite à la métamorphose (Marinelli and Strenger, 1954; Renaud, 2011)].

Cette perspective va notamment permettre de répondre aux questions suivantes. Quels sont développementaux caractérisant la croissance chez *Euphanerops* ? Ces patrons et processus sont-ils reconnus chez d'autres agnathes fossiles et actuels (*e.g.*, la lamproie) ? Ces processus et patrons sont-ils communs en partie à ce que l'on retrouve chez les gnathostomes ? Les nouvelles données anatomiques et morphologiques sont-elles informatives au niveau de la phylogénie des vertébrés ?

A long terme, une étude des séries de croissance de vertébrés paléozoïques est entrevue, fondée sur les méthodologies employées lors de cette thèse (voir la section "Futures recherches").

Limites de la recherche

Comme toutes les recherches en paléontologie, celle-ci est tout d'abord limitée par le nombre de spécimens d'étude qui peut être très faible (trois spécimens pour la description des organes d'intromission chez *Euphanerops*). De plus, l'altération taphonomique des fossiles, qui correspond à tous les processus biologiques, physiques et chimiques ayant lieu entre le moment de la mort de l'animal et celui où il est retrouvé en tant que fossile représente un biais lors de la description des espèces fossiles (Allison and Briggs, 1991; Chevrinais et al., 2015a). Ces processus englobent le charognage par des prédateurs, la décomposi-tion bactérienne ainsi que les conditions physico-chimiques et de température qui peuvent précipiter la décomposition des tissus. Et au delà de l'aspect purement descriptif, d'autres limites dues à l'altération taphonomique sont présentes et notamment relatives à la définition de caractères informatifs au niveau phylogénétique. Par exemple, la matrice dans Chevrinais et al. (submitted) contient près de 39 % de caractères non codés, parce que représentants des éléments anatomiques non préservés.

Travailler avec du matériel vieux de centaines de millions d'années implique l'absence de données génétiques directes. Les patrons développementaux et les cascades de gènes impliqués sont donc déduits des analyses. Cependant étant donné que la diversité des grands groupes de vertébrés primitifs fossiles surpasse de loin celle des représentants actuels, l'apport de données développementales, même si elles sont exclusivement morphologiques, est d'une aide précieuse dans la compréhension de l'évolution des structures anatomiques et des relations entre les taxons.

Malgré la présence de ces biais, les données fossiles sont primordiales étant donné que l'histoire évolutive des vertébrés est enregistrée majoritairement dans le registre fossile. La compréhension de cette histoire dépend des caractères morphologiques,

qui peuvent être perdus chez les fossiles à cause de processus *post-mortem* comme la décomposition. Mais les structures squelettiques définissant ces caractères peuvent aussi être absentes parce qu'elles ne sont pas encore développées durant la croissance. Une mauvaise interprétation de l'absence de caractères dans le registre fossile peut résulter dans un placement incorrect des espèces dans les arbres évolutifs. De plus, les caractères développementaux peuvent être sous-utilisés dans la construction de ces arbres (Mabee, 2000).

Afin de mieux comprendre les patrons et processus développementaux utilisés dans le registre fossile, un examen de multiples séries de taille de vertébrés montrant une bonne préservation et provenant de multiples *Lagerstätten* du Dévonien ainsi que la comparaison avec des vertébrés primitifs actuels est indispensable.

Futures recherches

Dans le contexte actuel, il y un faible consensus concernant les relations phylogénétiques entre les grands groupes de vertébrés paléozoïques (Forey, 1995; Janvier, 1996a; Donoghue et al., 2000; Shu et al., 2003; Gess et al., 2006; Brazeau, 2009; Sansom et al., 2010; Davis et al., 2012; Blom, 2012; Janvier, 2015; Burrow et al., 2016; Chevrinais et al., submitted). Ce travail de thèse a participé à fournir des données pour une meilleure interprétation de ces relations. Une meilleure interprétation est nécessaire parce qu'elle nous permet de retracer l'évolution des traits à travers l'histoire des vertébrés (*e.g.*, mâchoires, nageoires/pattes, éléments du crâne). Parce que les vertébrés primitifs sont principalement connus à partir de fossiles, spécialement durant le Paléozoïque, les relations doivent être reconstituées à partir des caractères homologues définis par des données morphologiques et anatomiques.

La qualité et la fidélité de la préservation des fossiles dépend de la nature des tissus impliqués, du taux de décomposition précédant la minéralisation et des conditions environnementales permettant la préservation. Normalement, la décomposition *post-mortem* retire une quantité substantielle de tissus mous et peu minéralisés, résultant en une perte de données morphologiques (correspondant à un biais potentiel - voir section Limites de la recherche). A cause de cette perte, les analyses phylogénétiques fondées sur des données fossiles anatomiques sont considérées comme étant biaisées par un "glissement vers le bas" (Sansom and Wills, 2013; Murdock et al., 2014, stem-ward slippage), où les fossiles sont résolus comme plus primitifs à cause de la perte non aléatoire d'éléments anatomiques importants pour la phylogénie (principalement des tissus mous). Ce "glissement vers le bas" a récemment été étudié *via* des études expérimentales de décomposition de vertébrés primitifs actuels (lamproies et myxines) (Sansom et al., 2011, 2013a; Sansom, 2014).

Cependant il est important de noter que les caractéristiques morphologiques des spécimens en décomposition (*e.g.*, perte du squelette des nageoires) peuvent être similaires aux caractéristiques des individus en début de développement (squelette des nageoires pas encore développé). Par exemple, il a été montré chez *Triazeugacanthus*, que les individus de stades développementaux précoces ont été mal identifiés par le passé, comme étant des spécimens en décomposition. De ce fait, une meilleure compréhension des morphologies communes de vertébrés primitifs résultant d'une perte par décomposition ou d'une absence développementale est l'objectif principal de la future recherche que je souhaite développer.

Cette problématique a amené le développement d'un projet de recherche de post-doctorat, en collaboration avec Zerina Johanson du Natural History Museum à Londres et Richard Cloutier (UQAR), qui fait l'objet de deux demandes de subvention (Leve-

rhulme Trust et Newton International Fellowship). Les objectifs de ce projet de recherche répondant à des questions spécifiques, sont de (1) décrire le développement des vertébrés primitifs à partir des espèces fossiles et actuelles, en se concentrant sur la variabilité anatomique à travers une gamme de tailles individuelles ; (2) de tester l'hypothèse selon laquelle la variabilité anatomique des séries de taille fossiles est due à l'ontogénie, plutôt qu'à la décomposition ; et (3) de formuler des caractères développementaux qui seront inclus dans des analyses phylogénétiques de vertébrés primitifs.

Ces objectifs peuvent être adressés et les hypothèses testées en ciblant trois localités du Dévonien : la carrière de Lode (Dévonien supérieur de Lettonie), le *Lagerstätte* de Miguasha (site référence de ma thèse) ainsi que la carrière d'Achanarras (Dévonien moyen d'Écosse). Dans la carrière de Lode, deux séries de croissance ont déjà été décrites (Upeniece, 2001). Le *Lagerstätte* de Miguasha, enregistre, quant à lui, des séries développementales pour 14 des 20 espèces de vertébrés présentes à la localité. Équivalent presque la diversité des espèces du *Lagerstätte* de Miguasha, 15 genres de vertébrés ont déjà été décrits à la carrière d'Achanarras (Dineley, 1999; Newman and Trewin, 2001; Newman, 2002) ; bien que des séries de croissance n'aient pas encore été étudiées.

1. Est ce que les morphologies développementales des vertébrés primitifs fossiles et actuels partagent des caractéristiques communes ?

   Quatorze ontogénies ont déjà été identifiées à Miguasha, très largement dû au travail effectué dans le laboratoire de Richard Cloutier (Cloutier, 2010). Cela inclut l'agnathe *Euphanerops longaevus* et l'acanthodien *Triazeugacanthus affinis* (décrits durant mon travail de thèse), le placoderme *Bothriolepis canadensis*, le dipnoiforme *Scaumenacia curta*, et l'ostéolépiforme *Eusthenopteron foordi*.

Parmi les fossiles de la carrière de Lode, les ontogénies du placoderme *Asterolepis ornata* et de l'acanthodien *Lodeacanthus gaujicus* ont été décrites (Upeniece, 2001). Au niveau des espèces actuelles, des ontogénies ont été décrites pour la lamproie *Petromyzon marinus* (Richardson et al., 2010, ainsi que dans le laboratoire de Richard Cloutier) et pour la myxine *Eptatretus burgeri* (Ota et al., 2011).

Les séries de taille n'ont pas encore été totalement examinées pour les spécimens de la carrière d'Achanarras, mais ils représentent cependant une comparaison importante, notamment avec les spécimens de Miguasha. A Achanarras, on retrouve deux espèces d'agnathes [*Cornovichthys blaauweni* (Newman and Trewin, 2001) et *Achanarella trewini* (Newman, 2002), cette dernière étant préservées sur de nombreuses plaques avec plus de dix spécimens par plaque] et plusieurs espèces de gnathostomes comme les dipnoiformes *Pentlandia* et *Dipterus* et les ostéolépiformes *Thursius* et *Tristichopterus*.

Ce futur axe de recherche nécessite une méthodologie adéquate, en partie développée durant ma thèse. Les données développementales pourront être collectées à partir de ces sources, et de nouvelles données pourront être ajoutées à partir de l'examen des fossiles des localités citées ci-dessus. Les séries développementales pourront être identifiées en utilisant une gamme aussi complète que possible d'individus de tailles différentes, et des métriques afin d'analyser les changements anatomiques ayant lieu pendant le développement des vertébrés primitifs pourront être déterminées et utilisées (à partir de celles déjà décrites dans cette thèse). Cela inclut : a) des corrélations entre la taille d'un élément squelettique et la longueur totale d'un spécimen, b) le nombre cumulatif d'éléments squelettiques en fonction de la longueur totale (courbe de la trajectoire ontogénétique), et c) une analyse des changements ontogénétiques en termes de changements de forme en utilisant des grilles de déformations et des analyses en composantes principales. De plus, les ontogénies de lamproies et de myxines pourront être examinées (*via*

un protocole de “clear and staining”, et du micro CT-scan), en utilisant les mêmes méthodologies et métriques que pour les espèces fossiles, afin de comparer avec les séries développementales fossiles.

2. L’hypothèse principale de ce projet de recherche est que la variation anatomique des fossiles est due à l’ontogénie plutôt qu’à la décomposition.

   L’étude des fossiles de ces trois sites, couplée à celle des ontogénies d’espèces actuelles, permettront de construire la plus large base de données existante pour examiner les variations morphologiques et anatomiques ayant lieu lors de la croissance. Ces données sont donc intéressantes pour répondre aux questions suivantes. Quelles sont les caractéristiques des séries développementales en opposition aux séries de décomposition ? Quels sont les patrons et les processus observés au niveau du développement des vertébrés paléozoïques ? Ces patrons et processus sont-ils communs aux différents groupes taxonomiques ? Ces données apporteront l’évidence nécessaire pour évaluer de façon plus critique les morphologies fossiles et pour tester les hypothèses relatives aux effets de la taphonomie (incluant la décomposition) sur ces morphologies.

3. Est ce que les données développementales sont informatives pour résoudre la phylogénie des vertébrés paléozoïques ?

   Actuellement, la phylogénie des vertébrés n’est pas complétement résolue (Zhu et al., 2013; Dupret et al., 2014; Brazeau and Friedman, 2014; Janvier, 2015). Les données développementales représentent cependant une source sous-estimée de caractères pour les analyses phylogénétiques, comme il a été montré avec ce travail de thèse à propos de *Triazeugacanthus*. Ces données ont le potentiel d’apporter une résolution à ce segment important de l’arbre évolutif des vertébrés.

Mot de la fin

A long terme, ce travail de thèse sur des fossiles du Dévonien s'inscrit dans une compréhension globale du développement des organismes et ce que cette compréhension apporte dans l'étude des relations phylogénétiques et l'évolution des structures anatomiques. Scientifiquement, je souhaite développer ce champ de recherche car il renferme nombres de résultats jusqu'alors très peu utilisés. En effet le développement des organismes étant très contraint et présentant des similitudes entre les grands groupes de vertébrés, le potentiel des données développementales pour une résolution des relations phylogénétiques entre les grands groupes est sous-estimé. La mise en place d'un groupe de recherche avec des spécialistes des grands groupes de vertébrés, afin de déterminer une liste de caractères pertinents pour coder une matrice de phylogénie avec un nombre le plus exhaustif possible de représentants fossiles et actuels pour chaque groupe, serait souhaitable et bénéfique dans un but de compréhension de l'histoire évolutive des vertébrés.

Plus largement, et dans le contexte sociétal actuel, la paléontologie satisfait une part de l'imaginaire collectif, relatif aux origines de la vie et à son évolution à travers le temps. Selon moi, il est important de faire perdurer et d'alimenter cet imaginaire car il sensibilise à la nature, à ses perturbations et à son changement. Le travail avec des spécimens vieux de centaines de millions d'années, enrichit l'humain d'un émerveillement pour le naturel qui, il me semble, est important à transmettre. Cet émerveillement pour le passé et l'évolution des espèces rend presque émouvante la contemplation de la nature actuelle. Peut être que le maintien de cet émerveillement est encore plus primordial aujourd'hui, quand on sait la crise de la biodiversité que nous traversons.

Mon point de vue est qu'il est tout a fait primordial d'être un bon chercheur, mais

qu'un bon chercheur qui ne vulgarise pas, ne remplit pas sa fonction à 100 %. Communiquer sur les nouveaux résultats permettant une compréhension du monde ; cette compréhension étant le seul moyen qui nous en rapproche et nous sensibilise à ses pertes. Un travail éducatif et de sensibilisation semble nécessaire parce que le travail scientifique mené par la raison, est fournisseur de résultats, de données concrètes et irréfutables mais ce sont bien les sentiments qui touchent les enfants, les gens, les communautés et les sociétés en général et qui permettront à terme de faire entendre raison. Le scientifique a donc ici un rôle à jouer, un rôle difficile auquel il n'est pas habitué et pas formé mais qui cependant est lié à la nature même de l'humain : transformer le concret et le rationnel en sentimental afin de mobiliser sur la vision la plus juste possible de l'état de la biodiversité.

ANNEXE I

GEOLOGICAL TIME SCALE

INTERNATIONAL CHRONOSTRATIGRAPHIC CHART

IUGS www.stratigraphy.org International Commission on Stratigraphy v 2016/04

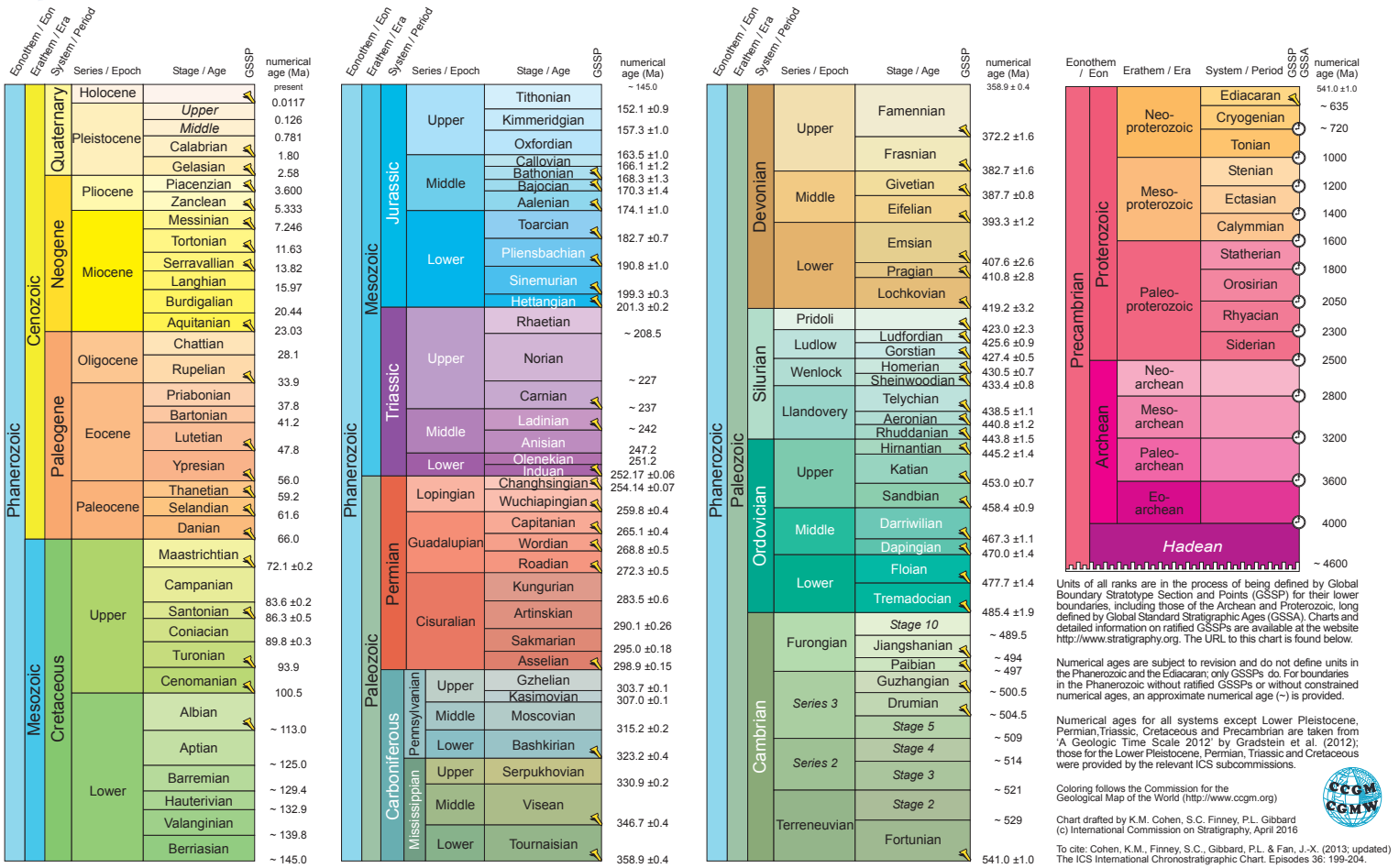

Units of all ranks are in the process of being defined by Global Boundary Stratotype Section and Points (GSSP) for their lower boundaries, including those of the Archean and Proterozoic, long defined by Global Standard Stratigraphic Ages (GSSA). Charts and detailed information on ratified GSSPs are available at the website http://www.stratigraphy.org. The URL to this chart is found below.

Numerical ages are subject to revision and do not define units in the Phanerozoic and the Ediacaran; only GSSPs do. For boundaries in the Phanerozoic without ratified GSSPs or without constrained numerical ages, an approximate numerical age (~) is provided.

Numerical ages for all systems except Lower Pleistocene, Permian,Triassic, Cretaceous and Precambrian are taken from 'A Geologic Time Scale 2012' by Gradstein et al. (2012); those for the Lower Pleistocene, Permian, Triassic and Cretaceous were provided by the relevant ICS subcommissions.

Coloring follows the Commission for the Geological Map of the World (http://www.ccgm.org)

Chart drafted by K.M. Cohen, S.C. Finney, P.L. Gibbard (c) International Commission on Stratigraphy, April 2016

To cite: Cohen, K.M., Finney, S.C., Gibbard, P.L. & Fan, J.-X. (2013; updated) The ICS International Chronostratigraphic Chart. Episodes 36: 199-204.

URL: http://www.stratigraphy.org/ICSchart/ChronostratChart2016-04.pdf

ANNEXE II

DIAGNOSTIC *TRIAZEUGACANTHUS* OTOLITHS IN MORPHOTYPE 1 (LARVAL) (A-B), MORPHOTYPE 2 (JUVENILE) (C-M) AND MORPHOTYPE 3 (ADULT) (N-O)

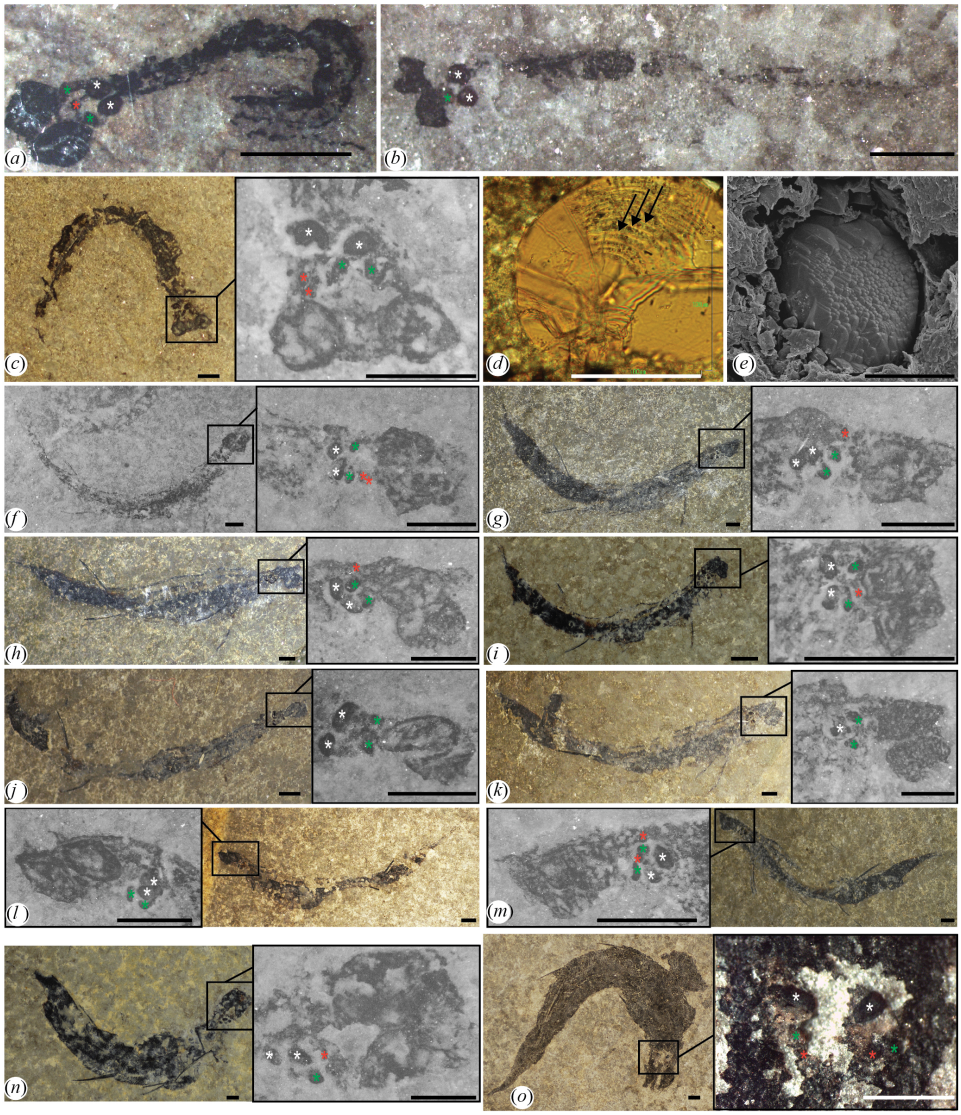

(a) MHNM 03-302. (b) MHNM 03-440. (c) MHNM 03-2684 and close-up of head region. (d) MHNM 03-1971 otolith thin section showing growth lines (arrows). (e) MHNM 03-210 SEM picture of otolith. (f) MHNM 03-1204 and close-up of head region. (g) MHNM 03-1879 and close-up of head region. (h) MHNM 03-1252 and close-up of head region. (i) MHNM 03-978 and close-up of head region. (j) MHNM 03-1408 and close-up of head region. (k) MHNM 03-1468 and close-up of head region. (l) MHNM 03-2033 and close-up of head region. (m) MHNM 03-1250 and close-up of head region. (n) MHNM 03-1962 and close-up of head region. (o) MHNM 03-176 and close-up of head region. *T. affinis* possesses three pairs of smooth bean-shaped otoliths. The hemispherical posterior otoliths (white stars) are approximately two times larger than the ovoid intermediate ones (green stars) and between two to three times larger than the spherical anterior ones (red stars). Scale bars = 1 mm except in (d) scale bar = 100 μm and (e) scale bar = 50 μm.

ANNEXE III

MORPHOMETRIC MEASUREMENTS TAKEN ON *TRIAZEUGACANTHUS AFFINIS*

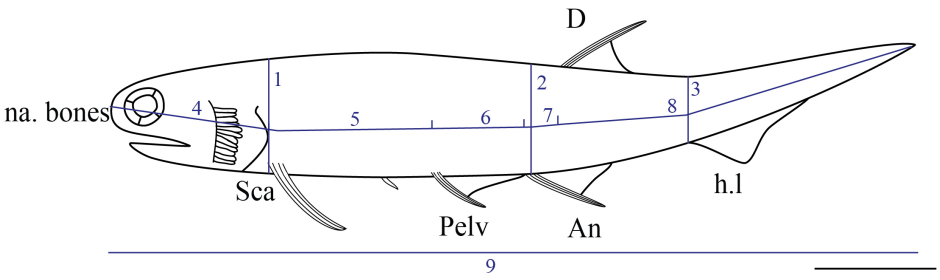

1, body height at the level of the scapula; 2, body height at the level of the anal spine; 3, body height at the level of the hypochordal lobe; 4, distance between tip of the snout and pectoral fin spine; 5, distance between pectoral and pelvic spines; 6, distance between pelvic and anal fin spines; 7, distance between anal and dorsal fin spines; 8, distance between the dorsal fin spine and the posterior extremity of the caudal fin; 9, total length. Drawing modified from Gagnier (1996). Scale bars = 5 mm.

ANNEXE IV

ONTOGENETIC SEQUENCE OF ENDOSKELETAL, EXOSKELETAL AND OTHER STRUCTURES OF *TRIAZEUGACANTHUS AFFINIS* RELATED TO SPECIMEN TOTAL LENGTH AND CLUSTERED BY MORPHOTYPES (RESPECTIVELY LARVAE, JUVENILES AND ADULTS)

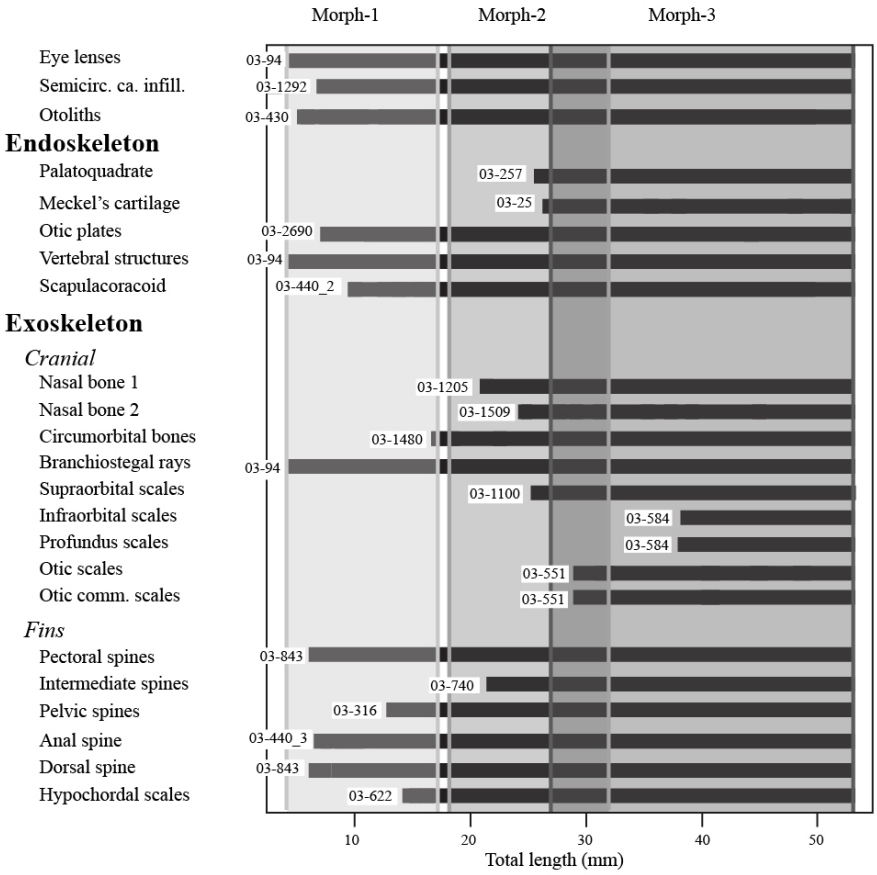

Horizontal black bars start at the size when the structure is identified first. Specimen numbers correspond to the smallest specimen (MHNM collections), in which a given structure has been recorded.

ANNEXE V

TAPHONOMIC ALTERATIONS OBSERVED IN *TRIAZEUGACANTHUS*

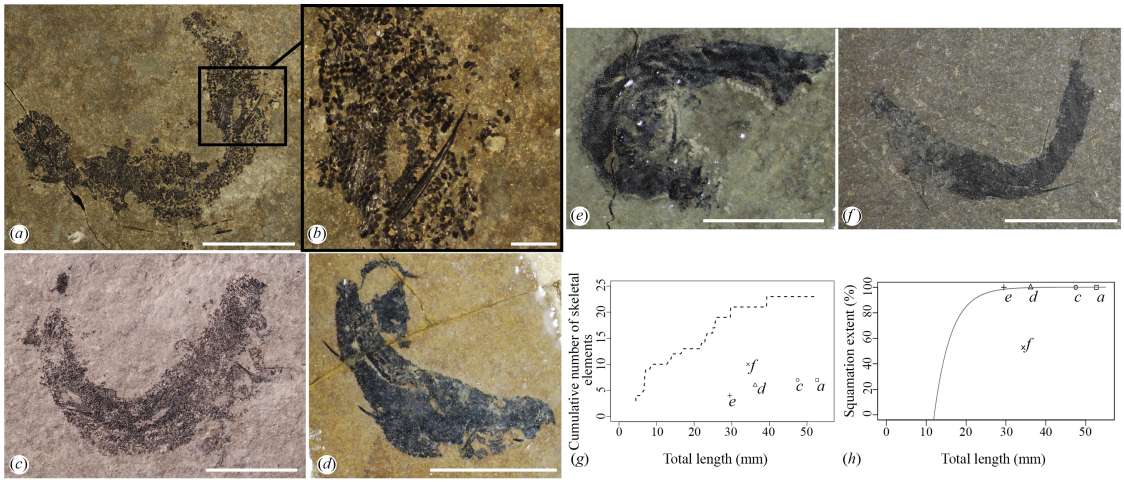

(a) MHNM 03-1107. (b) MHNM 03-1107 close-up of the posterior region. (c) MHNM 03-1817. (d) MHNM 03-452. (e) MHNM 03-164. (f) MHNM 03-1798. Taphonomic alterations include : (1) scattering of scales (a, b); (2) post-mortem gas rupture of the abdominal cavity (c-e) and, (3) a dorsal curvature of the body showing tetany (a-f). (g) Cumulative number of skeletal elements (dotted line) in relation to TL and positions of specimens showed above. Individual skeletal elements used to evaluate the cumulative number of 23 cranial and postcranial elements (paired and multiple elements are counted for one structure) are represented in the Annexe III (terminology primarily follows Gagnier (1996). (h) Squamation extent in relation to TL and positions of specimens showed above. Scale bars = 10 mm except in (b) = 2 mm.

ANNEXE VI

COMBINED PRINCIPAL COMPONENT ANALYSIS FOR 45 SPECIMENS OF MORPHOTYPES 2 (JUVENILE) AND 3 (ADULT) *TRIAZEUGACANTHUS*

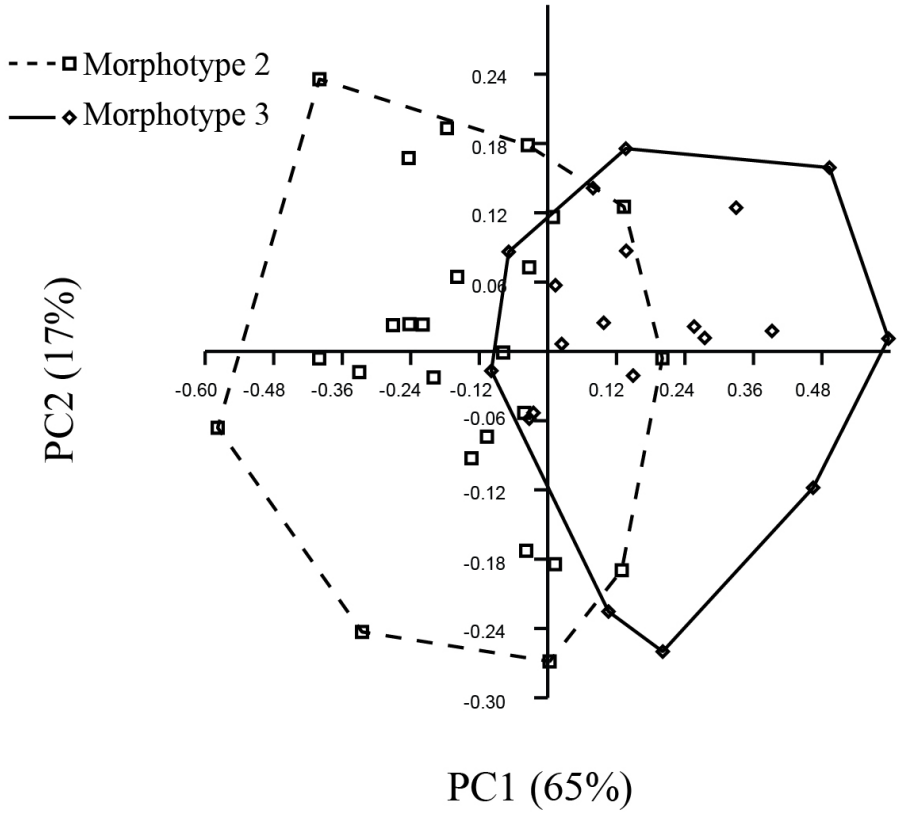

Five variables have been used : distance between tip of the snout and pectoral fin spine ; distance between pectoral and pelvic spines ; distance between pelvic and anal fin spines ; distance between anal and dorsal fin spines [log10(x+1) transformed] ; distance between the dorsal fin spine and the posterior extremity of the caudal fin. Minimum convex hulls delimit the juvenile and adult specimens. Percentages of variation are given in parentheses.

ANNEXE VII

SPECIMEN MHNM 03-1699 OF *TRIAZEUGACANTHUS AFFINIS* USED FOR FOURRIER-TRANSFORMED INFRA RED SPECTROMETRY AND X-RAY DIFFRACTION

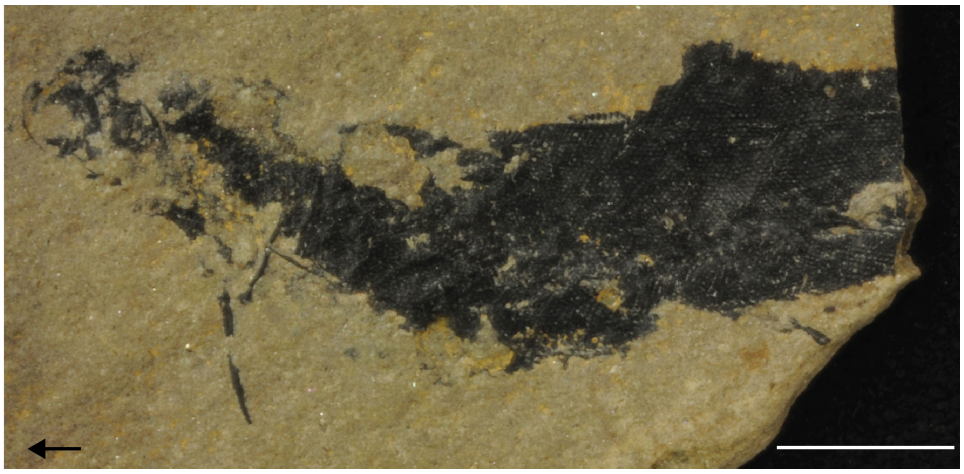

Scale bar = 10 mm. Arrow points anteriorly.

ANNEXE VIII

BLACK DOGFISH *CENTROSCYLLIUM FABRICII* ANATOMICAL ELEMENTS IMMERGED IN WATER.

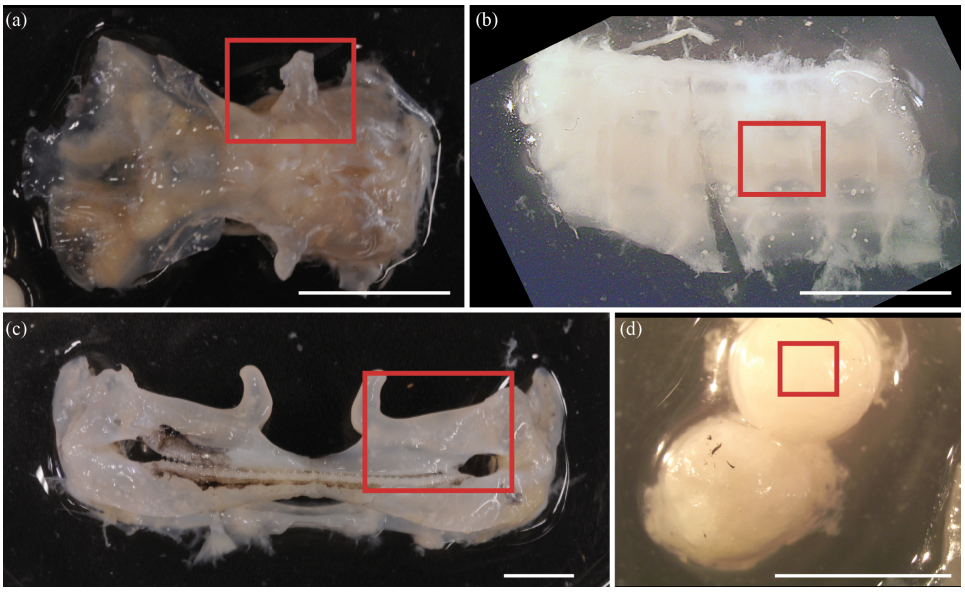

Specimen 0919 247F. (a) Dorsal view of the neurocranium. (b) Vertebral centra. (c) Mandibular and hyoid arches. (d) Eye lenses. Red squares represent areas of interest for EDX analyses. Scale bars = 10 mm in (a) and (d), and 5 mm in (b) and (c).

ANNEXE IX

ATLANTIC MACKEREL *SCOMBER SCOMBRUS* ANATOMICAL ELEMENTS, SEM IMAGES

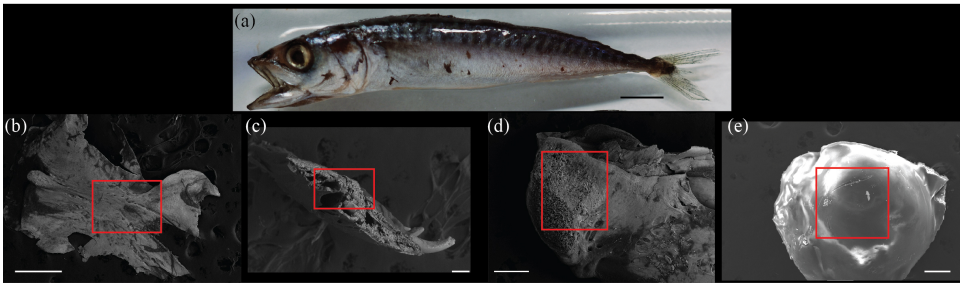

(a) Juvenile Atlantic mackerel. (b) Exoccipital. (c) Section of the dentary. (d) Basihyal. (e) Eye lens. Red squares represent areas of interest for EDX analyses. Scale bars = 10 mm in (a), 500 μm in (b), 100 μm in (c) and 200 μm in (d), (e).

ANNEXE X

REPRESENTATIVE SPECTRA OF *CENTROSCYLLIUM FABRICII* SAMPLES USING EDX PUNCTUAL MICROANALYSES

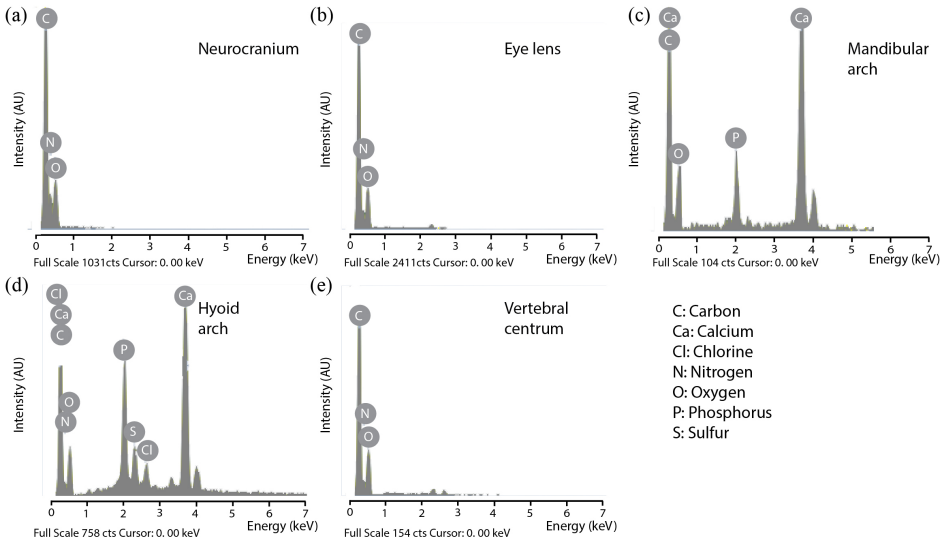

Spectra correspond to six different anatomical elements : (a) neurocranium, (b) eye lens, (c) Meckel's cartilage, (d) hyoid arch, and (e) vertebral centrum. Chemical elements are given only if they represent less than 1% of the relative composition. Elements were automatically identified and quantified in weight by the INCA software and results were normalized to 100%. Because we used an environmental EDX spectrometer, the amount of oxygen is non-significant for our analyses and depends essentially on the vacuum level in the chamber of the SEM.

ANNEXE XI

REPRESENTATIVE SPECTRA OF *SCOMBER SCOMBRUS* SAMPLES USING EDX PUNCTUAL MICROANALYSES

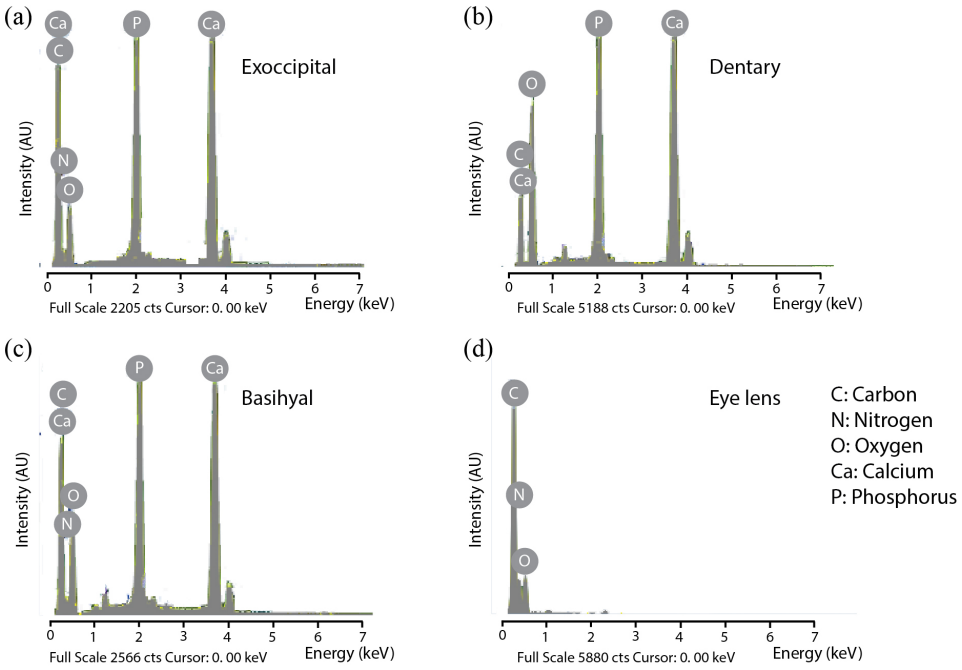

Spectra correspond to six different anatomical elements : (a) exoccipital, (b) dentary, (c) basihyal, and (d) eye lens. Chemical elements are given only if they represent less than 1% of the relative composition. Elements were automatically identified and quantified in weight by the INCA software and results were normalized to 100%. Because we used an environmental EDX spectrometer, the amount of oxygen is non-significant for our analyses and depends essentially on the vacuum level in the chamber of the SEM.

ANNEXE XII

TRIAZEUGACANTHUS AFFINIS SPECIMENS USED FOR EITHER HISTOLOGY OR SEM-EDS X-RAY ANALYSES

Squamation cover is indicated and its extent (as percentage of total length) is measured from head to tail.

Specimen ID	*Analyses*	*TL (mm)*	*Squamation extent (%)*
MHNM 03-1817	Histology	47.51	100
MHNM 03-1971	Histology	49.21	100
MHNM 03-78	Histology	26.52	100
MHNM 03-2620	Histology	35.44	100
MHNM 03-1497	EDS X-ray - SEM	45.29	100
MHNM 03-1819	Histology - SEM	23.9	48
MHNM 03-398	Histology - EDS X-ray - SEM	17.02	57
MHNM 03-701	Histology	33.18	49
MHNM 03-2684 2	Histology	12.71	NA
MHNM 03-529	Histology	43.28	NA
MHNM 03-372	Histology	16.02	13
MHNM 03-740	Histology	21.92	33
MHNM 03-1250	Histology	21.37	37
MHNM 03-210	Histology - SEM	17.55	33
MHNM 03-978	Histology	21.64	38
MHNM 03-2631	Histology - SEM	31.47	43
MHNM 03-259	Histology - SEM	13.82	55
MHNM 03-2570	Histology - SEM	22.96	63
MHNM 03-1460	SEM	NA	NA

ANNEXE XIII

TRIAZEUGACANTHUS AFFINIS SCALE MEASUREMENTS USED FOR LINEAR REGRESSIONS AND ANOVA ANALYSES RELATED TO ONTOGENETIC STAGES

Thickness and width values obtained from transverse ground sections of scales are given in $\log_{10}$ and μm, except for thickness/width where values were $\log_{10}(x+1)$-transformed.

Specimen ID	*Thickness*	*Width*	*Thickness/Width*
Adults			
MHNM 03-1817	1.98515692	2.37391744	0.1487706
	2.08149133	2.25880723	0.22135931
	2.02710079	2.23081919	0.21100786
	1.98237979	2.27596288	0.17858778
	1.85448823	2.25825405	0.14447147
	1.90661514	2.33804392	0.13682039
	1.93785877	2.28935703	0.1599115
	2.02391472	2.31377867	0.17984526
	1.85838078	2.32332224	0.12801586
	1.96465084	2.32939991	0.15587279
Continued on next page			

Continued from previous page

Specimen ID	*Thickness*	*Width*	*Thickness/Width*
	1.90661514	2.26083908	0.15907374
	1.84801043	2.38659527	0.11036896
	1.85692817	2.34220153	0.12291501
	1.87785491	2.33587494	0.12979338
	1.78843	2.42931454	0.08941781
	1.76285105	2.36087351	0.09772053
	1.84712209	2.32285992	0.12528501
	1.86486099	2.34399317	0.12443688
	1.76732658	2.34682223	0.10151765
	1.79919576	2.39244369	0.09868679
	1.75554711	2.40823318	0.08724594
	1.6531353	2.33231522	0.08254285
	1.89063895	2.41876517	0.11273801
	1.91450182	2.21415744	0.17654987
	1.93337085	2.28385731	0.16022341
	1.9006784	2.3290784	0.13764097
	1.89458188	2.34174703	0.13262369
	1.92292777	2.39874011	0.12526634
	1.96364146	2.28389571	0.16977726
	1.88910553	2.27324904	0.15011482
	1.89247862	2.35861813	0.12771031
	1.76732658	2.44797931	0.08228828
	1.84636186	2.38736313	0.10982785
	1.79342017	2.32698477	0.11150062

Continued on next page

Continued from previous page

Specimen ID	*Thickness*	*Width*	*Thickness/Width*
	1.82326551	2.30633494	0.12345931
	1.810864	2.42202979	0.09510406
	1.82030657	2.24539914	0.13854183
	1.79450199	2.35754228	0.10499946
	1.74697652	2.35296162	0.09612782
	1.83206161	2.38705864	0.10673946
	1.8297025	2.20988213	0.15127697
	1.71962955	2.29218516	0.10297342
	1.72662942	2.186801	0.12923857
	1.69838766	2.19892638	0.11920168
	1.75442479	2.13631779	0.15077372
	1.66238002	2.30477479	0.08913719
	1.72180237	2.29339571	0.10317673
	1.86987095	2.24166351	0.15376075
	1.87096543	2.25278994	0.15079381
	1.78947495	2.32767968	0.11045428
	1.75539458	2.4323968	0.08292058
	1.83126172	2.33489988	0.11845975
	1.78540102	2.41187045	0.09213665
	1.74873056	2.40717328	0.0862039
	1.74076521	2.39493474	0.08697633
	1.82548454	2.33250309	0.11765514
	1.82351987	2.39997814	0.10215252
	1.84551352	2.32263271	0.12493925

Continued on next page

Continued from previous page

Specimen ID	*Thickness*	*Width*	*Thickness/Width*
	1.81421429	2.31561143	0.11899579
	1.78730458	2.35867708	0.10322344
	1.78049013	2.35454828	0.10265668
	1.82836984	2.28187159	0.13096513
	1.86742624	2.4111734	0.1092158
	1.74413645	2.30968764	0.10446143
	1.85367388	2.37286599	0.1147969
	1.84147835	2.40419035	0.10506999
	1.84358779	2.31115179	0.12734784
	1.87588853	2.35894322	0.12346296
MHNM 03-78	1.52896809	2.159955	0.09127672
	1.41247735	2.06465263	0.08733895
	1.37021692	1.99353763	0.09274032
	1.37845241	2.17629099	0.06418837
	1.43507954	2.1725212	0.07300134
	1.38084413	2.03668877	0.08667279
	1.58593425	2.04339372	0.12993826
Juveniles			
MHNM 03-259	1.08075106	1.80247123	0.07547135
	0.98066972	1.82560538	0.05801225
	1.18953478	1.89971046	0.0773336
	1.19251814	1.82301293	0.09137004
	1.01154926	1.77589235	0.06894647
	1.06795629	1.84396604	0.06725337

Continued on next page

Continued from previous page

Specimen ID	*Thickness*	*Width*	*Thickness/Width*
MHNM 03-398	1.16346569	2.13291759	0.0442603
	1.79074948	2.2774052	0.12257467
	1.7816405	2.30105388	0.11474551
	1.81914236	2.34431759	0.11341447
	1.81931357	2.36654436	0.10844363
	1.80452106	2.16291672	0.15779856
	1.7706974	2.26426516	0.12088513
	1.78005075	2.27008229	0.12174697
	1.79025701	2.29747599	0.11760758
	1.67878234	2.37475384	0.07968244
	1.71594488	2.43429259	0.07601108
	1.75854857	2.19385616	0.13577559
	1.72914858	2.38246732	0.08713086
	1.79971264	2.3466209	0.10851491
	1.81603571	2.31550853	0.11945776
	1.81132696	2.14746917	0.16469972
	1.69334875	2.33663582	0.08897176
	1.82459438	2.31687575	0.12119803
	1.75472283	2.30942788	0.1068031
	1.71222024	2.31168183	0.09743094
	1.78712027	2.29399199	0.11768999
	1.74786218	2.27622736	0.11268339
	1.8012802	2.25870192	0.12994802
	1.76062601	2.26810504	0.11754591

Continued on next page

Continued from previous page

Specimen ID	*Thickness*	*Width*	*Thickness/Width*
	1.84653504	2.28897319	0.13387262
	1.77603252	2.3407276	0.1046446
	1.77321578	2.31116027	0.11051274
	1.82957392	2.40689258	0.10197232
	1.76964314	2.39021598	0.09327004
	1.69155003	2.34559523	0.0869989
	1.64443859	2.2861195	0.08926973
	1.74845938	2.35895652	0.09523564
	1.79025701	2.32248393	0.11180387
	1.78611939	2.3572295	0.10327896
	1.74179744	2.26527312	0.11380567
	1.69563925	2.32839388	0.09094219
	1.67878234	2.30483292	0.09221674
	1.72253521	2.28283728	0.10558899
	1.78173384	2.19257582	0.1424807
	1.74766035	2.19293525	0.13312192
	1.80953278	2.23450969	0.13857342
	1.69790903	2.28844598	0.09923921
	1.76324076	2.34992218	0.1000296
	1.66376687	2.35372201	0.08069678
	1.68946869	2.36597255	0.08300724
	1.72118386	2.29400965	0.1029164
	1.68946869	2.34325888	0.0870452
	1.27036818	2.17037483	0.0514962

Continued on next page

Continued from previous page

Specimen ID	*Thickness*	*Width*	*Thickness/Width*
	1.24970686	2.14386506	0.05215406
	1.38300136	2.09971295	0.07627419
	1.36240164	2.05037883	0.08103281
	1.16102729	2.01476847	0.05692091
	1.3510831	1.95397732	0.09674329
	1.22019248	1.86811954	0.08811596
	1.24367359	2.01156669	0.06842716
	1.19762174	1.94086226	0.07210916
	1.28764648	1.98637023	0.0792223
	1.19536891	2.02051645	0.06053646
	1.19611926	1.98205721	0.06584291
MHNM 03-529	1.35672862	2.22718892	0.05490149
	1.37341658	2.21878134	0.05795862
	1.35672862	2.22967831	0.05460662
	1.36461119	2.12762534	0.0691418
	1.27685162	2.13760379	0.05606576
	1.36864806	2.12964293	0.06943959
	1.53093605	2.23381551	0.07853211
	1.48452746	2.239636	0.07031441
	1.46093167	2.17352261	0.07694055
	1.48413842	2.31472983	0.059832
	1.463903	2.27603141	0.06225265
	1.70393435	2.32960887	0.09228871
	1.65620769	2.28604535	0.0914948

Continued on next page

Continued from previous page

Specimen ID	*Thickness*	*Width*	*Thickness/Width*
	1.6690414	2.21928354	0.10778002
	1.63007297	2.26798312	0.08997283
	1.71918433	2.1805098	0.12894187
	1.77674369	2.19760939	0.13970039
	1.4543844	2.213943	0.06965211
	1.4203791	2.00199307	0.10107695
	1.57754784	2.28363952	0.07800238
	1.53493856	2.20018804	0.08498631
	1.57506991	2.17684394	0.09696722
	1.53832862	2.15701595	0.09363508
	1.56037779	2.13020341	0.10355113
	1.54157557	2.00750296	0.12776437
	1.48110138	2.2459543	0.06887166
	1.38747458	2.13831897	0.07095447
	1.36632565	2.1607415	0.06466024
	1.43837018	2.14021501	0.07870343
	1.34289245	2.15885064	0.06174316
MHNM 03-701	1.40835604	2.06530944	0.08647241
	1.56336858	2.07669637	0.11616613
	1.43513006	2.03840855	0.09666659
	1.51767792	2.14303448	0.0923496
	1.76081438	2.37354091	0.09479756
	1.78237228	2.25071512	0.12715003
MHNM 03-2620	1.75208688	2.25109288	0.11957007

Continued on next page

Continued from previous page

Specimen ID	*Thickness*	*Width*	*Thickness/Width*
	1.77359631	2.26749322	0.12080518
	1.74245017	2.26784261	0.11336456
	1.74684429	2.24804442	0.11904302
	1.82901415	2.29775176	0.12704987
	1.7631059	2.28420732	0.11435415
	1.72978014	2.32752445	0.09777659
	1.71962955	2.29374695	0.10264421
	1.65292289	2.35816907	0.07814149
	1.65143309	2.29938743	0.08811095
	1.66238002	2.29045534	0.09183013
	1.76971695	2.24664627	0.12498673
	1.70137799	2.3701447	0.08436326
	1.73443176	2.25208567	0.11515468
	1.62772421	2.17090095	0.10934269
	1.78237228	2.13911052	0.15830416
	1.69958627	2.16577537	0.12769768
	1.7043393	2.12384511	0.14007487
	1.74684429	2.23396774	0.1224597
	1.69164721	2.16869779	0.12495641
	1.45552997	2.10094548	0.08857827
	1.41560304	1.98515209	0.10360982
	1.20086937	1.94930439	0.07131849
	1.51995576	2.03382763	0.1160385
	1.5395326	2.05426661	0.11583651

Continued on next page

Continued from previous page

Specimen ID	*Thickness*	*Width*	*Thickness/Width*
	1.55738758	2.06371916	0.11781827
	1.36944182	2.02349107	0.08699816
	1.50806872	2.06257302	0.10684688
	1.23450212	2.02896943	0.06465312
	1.54539915	1.93254043	0.14924088
MHNM 03-740	1.53874387	2.00598307	0.12743041
	1.50529559	1.97166848	0.12765087
	1.54407267	1.8015192	0.19111034
	1.57353117	1.90955919	0.16473576
	1.57353117	1.89409245	0.16967794
	1.34201338	1.89013305	0.10824737
	1.32783252	1.88029762	0.10729244
	1.35962989	1.97985877	0.09333654
	1.33697638	2.00754025	0.08404651
	1.34243944	2.06650821	0.07509756
	1.34201338	2.10398681	0.06929513

ANNEXE XIV

PHYLOGENETIC ANALYSIS OF EARLY GNATHOSTOMES

List of characters and coding matrix.

List of characters [modified from Burrow et al. (2016)] :

Modifications were made on 36 characters from the original data matrix from Burrow et al. (2016) : 16 characters have been rephrased (characters 9, 18, 19, 26, 31, 51, 81, 160, 177, 182, 190, 191, 241, 242, 257, 258), seven characters have been redefined (characters 7, 8, 149, 167, 195, 246, 260), 12 characters have been re-polarized (characters 7, 8, 11, 13, 104, 149, 167, 195, 196, 209, 246, 252), uninformative character 261 has been removed and six characters have been added (characters 262-267).

1. Tesselate prismatic calcified cartilage : absent (0) ; present (1).

In contrast to Burrow et al. (2016), but in agreement with Zhu et al. (2013), *Doliodus* has been re-coded as (1).

2. Perichondral bone : present (0) ; absent (1).

Perichondral bone is present in osteostracans [Donoghue and Smith (2001); Janvier et al. (2004); Qu et al. (2015); contra Zhu et al. (2013)]. Character 2 is coded as (0) for the Osteostraci. Since the presence of perichondral bone is ambiguous in galeaspids [see Wang et al. (2005) *versus* Zhu et al. (1999)], the Galeaspida is coded as (?). *Miguashaia* is coded as (0). *Diplacanthus* and *Rhadinacanthus* have been coded as (0) because perichondral ossification has been described in their scapulacoracoid (Burrow et al., 2016).

3. Extensive endochondral ossification : absent (0); present (1).
Because of the morphological incompleteness *Diabolepis*, *Styloichthys*, *Youngolepis*, *Psarolepis* and *Meemannia* have to be coded as (?) rather than (1). *Miguashaia* and *Cheirolepis* are coded as (1).

4. Dentine : absent (0); present (1).
Dentine is absent in the Galeaspida (Wang et al., 2005) but present in the Osteostraci (Qu et al., 2015). *Homalacanthus* and *Triazeugacanthus* are coded as (1).

5. Type of dentine : mesodentine (0); semidentine (1); orthodentine (2).
Homalacanthus and *Triazeugacanthus* are coded as (0). *Obtusacanthus* has been coded (2) (Hanke and Wilson, 2004). *Poracanthodes* has been coded (0&2) (Gross, 1971; Valiukevičius, 1995).

6. Cosmine : absent (0); present (1).

7. Lepidotrichia : absent (0); present (1).
Character 7 is modified to solely represent the presence or absent of lepidotrichia. Character 262 takes into account the presence or absence of lepidotrichia-like scale alignment. The polarity has been changed to reflect the absence of lepidotrichia in both the

Galeaspida and the Osteostraci. *Doliodus* is coded as (0).

8. Body scale growth pattern : polyodontode (0) ; monodontode (1).
The large rectangular body scales of osteostracans are considered to be polyodontodes because they are composed of multiple units (Hawthorn et al., 2008). Polyodontode composition has been described histologically in the Silurian osteostracan *Trematapis* and *Oeselaspis* (Qu et al., 2015). We refer to the information of the article 3 for our recognition of these two types. Thus, polyodontode is considered as the plesiomorphic condition. *Psarolepis* has been coded as (0) (Qu et al., 2016).

9. Body scale growth concentric "onion skin" pattern : absent (0) ; present (1).
Character 9 has been modified following (Brazeau, 2009, character 9). *Bothriolepis* has been coded as (?). *Cheirolepis*, *Homalacanthus* and *Triazeugacanthus* have been coded as (1). *Miguashaia* has been coded as (0).

10. Body scales with peg-and-socket articulation : absent (0) ; present (1).
Specimens of *Botrhiolepis* [Burrow and Turner (1999), R.C., pers. observ.] with scales lack peg-and-socket articulation ; *Bothriolepis* has been coded as (0). *Cheirolepis* has been coded as (0).

11. Body scale profile : flattened (0) ; distinct crown and base demarcated by a constriction (neck) (1).
Polarity of character 11 has been changed because there is no constriction neck in osteostracan body scales (Keating and Donoghue, 2016). *Bothriolepis* has been coded as (0). *Promesacanthus* has been recoded as (1) (Hanke, 2008).

12. Body scales with bulging base : absent (0) ; present (1).

13. Body scales with flattened base : present (0) ; absent (1).
Polarity of character 13 has been changed because of the presence of flattened base in the scales of galeaspids (Wang et al., 2005).

14. Flank scale alignment : vertical rows (0) ; oblique rows or hexagonal/rhombic packing (1) ; disorganised (2).

15. Sensory line canal : passes between or beneath scales (0) ; passes over scales and/or is partially enclosed or surrounded by scales (1) ; perforates and passes through scales (2).

16. Sensory line network : preserved as open grooves (sulci) in dermal bones (0) ; sensory lines pass through canals enclosed within dermal bones (1).

17. Jugal portion of infraorbital canal joins supramaxillary canal : present (0) ; absent (1).

18. Dermal skull roof : includes large dermal plates (0) ; consists of undifferentiated plates or small polygonal plates (1).
Tessera *sensu* Brazeau (2009) are defined as flat-based, plate-like head coverings that are differentiated from the body scales, but do not form as distinct pattern as the dermal skull roof of placoderms or osteichthyans. These are different from the endoskeletal mineralization of chondrichthyans (Kemp and Westrin, 1979). Because of this difference we rephrased the apomorphic character states.

19. Dermal skeleton morphology of the head : large interlocking polygonal plates (0) ; microsquamose, not larger than body squamation (1).
Character 19 has been rephrased because of the non-homologous conditions of dermal

"tessera" *sensu* (Brazeau, 2009) and the tessera of chondrichthyans.

20. Extent of dermatocranial cover : complete (0) ; incomplete (scale-free cheek and elsewhere) (1).

21. Endolymphatic ducts open in dermal skull roof : present (0) ; absent (1).

22. Endolymphatic ducts with oblique course through dermal skull bones : absent (0) ; present (1).

23. Series of paired median skull roofing bones that meet at the dorsal midline of the skull (rectilinear skull roof pattern) : absent (0) ; present (1).
Homalacanthus has been coded as (0) [Gagnier (1996) ; pers. observ.]. Acanthodians for which the head scale condition is known have been coded accordingly (0).

24. Consolidated cheek plates : absent (0) ; present (1).
Homalacanthus has been coded as (0) [Gagnier (1996) ; pers. observ.].

25. Pineal opening perforation in dermal skull roof : present (0) ; absent (1).
Cheirolepis has been coded as (0&1) ; *C. trailli* has an open pineal opening, whereas *C. canadensis* and *C. schultzei* lack a pineal opening (Arratia and Cloutier, 1996, 2004).

26. Enlarged postorbital dermal plate separate from orbital series, over the otic region : absent (0) ; present (1).
Character 26 has been rephrased.

27. Bony hyoidean gill-cover series (branchiostegals) : absent (0) ; present (1).
Andrews et al. (2005) interpreted a highly modified small element in *Onychodus jande-*

marrai as a possible branchiostegal ; it seems unlikely that this small element provided a hyoidean gill cover. This element was considered as absent by (Cloutier and Ahlberg, 1996, character 62). *Onychodus* has been coded as (0). *Homalacanthus* has been coded as (1) [Gagnier (1996) ; pers. observ.] and *Miguashaia* as (0).

28. Branchiostegal plate series along ventral margin of lower jaw : absent (0) ; present (1).
Homalacanthus has been coded as (1) [Gagnier (1996) ; pers. observ.].

29. Branchiostegal ossifications : plate-like (0) ; narrow and ribbon-like (1).
Homalacanthus has been coded as (1) [Gagnier (1996) ; pers. observ.].

30. Branchiostegal ossifications : ornamented (0) ; unornamented (1).

31. Branchiostegal ossifications : not imbricated (0) ; imbricated (1).
Character 31 and character states have been rephrased. *Homalacanthus* has been coded as (0).

32. Opercular cover of branchial chamber : complete or partial (0) ; separate gill covers and gill slits (1).

33. Opercular (submarginal) ossification : absent (0) ; present (1).
Dialipina is coded as (1) although a true opercular is absent (Schultze and Cumbaa, 2001; Cloutier and Arratia, 2004) but since the character takes into account the presence of an opercular (submarginal) ossification, such an element is present.

34. Shape of opercular (submarginal) ossification : broad plate that tapers towards its proximal end (0) ; narrow, rod-shaped (1).

Miguashaia has been coded as (0).

35. Gular plates : absent (0) ; present (1).

36. Size of lateral gular plates : extending most of length of the lower jaw (0) ; restricted to the anterior third of the jaw (no longer than the width of three or four branchiostegals) (1).

37. Basihyal : present (0) ; absent, hyoid arch articulates directly with basibranchial (1).

38. Interhyal : absent (0) ; present (1).

39. Oral dermal tubercles borne on jaw cartilages : absent (0) ; present (1).

40. Tooth whorls : absent (0) ; present (1).
Homalacanthus has been coded as (0).

41. Bases of tooth whorls : single, continuous plate (0) ; some or all whorls consist of separate tooth units (1).

42. Enlarged adsymphysial tooth whorl : absent (0) ; present (1).
Homalacanthus has been coded as (0).

43. Teeth ankylosed to dermal bones : absent (0) ; present (1).
Homalacanthus and *Miguashaia* have been coded as (0).

44. Dermal jaw plates on biting surface of jaw cartilages : absent (0) ; present (1).

45. Maxillary and dentary tooth-bearing bones : absent (0); present (1).

46. Large otic process of the palatoquadrate : absent (0); present (1).

47. Insertion area for jaw adductor muscles on palatoquadrate : ventral or medial (0); lateral (1).
Miguashaia has been coded as (1).

48. Oblique ridge or groove along medial face of palatoquadrate : absent (0); present (1).
Miguashaia has been coded as (1).

49. Fenestration of palatoquadrate at basipterygoid articulation : absent (0); present (1).

50. Perforate or fenestrate anterodorsal (metapterygoid) portion of palatoquadrate : absent (0); present (1).
Miguashaia has been coded as (0).

51. Dorsal process on Meckelian bone or cartilage : absent or weak (0); well-developed (pronounced) (1).
Character 51 and character states have been rephrased.

52. Preglenoid process : absent (0); present (1).

53. Jaw articulation located on rearmost extremity of mandible : absent (0); present (1).

54. Precerebral fontanelle : absent (0) ; present (1).
Gogonasus has been recoded as (0).

55. Median dermal bone of palate (parasphenoid) : absent (0) ; present (1).

56. Position of nasal opening(s) : dorsal, placed between orbits (0) ; ventral and anterior to orbit (1).

57. Olfactory tracts : short, with olfactory capsules situated close to telencephalon cavity (0) ; elongate and tubular (much longer than wide) (1).
Cheirolepis has been coded as (1) (Giles et al., 2015a).

58. Prominent pre-orbital rostral expansion of the neurocranium : present (0) ; absent (1).

59. Pronounced sub-ethmoidal keel : absent (0) ; present (1).

60. Position of myodome for superior oblique eye muscles : posterior and dorsal to foramen for nerve II (0) ; anterior and dorsal to foramen (1).

61. Endoskeletal intracranial joint : absent (0) ; present (1).
Cheirolepis and *Miguashaia* have been coded as (0).

62. Spiracular groove on basicranial surface : absent (0) ; present (1).
Cheirolepis has been coded as (1) (Giles et al., 2015a).

63. Spiracular groove on lateral commissure : absent (0) ; present (1).
Cheirolepis has been coded as (1) (Giles et al., 2015a).

64. Subpituitary fenestra : absent (0) ; present (1).
Gogonasus has been recoded as (0).

65. Supraorbital shelf broad with convex lateral margin : absent (0) ; present (1).
Cheirolepis has been coded as (1) (Giles et al., 2015a).

66. Orbit dorsal or facing dorsolaterally, surrounded laterally by endocranium : present (0) ; absent (1).

67. Extended prehypophysial portion of sphenoid : absent (0) ; present (1).
Homalacanthus has been coded as (?).

68. Narrow interorbital septum : absent (0) ; present (1).

69. Main trunk of facial nerve (N. VII) : elongate and passes anterolaterally through orbital floor (0) ; stout, divides within otic capsule at the level of the postorbital process (1).

70. Hyoid ramus of facial nerve (N. VII) exits through posterior jugular opening : absent (0) ; present (1).

71. Glossopharyngeal nerve (N. IX) exit : foramen situated posteroventral to otic capsule and anterior to metotic fissure (0) ; through metotic fissure (1).

72. Short otico-occipital region of braincase : absent (0) ; present (1).
Homalacanthus has been coded as (?). *Gogonasus* has been recoded as (0).

73. Ethmoid region elongate with dorsoventrally deep lateral walls : absent (0) ;

present (1).

74. Basicranial morphology : platybasic (0) ; tropibasic (1).

75. Ascending basisphenoid pillar pierced by common internal carotid : absent (0) ; present (1).

76. Jugular vein : invested in otic capsule wall posterior to the postorbital process (0) ; lateral wall of jugular canal incomplete or absent (1).
Cheirolepis has been coded as (1) (Giles et al., 2015a).

77. Canal for lateral dorsal aorta within basicranial cartilage : absent (0) ; present (1).
Cheirolepis has been coded as (1) (Giles et al., 2015a).

78. Entrance of internal carotids : through separate openings flanking the hypophyseal opening or recess (0) ; through a common opening at the midline of the basicranium (1).

79. Canal for efferent pseudobranchial artery within basicranial cartilage : absent (0) ; present (1).
Cheirolepis has been coded as (1) (Giles et al., 2015a).

80. Position of basal/basipterygoid articulation : same anteroposterior level as hypophysial opening (0) ; anterior to hypophysial opening (1).
Homalacanthus has been coded as (?).

81. Postorbital process : not articulated with palatoquadrate (0) ; articulating with pa-

latoquadrate (1).

Character 81 and character states have been rephrased from Zhu et al. (2013) and Burrow et al. (2016). *Cheirolepis* has been coded as (0) (Giles et al., 2015a). *Homalacanthus* has been coded as (?).

82. Labyrinth cavity : separated from the main neurocranial cavity by a cartilaginous or ossified capsular wall (0) ; skeletal capsular wall absent (1).

83. Basipterygoid process (basal articulation) with vertically oriented component : absent (0) ; present (1).

84. Pituitary vein canal : dorsal to level of basipterygoid process (0) ; flanked posteriorly by basipterygoid process (1).

85. External (horizontal) semicircular canal : absent (0) ; present (1).

86. Sinus superior : absent or indistinguishable from union of anterior and posterior canals with saccular chamber (0) ; present (1).

87. External (horizontal) semicircular canal : joins the vestibular region dorsal to posterior ampulla (0) ; joins the vestibular region levelling with posterior ampulla (1).

88. Trigemino-facial recess : absent (0) ; present (1).

89. Posterior dorsal fontanelle : absent (0) ; present (1).

Cheirolepis has been coded as (1) (Giles et al., 2015a).

90. Shape of posterior dorsal fontanelle : approximately as long as broad (0) ; much

longer than wide, slot-shaped (1).

Meemannia has been recoded as (0) (Lu et al., 2016).

91. Dorsal ridge : absent (0) ; present (1).

92. Endolymphatic ducts : posterodorsally angled tubes (0) ; tubes oriented vertically through median endolymphatic fossa (1).

93. Lateral otic process : absent (0) ; present (1).

94. Process forming part or complete wall of jugular groove or canal projecting from otic capsule wall : absent (0) ; present (1).

95. Position of hyomandibula articulation on neurocranium : below or anterior to orbit, on ventrolateral angle of braincase (0) ; posterior to orbit (1).

96. Ventral cranial fissure : absent (0) ; present (1).

Homalacanthus has been coded as (?).

97. Metotic (otico-occipital) fissure : absent (0) ; present (1).

Cheirolepis has been coded as (1) (Giles et al., 2015a).

98. Vestibular fontanelle : absent (0) ; present (1).

Cheirolepis has been coded as (1) (Giles et al., 2015a).

99. Occipital arch wedged in between otic capsules : absent (0) ; present (1).

100. Spino-occipital nerve foramina : two or more, aligned horizontally (0) ; one or

two, aligned dorsoventrally (1).

Cheirolepis has been coded as (1) (Giles et al., 2015a).

101. Ventral notch between parachordals : absent (0) ; present or entirely unfused (1).

Cheirolepis has been coded as (1) (Giles et al., 2015a).

102. Parachordal shape : broad, flat (0) ; keeled with sloping lateral margins (1).

Homalacanthus has been coded as (?).

103. Hypotic lamina (and dorsally directed glossopharyngeal canal) : absent (0) ; present (1).

104. Macromeric dermal shoulder girdle : absent (0), present (1).

The polarity of character 104 has been reversed because of the absence of macromeric dermal shoulder girdle in galeaspids and osteostracans. Burrow et al. (2016) consider that *Gyracanthides murrayi* lacks a macromeric pectoral girdle. However, based on the description of Warren et al. (2000), the proper identification of elements from the pectoral region remains questionable. The presence of small tubercules similar to dermal ornamentation on the element identified by (Warren et al., 2000, fig. 7) as the scapulocoracoid suggests the potential presence of a dermal ventral component. Because of this discrepancy of interpretation, *Gyracanthides* has been coded as (?).

105. Dermal shoulder girdle composition : ventral and dorsal (scapular) components (0) ; ventral components only (1).

106. Dermal shoulder girdle forming a complete ring around the trunk : present (0) ; absent (1).

Chondrichthyan taxa have been coded (1) as they lack such a structure independently if they have or not dermal components.

107. Pectoral fenestra completely encircled by dermal shoulder armour : present (0) ; absent (1).

108. Median dorsal plate : absent (0) ; present (1).

109. Pronounced internal crista ('keel') on median dorsal surface of shoulder girdle : absent (0) ; present (1).

110. Scapular process of endoskeletal shoulder girdle : absent (0) ; present (1).

111. Ventral margin of separate scapular ossification : horizontal (0) ; deeply angled (1).

112. Cross-sectional shape of scapular shaft : flattened or strongly ovate (0) ; subcircular (1).

113. Flange on trailing edge of scapulocoracoid : absent (0) ; present (1).

114. Scapular process with posterodorsal angle : absent (0) ; present (1).

115. Endoskeletal postbranchial lamina on scapular process : present (0) ; absent (1).

116. Mineralisation of internal surface of scapular shaft : mineralised all around (0) ; unmineralised on internal face forming a hemicylindrical crosssection (1).

117. Coracoid process : absent (0) ; present (1).

Cheirolepis has been coded as (1) (Giles et al., 2015a).

118. Procoracoid mineralisation : absent (0) ; present (1).

Cheirolepis and *Miguashaia* have been coded as (0).

119. Fin base articulation on scapulocoracoid : stenobasal (0) ; eurybasal (1).

Miguashaia has been coded as (0).

120. Perforate propterygium : absent (0) ; present (1).

121. Pelvic fins : absent (0) ; present (1).

122. Pelvic claspers : absent (0) ; present (1).

Homalacanthus has been coded as (0).

123. Dermal pelvic clasper ossifications : absent (0) ; present (1).

124. Pectoral fins covered in macromeric dermal armour : absent (0) ; present (1).

Miguashaia has been coded as (0).

125. Pectoral fin base has large, hemispherical dermal component : absent (0) ; present (1).

Miguashaia has been coded as (0).

126. Dorsal fin spines : absent (0) ; present (1).

127. Anal fin spine : absent (0) ; present (1).

128. Paired pectoral fin spines : absent (0) ; present (1).

Osteostraci has been coded as (0) as the pectoral fins of osteostracans are relatively well-known and lack such spines (Janvier et al., 2004).

129. Median fin spine insertion : shallow, not greatly deeper than dermal bones/scales (0) ; deep (1).

Miguashaia has been coded as (-).

130. Prepelvic fin spines : absent (0) ; present (1).

Miguashaia has been coded as (0).

131. Prepectoral fin spines : absent (0) ; present (1).

Miguashaia has been coded as (0).

132. Fin spines with ridges : absent (0) ; present (1).

133. Median and paired fin spines with nodes : absent (0) ; present (1).

134. Dorsal fin spines with rows of large retrorse denticles : absent (0) ; present (1).

Miguashaia has been coded as (-).

135. Synarcual : absent (0) ; present (1).

Miguashaia has been coded as (0).

136. Number of dorsal fins, if present : one (0) ; two (1).

Miguashaia has been coded as (1).

137. Anal fin : absent (0) ; present (1).

138. Caudal radials : extend beyond level of body wall and deep into hypochordal lobe (0) ; radials restricted to axial lobe (1).
Miguashaia has been coded as (1). *Onychodus* has been coded as (1) (Andrews et al., 2005).

139. Resorption and redeposition of odontodes : lacking or partially developed (0) ; developed (1).
Homalacanthus has been coded as (0).

140. Acrodin : absent (0) ; present (1).

141. Plicidentine : absent (0) ; simple or generalized polyplocodont (1).

142. Rostral tubuli : absent (0) ; present (1).
Cheirolepis, *Homalacanthus* and *Miguashaia* have been coded as (0).

143. Peg on rhomboid scale : narrow (0) ; broad (1).

144. Anterodorsal process on scale [*sensu* Schultze (1977)] : absent (0) ; present (1).

145. Fringing fulcra : absent (0) ; present (1).
Homalacanthus has been coded as (0).

146. Epichordal lepidotrichia in caudal fin : absent (0) ; present (1).
The fin elements present in the epichordal lobe of the caudal fin of *Bothriolepis* are interpreted as finrays rather than radials (Béchard et al., 2014).

147. Dermal intracranial joint : absent (0) ; present (1).

Homalacanthus and *Miguashaia* have been coded as (0).

148. Large unpaired median skull roofing bone anterior to the level of nasal capsules : absent (0) ; present (1).
Homalacanthus has been coded as (0).

149. Nasals : absent (0) ; many (1) ; one or two (2).
A new plesiomorphic condition has been included in character 149 to take into account the absence of nasals in osteostracans and galeaspids. The coding has been changed in *Acanthodes* (Zidek, 1976), *Cheiracanthus*, *Brochoadmones* (Hanke and Wilson, 2006), *Culmacanthus* (Burrow and Young, 2012), *Euthacanthus* (Newman et al., 2014), *Ischnacanthus* (Watson, 1937), *Kathemacanthus* (Wilson et al., 2010), *Obtusacanthus* (Hanke and Wilson, 2004), *Promesacanthus* (Hanke, 2008), and *Tetanopsyrus* (Hanke et al., 2001) for (0) because only head scales surround the nares. *Cassidiceps* (Gagnier and Wilson, 1996), *Homalacanthus* (Gagnier, 1996), *Mesacanthus* (Watson, 1937), *Climatius*, and *Nerepisacanthus* (Burrow and Rudkin, 2014) have been coded (2) because they have one or two pair(s) of nasal bones. *Ptomacanthus* has been coded as (?) because of the weak preservation of the snout area (Brazeau, 2012). All chondrichthyans have been coded as (0). *Pterichthyodes* has been coded (0).

150. Mesial margin of nasal : not notched (0) ; notched (1).
Mesacanthus has been coded as (1) (Watson, 1937).

151. Dermintermedial process : absent (0) ; present (1).

152. Posterior nostril : associated with orbit (0) ; not associated with orbit (1).
Homalacanthus and *Miguashaia* have been coded as (1).

153. Position of posterior nostril : external, far from jaw margin (0) ; external, close to jaw margin (1).

154. Supraorbital [*sensu* Cloutier and Ahlberg (1996) including posterior tectal of Jarvik] : absent (0) ; present (1).
Homalacanthus has been coded as (0).

155. Supraorbital, preorbital and nasal : unfused (0) ; fused (1).

156. Tectal [sensu Cloutier and Ahlberg (1996), not counting the 'posterior tectal' of Jarvik] : absent (0) ; present (1).
Homalacanthus has been coded as (0). *Miguashaia* and *Porolepis* have been coded as (1).

157. Lateral plates [*sensu* Zhu et al. (2013)] : absent (0) ; present (1).

158. Location of pineal foramen/eminence : level with posterior margin of orbits (0) ; well posterior of orbits (1).

159. Parietals (preorbitals of placoderms) surround pineal foramen/eminence : yes (0) ; no (1).

160. Spiracle : not completely enclosed by skull roof bones (0) ; completely enclosed by skull roof bones (1).
Character 160 and character states have been rephrased.

161. Number of marginal bones alongside paired median skull roofing bones over the otico-occipital division of braincase : single (0) ; two or more (1).

162. Number of paranuchals : one pair (0), two pairs (1).
Miguashaia has been coded as (?).

163. Large unpaired median bone contributing to posterior margin of skull roof : absent (0) ; present (1).
Cheirolepis and *Homalacanthus* have been coded as (0).

164. Contact of nuchal or centronuchal plate with paired preorbital plates : absent (0), present (1).

165. Posterior process of the paranuchal plate behind the nuchal plate (dorsal face) : absent (0), present (1).

166. Junction of posterior pitline and main lateral line : far in front of posterior margin of skull roof (0), close to posterior margin of skull roof (1).

167. Extrascapulars : absent (0) ; uneven number (1) ; paired number (2).
Character 167 has been redefined to include the new plesiomorphic condition.

168. Dermal neck-joint between paired main-lateral line-bearing bones of skull and shoulder girdle : absent (0) ; present (1).

169. Type of dermal neck-joint : sliding, dermal shoulder girdle plate with flat articular flange (0) ; ginglymoid, dermal shoulder girdle plate with articular condyle or fossa (1).

170. Number of sclerotic plates : four or less (0) ; more than four (1).

171. Foramina (similar to infradentary foramina) on cheek bones : absent (0) ; present (1).

172. Lacrimal posteriorly enclosing posterior nostril : absent (0) ; present (1).

173. Most posterior major bone of cheek bearing preopercular canal ("preopercular") extending forward, close to orbit : absent (0) ; present (1).
Eusthenopteron has been coded as (0).

174. Number of cheek bones bearing preopercular canal posterior to jugal : one (0) ; two (1).
Eusthenopteron, *Osteolepis*, *Gogonasus* and *Porolepis* have been coded as (1).

175. Bone bearing both quadratojugal pit-line and preopercular canal : absent (0) ; present (1).

176. Dermohyal : absent (0) ; present (1).

177. Premaxillae : without inturned adsymphysial processes (0) ; with inturned adsymphysial processes (1).
Character 177 and character states have been rephrased. *Miguashaia* has been coded as (0).

178. Premaxilla forming part of orbit : absent (0) ; present (1).

179. Preorbital process of premaxilla : absent (0) ; present (1).

180. Posterior expansion of maxilla (maxilla cleaver-shaped) : present (0) ; absent

(1). *Dialipina* has been recoded as (0) (Cloutier and Arratia, 2004; Schultze and Cumbaa, 2001).

181. Ventral margin of maxilla : straight (0), curved (1).

182. Maxilla : contributes to posterior margin of cheek (0) ; does not contribute to posterior margin of cheek (1).
Character 182 and character states have been rephrased. *Eusthenopteron* has been coded as (1).

183. Course of ethmoid commissure : middle portion through median rostral (0) ; sutural course (1) ; through bone center of premaxillary (2).
Eusthenopteron has been coded as (1).

184. Position of anterior pit-line : on paired median skull roofing bones over the otico-occipital division of braincase (0) ; on paired median skull roofing bones over the sphenoid division of braincase (1).
Eusthenopteron has been coded as (1) ; *Miguashaia* has been coded as (-).

185. Middle and posterior pit-lines on postparietal : posteriorly situated (0), mesially situated (1).
Eusthenopteron has been coded as (0).

186. Position of middle and posterior pit-lines : close to midline (0) ; near the central portion of each postparietal (1).
Eusthenopteron has been coded as (1).

187. Course of supraorbital canal : between anterior and posterior nostrils (0) ; ante-

rior to both nostrils (1).
Eusthenopteron has been coded as (-).

188. Course of supraorbital canal : straight (0) ; lyre-shaped (1).
Eusthenopteron has been coded as (0).

189. Posterior end of supraorbital canal : in postparietal (0) ; in parietal (1) ; in intertemporal (2).
Eusthenopteron has been coded as (2).

190. Otic and supraorbital canals : not in contact (0) ; in contact (1).
Character 190 has been rephrased.

191. Supraorbital and infraorbital canals : in contact rostrally (0) ; not in contact rostrally (1).
Character 191 has been rephrased. *Eusthenopteron* has been coded as (0).

192. Otic canal : runs through skull roof (0) ; follows edge of skull roof (1).
Eusthenopteron and *Miguashaia* have been coded as (0).

193. Infraorbital canal follows premaxillary suture : no (0) ; yes (1).

194. Sensory canal or pit-line associated with maxilla : absent (0) ; present (1).
Eusthenopteron has been coded as (0) ; *Miguashaia* has been coded as (-).

195. Preopercular canal : canal exits the dorso-posterior margin of the preopercular (0) ; canal exits at the antero-dorsal margin of the preopercular (1) ; canal exits the anterior margin of the preopercular at half-length (2).

Character 195 and character states of Zhu et al. (2013) have been redefined. All codings have been changed according to the newly defined character states.

196. Median gular : absent (0) ; present (1).
The polarity of character 196 was reversed because a median gular is absent in galeaspids and osteostracans.

197. Foramen in hyomandibular : absent (0) ; present (1).

198. Large dermal plates forming outer dental arcade : only with denticles (0), with a monolinear series of large, shedding teeth (1).
Eusthenopteron has been coded as (1).

199. Tooth-bearing median rostral : absent (0) ; present (1).
Eusthenopteron has been coded as (0).

200. Teeth of dentary : reaching anterior end of dentary (0) ; not reaching anterior end of dentary (1).
Eusthenopteron has been coded as (0).

201. Number of coronoids (*sensu lato*, including parasymphysial dental plate but excluding parasymphysial tooth whorl) : more than three (0) ; three (1).

202. Fangs of coronoids (*sensu stricto*) : absent (0) ; present (1).
Eusthenopteron has been coded as (1).

203. Marginal denticle band on coronoids : broad band, at least posteriorly (0) ; narrow band with 2-4 denticle rows (1).

Eusthenopteron has been coded as (-).

204. Infradentary bones : absent (0), present (1).

205. Infradentary foramina : always present (0) ; variable (1) ; always absent (2).

206. Large ventromesially directed flange of symphysial region of mandible : absent (0) ; present (1).
Friedman and Matt (2007) (character 156) coded *Miguashaia* as (1) although the condition is visible in *M. grossi* (Forey et al., 2000) but lacks clear evidence in *M. bureaui*. *Youngolepis* has been recoded as (0/1) since the condition of the flange is variable (Zhu Min, pers. comm.).

207. Flange-like extension composed of Meckelian ossification and prearticular that extends below ventral margin of infradentaries : absent (0), present (1).
Friedman and Matt (2007) (character 159) coded *Youngolepis* as (0), whereas Zhu et al. (2013) and Burrow et al. (2016) coded as (1).

208. Strong ascending flexion of symphysial region of mandible : absent (0) ; present (1).
Eusthenopteron has been coded as (0).

209. Parasymphysial plate : absent (0) ; detachable tooth whorl (1) ; long with posterior corner, sutured to coronoid, denticulated or with tooth row (2).
The polarity of character 209 has been changed to take into account the plesiomorphic condition given by galeaspids and osteostracans. *Eusthenopteron* has been coded as (2).

210. Anterior end of prearticular : far from jaw symphysis (0) ; near jaw symphysis

(1).

Eusthenopteron has been coded as (1).

211. Prearticular-dentary contact : present (0) ; absent (1).

Eusthenopteron has been coded as (1).

212. Meckelian bone exposed immediately anterior to first coronoid : yes (0) ; no (1).

Eusthenopteron has been coded as (1) (Porro et al., 2015).

213. Dermal plates on mesial (lingual) surfaces of Meckel's cartilage and palatoquadrate : absent (0) ; present (1).

Eusthenopteron has been coded as (1).

214. Biconcave glenoid on lower jaw : absent (0) ; present (1).

215. Contact between palatoquadrate and dermal cheek bones : continuous contact of metapterygoid and autopalatine (0) ; metapterygoid and autopalatine contacts separated by gap between commissural lamina of palatoquadrate and cheek bones (1).

216. Metapterygoid with developed mesial ventral protrusion (*i.e.*, commissural lamina *sensu stricto*) : absent (0) ; present (1).

217. Course of mandibular canal : not passing through most posterior infradentary (0) ; passing through most posterior infradentary (1).

218. Course of mandibular canal : passing through dentary (0) ; not passing through dentary (1).

Miguashaia has been recoded as (1).

219. Internasal pits : absent (0) ; undifferentiated or anterior palatal fossa (1) ; shallow, paired pits with strong midline ridge (2) ; deep, pear-shaped pits (3).

220. Fenestra ventrolateralis : absent (0) ; present (1) ; common ventral fenestra for anterior and posterior nostrils (2).

221. Ethmoid articulation for palatoquadrate : placed on postnasal wall (0) ; extends posteriorly to the level of N. II (1).

222. Eye stalk or unfinished area on neurocranial wall for eye stalk : absent (0) ; present (1).

223. Developed postorbital cavity : absent (0) ; present (1).

224. Postorbital pila ascending from basipterygoid process to postorbital process : absent (0) ; present (1).

225. Unconstricted cranial notochord : absent (0) ; present (1).

226. Descending process of sphenoid (with its posterior extremity lacking periostegeal lining) : absent (0) ; present (1).

227. Articulation facet with hyomandibular : single-headed (0), double-headed (1).

228. Hyoid arch articulation : on lateral commissure (0) ; on otic capsule wall (1).

229. Opercular suspension on braincase : absent (0) ; present (1).

230. Posterior postorbital process : absent (0) ; present (1).
Cheirolepis has been coded as (0) (Giles et al., 2015a).

231. Basicranial fenestra : absent (0) ; present (1).
Cheirolepis has been coded as (0) (Giles et al., 2015a).

232. Otical process (an outgrowth from the lateral wall of the braincase penetrated by the branches of the r. oticus lateralis) : absent (0) ; present (1).

233. Lateral cranial canal : absent (0) ; present (1).

234. Midline canal in basicranium for dorsal aorta : absent (0) ; present (1).

235. Vomerine fangs : absent (0) ; present (1).
Miguashaia has been coded as (0).

236. Vomeral area with grooves and raised areas : absent (0) ; present (1).

237. Parasphenoid : protruding forward into ethmoid region of endocranium (0) ; behind ethmoid region (1).

238. Denticulated field of parasphenoid : without spiracular groove (0) ; with spiracular groove (1).
Miguashaia has been coded as (0).

239. Ascending process of parasphenoid : absent (0) ; present (1).

Miguashaia has been coded as (0).

240. Shape of parasphenoid denticulated field : broad rhomboid or lozenge-shaped (0) ; broad, splint-shaped (1) ; slender, splint-shaped (2).
Miguashaia has been coded as (0).

241. Parasphenoid denticulated field : without multifid anterior margin (0) ; with multifid anterior margin (1).
Character 241 and character states have been rephrased. *Miguashaia* has been coded as (0).

242. Parasphenoid denticle field : without anteriorly divergent lateral margins (0) ; with anteriorly divergent lateral margins (1).
Character 242 and character states have been rephrased. *Miguashaia* has been coded as (1).

243. Parasphenoid denticle field : terminates at or anterior to level of foramina for internal carotid arteries (0) ; extends posterior to foramina for internal carotid arteries (1).

244. Presupracleithrum : absent (0) ; present (1).

245. Anocleithrum : absent (0), element developed as postcleithrum (1) ; element developed as anocleithrum sensu stricto (2).

246. Cleithra : absent (0) ; two cleithra (1) ; one cleithrum (2).
Character 246 as used by Burrow et al. (2016) and Zhu et al. (2013) and originally by Zhu and Yu (2002) (character 161) is redefined to minimize the assumption implied in

the apomorphic state. For example, the original coding of *Eusthenopteron* as (1) implied that the pectoral girdle element identified as the cleithrum included the dorsal and ventral cleithra [i.e., the anterolateral (AL) and anterior ventrolateral (AVL) plates of placoderms, respectively) as well as the pectoral spine (*i.e.*, spinal plate of placoderms), where in fact there is no indication of fusion. The character is rephrased to take into account the absence of cleithrum, the presence of two cleithra (including the AL and AVL plates of placoderms) or a single cleithrum. A new plesiomorphic condition is added to take into account the scope of the analysis. Character 128 takes into account the presence of pectoral spines, whereas character 265 has been added to take into account the presence of the spinal plate.

247. Relationship of clavicle to cleithrum : ascending process of clavicle overlapping cleithrum laterally (0) ; ascending process of clavicle wrapping round anterior edge of cleithrum, overlapping it both laterally and mesially (1).

248. Triradiate scapulocoracoid : absent (0) ; present (1).

249. Subscapular foramen/fossa : absent (0) ; present (1).

250. Endoskeletal supports in pectoral fin : multiple elements articulating with girdle (0) ; single element (“humerus”) articulating with girdle (1).

251. Pectoral propterygium : absent (0) ; present (1).

252. Pelvic girdle with substantial dermal component : absent (0) ; present (1).
The polarity of character 252 has been reversed.

253. Pelvic fin spines : absent (0) ; present (1).

254. Articulated jaws : absent (0) ; present (1).

255. Endocranial optic fissure : absent (0) ; present (1).

256. Admedian fin spines : absent (0) ; present (1).

257. Fin spine insertion : smooth (0) ; with fine parallel longitudinal ridges (1).
Character 257 and character states have been rephrased.

258. Retrorse denticles on adult pectoral spine : absent (0) ; present (1).
Character 258 has been rephrased.

259. Sclerotic plates : present (0) ; absent (1).

260. Areal growth in postcranial scale crowns : present (0) ; absent (1).
Character 260 of Burrow et al. (2016) has been divided into characters 260 and 265 to take into account the two modes of growth separately. Areal growth characterized polyodontode scales with addition of odontodes centripetally relative to the first odontode [as in type B2 growth of chondrichthyan scales (Karatajute-Talimaa, 1992)]. Areal growth of osteostracan scales represents the plesiomorphic condition (Sansom et al., 2008). *Climatius* (Burrow et al., 2015) and *Ptomacanthus* (Brazeau, 2012) have been coded as (1).

261. Scales with a canal system in the dentine of the crown, opening out through pores on the crown surface : absent (0) ; present (1).

262. Lepidotrichia-like scale alignment : present (0) ; absent (1).
Character 262 corresponds in part to character 7 of Zhu et al. (2013) and Burrow et al.

(2016). The presence of lepidotrichia-like scale alignment has been documented in osteostracans [see *Ilemanaspis* (Sansom et al., 2008) and *Escuminaspis* (Janvier et al., 2004)]. Fin webs preserved in specimens of *Parexus* and *Rhadinacanthus* show this type of scale alignment. *Triazeugacanthus*, *Homalacanthus* (MHNM collections) and *Acanthodes* (CMN and NHM collections) show this alignment. *Lupopsyrus* (Hanke and Davis, 2012) and *Obtusacanthus* (Hanke and Wilson, 2004) were previously coded as (0&1), but scale alignment are visible in the anterior part of the fin web.

263. Appositional growth in postcranial scales : absent (0) ; present (1).
Appositional growth characterized the apposition of odontodes on the side, on the back or on the front of the first odontode in polyodontode growing scales [growth type C, (Karatajute-Talimaa, 1992)]. Character 263 is complementary to character 260 ; it takes into account part of character 265 of (Burrow et al., 2016). *Parexus* (Burrow et al., 2013) and *Kathemacanthus* (Hanke and Wilson, 2010) have been coded as (1).

264. Hypermineralized superficial layer of scales : present (0), absent (1).
Character 264 and character states have been modified from Sansom et al. (2010) (character 82). Because *Trematapsis* (Osteostraci) shows the presence of a hypermineralized layer (Qu et al., 2015), the polarization is modified from Sansom et al. (2010).

265. Hypermineralized superficial layer of scales : enameloid (0), enamel (1).
Trematapsis (Osteostraci) shows the presence of enameloid (Qu et al., 2015), which represents the plesiomorphic condition.

266. Enamel : one layer (0), multi-layers (1).
Mimipiscis (Choo, 2011), *Moythomasia* (Schultze, 2015), *Ligulalepis* (Burrow, 1994), *Cheirolepis* and *Triazeugacanthus* have been coded (1) because they have ganoine.

267. Spinal plates : absent (0), present (1)

Matrix :

Osteostraci :

0001000000 ?000 ?0 ?100000-000-----0-0----0-- ?----------00000000- ?0000000-000 ?0-
--- ?0 ? ?00-00- ?00 ? ?000- ? ?000-00-0 ? ?-- ?0-100-0-000 ?00-00---00 ? ?---0-00 ?000---
-0-00 ?----0-- ?0-----0--0---------- ?----0-------0----0--------- ?0 ? ?0- ? ?--- ?0 ? ? ?------
---000- ? ? ?0-00000-0000000-0

Galeaspida :

0 ?00-0- ? ?00001 ?0 ?0&1000 ?0-000-----0-0----0-- ?----------000000 ?0- ?0000000-000
?0---- ?0 ? ?01 ?00- ?00 ? ?000-0000-- ?---- ?-- ?------0- ?-- ? ?0- ?----0 ? ? ?---0-00 ?000---
-0-001----0-- ?0-----0--0---------- ?----0-------0----0--------- ?0 ? ? ?- ? ?--- ?0 ? ? ?------
---000------000--- ? ?01 ? ?--0

Acanthodes :

000120011011111-0110- ?00 ?01110000-0-1 ?0----0011101010 ?01 ?1 ? ?010 ?0111 ?0
1101110100110011011010011 11 ?001100-1-0-1010010110010-0011110001000100--
?-00---0-- ? ?0-00 ?----0-- ?0--1-----0---------- ? ?-00--- ?00------0----0---00-1-- ? ? ? ? ?0 ?
001 ?00 ? ?0---------000- ?10101100000-00-00-0

Achoania :

001121 ? ? ? ? ? ? ? ? ?1 ?0- ? ? ? ?10 ? ? ? ? ? ? ? ? ? ? ? ? ?11 ?1 ?11 ? ? ? ? ? ?0 ?011010 ?1 ? ?0
0100 ? ? ?1 ? ? ? ? ?0 ? ? ? ? ? ? ? ? ? ? ? ? ? ? ? ? ?1 ? ? ? ? ? ? ?10 ?1 ? ? ? ? ? ? ? ? ? ?1 ? ? ? ? ? ? ?
?1 ? ? ? ? ? ? ? ? ? ?0 ?0 ? ? ? ?1 ? ? ?110 ? ? ?01 ? ? ? ? ? ? ? ? ? ? ? ?0 ? ? ? ?100 ? ? ? ? ? ? ?10

10 ? ? ?1 ? ? ?1110 ? ?10101111011 ? ? ? ?30110111 ? ? ? ? ? ? ? ? ?010 ?0010 ? ? ? ? ? ?01 ?0
100 ?- ? ? ? ? ?010 ?

Akmonistion :
10012001 ?0- ? ?21- ?1 ?1-----000---10-0- ?01110-0011 ?000 ?0101010 ?010011101011
00 ?111 ?11 ?001 ? ?110111010100 ?0010-1-0-1-0011011101100010010000000000 ?0 ?
?-0----0-- ?----0 ?------- ?--- ?---------------- ? ? ? ? ?--- ?00------0- ?- ? ?---0 ?-1--020 ?0 ? ?
? ?1 ?00 ?00---------000- ? ?01 ?01000- ? ?01 ?0100

Austroptyctodus :
0001 ?0 ?1 ?00000 ?1 ?0- ?1-001-00---0110-0010-01100 ? ? ? ?000 ?01010 ?0 ? ? ? ?101 ?
? ? ? ? ? ? ? ?0 ? ? ? ? ? ? ? ? ? ? ? ? ? ? ? ? ? ?0 ? ? ?0 ? ?001001101-00000100 ?111001000 ?0000
11 ? ? ? ? ? ? ?-0 ? ?00 ? ? ? ? ?0-00 ?10100--1-11 ?------------ ?- ? ? ?0 ? ? ?0---0 ?------0--- ? ?-
--0 ? ?0-- ? ? ? ? ? ? ? ? ? ? ?1 ? ? ? ? ? ? ? ? ? ? ? ? ? ?0 ?1 ? ? ? ? ? ? ? ?1 ?00-0 ?0 ? ? ? ? ? ?0

Bothriolepis :
0000-01 ? ?00-- ?10 ?0-000010-00---0100- ? ? ?0-- ?10000 ? ?00 ? ? ?0 ?0 ? ? ? ? ? ? ? ?0 ? ? ?
? ?00 ? ? ? ? ? ? ? ? ?0 ? ? ? ? ? ? ? ? ? ? ? ? ?0 ? ? ? ? ? ? ? ? ?100010 ? ? ? ? ? ?1--00-0--11000-00---00
0 ? ? ? ? ? ?-0-1 ?10 ? ?0 ?0-010-0101-0 ?011 ?0- ? ? ?0------ ?- ? ? ? ? ? ? ? ?0--- ? ?------0---00-
--0 ?00-- ?0 ?0 ?2 ? ? ? ?0--110--0-0 ?-1--0

Brachyacanthus :
000100 ?1000 ?010 ? ?100 ? ?-0 ?11000 ?0 ? ?0- ? ?0----00 ? ? ? ? ? ? ? ? ?01 ?1 ? ? ? ? ? ? ? ?
? ?11110-1000010 ?0 ? ?1 ?-0011101
1110011 ?0-- ?-00--- ?-- ? ?0-00 ?------- ?---1-- ?-- ?------- ?-- ? ?- ? ?--- ?0 ?------0----0---0
? ? ?-- ? ? ? ? ? ? ? ? ? ? ? ? ? ? ? ?0--------000- ? ? ? ?011 ?1000 ?00 ? ? ? ?0

Brindabellaspis :

000110?100111????0-?000?1-?????010??????????????????0?0100000000
00000-00000100?00??10000-00010000-0?0010????1-0001010??????0?????0?-
-???????0-?-?01???0?0-00010111100-11??-??????????-???0?000--??????
?????????????-????--02?100????11??00?????????????0?????110?-?-0?-??
?1

Brochoadmones :
0101000100?1010-0110??-0?000---10-0-??1100000?????????01?1?????????
?????????????????????????????????????0-1-0-??????--?0?10-001111111
11011?0-0?-00---0--??0-00?------- ?---------- ??-??--- ?0??-----0----0---0?-?
--?????????????????0--------000-????011?0001-00-1--0

Buchanosteus :
00?1?0?100111??0?0-001111-00---0110-??1--0?10010??0?00110100001010010
-00000000?00??1000???0011000-0100100011?0?--1?1???????00?0??000-???
???0-?-?00?????0-00010101011-11??-????------?-???????0---??------0---00--
-0000--02??100000110000001000010010??????110--0-0?-???1

Campbellodus :
000??001?00000?1?0-?1-001-00---0100-0010-01100?0??000?0??????????????
?????????????????????????????0????????100110???--1-?0??111001000?0-0
01?01????-?--?0?????0-00?10100--1-11?---------- ?-???0???0---0?------0---??
---00-0--??????????1?????????????0?001?????1?1?0--0-0?-???1

Cassidiceps :
0001?00??0111100?10???-???111?10??0-??0----00?????????01?1????????
?????????????????????????????????????0---0-110????????10-0011101

0010011 ?0-- ?-00--02-- ? ?0-00 ?----0-- ?0-- ?-- ?-- ?------- ?-- ? ? ? ? ?--- ?0 ?------0----0--
-0 ? ? ?-- ? ? ? ? ? ? ? ? ? ? ? ? ? ? ? ?0--------000- ? ? ? ?011 ?000 ?-00- ? ? ?0

Cheiracanthus :

0001200110111110- ?111- ?00 ?01110000-0- ? ?0----0011001010 ?01 ?1 ? ? ? ? ? ? ? ?1 ? ? ?
? ? ? ? ? ? ? ? ? ? ?01 ?0-1-0-1110010010 ?10-001111000100
01 ?0-- ?-00--00-- ? ?0-00 ?----0-- ?0--1-----0---------- ? ?- ? ?--- ?0 ?------0----0---0 ?-1-- ?
? ? ? ? ? ? ? ? ? ? ? ? ? ? ?0--------000- ? ? ? ?011 ?0000-00- ? ? ?0

Cheirolepis :

0011001110111112110-01-110&1-1100101011 ? ?10-001111 ?10000 ?11110 ?011 ?011
? ? ? ?101 ?100000 ?00 ? ? ? ?1 ? ? ? ? ? ?111 ?11 ? ?10110- ? ? ? ? ?1 ?101010-00000-00---
001 ?0000-011 ?0200101000011010-- ?20-000100100&10000 ? ?0 ?000010010101000
0011000000 ?111100 ?0 ? ? ? ? ? ?0 ? ?00 ? ?10 ?000101 ?0&11201 ?0100100--0-0--0110

Chondrenchelys :

11012001 ?0 ? ? ?-1- ?1 ?1-----000---00-0- ? ?1100-0011 ?00011001110 ?0 ?000110 ? ?-1
11 ? ?0 ? ? ? ? ? ? ? ? ? ? ? ? ?0 ?00110 ?0 ?0010-1-0-1-00110100-11000000-00---000 ? ? ? ?
?- ? ? ?--0-- ?----0 ?------- ?--- ?-- ?-- ? ? ? ?---- ?-- ? ? ? ? ?--- ?0 ? ? ? ?---0- ?- ? ? ?-- ? ? ?1-- ?
? ? ? ? ? ? ? ? ? ? ? ? ? ? ?--- ?- ? ?--000- ? ? ? ? ? ?100-- ? ? ? ? ? ? ? ?0

Cladodoides :

110 ? ? ? ? ? ? ? ? ? ? ? ? ?- ? ? ? ?--- ?- ? ? ? ? ? ? ? ? ? ? ? ? ?111 ?-0011 ?00 ? ? ?1010 ? ? ?00000
110101000011111100110111111 ?0101010001 ?
? ? ? ? ? ? ? ? ? ? ? ?- ?----0-- ?----0 ?------- ?--- ?-- ?-- ? ? ? ?------- ? ? ? ? ?--- ? ? ? ? ? ?---0- ?-
? ? ?--0 ?-1--02 ?100 ? ? ?1 ?0 ? ?00--- ?- ? ?-- ? ? ?- ? ? ? ? ? ?100 ?- ? ?0 ? ? ? ? ? ?

Cladoselache :

1101200100-??2?-?1?1-----000---10-0-?01110-00110000?0?01?10?0??0111????10???11?11???????1?1?101010??10?0-1-0-1-0011010101?-001000000?00000????-?----0--?----0?-------?---?--?--????----?--?????---?00???---0-?-???--???1--???????????1??????---?-??--000-????001000-0?0?????0

Climatius :

000100000000010-?100?-00?11100?0??0-??1100000111000?0?0??1????????1??11110-100001000??10-00111011110011?000?-00--02--??0-00?----0--?0--1--?--?---------- ??-??---?0??-----0----0---00?1--??????????????????0--------000-????011?100000111--0

Cobelodus :

1101?00??0-????-?1?1-----000---10-0-001110-0011?00010101?1??01000111101101011111110011011011001010000010-1-0-1-0011011101100000-00---0000?????-???--0--?----0?-------?---?--?--????----?--?????---?0????---0-?-???--???1--02?1?0?0????0?00---?-??--000-??????1?0?-??0????0

Coccosteus

000??00?0??????0?0-001111-00---0110-??10-0110?????00?11?1??????????????00???????????????????0?????????????100011?0?--1?????1?000000-0010-100?????-?--?0?????0-00010101011011?0-???0------?-01?000?0---0?------0---00---000?--???????????????????????????001?????00110--?-0?-???1

Cowralepis :

000??0?????????0?0-1?-0-1-0????0110-0?10-0110?????00??1???0?????????????100110???????01?1?000000-00?0?1-00????-?--?0?????0-00?10101111010??-????------?-???010?0---0?----

--0---00---00??-- ??????????????????????????001?????001?0--??0?????1

Culmacanthus :

?001?00110111101?100???1?000---0??0-??0----10?????1???01?1??????????
??11110-1011010????10-00111100
010011??-- ?-00--00--000-000----0-- ?0-- ?-- ?--0---------- ??-??--- ???------0----0---0
???-- ??????????????????0--------000-????011??101-?0-???0

Debeerius :

1101200??0???-1-?1?1-----000---00-0-00101?-0001?000?1001110?0?0?0111??-
111??0?110??????10-0100100?0?00?0-1-0-1-00110100011?001-01000100100??
??-???--0--?----0?------- ?--- ?-- ?-- ????---- ?-- ?????--- ?0????---0-?-???-- ???1--
??????????????????--- ?-??--000-???00?1?00-?????00-0

Diabolepis :

00?121??????????1?0-?1-1??????????????10-0011?????000011?10?0?100
110???101?1?0?0?1??11??????00111????????????????????????????????
??????????1001????0?1011110?00101??????0-??1????000???11011110?1
1????100---11000010?????1101000??0?0?0?0??010101011??????????100?-
?????010?

Dialipina :

0??1?01?010001?0?0-01-101??????00?10??1?-00?1??????????1?1???????
???????0????????????????????????????????10110-??????????10-00000
-00--??11?0???????1??20??00/1?00?110???-??0-?0????????00????01010?0
???1?10????11??0?????????1????????????????????????????10????01
?0--?-0?-0100

Dicksonosteus :

00?110?1?0?????0?0-001111-00---0100-??1??0110000????0011010000010100
10-00001000?00??10000-0001100000?0010001000?--1-101????000?0-?010-1??
????0-???00?????0-00010101011-1100-???0------?-0/11?01000---00------0---00-
--0000--02111000001100000010000010010000???110--0???????1

Diplacanthus :

000100011010010?0100-?01?000---00?0-??0--0-10?????0???01?1??????????
??11110-111100001??10-001111100
10011?0--?-00--00--??0-00?----0--?0-----?--0---------??-0?---?0?------0----0---0??
?--?????????????????0--------000-?1??011?1111-10-1--0

Doliodus :

1?01?0010000???-?1???--0??00---?0?0-??1110-0011??????101010?00?00010
??00??111?11?00????11??10101000?0?0-1??????????????????00??1???1
1?????000?-??--00--?----0?------- ?0--?--?--?---------- ?????---?0??-----0-?-???--
0?-1--02??0????1?0??00--------- ?-0-????0?10?00?-0?-???0

Entelognathus :

000??0???0000??0?0-01-111-110010101???1?????101????00?1010?0000010
???00?01????0???????????011000??10?100010???????????????00??0??
???0?????????-???00????00-00??0111-00?10000???0000?1?????????00??
1?0?????110?0??????01??0???1??0?01100?00???????0010??????1?0?-0
?0?????1

Eusthenopteron :

00112011000001210 0-01-110-110010101011 10-00111110000001111011110011011

0101110000 ?1111111100 ?0011110101010110-0------000-10-00000-00---0111 ?010-00110101--10100001110- ?10-10-01000001011101-02100 ?021110001-11 ? ?021111 ?111111000010100010001000020000221111000100--0-0 ?-00&100

Euthacanthus :

000100011011010-0100- ?00 ?01100100-0- ? ?0--0-0011 ? ? ?0 ?0 ?01 ?1 ? ? ? ? ? ? ? ?1 ?11110-10100100 ? ? ?10-001110110 10011 ?0-- ?-00--00-- ? ?0-00 ?----0-- ?0--1----- ? ? ? ?------- ? ?-0 ?--- ?0 ?------0----0---0 ? - ?-- ? ? ? ? ? ? ? ? ? ? ? ? ? ? ? ?0--------000- ? ? ? ?011 ?0000-00- ? ? ?0

Gogonasus 0011211100000 ?2100-01-110-1101 ?010101 ?10-0011111000000111101 110001101101011110000 ? ?1111 ?1 ? ? ? ?0011110101010110- ? ? ? ? ? ? ? ? ? ?0 ? ? ? ? ? ?0 ? ?0 ? ? ? ? ? ?0 ?1 ?1010100 ?10101--10100001110- ?10-10- ?10000010 ? ? ? ? ? ? ? ?1 ? ? ? ?1 ?1 ? ? ?0 ? ?1 ? ? ? ? ? ? ? ? ? ?11111100001010001000100002000002111 1 ?00100--0 ? 0 ? ? ? ? ?0

Guiyu :

0011201101000121 ?0-01-110-1100101010 ? ?11-1011 ? ? ? ? ?000011 ?10 ?1 ? ? ?0100 1 ? ?10 ?1 ? ?0 ?0 ? ? ? ? ? ? ? ? ? ? ? ? ? ? ?1 ? ? ? ? ? ? ?10 ?110 ?-- ?-1 ? ? ? ? ?1 ? ?001 ?10000 10 ?11 ?000001 ? ?102001010001001110- ?10- ?0110000000000 ?001000 ?0 ?110 ?111 01111001 ?11011 ? ?1 ?301 ?0110 ? ? ?0 ? ? ? ? ?010000001220 ? ? ? ?11100 ?- ? ?0 ? ?010 1

Gyracanthides :

000120010 ?100 ?-- ?11 ?- ?-0-000---10-0- ? ?0--0-00 ? ? ? ? ? ? ? ? ?0 ?-0-100001001 ? ?10-00111101100 011 ?0-- ?- ? ?--- ?-- ? ? ?- ?0 ?------- ?---------0---------- ? ?- ? ?--- ? ? ?------0---- ?---0 ? ? ?--

? ? ? ? ? ? ? ? ? ? ? ? ? ? ? ?--------- ? ?0- ? ? ? ?011 ?1001-00- ? ? ?0

Hamiltonichthys :

11012001 ?00 ?020- ?110---0-000---10-0-0 ?1110-0001 ?0 ?010101 ?11 ?00 ? ?0110 ? ?-
?0 ? ?1 ? ? ?1 ? ? ? ? ? ? ? ?110 ?0 ?10001 ? ?010-1-0-1-000101000110001001000110110 ?
? ? ?-00---0-- ?----0 ?------- ?--- ?-- ?-- ?---------- ? ? ? ? ?--- ?0 ? ?-----0- ?- ? ? ?--00 ?1--0 ? ?
?0 ? ? ? ?1 ?0 ? ?0 ?---------000- ? ? ?1 ?01000- ? ?0 ? ? ? ? ?0

Homalacanthus :

000100011011111-0111- ?00 ?01111000-0- ? ?00-0000110010 ?0 ?01 ?1 ? ? ? ? ? ?01 ? ?
? ? ? ? ?1 ?1 ? ? ? ? ? ? ? ?0-1-0-1110010 ?1 ? ?10-0011110001
000100--0-00-002-- ? ?0-00 ?----0-- ?0--0-- ?--0---------- ? ?-0 ?--- ?0 ?------0----0---0 ?-1
-- ? ? ? ? ? ? ? ? ? ? ? ? ? ? ? ?0--------000- ? ? ? ?011 ?0000-00-00- ?

Howqualepis :

? ? ? ? ?01 ?0100012110-01-110-1100101011 ?1110101111 ?1 ? ?00 ?11 ?10 ?0110 ?111
? ? ?101 ? ? ? ? ?0 ? ? ? ? ? ? ? ? ? ? ? ?0 ?1111 ? ? ?1010110- ?- ? ? ?1 ? ?01110-00000-00--- ?
011010 ?0110002100001000010110- ?20-0001001 ?1100000 ?00000100101011 ?0001
1001000 ?1 ?110000 ? ? ? ?0 ?000 ?0 ? ?10001111111120 ? ?01001 ?0--0 ? ? ? ? ? ? ? ?

Ischnacanthus :

000120011011110-0100- ?00 ?01101000-0- ? ?110111011100010 ?0 ? ?1 ? ? ? ? ? ? ?1 ? ?
? ?1 ? ? ? ? ? ? ? ?0-1-0-111001101 ? ?10-0011110001
0011 ?000 ?-00--00-- ? ?0-00 ?----0-- ?0--------0---------- ? ?-0 ?--- ?0 ? ?-----0----0---00-1
-- ? ? ? ? ? ? ? ? ? ? ? ? ? ? ? ?0--------000- ? ? ? ?011 ?0001-00- ? ? ? ?

Kathemacanthus :

0101000000 ?001 ?- ?110- ?00 ?000---00-0- ? ?0----00 ? ? ? ? ?000 ?01 ?1 ? ? ? ? ? ? ? ? ? ? ?

???0??????????????????????????????0-1-0-?????-?00?10-00111010010
011?0--?-00--00--??0-00?----0--?0--------0----------??-??---?0?------0----0---0?-1--
????????????????0--------000-????011?10011000???0

Kenichthys:
00?121?101000??100-01-11?-??00101010??10--011????000011??0?1?100110
???1011????0??11??????????111??????10110-0----1-000-????????????????
????101010??1??011110100101110-?10-?1100100001011101112100 10-1?10001
0111002110????1111000?10???0?????00002001001???????100?-?????????

Ligulalepis:
001??0?10???????1?0-?1-1????????????????????????????????0?101010?1
?011010010??1?000010011?1100000111????????????????????????????????
??????????0???????0??????0?0??10????-??0-????????????????00?000
?0?????1????????????????????????101?000?0??1????????????????????
?10?????0??011?

Lodeacanthus:
000100011011110-?110??00?01111100-0-??00-000011101000?01??????????
????????????????????1????????????????0-1-0?100?0?000??10-00111110
100001?0--0-00-0021???0-00?-?--0--?0--1?----0-------?-??????----0?------0---00--
-0?-?--???0??????-?????0--------000-??-?011?0100-00-0??0

Lophosteus:
???120?101?????0?0-?????????????????????????1??????????????????
??
????????????????0???-??

? ? ? ? ? ? ? ? ? ? ? ? ?0 ? ? ? ? ? ? ? ? ? ? ?1 ?
? ? ? ? ? ? ? ? ?1 ? ?0 ? ?-0 ?-1-- ?

Lupopsyrus :
000100010 ?10020- ? ?1 ?- ?00 ?01010 ?00-0 ? ? ?0--0-00 ? ? ? ? ? ? ? ? ?0 ? ?1 ? ? ? ? ? ? ? ? ?
? ?0-1-0-100001001 ? ?10-001110111
10011 ?0-- ?-00--0 ?-- ? ?0-00 ?----0-- ?0--------0---------- ? ?- ? ?--- ?0 ?------0----0---0 ? ?
?-- ? ? ? ? ? ? ? ? ? ? ? ? ? ? ? ?0--------000- ? ? ? ?011 ?0011-00 ?1--0

Macropetalichthys :
00 ?110 ? ? ? ? ? ? ? ? ? ?1 ?0- ?00001- ? ? ? ? ? ? ?0 ? ? ? ? ?0 ? ? ? ? ? ? ? ? ? ? ? ? ?001100 ?0000
000000-0000 ?1-1 ?0 ? ? ?10 ?00- ?0010000- ?00 ?10 ?1 ?1 ? ?
?10 ? ? ? ? ? ? ? ?0- ? ? ?00 ? ? ? ? ?0-000101111000 ? ? ? ?- ? ? ? ?------ ?- ? ? ?0 ?0 ?0--- ? ?---
---0--- ? ?--- ? ? ? ?-- ? ? ?100 ? ? ? ?110000 ? ? ? ? ? ? ? ? ?001 ? ? ? ? ? ? ?1 ? ?- ? ? ? ? ? ? ? ? ? ?

Meemannia :
00 ?121 ? ? ? ? ? ? ? ? ? ?1 ?0- ?1-1 ? ? ? ? ? ? ? ? ? ? ? ? ? ? ? ?1 ?-0011 ? ? ? ? ?000 ? ? ? ? ? ? ?0 ? ? ?
? ? ? ? ? ?01 ? ? ? ? ? ? ? ? ?1 ? ?11 ? ?10 ? ?00111 ? ?1 ?
? ? ? ? ? ? ? ? ? ? ? ?0 ? ? ? ? ? ? ?0 ? ? ? ? ? ?0 ? ?0 ?100 ?0 ?0
10 ? ? ? ? ? ? ? ?1 ? ?0 ? ?10 ?0 ? ?1 ? ? ? ? ? ? ? ? ? ? ? ? ? ? ? ?
? ? ? ?1 ?0 ?- ? ? ? ? ?010 ?

Mesacanthus :
000120011 ?11110- ?100 ? ?00 ?01110000-0- ? ?0----0011 ?000 ?0 ?01 ?1 ? ? ? ? ? ? ?1 ? ?
? ? ? ? ? ? ? ? ? ? ?0 ?0-110-111001100 ? ?10-0011101001
0001 ?0-- ?-00--021- ? ?0-00 ?----0-- ?0--1-----0---------- ? ?-0 ?--- ?0 ?------0----0---00-1-
- ? ? ? ? ? ? ? ? ? ? ? ? ? ? ? ?0--------000- ? ? ? ?011 ?0000-00- ? ? ?0

Miguashaia :

0011201100000012100-01-111-00---01010 ? ?10-001111100 ?00 ?11 ?1 ? ?0 ? ? ? ?1 ? ? ?
? ?10110- ? ? ? ? ? ? ? ?00 ?10-00000-00---
0111 ?000-0010010 ?101010 ?101 ?10- ?10-10 ?011000 ?--- ?-11 ?021 ?00-10 ?1000001
1110011 ?11 ? ?11 ? ? ? ? ? ?1 ? ? ? ? ? ? ? ? ?0 ? ?00001 ?0210 ? ? ? ?001 ?0--0 ?0 ? ?0100

Mimipiscis :

0011201101000012110-01-110-11001010111110-00111111000001111010110011111
0101111000010011111000001111011101011 0-0----1-001110000000-00---00110100
0110002100001000010110- ?20-0001001011010000100001001011100000011000000
11111000000001000000001100010110111201001001 00--0 ?0 ? ?0110

Moythomasia :

0011201101000012110-01-11 ?-1100101011 ?110-00111111000001111010110011111
0101111000010011111000001111011101011 0-0----1-001110000000-00---00110100
0110002100001000010110- ?20-00010010110100001000010010111 0/100001100000
01 ? ?110000000 ?0000000 ?110001111111120100100100--0 ?0 ? ?0110

Nerepisacanthus :

00010000&11011110- ?11 ?- ?00 ?000---10-0- ? ?11 ?1110 ? ? ? ? ?0 ?0 ?01 ?1 ? ? ? ? ? ? ? ?
1 ?0-110-101001100 ? ?10-001110
00010 ?11 ?000 ?-00---2-- ? ?0-00 ?------- ?--- ?----- ?---------- ? ?- ? ?--- ?0 ? ?-----0----0---
0 ? ?1-- ? ? ? ? ? ? ? ? ? ? ? ? ? ? ? ?0--------000- ? ? ? ?111 ?000100 ?01--0

Obtusacanthus :

01012000-0 ?0020- ?110- ?00 ?000---00-0- ? ?0----00 ? ? ? ? ? ? ? ? ? ?0 ? ?1 ? ? ? ? ? ? ? ? ? ? ?
? ?0-1-0- ? ? ? ? ? ? ?- ?0 ? ?10-00111001110

011 ?0-- ?-00--00-- ? ?0-00 ?------- ?0--------0---------- ? ?- ? ?--- ?0 ?------0----0---0 ?- ?--
? ? ? ? ? ? ? ? ? ? ? ? ? ? ? ?0--------000- ? ? ? ?011 ?0001-00 ?1--0

Onychodus :
001120110000112100-01-111-00---01010 ?111010111110 ? ?00 ?11 ?10111 ?001001-
?10111 ?0 ?0 ?1001 ? ? ? ? ? ? ?0 ?1111 ? ? ? ? ?10110-0----1-000 ?10-00000-00---0111 ?0
0 ?-00110100101010 ?101110- ?10-1010110100000011110 ?10001100101001110011
11011 ?11130100010000 ? ? ?0 ? ?010010000220001000100--0-0 ? ?0100

Onychoselache :
1101 ?001 ?0-00-0- ?1 ?1---0-000--- ?0-0- ? ?1110-0001 ?0 ?0 ?0101 ?1 ? ?0 ? ? ? ?11 ? ? ?
? ?0 ? ? ? ? ? ? ?0 ? ? ? ? ? ? ? ? ? ? ? ? ? ? ? ? ?1 ? ? ? ?0-1-0-1-1001010001100010010001001
10 ? ? ? ?-0- ?--0-- ?----0 ?------- ?--- ?-- ?-- ? ? ? ?---- ?-- ? ? ? ? ?--- ?0 ? ? ? ?---0- ?- ? ? ?-- ? ?
?1-- ? ? ? ? ? ? ? ? ? ? ? ? ? ? ? ?--- ?- ? ?--000- ? ? ?10 ?1000- ?-0 ?-0100

Orthacanthus :
1101200 ? ? ? ? ? ? ? ?- ?1 ? ?---0- ?00---10-0-001110-00111000101010 ?1 ?0000011010
1000011111110011011111101010100010-1-0-1-0011011 ? ?11000100 ?00 ? ?10-10 ?
? ? ?-0 ? ?--0-- ?----0 ?------- ?--- ?-- ?-- ? ? ? ?---- ?-- ? ? ? ? ?--- ?00 ? ? ?---0- ?- ? ? ?-- ? ? ?1-
- ? ? ? ? ? ? ? ? ?1 ? ? ? ? ? ?0-- ?- ? ?--000- ? ? ? ? ? ?1000- ? ? ? ? ?1--0

Osorioichthys :
00 ?1201 ?0 ? ? ? ?1 ?110-01-11 ?-1100101011 ? ?1 ? ? ?0 ?1 ? ? ? ? ? ? ? ? ? ?1 ? ? ? ? ? ? ? ? ?
? ?10110- ? ? ? ? ? ? ? ? ? ? ? ? ? ? ?00 ? ?
0-00--- ? ? ? ?010 ?0 ? ? ? ?0210000100 ?1001 ? ? ? ?20-0001 ? ?1 ?1100 ?0 ? ? ?0000 ?00 ?
11 ?10 ?00 ?110 ?00 ? ? ? ? ? ? ?00 ?1120 ? ? ? ? ? ? ?1 ?0 ?
-0 ? ? ? ? ? ? ?0

Osteolepis :

001121110100012100-01-11 ?-1100101010 ? ?10-001111 ? ? ? ? ?0011110 ?1 ?1001101
1 ?101110 ? ?0011 ?1111 ? ?0 ?00111 ?0101010110- ? ? ? ? ? ? ? ? ? ? ? ?10-00000-00--- ?11
110 ?0100110101--10100001110- ?10-10- ?1 ? ? ? ? ? ? ? ? ? ? ? ? ? ? ? ?1 ? ? ? ?2111 ? ?0 ? ?1
1 ? ? ? ? ? ? ? ? ? ? ?11111000010100010001000020000221111 ?00100--0 ?0 ? ?0100

Parayunnanolepis :

0 ? ?1 ?0 ?1 ?0 ?11 ?10 ?0-000010-0----0100- ? ? ? ? ? ? ? ? ?0 ? ? ? ? ? ? ? ? ? ? ?0 ? ? ? ? ? ? ? ? ? ?
? ?100010 ? ? ? ? ? ? ? ? ?0 ?10010000
?00--- ?00 ? ? ? ? ?- ?-- ?1 ? ? ?0 ?0 ?010-0101-0 ?-11 ? ?- ? ? ?0------ ?- ? ? ? ? ? ? ? ?0---0 ?----
--0--- ? ?--- ? ? ? ?-- ?0 ?002 ? ? ? ?010110-- ? ? ? ? ? ? ? ?0

Parexus :

000100000000010- ?100 ? ? ?0 ?11 ?0000 ? ?0- ? ?1100000 ? ? ? ? ? ? ? ? ?01 ?1 ? ? ? ? ? ? ? ?
? ?11110-101001000 ? ?10-001110
11111011 ?000 ?-00--0 ?-- ? ?0-00 ?----0-- ?0--1-- ?-- ?------- ?-- ? ? ? ? ?--- ?0 ? ?-----0----
0---0 ? ? ?-- ? ? ? ? ? ? ? ? ? ? ? ? ? ? ? ?0--------000- ? ? ? ?011 ?100010001--0

Poracanthodes :

00010&20010011110- ?10 ? ? ? ?0 ? ? ? ? ? ? ? ? ? ?0- ? ?110111011 ?000 ?0 ? ? ? ? ? ? ? ? ? ?
? ?1 ?0-1-0-111001100 ? ?10-00111
000010011 ?000 ?-00--- ?-- ? ?0-00 ?------- ?--- ?----- ?------- ?-- ? ?- ? ?--- ?0 ? ?-----0----0
---00-1-- ? ? ? ? ? ? ? ? ? ? ? ? ? ? ? ?0--------000- ? ? ? ?011 ?0001-10-1--0

Porolepis :

001121110100012100-01-110-110 ?101010 ?1110101111100000011110 ?11 ?001101
1 ?1011100 ?0 ? ?101 ? ?1 ? ? ? ?001111 ? ?01 ?10110-0----1-000 ?10-00000-00--- ?11 ?1

010100110???10??10??00110-??0-???01??000??????1?1??10???2111?11101??0?11?11111121?0001??000???0???1010???2????1000100--??0???????

Powichthys :

001121?10100012100-01-11?-1100?0101???11??011?????000011110?11100110 1??101?1?0?0??10????????0011110?01010110-??????????????????????????????????101111??0010111101011011????10-??10??0000101110111100010?1?10 1110101001110????1121000?1110?011?0101101001021111100?100--????????? ?

Promesacanthus :

00012001101111?-?101??00?01110000-0-??0----0011???010?01?1???????1??????????????1?????????????????????????0-1-0-11100?001??10-0011101101 0001?0--?-00--00--??0-00?----0--?0--?-----0---------??-??---?0?------0----0---0?-1--???????????????????0--------000-????011?0000-00-???0

Psarolepis :

00?121?101?0??21?0-01-?10-??????????????11?1011?????000011010?1?1001 0011?10?11?0?0?1001???100000111?????10?1??????-1??01????01?10?0 010????000001??10??110???0100??10-??0-?1010??1110000101100000?011?? 11101110101111011??113011011000?0001??01000000??1/200001111000-??0?? 0101

Pterichthyodes :

0?0??0-1?0???010?0-00??10-0?---0100-??0--???0?????????0?0?0?????0?? ??????????????????????????????0?????????1?0010?????1--00-0--11?00?00--?000?????-?--?10??0?0-010-0101-0?011??-???0------?-???????0---??------0--

-??---????--??????????????????????????002??????110?-??0?????0

Ptomacanthus :

?00100?00011010-?100??00?01?0001?????1100-00110000???01?10??0????
0????0????0000??????????????????????10?11110-100001010??10-00111011
110011?000?-00---?--??0-00?-------?---1--?--?---------?????---?0??-----0-?-???-
-0?-1--??????????????0??00--------000-?????11?00000001???0

Pucapampella :

110??0?????????-????---?-??????????????????????????????1????000
001101?1100?1101011001?0?101010111?00100?????????????????????????
???????????????-???-?0--?----??-???????---?--?--????-------?????---?????
?---0-?-???--????--?2?10????1?0??00---?-??--00?-??????10???????????

Rhadinacanthus :

000100011011110?0100-?01?000---0??0-??0--0-10?????0???01?1??????????
??????????????????????????????????????11110-111100001??10-001111100
10011?0--?-00--00--?-0-00?----0--?0-----?--0----------??-??---?0?------0----0---0??
?--??????????????0--------000-????011?1111-00-1--0

Rhamphodopsis :

000??0???????0?1?0-?1-001-00---0110-??10-01100????????0?????????????
??????????????????????????????0????????10011??0?--1-????111001000?0
110?10?????-?0??0????0-00?1010??01-11?---------?-???0???0---0?------0-
--??---0???--??????????1??????????????000?????01?0--??0?????1

Sigaspis :

0????0???0???010?0-00111?-00---010??????????0????????????????????

? ?100010 ? ? ? ? ? ? ? ? ?1 ?1 ?0000 ? 0 ? ?000- ? ? ? ? ? ? ? ? ? ? ? ? ?0 ? ? ? ? ?0 ?00 ?10101000 ?10 ?0- ? ? ?0------ ?-11 ? ? ? ? ?0-- ? 0 ?------0--- ? ?--- ? ? ? ?-- ?000 ? ? ? ? ?101 ?0-- ? ?0 ? ? ? ? ?1

Styloichthys :

00 ?121 ?101000 ?2100-01-11 ?- ? ? ? ? ? ? ? ? ? ? ? ?11 ? ?011 ? ? ? ? ?000011110 ?1 ?1001 101 ?0101110 ? ?0 ?1101 ? ? ? ? ?0 ?0011100101010110-0----1-000- ? ? ? ? ? ? ?0 ? ? ? ? ? ? ? ? ? ?00 ?011 ? ?1 ? ? ?01 ? ? ? ?00 ?01110- ? ?0- ?1 ?0010 ? ?0101110111200 ?101 ? ?101 ? ? ?100101110 ? ? ? ?1121010 ?1110 ?01 ? ?0 ?00001011 ? ?211110 ? ?100 ?- ? ? ? ? ?010 ?

Tamiobatis :

1101 ?0 ?000-00 ? ?- ?11 ?---0- ? ? ? ? ? ? ? ? ? ? ? ? ?1110-0011 ?000 ? ?101 ? ?0 ?00000110 1010000111111 ?001 ? ? ?111110101000001 ?-1- ? ? ? ? ? ?1 ? ? ? ? ? ? ? ? ? ? ?1 ?01 ? ?110 ? ? ?00 ? ? ?- ? ? ?--0-- ?----0 ?------- ?--- ?-- ?-- ? ? ? ?---- ?-- ? ? ? ? ?--- ? ? ? ? ?----0- ?- ? ? ?-- ? ? ?1--02 ? ? ?0 ?0 ?1 ? ?0 ?00--- ?- ? ?--000- ? ? ? ? ?11 ?00- ?10 ?1 ? ? ?0

Tetanopsyrus :

0001200110111110- ?110 ? ?00 ?000---00-0- ? ?10-0010010001 ?0 ?01 ?1 ?0-1-0-100001 ?010 ?10-0011100011 0011 ?0-- ?-00--00-- ? ?0-00 ?----0-- ?0--------0---------- ? ?- ? ?--- ?0 ?------0----0---00-1- - ? ? ? ? ? ? ? ? ? ? ? ? ? ? ?0--------000- ? ? ? ?011 ?0001-00- ? ? ?0

Tristychius :

11012001 ?0- ? ?- ?- ?1 ?1-----000---00-0- ?01110-0001 ?0 ?010101010 ?000001101 ?-1 000101 ?-0 ?001 ? ? ? ? ?11101000 ?10010-1-0-1-0011010001100010010001101100 ? ? ?

?-???--0--?----0?-------?---?--?--????----?--?????---?0???----0-?-???--???1--??
???????????????---?-??----0-???1001000-????????0

Triazeugacanthus :

000100011011110-111???00?01011000-0-??00-0000?1???????01????????????
????????????????????1????????????????????0-1-0???0?0?000??10-00111110
100001?0--0-00-0021???0-00?-?--0--?0--0?----0-------?-??????----0?------0---00--
-0?-?--???0???????-?????0--------000-??-?011?0000-00-0110

Uraniacanthus :

000100011011110-?100-?01?01000100-0-??0----10??????1???0??1??????????
??0-1-0-1011000?00?10-0011111111
0?11?0--?-00--0?--??0-00?----0--?0--------0---------- ??-??---???------0----0---0?-?
--???????????????????0--------000-????011??101-1?-1--0

Vernicomacanthus :

000??0???????1?-??0???0???100??0??????11?0000?????????0????????
??110-1?000???1??10-001
11011110011?0?0?-00---?--??0-00?-------?---?--?--?-------?--?????---????-----0-
---0---0???--??????????????0--------000-?????1101010???????0

Youngolepis :

00?121?101000?2100-01-11?-?????0101???11??01111???000011110?0110011
01101011100?0011011111?000011110101010110-0----1-000-???????0????????
??101111??0?10111???00101110-?10-?1100100001011101111001 10-1?1001101
00&1101110???11121000?1110?0010011010100/11??211110??1?0?-????0100

ANNEXE XV

SCALES OF THE FRASNIAN ACANTHODIFORM *HOMALACANTHUS CONCINNUS*, ESCUMINAC FORMATION, MIGUASHA, QUEBEC, CANADA

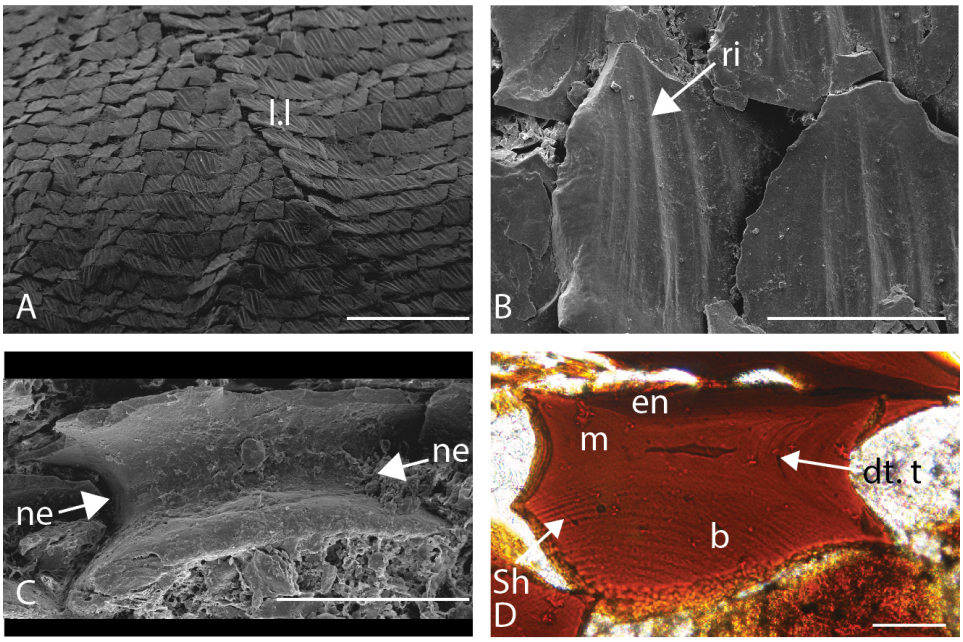

A-D : MHNM 03-2215. A : SEM of the body squamation showing the alignment. B : Details from two scales showing the superficial ridges. C : SEM observations of a transverse section. D : Transverse ground section under polarised light. Scale bar = 1 mm in A, 200 μm in B, 100 μm in C, 50 μm in D.

ANNEXE XVI

SCALES OF THE FRASNIAN ACTINOPTERYGIAN *CHEIROLEPIS CANADENSIS*, ESCUMINAC FORMATION, MIGUASHA, QUEBEC, CANADA

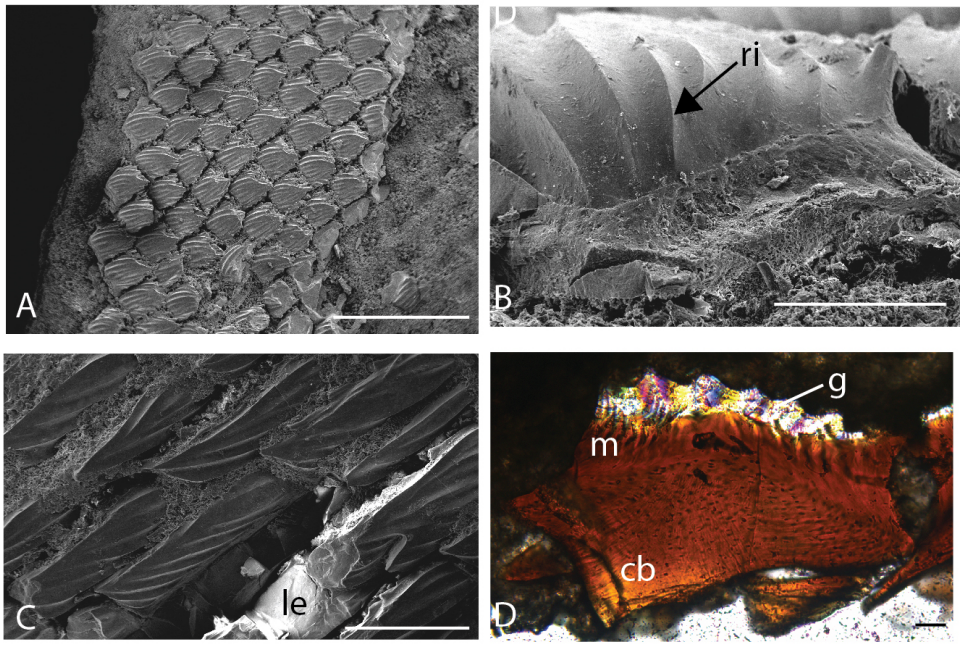

A : MHNM 05-53, SEM of the body squamation. B : MHNM 05-53, details showing the ridged scale surface and the broad base. C : MHNM 05-152, SEM of lepidotrichial segments showing the ornamentation. D : Transverse ground section of a scale under polarised light. Scale bar = 2 mm in A, 200 μm in B, 500 μm in C, 50 μm in D.

ANNEXE XVII

REPRESENTATIVE SPECTRA OF *TRIAZEUGACANTHUS AFFINIS* SAMPLES USING EDX PUNCTUAL MICROANALYSIS OF MHNM 03-1497 SCALES

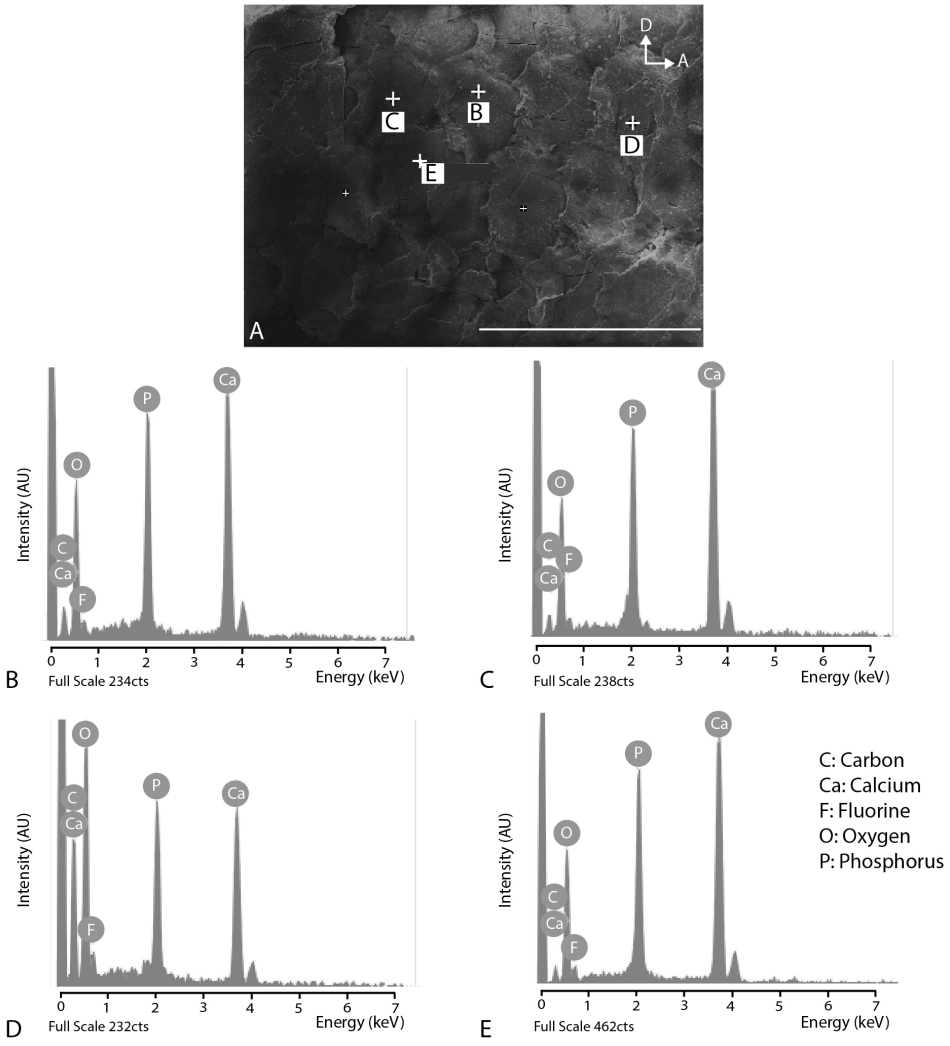

A : MHNM 03-1497, location of spectra for EDX analyses. Note that the oxygen peak is non-significant and depends essentially on the vacuum level in the chamber of the environmental SEM. Scale bar : A = 1 mm.

ANNEXE XVIII

DISTANCES BETWEEN GROWTH LINES IN THE SCALES OF FOUR ADULT SPECIMENS OF *TRIAZEUGACANTHUS AFFINIS*

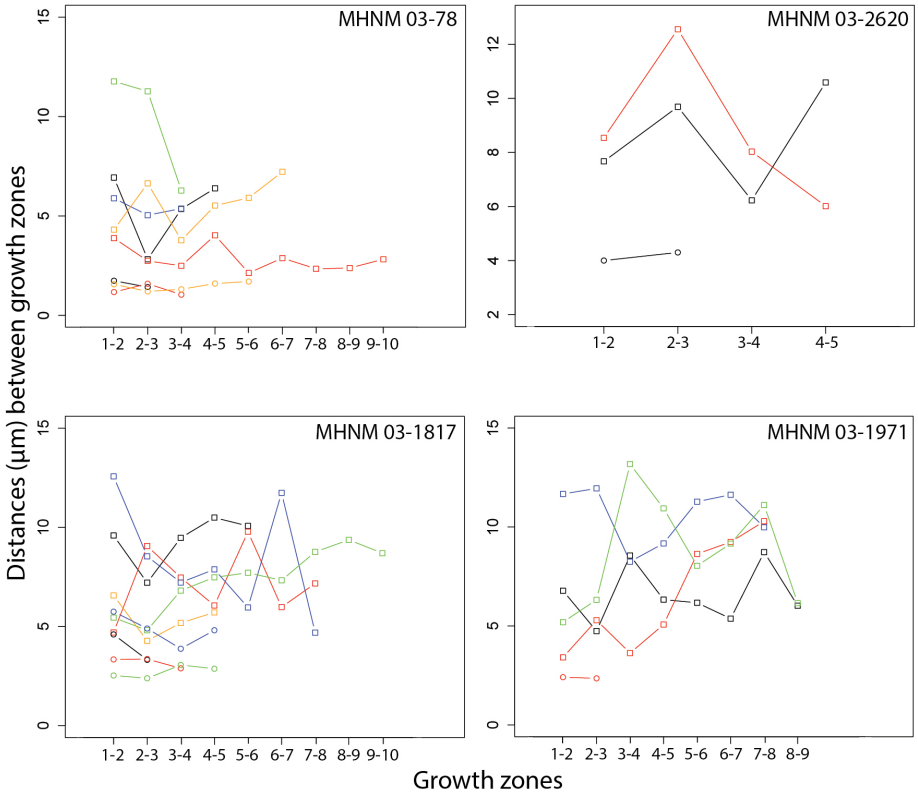

Circles are for the ganoine layers (superimpositional growth), squares for mesodentine and bone layers (“box-in-box” growth). The ”box-in-box” patttern of growth is more irregular than the superimpositional growth of the multi-layered ganoine. Growth zones are numbered by the two growth lines that delimit the zone. Each coloured line represents one scale.

ANNEXE XIX

TRIAZEUGACANTHUS AFFINIS MEDIAN RIDGE SCALES

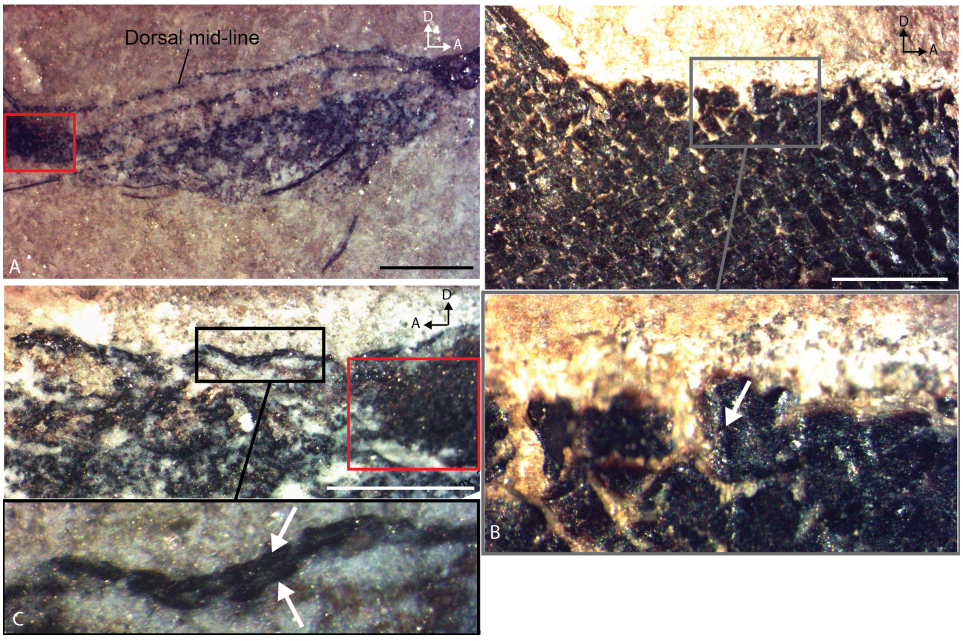

A : Early juvenile, MHNM 03-1252. Dorsal mid-line scales develop before trunk scales; the latter are only present in the posterior region (red rectangle). B : Adult, MHNM 03-1497. Dorsal scale showing the presence of a median ridge (white arrow). C : Late juvenile, MHNM 03-2684. Two parallel scale rows (white arrows) are present anterior to trunk scales (red rectangle). Scale bars : A = 2 mm, B, C = 1mm.

ANNEXE XX

TREES GENERATED IN THE PHYLOGENETIC ANALYSES OF SELECTED EARLY GNATHOSTOMES (79 TAXA, 267 CHARACTERS)

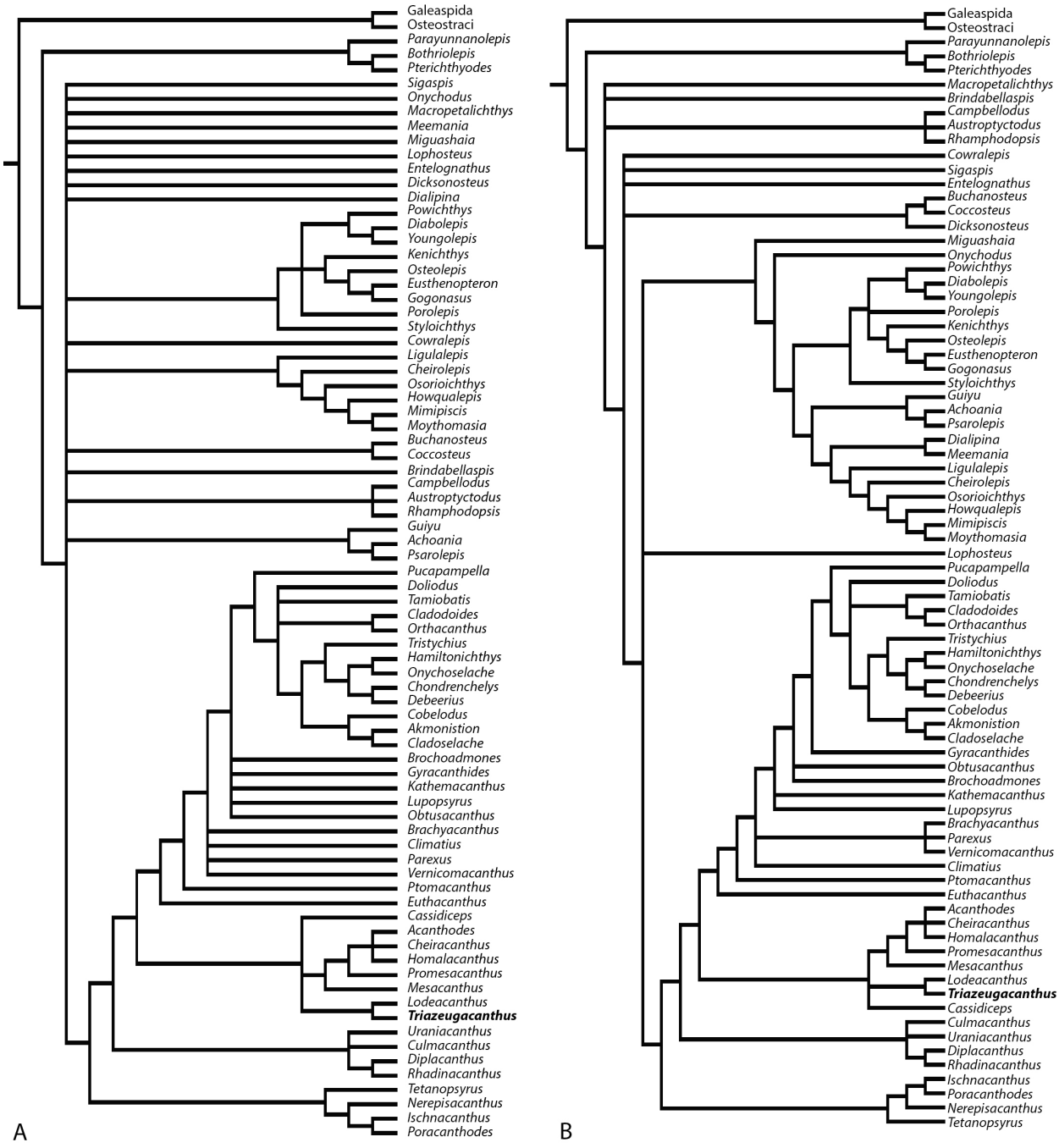

A : Strict consensus of 10 000 most parsimonious trees (711 steps). B : Adams consensus of 10 000 most parsimonious trees (711 steps).

ANNEXE XXI

TREES GENERATED IN THE PHYLOGENETIC ANALYSES OF SELECTED EARLY GNATHOSTOMES (79 TAXA, 267 CHARACTERS).

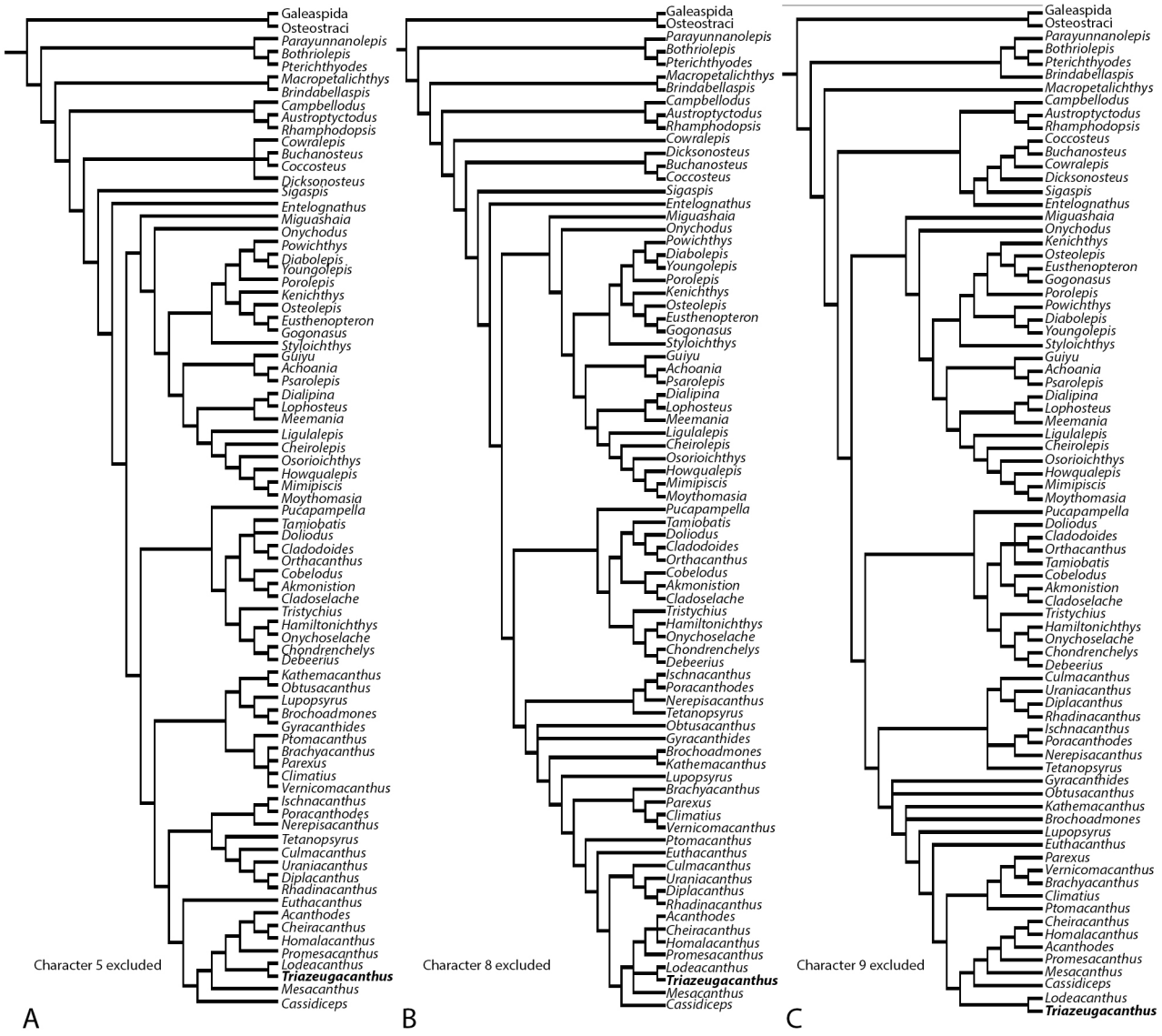

Each analysis is realized with the exclusion of one character related to scales.

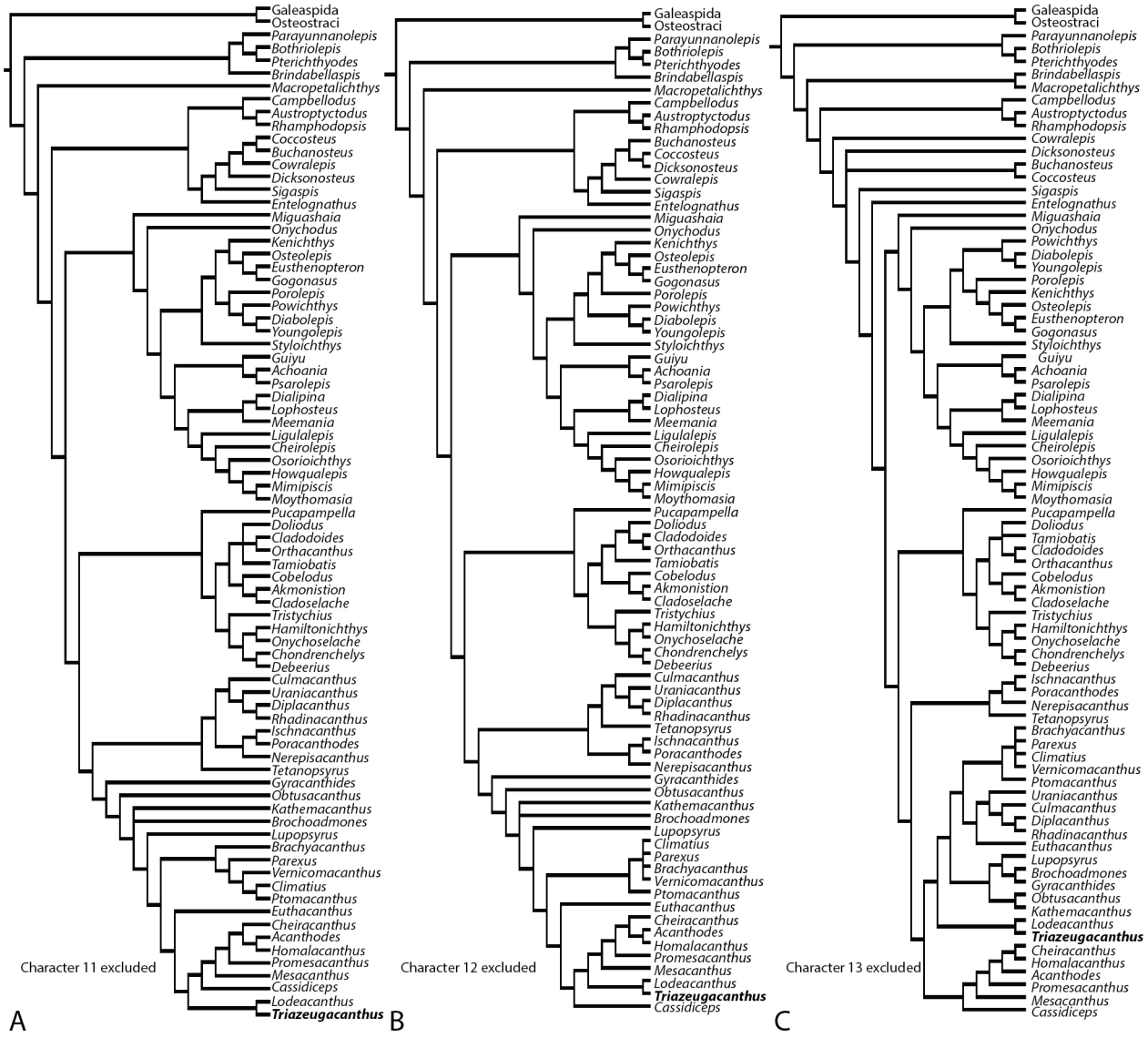

Each analysis is realized with the exclusion of one character related to scales.

Each analysis is realized with the exclusion of one character related to scales.

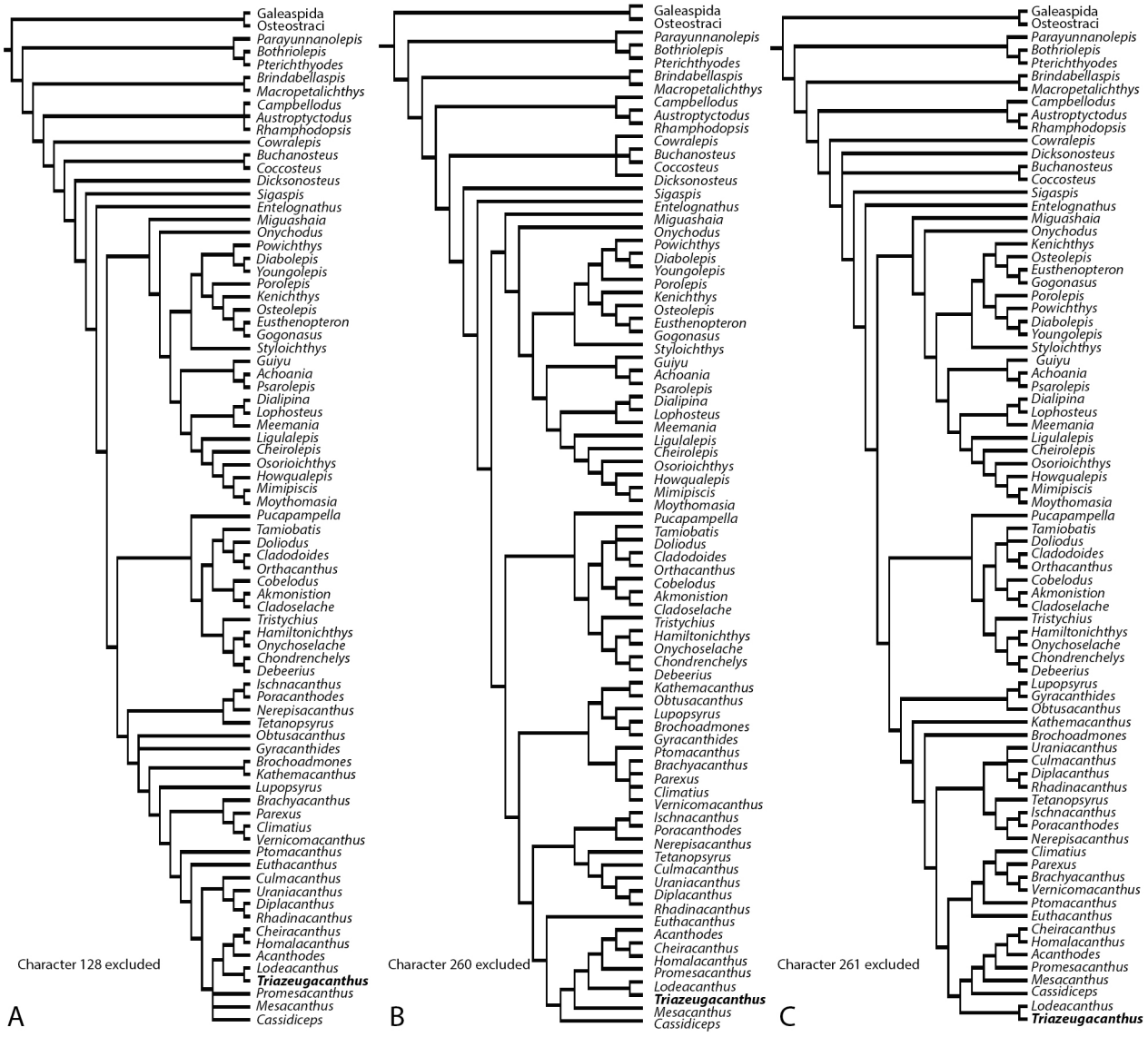

Each analysis is realized with the exclusion of one character related to scales

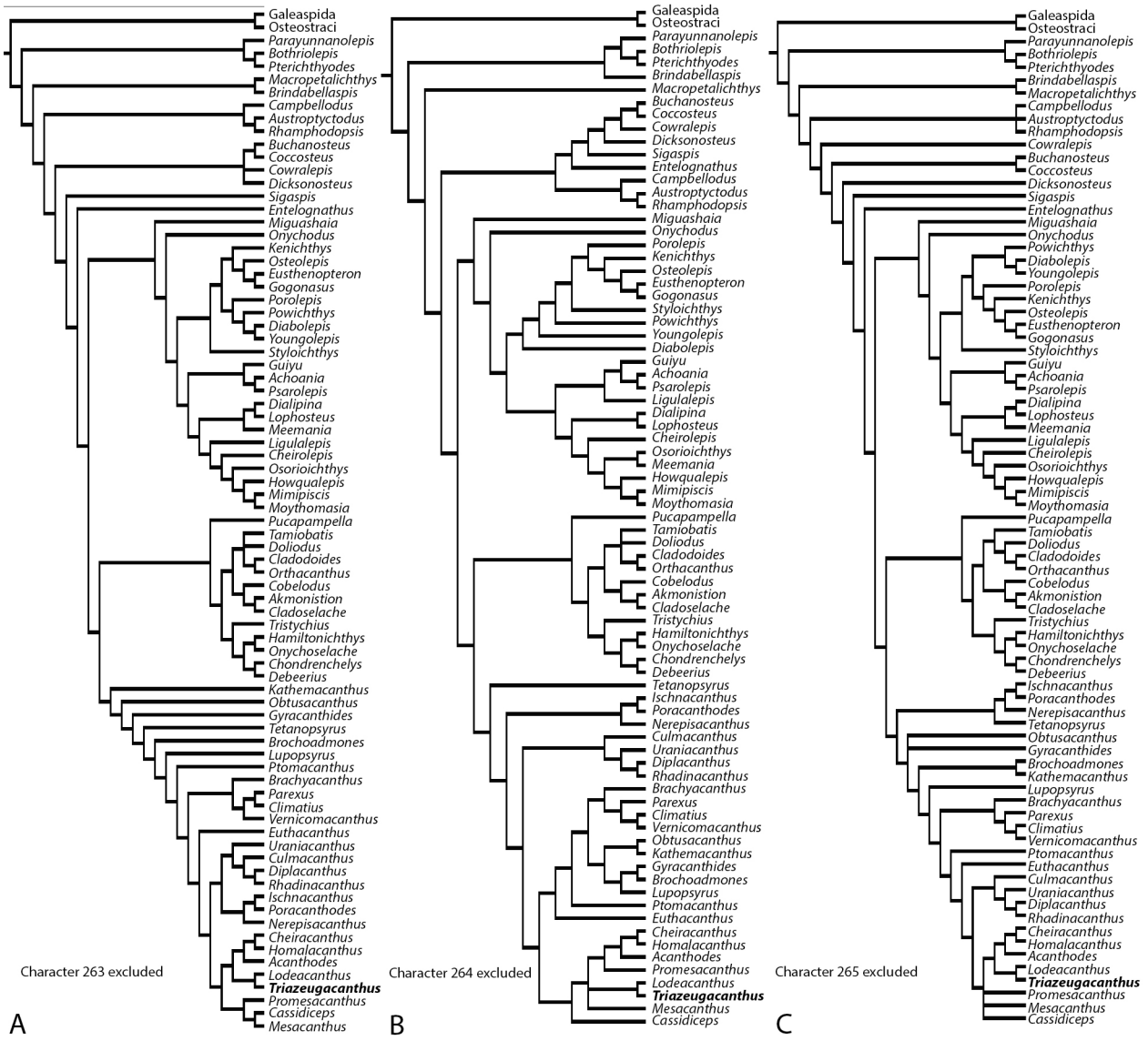

Each analysis is realized with the exclusion of one character related to scales.

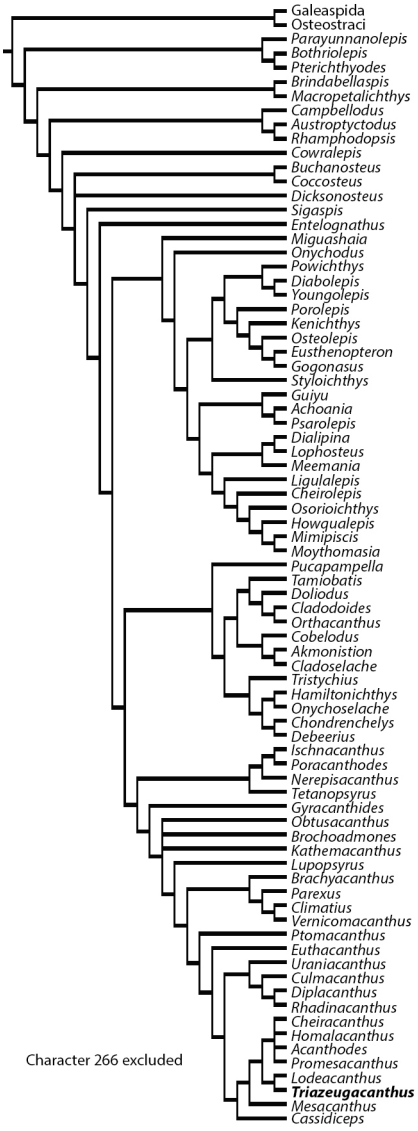

Analysis realized with the exclusion of one character related to scales.

ANNEXE XXII

RESULTS FROM SUCCESSIVE DELETION OF CHARACTERS PERTAINING TO THE HISTOLOGY, MORPHOLOGY AND GROWTH OF SCALES AND TWO SPINE CHARACTERS

Only the characters relevant to acanthodian taxa have been deleted. For each analysis the length of the trees, the number of trees, as well as the resulting phylogenetic status of the acanthodians and the identification of the taxa at the base of either the monophyletic acanthodians or the total-group chondrichthyans have been recorded.

Character	*Length of MPTs*	*Number of trees*	*Acanthodii*	*Basal*
5 - Dentine types	700	16,976	monophyly	[climatiids and putative chondrichthyans]
8 - Odontode	704	100,000	monophyly	Ischnacanthiformes
9 - Box-in-box growth	706	10,463	monophyly	[Ischnacanthiformes + Diplacanthiformes]

Continued on next page

Continued from previous page

Character	*Length of MPTs*	*Number of trees*	*Acanthodii*	*Basal*
11 - Profile (neck)	705	6,539	monophyly	[Ischnacanthiformes + Diplacanthiformes]
12 - Bulging base	702	71,665	monophyly	[Ischnacanthiformes + Diplacanthiformes]
13 - Flat base	702	2,659	monophyly	Ischnacanthiformes
14 - Flank scale alignement	706	95,702	monophyly	[Ischnacanthiformes + Diplacanthiformes]
15 - Sensory line canals	705	44,128	paraphyly	[Ischnacanthiformes + Diplacanthiformes]
127 - Anal fin spine	710	100,000	monophyly	[Ischnacanthiformes + Diplacanthiformes]
128 - Paired pectoral fin spines	707	100,000	monophyly	Ischnacanthiformes

Continued on next page

Continued from previous page

Character	*Length of MPTs*	*Number of trees*	*Acanthodii*	*Basal*
260 - Areal growth	708	998	monophyly	[climatiids and putative chondrichthyans]
261 - Pore canal system	709	100,000	paraphyly	Ischnacanthiformes
263 - Appositional growth	708	19,667	monophyly	putative chondrichthyans
264 - Hypermineralized superficial layer of scales	706	934	monophyly	putative chondrichthyans
265 - Enameloid / Enamel	708	100,000	monophyly	Ischnacanthiformes
266 - Mono / multilayered enamel	709	37,095	monophyly	Ischnacanthiformes

ANNEXE XXIII

COMPARISON OF SCALE COMPOSITION IN EARLY GNATHOSTOMES

	Superficial layer			*Middle layer*				*Basal layer*			*Size of flank scales*	*Box-in-box growth*	*Superpositional growth*	*Polyodontode growth*	*Squamation primordium*	*Squamation direction*
	Surface	*Micro relief*	*Enamel-like*	*Vascular canal*	*Pore canal*	*Dentine*	*Neck*	*Bone*	*Sharpey's fibers*	*Shape*						
Diplacanthiformes																
Diplacanthus (Denison 1979; Burrow et al. 2016)	ridges	?	absent	present	present	mesodentine	slightly cons-tricted	acellular	present	convex	3/mm	5-6 GZ	?	absent	?	?
Uraniacanthus (Newman et al. 2012)	3-5 grooves	absent	absent	present	present	dentine	present	acellular	present	flat	2-5/mm	2-4 GZ	absent	absent	?	?
Rhadinacanthus (Burrow et al. 2016)	around 12	absent	absent	present	present	mesodentine	constricted	acellular	present	slightly convex	1/mm	> 6-7 GZ	absent	absent	?	?
Milesacanthus (Burrow et al. 2009)	14-24 ridges	absent	absent	present	present	mesodentine	constricted	acellular	present	convex	1-2/2mm	12 GZ	absent	absent	?	?
Culmacanthus stewarti (Long 1983)	6-7 ridges	?	?	?	present	?	constricted	?	?	convex	?	?	?	?	?	?
Tetanopsyrus lindoei (Hanke et al. 2001)	smooth	?	?								6/mm	?	?	absent	?	?
Gladiobranchus probaton (Hanke and Davis 2008)	6-9 ridges	absent	absent	present	absent	orthodentine	constricted	acellular	present	slightly convex	2/mm	6 GZ	absent	absent	?	?

Climatiiformes																
Nostolepis gaujensis (Gross 1971; Valiukevičius and Burrow 2005; Burrow et al. 2009)	4-6 ridges	15 µm diameter	birefringent durodentine	present	present	mesodentine	absent	cellular	present	moderately convex	1/1.5 mm	> 6 GZ	present	absent	?	?
Cassidiceps vermiculatus (Gagnier and Wilson 1996)	smooth	absent	?	?	?	?	high and constricted	?	?	convex	?	?	?	?	??	??
Climatius reticulatus (Burrow et al. 2015)	ridges	?	absent	present	absent	mesodentine	present	cellular	present	slightly convex	3-4/mm	absent	absent	areal	?	?
Parexus recurvus (Burrow et al. 2013)	ridges	?	absent	?	?	?	absent	acellular		flat or slightly concave	1-2/mm	absent	absent	3-5 appositional GZ	?	?
Vernicomacanthus waynensis (Miles 1973)	ridges	?	?								2/mm	?	?	?	?	?
Acanthodiformes																
Triazeugacanthus affinis – juveniles	smooth	?	absent	absent	absent	mesodentine	poorly developed	N/A	absent	flat	12/mm	1-2 GZ	absent	absent	dorsal region	bidirectional
Triazeugacanthus affinis – adults	smooth	2.5 µm diameter	ganoine	absent	absent	mesodentine	poorly developed	acellular	present	convex	5/mm	> 11 GZ	present	absent	N/A	N/A
Lodeacanthus gaujicus (Upeniece 2011)	smooth	absent	present	absent	absent	mesodentine	constricted	acellular	?	convex	7/mm	?	absent	absent	caudal	P > A

Acanthodes sp. (Derycke and Chancogne-Weber 1995)	smooth	present	ganoine	absent	absent	mesodentine	?	acellular	?	?	?	?	?	?	?	?
Acanthodes bridgei (Zidek 1985)	smooth	absent	?									present	?	?	caudal	P > A
Acanthodes bronni (Heidtke 1990)	?														caudal	P > A
Acanthodes gracilis (Zajic 2005)	?										5/mm	?	?	?	caudal	P > A
Acanthodes lopatini (Beznosov 2009)	smooth	absent	ename-loid	absent	absent	dentine	developed	acellular	?	convex	?	present	absent	absent	caudal	P > A
Acanthodes ovensi (Dineley 1999)	?														caudal	P > A
Promesacanthus milesi (Hanke 2008)	smooth	?	?	?	present	dentine	present	acellular	present	tumid/ convex	4/mm	4-5 GZ	absent	absent	?	?
Melanoacanthus minutus (Cumbaa and Schultze 2002)	smooth	?	?	absent	absent	dentine	?	acellular	?	?	9/mm	present	absent	absent	?	?
Teneracanthus (Burrow and Young 2005)	smooth	?	present	absent	absent	mesodentine	present	acellular	?	convex	4-5/mm	present	absent	absent	?	?
Mesacanthus mitchelli (Watson 1937; Baron 2015)	smooth	?	?	?	?	orthodentine	?	?	?	?	16/mm	?	?	?	?	P > A

Homalacanthus concinnus (S1 Fig)	ridges	absent	present	absent	absent	mesodentine	constricted	acellular	present	convex	4/mm	present	present	absent	dorsal	?
Cheiracanthus splendens (Denison 1979; Trinajstic 2001)	ridges	?	?	present	absent	orthodentine	constricted	cellular	?	tumid/ convex	2-3/mm	present	absent	absent	?	?
Acanthodidae indet. (Burrow *et al.* 2009)	smooth	?	duro-dentine	present	absent	dentine	slightly cons-tricted	acellular	?	convex	2-3/mm	10 GZ	absent	absent	?	?
Halimacanthodes ahlbergi (Burrow *et al.* 2012)	smooth	present	ename-loid	absent	absent	dentine	shallow	acellular	present	convex	2-3/mm	?	?	?	?	?
Ischnacanthiformes																
Gomphonchus (Gross 1971; Burrow and Young 1999)	ridges	?	?	?	absent	?	?	?	present	?	?	present	?	?	?	?
Poracanthodes (Gross 1971; Valiukevičius 1995; Burrow and Young 1999)	ridges	?	absent	present	present	mesodentine and/or orthodentine	constricted	cellular and acellular	?	?	?	12 GZ	absent	absent	?	?
Radioporacanthodes scheii (Burrow and Sues 2013)	4-8 ridges	honey-comb	durodentine	present	present	mesodentine	constricted	cellular	?	convex	9-10/mm	14 GZ	absent	absent	?	?
Ischnacanthus gracilis (Watson 1937)	smooth	?	?								4/mm	?	?	?	?	?
Nerepisacanthus (Burrow and Rudkin	smooth	?	absent	absent	absent	mesodentine	absent	cellular	?	convex		absent	present	present	?	?

2014)															
Acanthodian Indet.															
Paucicanthus vanelsti (Hanke 2002)	smooth	?					low	no histology		flat	?			?	?
Machaeracanthus pectinatus (Burrow and Young 2005)	4-12 ridges	absent	absent	absent	absent	orthodentine + mesodentine	constricted	acellular	?	slightly convex	0.5-1/mm	present	present	absent	?	?
Machaeracanthus goujeti (Botella *et al.* 2012)	8-12 ridges	absent	absent	absent	absent	mesodentine	pronounced	cellular	present	slightly convex	0.5-1/mm	present	absent	absent	?	?
Lupopsyrus pygmaeus (Hanke and Davis 2012)	smooth edges	absent	absent	absent	absent	mesodentine	present	no basal tissue	absent	flat	?	absent	absent	absent	2nd dorsal fin	?
Pechoralepis (acritolepidae) (Burrow et al. 2009)	ridges	absent	absent	present	absent	mesodentine	short or absent	cellular	?	convex	1-2/mm	absent	4-7	absent	?	?
Brochoadmones milesi (Hanke and Wilson 2006)	rings	?	absent	?	absent	mesodentine	low	cellular	present	Flat or slightly convex	3-4/mm	present	absent	absent	?	?
Acritolepis (Valiukevičius 2003)	2-6	absent	absent	present	absent	mesodentine	present	cellular	present	slightly convex	3-7/mm	absent	present	absent	?	?
Obtusacanthus corroconis (Hanke and Wilson 2004)	ridges	?	absent	present	absent	orthodentine	absent	?	?	flat	2/mm	?	?	?	?	?
Kathemacanthus	ridges	?	?								2-3/mm	absent	absent	appositional	?	?

rosulentus (Hanke and Wilson 2010)																
Euthacanthus gracilis (Newman et al. 2012)	> 4 ridges		?							slightly convex	2-3/mm	?	?	?	?	?
Ptomacanthus anglicus (Brazeau 2012)	ridges	?	?	present	absent	mesodentine	present	cellular	absent	convex	1-2/mm	absent	present	areal	?	?
Early osteichthyans																
Cheirolepis canadensis (S2 Fig)	ridges	present	ganoine	present	absent	mesodentine	short	cellular	?	convex	2/mm	>8	absent	absent	?	?
Psarolepis romeri (Qu et al. 2013)	smooth with pores	10-50 µm pore diameter	cosmine	present	present	orthodentine	present	cellular	present	convex	?	absent	present	present	?	?
Elonichthys peltigerus (Schultze and Bardack 1987)	?														lateral line – abdominal	A > P then, P > A
Eurynotus crenatus (Schultze 2015)	smooth	present	ganoine	present	present	dentine	absent	cellular	?	flat	?	?	present	absent	?	?
Early chondrichthyan growing scales (Karatajute-Talimaa 1992)																
Ctenacanthus	ridges	absent	present	?	?	dentine	?	?	?	concave	?	absent	absent	present	scales of various ages with different # of odontodes	?

Altholepis	ridges	absent	present	?	?	dentine				concave		absent	absent	present	?	?
Seretolepis	ridges	absent	present			dentine				concave		absent	absent	present	increasing # of scales during life	?
Protacrodus	ridges	absent	present			dentine				convex		absent	absent	present	?	?

ANNEXE XXIV

TRIAZEUGACANTHUS SKELETAL STRUCTURE MEASUREMENTS

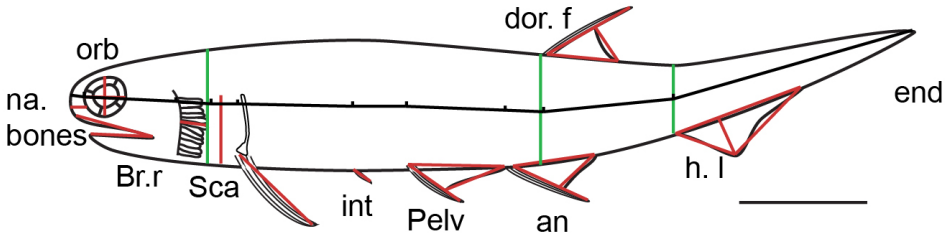

Scale bar = 5 mm.

ANNEXE XXV

RAW DATA OF PRESENCE/ABSENCE OF SKELETAL ELEMENTS IN *TRIAZEUGACANTHUS AFFINIS* USED FOR RELIABILITY INDEX CALCULATION

White is for absence. Grey is for presence.

Specimen MHNM	Estimated TL (mm)	Eye lenses	Semicircular canals	Otoliths			Nasal plate	Palatoquadrate	Meckel's cartilage
				Saccular	Lagenar	Utricular			
03-94	4.5	■							
03-403	4.51	■		■	■				
01-260	5.5	■		■	■	■	■		
01-250	6.64	■		■			■		
03-843	6.79	■							
03-440	6.9	■		■	■				
03-1292	7.17	■	■	■	■		■		
03-440	7.29	■		■	■				
01-271	7.82	■		■	■				
03-403	8.12	■		■	■				
03-440	8.76	■		■					
01-275	9.14	■							
03-2729	9.94	■		■	■	■			
01-256	9.99	■		■	■				
03-1292	10.84	■	■	■	■		■		
01-253	11.4	■	■	■			■		
03-2684	12.71	■	■	■	■	■			
03-316	13.58	■	■	■	■		■		
01-230	13.6	■		■	■		■		
03-259	13.82	■	■	■					
03-622	14.1	■	■	■	■	■			
03-418	14.17	■		■	■				
03-1378	14.65	■					■		
01-230	15.1	■					■		

Continued on next page

Continued from previous page

Specimen MHNM	Estimated TL (mm)	Eye lenses	Semicircular canals	Otoliths			Nasal plate	Palatoquadrate	Meckel's cartilage
				Saccular	Lagenar	Utricular			
03-417	15.11	■		■	■				
03-1778	15.32	■	■	■	■	■	■		
03-2015	15.59	■	■	■	■	■	■		
03-890	15.67	■					■		
03-1515	15.98		■	■	■				
03-372	16.2	■	■	■	■				
03-1438	16.42	■	■	■					
03-2684	16.43	■	■	■	■	■			
03-1480	17.15	■	■	■					
03-398	17.2	■	■	■	■		■		
03-1204	17.22	■	■	■	■	■	■		
03-2756	17.47	■	■	■	■	■	■		
03-210	17.55	■	■	■	■	■			
03-1976	17.55	■	■	■	■	■	■		
03-319	17.58	■	■	■	■	■	■		
03-1897	17.7	■	■	■	■				
03-1408	17.9	■	■	■	■		■		
03-1252	18.1	■	■	■	■	■	■		
03-435	18.46	■	■	■	■		■		
03-654	18.55	■	■	■	■	■	■		
03-2033	18.86	■	■	■	■				
03-2001	18.91	■	■	■	■	■			
03-2015	19.2	■	■	■	■	■			
03-503	19.34	■	■	■	■		■		

Continued on next page

Continued from previous page

Specimen MHNM	Estimated TL (mm)	Eye lenses	Semicircular canals	Otoliths			Nasal plate	Palatoquadrate	Meckel's cartilage
				Saccular	Lagenar	Utricular			
03-1427	19.5	■	■	■	■	■	■		
03-1916	19.58	■	■	■	■				
03-2599	19.93	■	■	■	■	■	■		
03-1516	20.12	■	■	■	■		■		
03-401	20.14	■	■	■	■	■	■		
03-354	20.3	■	■	■	■				
03-1916	20.35	■	■	■	■	■	■		
03-1881	20.59	■	■	■	■	■	■		
03-1378	20.65	■					■		
03-1250	21.37	■	■	■	■	■	■		
03-433	21.55	■	■	■			■		
03-2684	21.57	■	■	■	■	■	■		
03-549	21.64	■	■	■	■				
03-978	21.64	■	■	■	■	■	■		
03-740	21.92	■	■	■	■	■			
03-531	22.43	■		■					
03-1961	22.48	■	■	■	■		■		
03-561	22.59	■	■	■	■	■	■		
03-1963	22.73		■						
03-1192	22.75	■	■	■	■	■			
03-2570	22.96	■	■	■	■		■		■
03-1515	23.15	■	■	■	■		■		
03-1205	23.47	■	■	■	■				
03-1833	23.75	■					■		
03-1962	23.79	■	■	■	■	■			
03-363	23.88	■							

Continued on next page

Continued from previous page

Specimen MHNM	Estimated TL (mm)	Eye lenses	Semicircular canals	Otoliths			Nasal plate	Palatoquadrate	Meckel's cartilage
				Saccular	Lagenar	Utricular			
03-1819	23.9	■	■	■	■				
03-813	23.9	■	■	■	■		■		
03-2480	24.05	■	■	■	■				
03-1236	24.25	■	■	■	■				
03-432	24.31	■	■	■	■	■			
03-2477	24.55	■	■	■	■	■	■		
03-916	24.7	■							
03-2483	24.86	■	■	■	■	■	■		
03-1985	24.93	■	■	■					
03-1509	24.95	■	■	■	■				
03-2440	25.12	■	■	■	■		■		
03-450	25.21	■	■	■	■				
03-558	25.3	■		■			■		
03-1879	25.3	■	■	■	■	■			
03-2629	25.51	■	■	■					
03-1847	25.53	■	■	■	■	■			
03-25	25.57							■	■
03-1100	25.88	■						■	
03-1311	25.97	■	■	■	■	■	■		
03-2660	25.97	■	■	■	■		■		
03-220	26.16	■	■	■					
03-2025	26.27	■	■	■	■	■	■		
03-1538	26.28	■	■	■	■		■		
03-78	26.52	■							
03-235	26.69	■	■	■					
03-2654	26.73	■	■	■	■				

Continued on next page

Continued from previous page

Specimen MHNM	Estimated TL (mm)	Eye lenses	Semicircular canals	Otoliths			Nasal plate	Palatoquadrate	Meckel's cartilage
				Saccular	Lagenar	Utricular			
03-695	26.87	■						■	■
03-108	27.58	■	■	■				■	■
03-1406	27.79	■		■					
03-2030	27.84	■	■						
03-2487	27.88	■	■	■	■				
03-369	27.96		■	■	■				
03-773	28.13	■	■	■					
03-1295	28.2	■	■	■	■				
03-1496	28.2	■	■	■	■				
03-2589	28.36	■	■	■					
03-2613	28.62	■							
03-1969	28.73	■	■	■					
03-1306	28.79		■	■	■				
03-123	29.13	■							
03-176	29.2	■		■	■	■			
03-2630	29.29	■	■						
03-867	29.34	■	■	■					
03-699	29.36	■	■	■					
03-1994	29.37	■	■	■	■				
03-164	29.47	■							
03-1051	29.49	■	■	■	■	■			
03-2025	29.57	■	■	■	■	■	■		
03-2612	29.63	■	■	■	■				
03-551	29.71	■	■	■					
03-1909	29.72	■	■	■					
03-336	29.87	■	■	■	■				

Continued on next page

Continued from previous page

Specimen MHNM	Estimated TL (mm)	Eye lenses	Semicircular canals	Otoliths			Nasal plate	Palatoquadrate	Meckel's cartilage
				Saccular	Lagenar	Utricular			
03-1687	30.24	■		■					
03-217	31.12	■	■	■					
03-868	31.17	■							■
03-716	31.34	■		■					
03-2631	31.47	■	■	■			■		
03-1008	31.53	■	■	■	■		■		
03-1314	31.64	■	■	■					
03-55	31.71	■		■					
03-2589	32.42		■	■					
03-1550	33.1	■	■	■	■				
03-701	33.18	■	■	■	■	■	■		
03-1533	33.29	■	■	■	■				
03-38	33.64	■	■	■				■	■
03-530	33.7								
03-2614	33.74	■	■						
03-1798	34.34	■	■	■	■				
03-723	34.48	■							
03-88	35.12	■	■	■					
03-2620	35.44			■					
03-597	35.6	■							■
03-570	35.75								
03-1083	35.92								
03-98	35.93	■	■	■	■			■	■
03-452	36.19	■							
03-1233	36.29								
03-1215	36.35		■	■					

Continued on next page

Continued from previous page

Specimen MHNM	Estimated TL (mm)	Eye lenses	Semicircular canals	Otoliths			Nasal plate	Palatoquadrate	Meckel's cartilage
				Saccular	Lagenar	Utricular			
03-1031	36.4	■	■						
03-933	36.41	■	■	■					
03-1731	37.11	■							
03-388	37.6	■		■					
03-1545	38.21	■	■	■	■	■			
03-525	38.3								
03-2719	38.41	■	■	■					
03-971	39.27	■	■	■					
03-584	39.31	■							
03-2621	40.8	■	■	■	■				■
03-534	40.98	■	■	■					
03-347	41.2	■							■
03-2637A	41.2		■	■					
03-2761	41.29		■						
03-198	42.5	■	■	■	■	■			
03-529	43.28								
03-528	43.6								
03-139	43.8	■							
03-58	44	■							
03-1497	45.29	■	■					■	■
03-715	45.8	■	■	■					
03-961	46.45								
03-1817	47.51								
03-1971	49.21								
03-2679	49.27	■	■					■	■
03-1107	52.72								

Continued on next page

Continued from previous page

Specimen MHNM	Estimated TL (mm)	Otic plates	Vertebral structures	Scapulo-coracoid	Body scales	Nasal bones	Sclerotic bones				Branchiostegal rays	
							Dorsal	Anterior	Posterior	Ventral	1	2
03-94	4.5		■								■	■
03-403	4.51											
01-260	5.5											
01-250	6.64											
03-843	6.79	■	■									
03-440	6.9	■	■									
03-1292	7.17		■									
03-440	7.29											
01-271	7.82											
03-403	8.12											
03-440	8.76		■	■								
01-275	9.14		■								■	
03-2729	9.94											
01-256	9.99			■								
03-1292	10.84											
01-253	11.4											
03-2684	12.71		■		■						■	
03-316	13.58		■		■						■	■
01-230	13.6	■			■							
03-259	13.82		■	■	■							
03-622	14.1		■		■						■	
03-418	14.17		■		■						■	■
03-1378	14.65		■		■						■	■
01-230	15.1		■		■						■	■

Continued on next page

Continued from previous page

Specimen MHNM	Estimated TL (mm)	Otic plates	Vertebral structures	Scapulo-coracoid	Body scales	Nasal bones	Sclerotic bones				Branchiostegal rays	
							Dorsal	Anterior	Posterior	Ventral	1	2
03-417	15.11		■		■						■	■
03-1778	15.32	■	■	■	■							
03-2015	15.59				■							
03-890	15.67		■		■							
03-1515	15.98		■		■							
03-372	16.2	■	■	■	■							
03-1438	16.42		■		■						■	■
03-2684	16.43	■	■		■						■	■
03-1480	17.15				■		■					
03-398	17.2				■							
03-1204	17.22		■		■							
03-2756	17.47		■	■	■		■					
03-210	17.55	■	■		■						■	
03-1976	17.55	■		■	■							
03-319	17.58		■		■						■	■
03-1897	17.7		■		■							
03-1408	17.9		■		■							
03-1252	18.1	■	■	■	■							
03-435	18.46				■		■				■	■
03-654	18.55		■		■							
03-2033	18.86		■		■						■	■
03-2001	18.91	■	■	■	■						■	
03-2015	19.2			■	■							
03-503	19.34				■						■	■

Continued on next page

Continued from previous page

Specimen MHNM	Estimated TL (mm)	Otic plates	Vertebral structures	Scapulo-coracoid	Body scales	Nasal bones	Sclerotic bones				Branchiostegal rays	
							Dorsal	Anterior	Posterior	Ventral	1	2
03-1427	19.5		■	■	■						■	■
03-1916	19.58				■							
03-2599	19.93				■						■	■
03-1516	20.12		■		■							
03-401	20.14		■		■						■	■
03-354	20.3				■							
03-1916	20.35		■	■	■							
03-1881	20.59	■		■	■							
03-1378	20.65		■	■	■							
03-1250	21.37		■	■	■						■	■
03-433	21.55		■	■	■							
03-2684	21.57	■		■	■						■	■
03-549	21.64		■		■		■				■	■
03-978	21.64	■	■		■							
03-740	21.92			■	■							
03-531	22.43		■	■	■		■				■	■
03-1961	22.48		■	■	■							
03-561	22.59				■							
03-1963	22.73			■	■							
03-1192	22.75		■		■							
03-2570	22.96		■	■	■						■	
03-1515	23.15				■						■	■
03-1205	23.47	■	■	■	■	■						
03-1833	23.75				■							
03-1962	23.79			■	■							
03-363	23.88		■	■	■	■	■					

Continued on next page

Continued from previous page

Specimen MHNM	Estimated TL (mm)	Otic plates	Vertebral structures	Scapulo-coracoid	Body scales	Nasal bones	Sclerotic bones				Branchiostegal rays	
							Dorsal	Anterior	Posterior	Ventral	1	2
03-1819	23.9		■	■	■						■	■
03-813	23.9	■	■		■							
03-2480	24.05			■	■							
03-1236	24.25	■	■		■						■	■
03-432	24.31		■	■	■							
03-2477	24.55		■	■	■							
03-916	24.7			■	■		■	■			■	■
03-2483	24.86		■	■	■							
03-1985	24.93			■	■							
03-1509	24.95				■	■	■				■	■
03-2440	25.12			■	■							
03-450	25.21		■		■							
03-558	25.3			■	■		■				■	■
03-1879	25.3		■		■						■	■
03-2629	25.51			■	■						■	■
03-1847	25.53	■	■		■							
03-25	25.57			■	■						■	■
03-1100	25.88			■	■	■	■				■	■
03-1311	25.97			■	■							
03-2660	25.97			■	■							
03-220	26.16			■	■	■					■	■
03-2025	26.27		■	■	■							
03-1538	26.28		■	■	■							
03-78	26.52				■						■	■
03-235	26.69			■	■		■	■	■		■	
03-2654	26.73	■	■		■							

Continued on next page

Continued from previous page

Specimen MHNM	Estimated TL (mm)	Otic plates	Vertebral structures	Scapulo-coracoid	Body scales	Nasal bones	Sclerotic bones				Branchiostegal rays	
							Dorsal	Anterior	Posterior	Ventral	1	2
03-695	26.87											
03-108	27.58											
03-1406	27.79											
03-2030	27.84											
03-2487	27.88											
03-369	27.96											
03-773	28.13											
03-1295	28.2											
03-1496	28.2											
03-2589	28.36											
03-2613	28.62											
03-1969	28.73											
03-1306	28.79											
03-123	29.13											
03-176	29.2											
03-2630	29.29											
03-867	29.34											
03-699	29.36											
03-1994	29.37											
03-164	29.47											
03-1051	29.49											
03-2025	29.57											
03-2612	29.63											
03-551	29.71											
03-1909	29.72											
03-336	29.87											

Continued on next page

Continued from previous page

Specimen MHNM	Estimated TL (mm)	Otic plates	Vertebral structures	Scapulo-coracoid	Body scales	Nasal bones	Sclerotic bones				Branchiostegal rays	
							Dorsal	Anterior	Posterior	Ventral	1	2
03-1687	30.24			■	■		■	■	■			
03-217	31.12			■	■	■	■	■			■	■
03-868	31.17			■	■	■	■	■	■	■	■	■
03-716	31.34			■	■	■	■	■	■		■	■
03-2631	31.47		■	■	■							
03-1008	31.53		■	■	■							
03-1314	31.64		■	■	■						■	
03-55	31.71			■	■	■	■				■	■
03-2589	32.42			■	■						■	■
03-1550	33.1			■	■	■						
03-701	33.18		■	■	■							
03-1533	33.29		■		■							
03-38	33.64			■	■	■	■				■	■
03-530	33.7			■	■		■	■	■		■	■
03-2614	33.74			■	■		■				■	■
03-1798	34.34			■	■							
03-723	34.48			■	■	■	■	■			■	■
03-88	35.12			■	■	■	■	■	■	■	■	■
03-2620	35.44			■	■	■					■	■
03-597	35.6			■	■	■	■	■	■		■	■
03-570	35.75				■							
03-1083	35.92				■							
03-98	35.93			■	■	■	■				■	■
03-452	36.19			■	■		■	■			■	■
03-1233	36.29			■	■							
03-1215	36.35			■	■						■	■

Continued on next page

Continued from previous page

Specimen MHNM	Estimated TL (mm)	Otic plates	Vertebral structures	Scapulo-coracoid	Body scales	Nasal bones	Sclerotic bones				Branchiostegal rays	
							Dorsal	Anterior	Posterior	Ventral	1	2
03-1031	36.4			■	■		■	■			■	■
03-933	36.41			■	■						■	■
03-1731	37.11			■	■	■	■	■	■			
03-388	37.6			■	■	■	■				■	■
03-1545	38.21			■	■	■						
03-525	38.3			■	■							
03-2719	38.41			■	■		■	■				
03-971	39.27			■	■		■				■	■
03-584	39.31			■	■	■					■	■
03-2621	40.8			■	■		■				■	■
03-534	40.98			■	■	■	■					
03-347	41.2			■	■	■	■	■	■		■	■
03-2637A	41.2			■	■							
03-2761	41.29			■	■	■					■	■
03-198	42.5			■	■		■	■				
03-529	43.28			■	■							
03-528	43.6			■	■						■	■
03-139	43.8	■		■	■							
03-58	44			■	■		■					
03-1497	45.29			■	■	■	■	■	■	■	■	■
03-715	45.8			■	■	■					■	■
03-961	46.45			■	■							
03-1817	47.51			■	■	■						
03-1971	49.21			■	■	■					■	■
03-2679	49.27			■	■	■	■	■	■	■	■	■
03-1107	52.72				■	■	■	■			■	■

Continued on next page

Continued from previous page

Specimen MHNM	Estimated TL (mm)	Branchiostegal rays										Supra-orbital sc	Sub-orbital sc
		3	4	5	6	7	8	9	10	11	12		
03-94	4.5												
03-403	4.51												
01-260	5.5												
01-250	6.64												
03-843	6.79												
03-440	6.9												
03-1292	7.17												
03-440	7.29												
01-271	7.82												
03-403	8.12												
03-440	8.76												
01-275	9.14												
03-2729	9.94												
01-256	9.99												
03-1292	10.84												
01-253	11.4												
03-2684	12.71												
03-316	13.58												
01-230	13.6												
03-259	13.82												
03-622	14.1												
03-418	14.17												
03-1378	14.65												
01-230	15.1												

Continued on next page

Continued from previous page

Specimen MHNM	Estimated TL (mm)	Branchiostegal rays										Supra-orbital sc	Sub-orbital sc
		3	4	5	6	7	8	9	10	11	12		
03-417	15.11												
03-1778	15.32												
03-2015	15.59												
03-890	15.67												
03-1515	15.98												
03-372	16.2												
03-1438	16.42												
03-2684	16.43												
03-1480	17.15												
03-398	17.2												
03-1204	17.22												
03-2756	17.47												
03-210	17.55												
03-1976	17.55												
03-319	17.58												
03-1897	17.7												
03-1408	17.9												
03-1252	18.1												
03-435	18.46												
03-654	18.55												
03-2033	18.86												
03-2001	18.91												
03-2015	19.2												
03-503	19.34												

Continued on next page

Continued from previous page

Specimen MHNM	Estimated TL (mm)	Branchiostegal rays										Supra-orbital sc	Sub-orbital sc
		3	4	5	6	7	8	9	10	11	12		
03-1427	19.5												
03-1916	19.58												
03-2599	19.93												
03-1516	20.12												
03-401	20.14												
03-354	20.3												
03-1916	20.35												
03-1881	20.59												
03-1378	20.65												
03-1250	21.37												
03-433	21.55												
03-2684	21.57												
03-549	21.64												
03-978	21.64												
03-740	21.92												
03-531	22.43												
03-1961	22.48												
03-561	22.59												
03-1963	22.73												
03-1192	22.75												
03-2570	22.96												
03-1515	23.15												
03-1205	23.47												
03-1833	23.75												
03-1962	23.79												
03-363	23.88												

Continued on next page

Continued from previous page

Specimen MHNM	Estimated TL (mm)	Branchiostegal rays										Supra-orbital sc	Sub-orbital sc
		3	4	5	6	7	8	9	10	11	12		
03-1819	23.9	■											
03-813	23.9												
03-2480	24.05												
03-1236	24.25												
03-432	24.31												
03-2477	24.55												
03-916	24.7	■	■	■	■	■							
03-2483	24.86												
03-1985	24.93												
03-1509	24.95	■	■	■	■	■	■	■	■	■	■		
03-2440	25.12												
03-450	25.21												
03-558	25.3												
03-1879	25.3												
03-2629	25.51	■	■	■	■	■	■						
03-1847	25.53												
03-25	25.57	■	■	■									
03-1100	25.88	■	■	■	■	■	■	■	■			■	
03-1311	25.97												
03-2660	25.97												
03-220	26.16	■	■	■									
03-2025	26.27												
03-1538	26.28												
03-78	26.52	■	■	■	■	■	■	■	■	■	■		
03-235	26.69												
03-2654	26.73												

Continued on next page

Continued from previous page

Specimen MHNM	Estimated TL (mm)	Branchiostegal rays										Supra-orbital sc	Sub-orbital sc
		3	4	5	6	7	8	9	10	11	12		
03-695	26.87	■	■	■									
03-108	27.58												
03-1406	27.79	■	■	■	■	■						■	
03-2030	27.84	■	■	■	■	■	■	■	■	■	■		
03-2487	27.88												
03-369	27.96	■	■									■	
03-773	28.13												
03-1295	28.2	■	■	■	■	■	■						
03-1496	28.2	■	■	■	■	■	■	■	■	■	■	■	
03-2589	28.36												
03-2613	28.62	■	■	■	■	■							
03-1969	28.73	■	■										
03-1306	28.79	■	■	■	■	■	■						
03-123	29.13												
03-176	29.2												
03-2630	29.29	■	■	■	■	■	■						
03-867	29.34											■	
03-699	29.36											■	
03-1994	29.37												
03-164	29.47												
03-1051	29.49	■	■	■	■	■	■	■	■	■	■		
03-2025	29.57												
03-2612	29.63												
03-551	29.71	■	■	■	■	■	■					■	
03-1909	29.72												
03-336	29.87	■	■	■	■								

Continued on next page

Continued from previous page

Specimen MHNM	Estimated TL (mm)	Branchiostegal rays										Supra-orbital sc	Sub-orbital sc
		3	4	5	6	7	8	9	10	11	12		
03-1687	30.24	■	■	■	■								
03-217	31.12											■	
03-868	31.17	■	■	■								■	
03-716	31.34	■	■	■	■	■	■	■	■	■	■		
03-2631	31.47	■	■	■	■	■	■	■	■				
03-1008	31.53												
03-1314	31.64												
03-55	31.71											■	
03-2589	32.42	■											
03-1550	33.1	■	■	■	■	■	■						
03-701	33.18												
03-1533	33.29												
03-38	33.64											■	
03-530	33.7	■	■	■	■	■	■	■					
03-2614	33.74	■	■									■	
03-1798	34.34	■	■	■									
03-723	34.48											■	
03-88	35.12	■	■	■	■	■	■					■	
03-2620	35.44	■											
03-597	35.6	■	■	■	■	■						■	
03-570	35.75	■	■	■	■	■	■	■	■	■			
03-1083	35.92												
03-98	35.93											■	
03-452	36.19	■	■	■	■								
03-1233	36.29	■	■	■	■	■	■						
03-1215	36.35											■	

Continued on next page

Continued from previous page

Specimen MHNM	Estimated TL (mm)	Branchiostegal rays										Supra-orbital sc	Sub-orbital sc
		3	4	5	6	7	8	9	10	11	12		
03-1031	36.4	■	■	■	■	■	■	■				■	
03-933	36.41	■	■	■									
03-1731	37.11												
03-388	37.6	■	■	■								■	
03-1545	38.21											■	
03-525	38.3												
03-2719	38.41												
03-971	39.27	■	■	■	■	■	■	■	■	■		■	■
03-584	39.31	■										■	
03-2621	40.8	■	■	■								■	
03-534	40.98											■	
03-347	41.2	■	■	■	■							■	
03-2637A	41.2												
03-2761	41.29	■	■	■	■	■							
03-198	42.5												
03-529	43.28												
03-528	43.6	■	■	■	■							■	
03-139	43.8												
03-58	44												
03-1497	45.29	■	■	■	■	■	■	■	■	■			■
03-715	45.8	■	■	■	■	■	■	■	■	■		■	
03-961	46.45												
03-1817	47.51												
03-1971	49.21	■											
03-2679	49.27	■	■	■	■	■	■	■	■	■	■	■	
03-1107	52.72	■	■	■	■	■						■	

Continued on next page

Continued from previous page

Specimen MHNM	Estimated TL (mm)	Profundus scales	Otic scales	Otic comm. sc	Pectoral spines	Interm. spines	Pelvic spines	Pelvic scales	Anal spine	Anal scales	Dorsal spine	Dorsal scales	Hypoch. scales
03-94	4.5												
03-403	4.51												
01-260	5.5												
01-250	6.64												
03-843	6.79				■						■		
03-440	6.9				■				■		■		
03-1292	7.17												
03-440	7.29								■		■		
01-271	7.82												
03-403	8.12												
03-440	8.76				■				■		■		
01-275	9.14				■				■		■		
03-2729	9.94				■				■		■		
01-256	9.99				■						■		
03-1292	10.84										■		
01-253	11.4												
03-2684	12.71										■		
03-316	13.58				■		■		■		■		
01-230	13.6												
03-259	13.82				■		■				■	■	
03-622	14.1						■		■				■
03-418	14.17				■								
03-1378	14.65												
01-230	15.1								■				

Continued on next page

Continued from previous page

Specimen MHNM	Estimated TL (mm)	Profundus scales	Otic scales	Otic comm. sc	Pectoral spines	Interm. spines	Pelvic spines	Pelvic scales	Anal spine	Anal scales	Dorsal spine	Dorsal scales	Hypoch. scales
03-417	15.11				■				■				
03-1778	15.32												
03-2015	15.59				■								
03-890	15.67						■		■		■		■
03-1515	15.98				■						■		
03-372	16.2				■		■		■		■	■	
03-1438	16.42				■				■				
03-2684	16.43												
03-1480	17.15				■		■		■		■		■
03-398	17.2				■		■						■
03-1204	17.22				■		■						
03-2756	17.47				■		■		■				
03-210	17.55				■		■		■		■		■
03-1976	17.55				■								
03-319	17.58				■						■		
03-1897	17.7												
03-1408	17.9				■				■		■		
03-1252	18.1				■		■		■		■		
03-435	18.46				■		■		■		■		
03-654	18.55				■		■						■
03-2033	18.86				■		■		■		■		
03-2001	18.91				■				■		■		
03-2015	19.2				■		■		■		■		■
03-503	19.34						■		■		■		■

Continued on next page

Continued from previous page

Specimen MHNM	Estimated TL (mm)	Profundus scales	Otic scales	Otic comm. sc	Pectoral spines	Interm. spines	Pelvic spines	Pelvic scales	Anal spine	Anal scales	Dorsal spine	Dorsal scales	Hypoch. scales
03-1427	19.5				■		■		■		■		
03-1916	19.58				■							■	
03-2599	19.93										■		■
03-1516	20.12				■		■		■		■	■	■
03-401	20.14						■		■		■		
03-354	20.3				■				■		■		
03-1916	20.35				■		■				■		
03-1881	20.59				■		■		■		■	■	
03-1378	20.65				■		■		■				
03-1250	21.37				■		■		■		■	■	■
03-433	21.55				■				■		■	■	
03-2684	21.57				■		■		■				■
03-549	21.64				■				■		■		■
03-978	21.64				■		■		■		■		
03-740	21.92				■	■	■		■		■		■
03-531	22.43				■		■		■		■	■	■
03-1961	22.48				■	■	■				■		
03-561	22.59				■		■		■				
03-1963	22.73				■						■		
03-1192	22.75				■	■	■		■		■		■
03-2570	22.96				■	■	■		■		■		■
03-1515	23.15				■								■
03-1205	23.47								■		■		
03-1833	23.75				■				■		■		
03-1962	23.79				■	■	■		■		■		
03-363	23.88				■		■		■		■		■

Continued on next page

Continued from previous page

Specimen MHNM	Estimated TL (mm)	Profundus scales	Otic scales	Otic comm. sc	Pectoral spines	Interm. spines	Pelvic spines	Pelvic scales	Anal spine	Anal scales	Dorsal spine	Dorsal scales	Hypoch. scales
03-1819	23.9						■		■		■		
03-813	23.9				■		■						
03-2480	24.05				■		■		■				
03-1236	24.25				■		■		■		■		
03-432	24.31				■		■		■		■	■	■
03-2477	24.55				■		■		■		■		■
03-916	24.7				■						■		■
03-2483	24.86				■		■		■				■
03-1985	24.93				■		■		■				■
03-1509	24.95				■		■						■
03-2440	25.12				■		■						
03-450	25.21				■		■		■		■		
03-558	25.3				■		■		■		■	■	■
03-1879	25.3				■		■		■		■		
03-2629	25.51				■		■		■		■		■
03-1847	25.53				■		■		■				
03-25	25.57				■		■	■	■	■	■	■	
03-1100	25.88				■		■		■		■	■	■
03-1311	25.97				■	■	■		■		■		■
03-2660	25.97				■		■		■				■
03-220	26.16				■		■	■		■	■	■	■
03-2025	26.27				■	■	■		■		■		
03-1538	26.28				■		■		■		■		
03-78	26.52				■		■		■				■
03-235	26.69				■	■	■		■		■		
03-2654	26.73						■		■		■		■

Continued on next page

Continued from previous page

Specimen MHNM	Estimated TL (mm)	Profundus scales	Otic scales	Otic comm. sc	Pectoral spines	Interm. spines	Pelvic spines	Pelvic scales	Anal spine	Anal scales	Dorsal spine	Dorsal scales	Hypoch. scales
03-695	26.87												
03-108	27.58												
03-1406	27.79												
03-2030	27.84												
03-2487	27.88												
03-369	27.96												
03-773	28.13												
03-1295	28.2												
03-1496	28.2												
03-2589	28.36												
03-2613	28.62												
03-1969	28.73												
03-1306	28.79												
03-123	29.13												
03-176	29.2												
03-2630	29.29												
03-867	29.34												
03-699	29.36												
03-1994	29.37												
03-164	29.47												
03-1051	29.49												
03-2025	29.57												
03-2612	29.63												
03-551	29.71												
03-1909	29.72												
03-336	29.87												

Continued on next page

Continued from previous page

n MHNM	Estimated TL (mm)	Profundus scales	Otic scales	Otic comm. sc	Pectoral spines	Interm. spines	Pelvic spines	Pelvic scales	Anal spine	Anal scales	Dorsal spine	Dorsal scales	Hypoch. scales
03-1687	30.24												
03-217	31.12												
03-868	31.17												
03-716	31.34												
03-2631	31.47												
03-1008	31.53												
03-1314	31.64												
03-55	31.71												
03-2589	32.42												
03-1550	33.1												
03-701	33.18												
03-1533	33.29												
03-38	33.64												
03-530	33.7												
03-2614	33.74												
03-1798	34.34												
03-723	34.48												
03-88	35.12												
03-2620	35.44												
03-597	35.6												
03-570	35.75												
03-1083	35.92												
03-98	35.93												
03-452	36.19												
03-1233	36.29												
03-1215	36.35												

Continued on next page

Continued from previous page

Specimen MHNM	Estimated TL (mm)	Profundus scales	Otic scales	Otic comm. sc	Pectoral spines	Interm. spines	Pelvic spines	Pelvic scales	Anal spine	Anal scales	Dorsal spine	Dorsal scales	Hypoch. scales
03-1031	36.4				■		■	■	■	■	■	■	■
03-933	36.41				■		■		■	■	■	■	
03-1731	37.11				■	■	■		■		■		
03-388	37.6				■		■				■	■	
03-1545	38.21				■	■	■		■		■		■
03-525	38.3				■		■	■	■	■	■		■
03-2719	38.41				■	■	■				■		■
03-971	39.27				■		■	■	■	■	■	■	
03-584	39.31	■			■		■		■			■	
03-2621	40.8				■		■		■	■	■	■	
03-534	40.98				■	■	■		■	■	■		■
03-347	41.2		■	■	■		■		■			■	
03-2637A	41.2				■	■	■		■		■		■
03-2761	41.29				■		■	■	■	■	■	■	■
03-198	42.5				■	■	■		■		■		■
03-529	43.28				■		■		■				■
03-528	43.6				■		■		■		■	■	■
03-139	43.8				■	■	■		■		■		
03-58	44				■				■		■		■
03-1497	45.29				■		■		■		■	■	■
03-715	45.8		■		■		■		■		■	■	■
03-961	46.45				■		■		■	■	■		
03-1817	47.51				■		■		■				■
03-1971	49.21				■		■		■		■	■	■
03-2679	49.27		■		■							■	
03-1107	52.72				■		■				■	■	

Continued on next page

Continued from previous page

	Eye lenses	Semi-circular canals	Otoliths			Nasal plates	Palatoquadrate	Meckel's cartilage
			Saccular	Lagenar	Utricular			
Observed	157	119	133	93	41	51	12	8
Expected	178	172	177	177	176	176	110	88
RE (%)	**88.2**	**69.19**	**75.14**	**52.54**	23.30	28.98	10.1	9.09
Max. Gap	3	7	5	7	19	24	26	36
Position	end	early	late	middle	end	middle	middle	middle
TL 1st appearance (mm)	4.5	7.17	4.51	4.51	5.5	5.5	22.96	25.57

	Otic plates	Vertebral structures	Scapulo-coracoid	Body scales	Nasal bones	Sclerotic bones				Branchiostegal rays	
						Dorsal	Anterior	Posterior	Ventral	1	2
Observed	2	63	112	162	36	50	26	13	4	85	77
Expected	18	178	168	162	108	146	98	80	50	178	178
RE (%)	11.11	35.39	**66.67**	**100**	33.33	34.25	26.53	16.25	8	47.75	43.26
Max. Gap	11	40	6	NA	9	17	17	9	27	10	16
Position	late	late	early	NA	early	early	early	early	late	early	early
TL 1st appearance (mm)	39.31	4.5	8.76	12.71	23.47	17.15	24.7	26.69	31.17	4.5	4.5

Continued on next page

Continued from previous page

	Branchiostegal rays										Supra-orbital sc	Infra-orbital sc
	3	4	5	6	7	8	9	10	11	12		
Observed	63	49	45	36	32	23	15	13	11	7	29	2
Expected	157	148	140	136	136	95	95	95	95	95	87	18
RE (%)	40.13	33.11	32.14	26.47	23.53	24.21	15.79	13.68	11.58	7.37	33.33	11.11
Max. Gap	10	22	22	22	22	11	11	15	16	47	10	11
Position	early	middle	middle	early	early	late	late	middle	middle	end	middle	late
TL 1st appearance (mm)	14.17	16.42	17.58	18.46	18.46	24.95	24.95	24.95	24.95	24.95	25.88	39.31

	Profundus scales	Otic scales	Otic comm. scales	Pectoral spines	Interm. spines	Pelvic spines	Pelvic scales	Anal spine	Anal scales	Dorsal spine	Dorsal scales	Hypoch. scales
Observed	1	5	2	148	35	127	13	133	23	123	34	88
Expected	18	55	55	174	116	161	88	173	88	174	159	158
RE (%)	5.56	9.09	3.64	**85.06**	30.17	**78.88**	14.77	**76.88**	26.14	**70.69**	21.38	**55.7**
Max. Gap	NA	33	39	5	18	6	16	4	12	7	19	6
Position	NA	middle	middle	early	middle	early	middle	early	middle	early	early	early
TL 1st appearance (mm)	39.31	29.71	29.71	6.79	21.92	13.58	25.57	6.9	25.57	6.79	13.82	14.1

ANNEXE XXVI

RELIABILITY INDEX

Inter-individual variation in developmental sequence (*i.e.*, timing and order of appearance of events) has been reported in developmental sequences of living organisms (Colbert and Rowe, 2008; de Jong et al., 2009; Maxwell, 2008; Fischer-Rousseau et al., 2009). Here, we developed a reliability estimate (RE) which is calculated for each event rather than for the complete sequence because non-developmental sources of variation have the potential to be included in fossilized ontogenies (*e.g.*, taphonomic alteration). Departure from the expected occurrence of skeletal events within a growth series owing to inter-individual growth difference has been designate as disparity by dividing the total number of non-occurrences of events after their initial appearance by the total number of occurrences for all events (Maisano, 2002). The RE is calculated for each structure by dividing the actual number of specimens having an anatomical structure by the number of specimens expected to have this structure [*i.e.*, number of specimens longer (in terms of TL) than the smallest specimen that displays the structure] (Annexe XXV). Four parameters are calculated for each structure forming a sequence : (1) the actual number of specimens in which a structure has been observed ; (2) the expected number of specimens in which the structure should be present ; and the maximal gap in the sequence in terms of (3) the number of specimens lacking the structure, and (4) the difference in TL [*i.e.*, number of specimens longer (in terms of TL) than the smallest

specimen that displays the structure] (Annexe XXV). Only the specimens for which the parts are preserved are taken into account in these four parameters. A high RE (> 50%) means that many specimens expected to have a structure do have it and that the variation for this structure is low. A low RE (< 50%) suggests the sample might be less reliable for this structure, especially when there is an important gap in the early part of the ontogenetic sequence.

ANNEXE XXVII

RAW DATA (IN PERCENTAGE OF WEIGHT) FROM EDS X-RAY ANALYSES IN *TRIAZEUGACANTHUS AFFINIS*

Data for each skeletal structures is recorded from the mean of several punctual spectra (Spectra #) and given in percentage of the total weight of the sample. Traces include elements which are not implied in the biomineral but are present in the SEM chamber as the EDS Xray is an environmental one or are remains of sedimentary matrix.

		C	O	Ca	P	F	Traces	Spectra #
MHNM 03-440 2	Head structures	59.46	34.93				5.71	2
	Otoliths	15.98	61.72	13.73			8.57	2
	Scapula	16.22	44.9	19.02	8.72	2.85	8.29	5
	Pectoral spine	16.98	43.37	19.47	9.88	5.54	4.76	2
	Vertebral structures	59.23	29.24	5.17			6.36	1
MHNM 03-440 2	Head structures	66.49	21.34	1.12			1.05	2
	Otoliths	15.95	56.25	23.65			4.15	2
MHNM 03-398 sc	Endoskeleton	21.66	16.98	56.41			4.95	1
	Scale inner layer	36.06	20.15	34.03	5.72		4.04	2
	Scale outer layer	42.04	19.89	32.03	2.63		3.41	1

Continued on next page

Continued from previous page

		C	O	Ca	P	F	Traces	Spectra #
	Scale surface	33.76	21	38.11	3.51		3.62	1
MHNM 03-398An	Vascular cavity	32.59	18.89	45.50			1.02	1
	Endoskeleton	31.63	16.84	48.65			2.88	2
MHNM 03-398An	Spine outer layer	40.03	13.06	39.45	1.29		6.17	1
	Spine piece	39.14	15.77	39.45	3.11		2.53	1
	Spine inner layer	36.7	17.05	38.01	3.09		5.15	3
MHNM 03-1497	Sclerotic bone	22.02	41.72	20.40	9.89	3.67	2.3	1
	Palatoquadrate	25.82	42.08	16.40	9.26	6.17	0.27	2
	Branchiostegal rays	27.42	43.11	13.72	7.54	6.32	1.89	2
	Scapula	11.10	50.19	20.74	10.02	6.26	1.69	3
	Pectoral spine	28.68	45.25	12.65	6.77	4.68	1.97	3
	Scales	13.10	47.99	20.03	8.75	7.95	2.18	4

ANNEXE XXVIII

TRIAZEUGACANTHUS LATERAL LINE CANAL AND SCALES

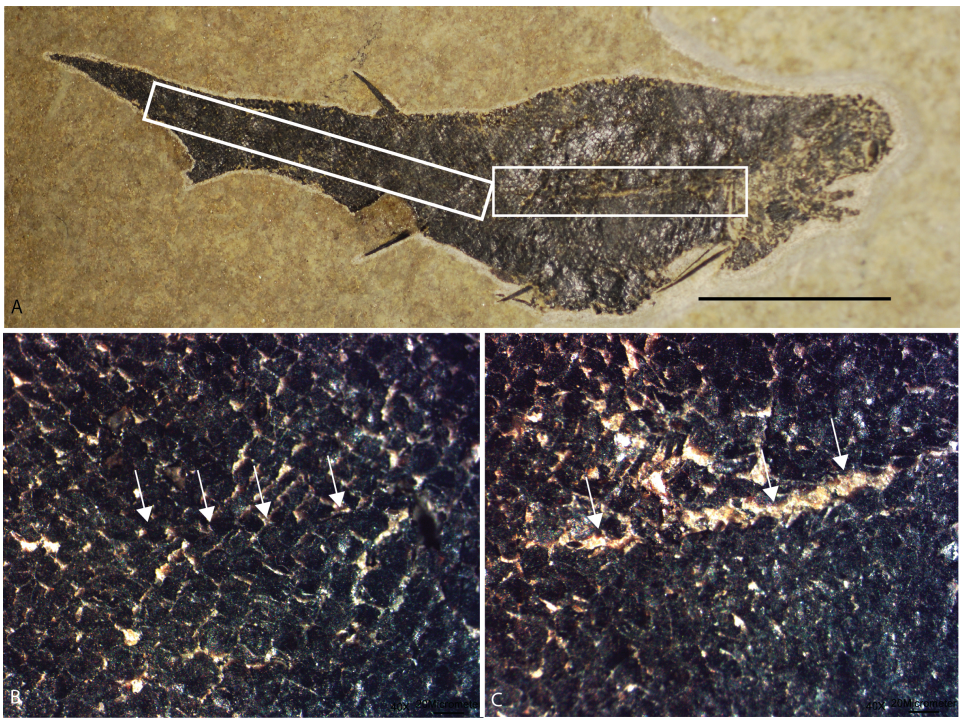

MHNM 03-1497 A. Anterior and posterior portion of the lateral line canal, morphologically different concerning the arrangement of scales. Anterior rectangle : gap between the rows of scales surrounding the lateral line. Posterior rectangle : no such a gap. B. Close-up of the posterior region. C. Close-up of the anterior region. Arrows indicate the position of the lateral line canal. Scale bar = 10 mm.

ANNEXE XXIX

PELVIC, ANAL AND DORSAL FIN WEBS IN *TRIAZEUGACANTHUS*

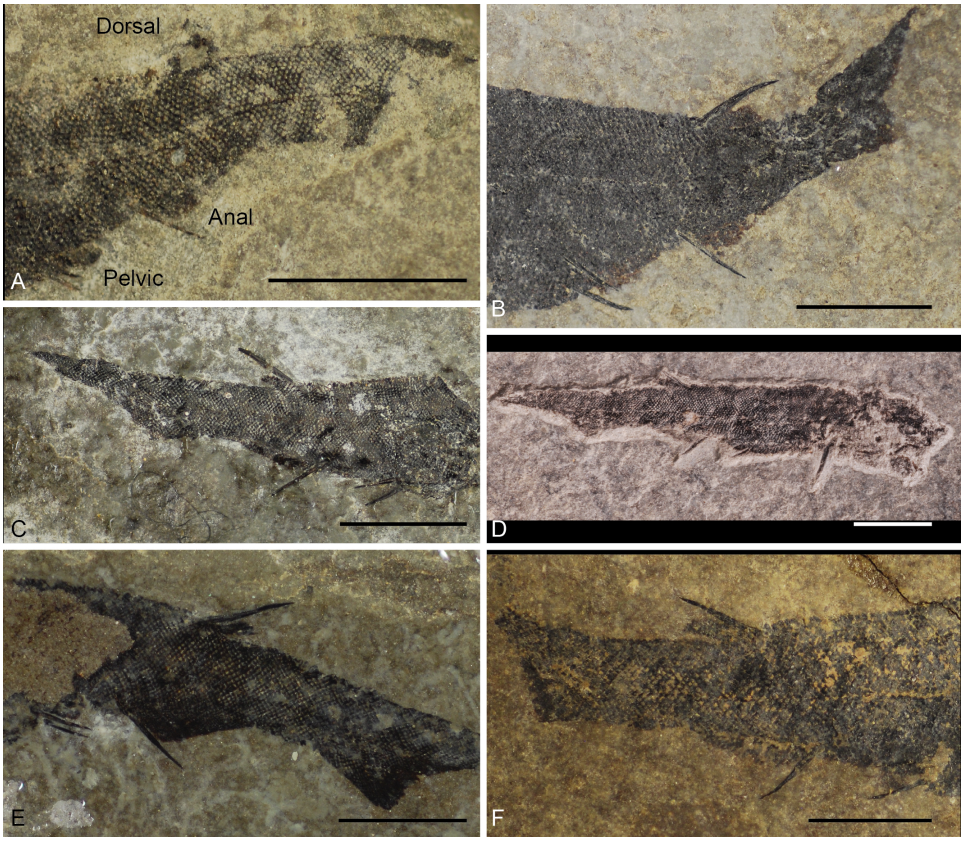

(A) MHNM 03-25. (B) MHNM 03-867. (C) MHNM 03-220. (D) MHNM 03-2589 2. (E) MHNM 03-525. (F) MHNM 03-2761. Scale bars = 5 mm.

ANNEXE XXX

ELONGATION RATIO IN VARIOUS CHONDRICHTHYAN SPECIES

Length and depth of chondrichthyan species collected from Wyffels (2009)

Species	Stage	Length (mm)	Depth (mm)	Elongation ratio
Squalus acanthias	Embryo	120	13.8	8.7
	Juvenile	230	24.3	9.5
	Adult	1010	110	9.1
Lamna nasus	Embryo	394	59	6.7
	Juvenile	580	125	4.6
	Adult	840	190	4.4
Carcharias taurus	Embryo	131	17	7.7
	Juvenile	271	43	6.3
	Adult	1110	170	6.5
Callorhinchus milii	Embryo	75	7.1	10.7
	Embryo	105	12	8.7
	Juvenile	133	24	5.5
	Adult	920	137	6.7

ANNEXE XXXI

RAW DATA FOR RELIABILITY INDEX CALCULATION IN *LODEACANTHUS GAUJICUS*

Data from Upeniece (2011). White is for absence. Grey is for presence.

Specimen ID LDM	*Estimated TL (mm)*	*Scapula*	*Endo-cranium*	*Jaws*	*Branch arches*	*Branch rays*	*Sclerotic bones*	*Nasals*	*Cheek bones*	*Tesserae*	*Trunk SL*	*Head SL*
270/45	8	■				■						
270/28	13.6	■	■			■	■	■	■			
270/25	19.6					■					■	
270/22	20.5	■	■			■	■	■	■		■	■
270/23	20.6	■				■	■		■		■	■
270/3	20.8	■	■			■	■		■		■	■
270/12	23	■				■	■	■	■	■	■	■
270/37	25	■		■		■	■	■		■	■	■
270/2	NA	■		■	■	■	■	■		■		
270/19	34.7	■		■		■	■	■	■	■		
270/38	37.6	■	■	■		■	■		■	■	■	
270/41	38.3	■	■	■		■	■	■	■	■		
270/9	38.9	■	■	■		■			■			

Continued on next page

Continued from previous page

Specimen ID LDM		*Scapula*	*Endo-cranium*	*Jaws*	*Branch arches*	*Branch rays*	*Sclerotic bones*	*Nasals*	*Cheek bones*	*Tesserae*	*Trunk SL*	*Head SL*
270/14	NA											
Observed		13	10	7	2	14	11	7	9	7	7	5
Expected		14	13	14	6	14	13	13	13	8	12	11
RE (%)		92.86	76.92	50	33.33	100	84.62	53.85	69.23	87.5	58.33	45.45
Max. Gap		1	1	0	4	0	1	2	2	1	3	6
Position		early	early		late			early and late	middle	late	late	late
TL 1st appearance (mm)		8	13.6	25	?	8	13.6	13.6	13.6	23	19.6	20.5

ANNEXE XXXII

PAIRED FINS AND AXIAL SKELETON

Distinction between fin rays and fin radials

Fin rays are defined as the structures internally strengthening and supporting the fins (Francillon Vieillot et al., 1990; Arratia et al., 2001; Witten and Huysseune, 2007). Fin rays can consist of cartilaginous, mineralized and osseous tissues. Four kinds of fin rays have been described to date. Lepidotrichia, present in actinopterygians and sarcopterygians with the exception of dipnoans, are flexible rays composed of mineralized hemisegments connected by ligaments (Francillon Vieillot et al., 1990; Witten and Huysseune, 2007). The distal ends are dichotomously branched. Actinotrichia are present between the most distal hemisegments of the lepidotrichia. Actinotrichia consists of short, tapered cartilaginous rods that are generally distally branched (Francillon Vieillot et al., 1990; Witten and Huysseune, 2007). Ceratotrichia are flexible, unsegmented cartilaginous rods present in the fins of chondrichthyans. Those fin rays are longer and thicker than actinotrichia and are usually branched distally (Kemp, 1977; Geraudie and Meunier, 1982; Francillon Vieillot et al., 1990). Lastly, camptotrichia, present only in dipnoans, consist of straight cylindrical rods arranged in two asymmetrical rows (Geraudie and Meunier, 1982; Arratia et al., 2001). This kind of fin ray is usually dichotomous at the margin and is composed of acellular fibrous tissues and

mineralized bones (Arratia et al., 2001).

In *Euphanerops*, we observed both fin radials and rays in the paired anteroventral and anal fins. The fin radials are described as proximal cartilaginous (composed of spherulic chondrocytes) endoskeletal elements whereas the fin rays are more distal, and composed of stacked chondrocytes (main text Figure 32 and Annexes XXXIII and XXXIV). Previous interpretations of *Euphanerops* called the fin distal elements 'radials' because of the homology with "Radii pterygiales" of lamprey (Marinelli and Strenger, 1954). But even in lamprey, the dorsal fin distal elements are bifurcating and composed of stacked chondrocytes (Annexe XXXVi). Despite the terms that have been used in previous studies (*i.e.*, fin radials) (Goodrich, 1958; Janvier and Arsenault, 2007; Sansom et al., 2013b) we use the term fin ray for lampreys and *Euphanerops* in the present study.

Multiple or elongate paired ventral fins

In Annexe XXXV d, we proposed a reconstruction of *Euphanerops* MHNM 01-123 paired ventral fins. These fins are composed of basal (radials) and distal (rays) elements. One unit is composed of one radial, one meso- or metapterygium-like structure and several (more than four or five, but the number is difficult to determine) fin rays (Annexe XXXV). Because we observed more than one ray per radial, and the fins are formed as repetitive anatomical units, we proposed that instead of having a unique ventral fin on each side of the body (Janvier and Arsenault, 2007), *Euphanerops* could display multiple ventral fins [that could be arranged along the body in a manner comparable to acanthodian intermediate or pre-pelvic spines (Wilson et al., 2007)]. Currently, we cannot distinguish between these two hypotheses.

Axial skeleton

In the caudal region of *Petromyzon marinus*, chondrocytes form irregular agglomerates of cartilages dorsolaterally to the notochord (Figure 33 a-d). These cartilaginous elements are proposed to correspond to **notochordal cartilages** or dorsolateral cartilages. Histological sections on an adult revealed the presence of two dorsolateral rods positioned dorsally to the notochord and encompassing both sides of the neural tube (Figure 33 b-d); such notochordal cartilage has never been described in lampreys before. The dorsolateral rods are fused to the ventral parts of the dorsomedian rod, thus forming a continuous arch encompassing the neural tube. Surprisingly, this notochordal cartilage was also observed in the posteriormost region of ammocoetes (*i.e.*, small amounts of chondrocytes dorsally to the notochord in the posteriormost region of the caudal fin), indicating that chondrogenesis for this cartilage has occurred in earlier stages of development. However, whether these chondrocytes are the results of a notochordal chondrogenesis or the result of the extension of the dorsomedian rod is not clear.

Arcualia are defined as the primary cartilaginous elements forming dorsally along the notochord in vertebrates (Parker, 1883; Arratia et al., 2001). During embryonic development, the first mesenchymal cells gather around the notochord, forming discrete blocks of cartilage (Arratia et al., 2001). These structures, mainly formed of hyaline cartilage, develop into neural arches in derived groups of fishes (Arratia et al., 2001; Grotmol et al., 2003, 2006). This term is also used to designate the dorsal vertebral elements in the Petromyzontiformes (Damas, 1944; Janvier, 2003; Richardson et al., 2010; Renaud, 2011).

In *Petromyzon marinus*, the development of arcualia was categorized in terms of their position along the body axis (main text Figure 33 a, Annexe XXXVII). Two centres of development of arcualia have been recorded. The first centre of development is located in the branchial region where the arcualia developed antero-posteriorly. The number of

arcualia formed in this region varied from 6 to 12 regardless of the metamorphosing stage. We also observed that arcualia decreased in size posteriorly along this region (Figure 33 e). The morphology of the first arcualium is distinctive from the others ; it is noticeably larger and its distal extremity is always bifid rather than undivided. The second centre is located in the second dorsal region where the arcualia developed bidirectionally (Figure 33 e).

In adults, the first 7-8 arcualia located in the branchial region were always the largest and the most developed. Besides the size and the typical 'hook'-shape, the general morphology of arcualia in the branchial region is variable (Figure 33 e). The distal extremity is either undivided, bifurcated or trifurcated ; it can either point anteriorly or posteriorly. The proximal base of the arcualia is generally well rounded and perforated, as observed previously in metamorphosing specimens. No arcualia was present in the terminal section of the caudal region. Unlike the trunk region, the caudal region contains arcualia with variable morphologies. Caudal region (Annexe XXXVII) is composed of arcualia with a great variation of size and shape, in addition to being irregularly spaced along the notochord (Figure 33 e).

We defined the **mediodorsal vertebral elements** as the cartilaginous structures inward of the arcualia and sitting dorsally on the notochord (Figure 33 e, mde). The shape of the mediodorsal vertebral elements is either elongated, short, crumpled, notched or twisted. Their size varies as being the same height as the arcualia, whereas other elements are small, stocky and barely visible along the notochord. These elements were present only in the branchial region, developing anteroposteriorly, mostly interspersed between the third to the seventh arcualia. Some specimens possessed two mediodorsal vertebral elements between two consecutive arcualia.

ANNEXE XXXIII

EUPHANEROPS LONGAEVUS, IMMATURE SPECIMENS

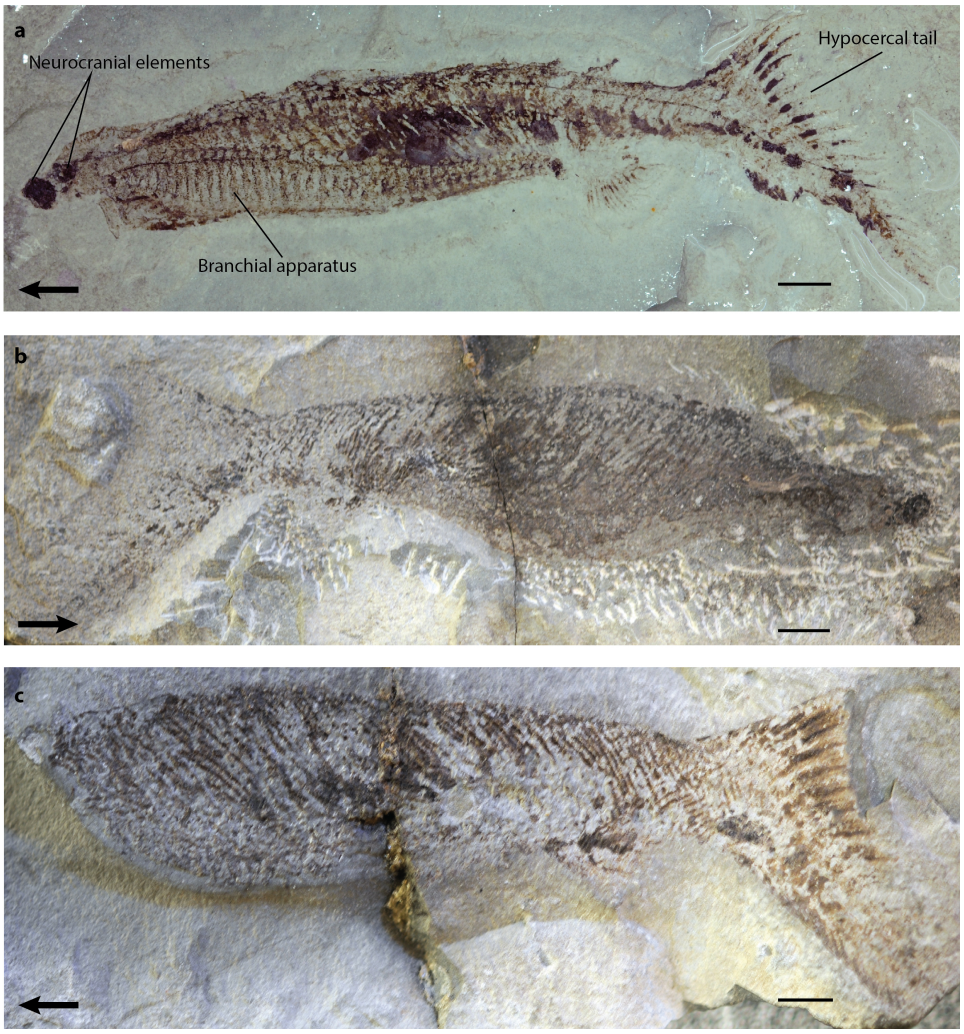

a. MHNM 01-02A, photographed in water immersion. b, c. NHM P6813. Arrows indicate anterior. Scale bars = 5 mm.

ANNEXE XXXIV

EUPHANEROPS PAIRED VENTRAL FINS

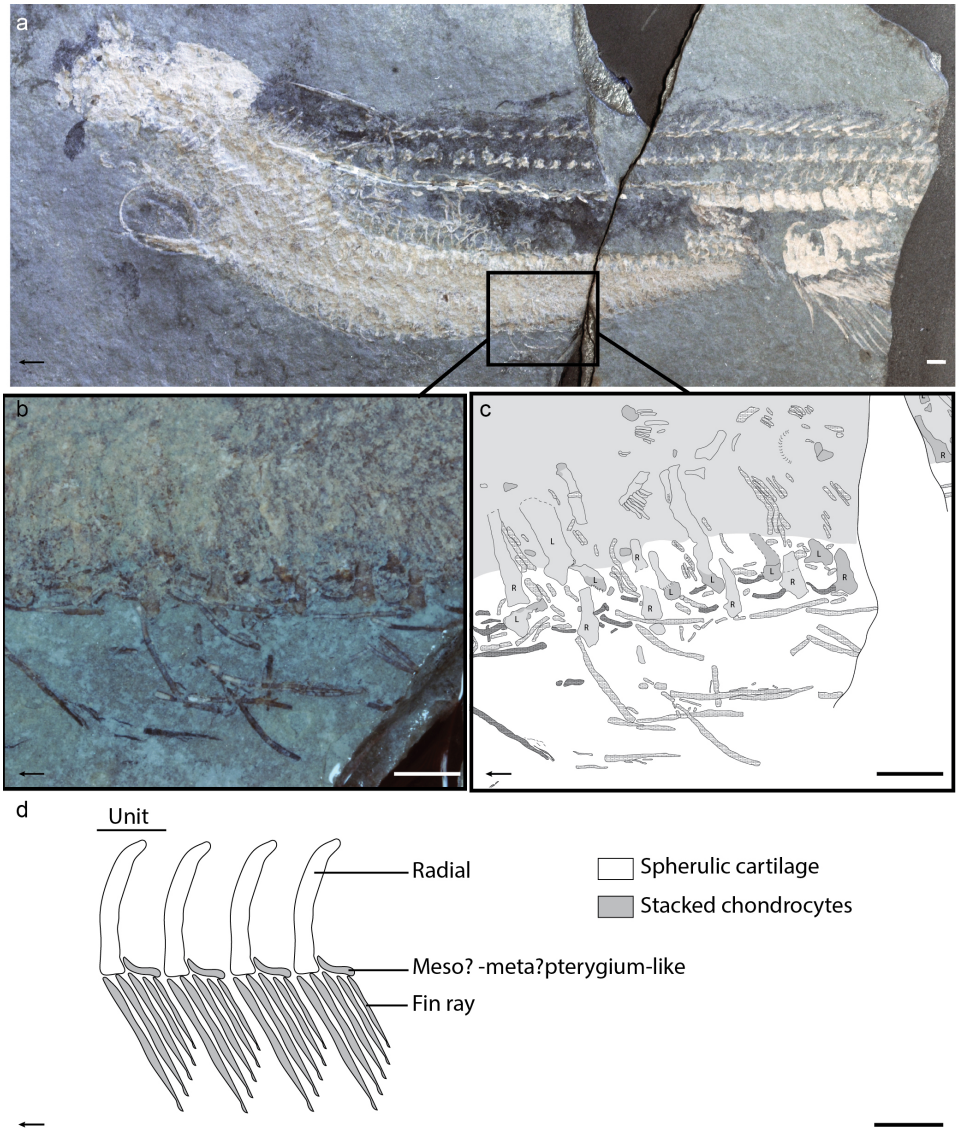

a, *Euphanerops* MHNM 01-123. b, c close-up of the black square in a showing paired ventral fins radials and fin rays. d, interpretation of the paired ventral fin elements, one body side is represented. Arrows point anteriorly, L = left, R = right. Scale bars = 3 mm.

ANNEXE XXXV

SECOND ORDER BIFURCATION IN MEDIAN FINS OF *PETROMYZON MARINUS* AMMOCOETE (CMNFI 2013-0019-S2-02, 103.4 MM TL)

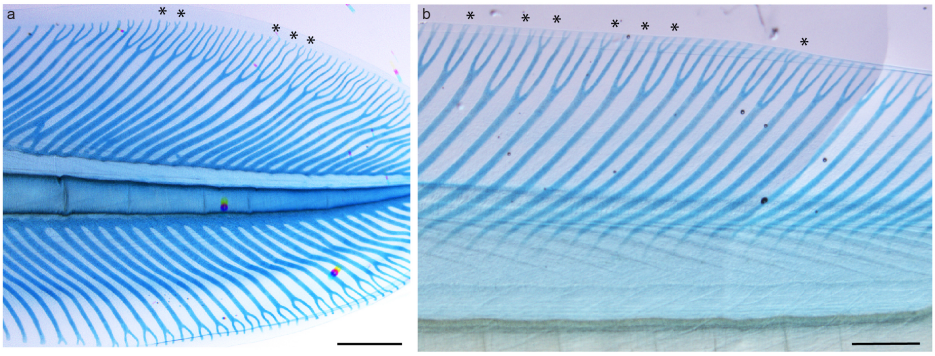

Second order bifurcation of fin rays is present in (a) epichordal lobe of the caudal fin and (b) second dorsal fin. Note that bifurcation is not present on every fin ray. Black asterisks indicate rays with second order bifurcation. Scale bar = 0.1 mm.

ANNEXE XXXVI

DEVELOPMENT OF THE ARCUALIA IN 14 METAMORPHOSING AMMOCOETES OF *PETROMYZON MARINUS* WITH RESPECT TO FIVE BODY SECTIONS

The branchial region (B) starts at the first branchial arch and finishes at the level of the seventh branchial arch. The predorsal region (P) covers the area from the seventh arch to the first fin ray of the first dorsal fin (D1). The D1 region contains the first to last rays of the first dorsal fin. The D2 region is delimited between the first and the last ray of the second dorsal fin ; since the second dorsal fin is continuous with the caudal fin, we considered the shortest ray of the posteriormost region of D2 as the limit between D2 and the caudal fin. The caudal region (C) encompasses the last fin ray of the second dorsal fin to the posterior extremity of the notochord. Each region was grossly separated into three zones : (1) anterior, (2) middle and (3) posterior. Development of arcualia was defined as follows : absent if no arcualia is observed (0) ; weakly developed if arcualia are small cartilaginous nodules that are barely visible along the notochord (+) ; moderately developed if arcualia are rather small but well visible along the notochord (++) and well developed if arcualia are noticeably long and large (+++).

	Branchial			Predorsal			D1			D2			Caudal			TL (mm)
	1	2	3	1	2	3	1	2	3	1	2	3	1	2	3	
S3-1	+++	++	+	0	0	0	0	0	0	0	0	0	0	0	0	125.6
S3-2	+++	++	+	0	0	0	0	0	0	0	0	0	0	0	0	128.6
S3-3	+++	+++	+	0	0	0	0	0	0	0	0	0	0	0	0	129.1
S3-4	+++	++	+	0	0	0	0	0	0	0	0	0	0	0	0	131.4
S3-5	+++	+++	++	0	0	0	0	0	0	0	0	0	0	0	0	131.5
S3-6	+++	++	+	0	0	0	0	0	0	0	0	0	0	0	0	132.8
S3-7	+++	+++	+	0	0	0	0	0	0	0	0	0	0	0	0	133
S3-8	+++	++	0	0	0	0	0	0	0	0	0	0	0	0	0	136.6
S3-9	++	+	0	0	0	0	0	0	0	0	0	0	0	0	0	138
S3-10	+++	++	+	0	0	0	0	0	0	0	+	0	0	0	0	138.1
S3-11	+++	++	+	0	0	0	0	0	+	+	++	0	0	0	0	139
S3-12	+++	++	+	+	0	0	0	0	+	+	++	+	0	0	0	140.3
S3-13	+++	++	+	+	0	0	0	0	0	+	++	0	0	0	0	142.9
S3-14	+++	++	+	0	0	0	0	0	+	+	++	+	0	0	0	144.1

RÉFÉRENCES

Aldridge, R. J., Briggs, D. E. G., Smith, M. P., Clarkson, E. N. K., Clark, N. D. L., 1993. The anatomy of conodonts. Philosophical Transactions: Biological Sciences 340 (1294), 405–421.

Allison, P. A., 1988. The role of anoxia in the decay and mineralization of proteinaceous macro-fossils. Paleobiology 14 (2), 139–154.

Allison, P. A., Briggs, D. E. G., 1991. Taphonomy of nonmineralized tissues. In: Allison, P. A., Briggs, D. E. G. (Eds.), Taphonomy: Releasing the Data Locked in the Fossil Record. Vol. 9. Plenum Press, New York.

Andreev, P. S., Coates, M. I., Shelton, R. M., Cooper, P. R., Smith, M. P., Sansom, I. J., 2015. Upper Ordovician chondrichthyan-like scales from North America. Palaeontology 58 (4), 691–704.

Andrews, M., Long, J., Ahlberg, P., Barwick, R., Campbell, K., 2005. The structure of the sarcopterygian *Onychodus jandemarrai* n. sp. from Gogo, Western Australia: With a functional interpretation of the skeleton. Transactions of the Royal Society of Edinburgh: Earth Sciences 96 (03), 197–307.

Arratia, G., 2009. Identifying patterns of diversity of the actinopterygian fulcra. Acta Zoologica 90 (s1), 220–235.

Arratia, G., Cloutier, R., 1996. Reassessment of the morphology of *Cheirolepis canadensis* (Actinopterygii). In: Schultze, H.-P., Cloutier, R. (Eds.), Devonian Fishes and Plants of Miguasha, Quebec, Canada. Verlag Dr. Friedrich Pfeil, München, Ch. 17, pp. 165–197.

Arratia, G., Cloutier, R., 2004. A new cheirolepidid fish from the Middle-Upper Devonian of Red Hill, Nevada, USA. In: Arratia, G., Wilson, M. V. H., Cloutier, R. (Eds.), Recent Advances in the Origin and Early Radiation of Vertebrates. Verlag Dr. Friedrich Pfeil, München, Germany, pp. 583–598.

Arratia, G., Schultze, H.-P., Casciotta, J., 2001. Vertebral column and associated elements in dipnoans and comparison with other fishes: Development and homology. Journal of Morphology 250 (2), 101–172.

Arsenault, M., Desbiens, S., Janvier, P., Kerr, J., 2004. New data on the soft tissues and external morphology of the antiarch *Bothriolepis canadensis* (Whiteaves, 1880), from the Upper Devonian of Miguasha, Quebec. In: Arratia, G., Wilson, M. V. H., Cloutier, R. (Eds.), Recent Advances in the Origin and Early Radiation of Vertebrates. Verlag Dr Friedrich Pfeil, pp. 439–454.

Arsenault, M., Janvier, P., 1995. Combien d'Ostéostracés à Miguasha? Geobios 28, 19–22.

Baguna, J., Garcia-Fernandez, J., 2003. Evo-Devo: The long and winding road. International Journal of Developmental Biology 47, 705–713.

Balan, E., Delattre, S., Roche, D., Segalen, L., Morin, G., Guillaumet, M., Blanchard, M., Lazzeri, M., Brouder, C., Salje, E. K. H., 2011. Line-broadening effects in the powder infrared spectrum of apatite. Physics and Chemistry of Minerals 38 (2), 111–122.

Balon, E. K., 1981. Saltatory processes and altricial to precocial forms in the ontogeny of fishes. American Zoologist 21 (2), 573–596.

Balon, E. K., 2001. Saltatory ontogeny and the life-history model: Neglected processes and patterns of evolution. Journal of Bioeconomics 3 (1), 1–26.

Balon, E. K., 2002. Epigenetic processes, when *natura non facit saltum* becomes a myth, and alternative ontogenies a mechanism of evolution. Environmental Biology of Fishes 65 (1), 1–35.

Bardack, D., 1991. First fossil hagfish (Myxinoidea): A record from the Pennsylvanian of Illinois. Science 254 (5032), 701–703.

Baron, M. G., 2015. An investigation of the genus *Mesacanthus* (Chordata: Acanthodii) from the Orcadian Basin and Midland Valley areas of Northern and Central Scotland using traditional morphometrics. PeerJ 3, e1331.

Barton, M., Bond, C. E., 2007. Bond's Biology of Fishes. Vol. 3. Belmont, CA.

Bartsch, P., Gemballa, S., Piotrowski, T., 1997. The embryonic and larval development of *Polypterus senegalus* Cuvier, 1829: Its staging with reference to external and skeletal features, behaviour and locomotory habits. Acta Zoologica 78 (4), 309–328.

Béchard, I., Arsenault, F., Cloutier, R., Kerr, J., 2014. The Devonian placoderm fish *Bothriolepis canadensis* revisited with three-dimensional digital imagery. Palaeontologia Electronica 17 (1), 1–19.

Béland, P., Arsenault, M., 1985. Scauménellisation de l'Acanthodii *Triazeugacanthus affinis* (Whiteaves) de la Formation d'Escuminac (Dévonien supérieur de Miguasha, Québec) : Révision du *Scaumenella mesacanthi* Graham-Smith. Canadian Journal of Earth Sciences 22 (4), 514–524.

Belanger, S. E., Balon, E. K., Rawlings, J. M., 2010. Saltatory ontogeny of fishes and sensitive early life stages for ecotoxicology tests. Aquatic Toxicology 97 (2), 88–95.

Belles-Isles, M., 1989. *Yvonaspis*, nouveau genre d'Osteostraci (Vertebrata, Agnatha) du Dévonien (Emsien - Eifélien) des Grès de Gaspé (Québec, Canada). Canadian Journal of Earth Sciences 26, 2396–2401.

Bemis, W. E., Grande, L., 1992. Early development of the actinopterygian head. I. External development and staging of the paddlefish *Polyodon spathula*. Journal of Morphology 213 (1), 47–83.

Beznosov, P., 2009. A redescription of the Early Carboniferous acanthodian *Acanthodes lopatini* Rohon, 1889. Acta Zoologica 90, 183–193.

Beznosov, P. A., 2000. The dependence of scale shape and size on their position on the body of the acanthodian *Carycinacanthus lopatini* (Rohon). In: Burtsev, I. N., Lukin, V. Y. (Eds.), Proceedings of the 9th Scientific Conference "Structure, Composition, History of Lithosphaere of the Timan - North Urals Segment". pp. 7–10.

Bird, N. C., Hernandez, L. P., 2007. Morphological variation in the Weberian apparatus of Cypriniformes. Journal of Morphology 268 (9), 739–757.

Blieck, A., 1984. Les Hétérostracés Ptéraspidiformes, Agnathes du Silurien-Dévonien du continent nord-atlantique et des blocs avoisinants: Révision systématique, phylogénie, biostratigraphie, biogéographie. Cahiers de Paléontologie, 1–205.

Blieck, A., Heintz, N., 1983. The cyathaspids of the Red Bay Group (Lower Devonian) of Spitsbergen. Polar Research 1 (1), 49–74.

Blom, H., 2012. New birkeniid anaspid from the Lower Devonian of Scotland and its phylogenetic implications. Palaeontology 55 (3), 641–652.

Botella, H., Blom, H., Dorka, M., Ahlberg, P. E., Janvier, P., 2007. Jaws and teeth of the earliest bony fishes. Nature 448, 583–586.

Botella, H., Martinez-Perez, C., Soler-Gijon, R., 2012. *Machaerancathus gaujeti* n. sp. (Acanthodii) from the Lower Devonian of Spain and Northwest France, with special reference to spine histology. Geodiversitas 34 (4), 761–783.

Brazeau, M. D., 2008. Endocranial morphology and phylogeny of Palaeozoic gnathostomes (jawed vertebrates). In: Upsaliensis, A. U. (Ed.), Digital comprehensive summaries of Uppsala dissertations from the Faculty of Science and Technology. Vol. 570. Uppsala.

Brazeau, M. D., 2009. The braincase and jaws of a Devonian "acanthodian" and modern gnathostome origins. Nature 457 (15), 305–308.

Brazeau, M. D., 2012. A revision of the anatomy of the Early Devonian jawed vertebrate *Ptomacanthus anglicus* Miles. Palaeontology 55 (2), 355–367.

Brazeau, M. D., Friedman, M., 2014. The characters of Palaeozoic jawed vertebrates. Zoological Journal of the Linnean Society 170 (4), 779–821.

Brazeau, M. D., Friedman, M., 2015. The origin and early phylogenetic history of jawed vertebrates. Nature 520 (7548), 490–497.

Briggs, D. E., Clarkson, E. N., Aldridge, R. J., 1983. The conodont animal. Lethaia 16 (1), 1–14.

Briggs, D. E. G., 2003. The role of decay and mineralization in the preservation of soft-bodied fossils. Annual Review of Earth & Planetary Sciences 31 (1), 275–301.

Bürgin, T., 1990. Reproduction in Middle Triassic actinopterygians; complex fin structures and evidence of viviparity in fossil fishes. Zoological Journal of the Linnean Society 100 (4), 379–391.

Burke, A. C., Nelson, C. E., Morgan, B. A., Tabin, C., 1995. *Hox* genes and the evolution of vertebrate axial morphology. Development 121 (2), 333–346.

Burrow, C. J., 1994. Form and function in scales of *Ligulalepis toombsi* Schultze, a palaeoniscoid from the Early Devonian of Australia. Records of the South Australian Museum 27 (2), 175–185.

Burrow, C. J., 1995. A new lophosteiform (Osteichthyes) from the Lower Devonian of Australia. Geobios 28, Supple (0), 327–333.

Burrow, C. J., Davidson, R. G., Den Blaauwen, J. L., Newman, M. J., 2015. Revision of *Climatius reticulatus* Agassiz, 1844 (Acanthodii, Climatiidae), from the Lower Devonian of Scotland, based on new histological and morphological data. Journal of Vertebrate Paleontology, e913421.

Burrow, C. J., Den Blaauwen, J. L., Newman, M., Davidson, R. G., 2016. The diplacanthid fishes (Acanthodii, Diplacanthiformes, Diplacanthidae) from the Middle Devonian of Scotland. Palaeontologica Electronica 19 (1.10A), 1–83.

Burrow, C. J., Long, J. A., Trinajstic, K., 2009. Disarticulated acanthodian and chondrichthyan remains from the upper Middle Devonian Aztec Siltstone, southern Victoria Land, Antarctica. Antarctic Science 21 (01), 71–88.

Burrow, C. J., Newman, M. J., Davidson, R. G., Den Blaauwen, J. L., 2011. Sclerotic plates or circumorbital bones in early jawed fishes? Palaeontology 54 (1), 207–214.

Burrow, C. J., Newman, M. J., Davidson, R. G., Den Blaauwen, J. L., 2013. Redescription of *Parexus recurvus*, an Early Devonian acanthodian from the Midland Valley of Scotland. Alcheringa 37, 1–23.

Burrow, C. J., Rudkin, D., 2014. Oldest near-complete acanthodian: The first vertebrate from the Silurian Bertie Formation Konservat-Lagerstätte, Ontario. PLoS ONE 9 (8), e104171.

Burrow, C. J., Sues, H., 2013. Reassessment of *Ischnacanthus? scheii* Spjeldnaes (Acanthodii, Ischnacanthiformes) from the latest Silurian or earliest Devonian of Ellesmere Island, arctic Canada. Canadian Journal of Earth Sciences 50 (9), 945–954.

Burrow, C. J., Trinajstic, K., Long, J. A., 2012. First acanthodian form the Upper Devonian (Frasnian) Gogo Fromation, Western Australia. Historical Biology, 1–12.

Burrow, C. J., Turner, S., 1999. A review of placoderm scales, and their significance in placoderm phylogeny. Journal of Vertebrate Paleontology 19 (2), 204–219.

Burrow, C. J., Turner, S., 2010. Reassessment of *"Protodus" scoticus* from the Early Devonian of Scotland. In: Elliott, D. K., Maisey, J. G., Yu, X., Miao, D. (Eds.), Morphology, Phylogeny and Paleobiogeography of Fossil Fishes. Dr Friedrich Pfeil, München, pp. 123–144.

Burrow, C. J., Turner, S., 2012. Scale structure of putative chondrichthyan *Gladbachus adentatus* Heidtke & Krätschmer, 2001 from the Middle Devonian Rheinisches Schiefergebirge, Germany. Historical Biology 25 (3), 385–390.

Burrow, C. J., Young, G. C., 1999. An articulated teleostome fish from the Late Silurian (Ludlow) of Victoria, Australia. Records of the Western Australian Museum 57, 1–14.

Burrow, C. J., Young, G. C., 2005. The acanthodian fauna of the Craven Peaks beds (Early to Middle Devonian), Western Queensland. Queensland Museum. Memoirs 51 (1), 3–25.

Burrow, C. J., Young, G. C., 2012. New information on *Culmacanthus* (Acanthodii: Diplacanthiformes) from the ?Early–Middle Devonian of Southeastern Australia. Proceedings of the Linnean Society of New South Wales 134, 21–29.

Cambra-Moo, O., Nacarino-Meneses, C., Díaz-Güemes, I., Enciso, S., Gil, O. G., Rodríguez, L. L., Barbero, M. Á. R., Antonio, H., Martín, A. G., 2015. Multidisciplinary characterization of the long-bone cortex growth patterns through sheep's ontogeny. Journal of Structural Biology 191 (1), 1–9.

Chang, M.-M., Wu, F., Miao, D., Zhang, J., 2014. Discovery of fossil lamprey larva from the Lower Cretaceous reveals its three-phased life cycle. Proceedings of the National Academy of Sciences 111 (43), 15486–15490.

Chevrinais, M., Balan, E., Cloutier, R., 2015a. New insights in the ontogeny and taphonomy of the Devonian acanthodian *Triazeugacanthus affinis* from the Miguasha *Fossil-Lagerstätte*, Eastern Canada. Minerals 6 (1), 1–17.

Chevrinais, M., Cloutier, R., Sire, J.-Y., 2015b. The revival of a so-called rotten fish: The ontogeny of the Devonian acanthodian *Triazeugacanthus*. Biology Letters 11 (2), 20140950.

Chevrinais, M., Sire, J.-Y., Cloutier, R., submitted. From body scale ontogeny to species ontogeny: Histological and morphological assessment of the Late Devonian acanthodian *Triazeugacanthus affinis* from Miguasha, Canada. PLoS ONE.

Chidiac, Y., 1996. Paleoenvironmental interpretation of the Escuminac Formation based on geochemical evidence. In: Schultze, H.-P., Cloutier, R. (Eds.), Devonian Fishes and Plants of Miguasha, Quebec, Canada. Verlag Dr Friedrich Pfeil, München, Ch. 5, pp. 47–53.

Choo, B., 2011. Revision of the actinopterygian genus *Mimipiscis* (= *Mimia*) from the Upper Devonian Gogo Formation of Western Australia and the interrelationships of the early Actinopterygii. Earth and Environmental Science Transactions of the Royal Society of Edinburgh 102 (02), 77–104.

Choo, B., 2015. A new species of the Devonian actinopterygian *Moythomasia* from Bergisch Gladbach, Germany, and fresh observations on *M. durgaringa* from the Gogo Formation of Western Australia. Journal of Vertebrate Paleontology 35 (4), e952817.

Cloutier, R., 2010. The fossil record of fish ontogenies: Insights into developmental patterns and processes. Seminars in Cell & Developmental Biology 21, 400–413.

Cloutier, R., 2013. Great Canadian *Lagerstätten* 4. The Devonian Miguasha biota (Québec): UNESCO World Heritage Site and a time capsule in the early history of vertebrates. Geoscience Canada 40, 149–163.

Cloutier, R., Ahlberg, P. E., 1996. Morphology, characters and the interrelationships of basal sarcopterygians. In: Stiassny, M. L. J., Parenti, L. R., Johnson, G. D. (Eds.), Interrelationships of Fishes. Academic Press Inc., USA, pp. 445–469.

Cloutier, R., Arratia, G., 2004. Early diversification of actinopterygians. In: Arratia, G., Wilson, M. V. H., Cloutier, R. (Eds.), Recent Advances in the Origin and Early Radiation of Vertebrates. Verlag Dr. Friedrich Pfeil, München, pp. 217–270.

Cloutier, R., Béchard, I., Charest, F., Matton, O., 2009. La contribution des poissons fossiles du parc national de Miguasha à la biologie évolutive du développement. Le Naturaliste canadien 133 (3), 84–95.

Cloutier, R., Lambrey de Souza, J., Browman, H. I., Skiftesvik, A. B., 2011a. Early ontogeny of the Atlantic halibut *Hippoglossus hippoglossus* head. Journal of Fish Biology 78 (4), 1035–1053.

Cloutier, R., Loboziak, S., Candilier, A.-M., Blieck, A., 1996. Biostratigraphy of the Upper Devonian Escuminac Formation, eastern Québec, Canada: A comparative study based on miospores and fishes. Review of Palaeobotany and Palynology 93 (1–4), 191–215.

Cloutier, R., Proust, J.-N., Tessier, B., 2011b. The Miguasha Fossil-Fish-Lagerstätte: A consequence of the Devonian land-sea interactions. Palaeobiodiversity and Palaeoenvironments 91, 293–323.

Coates, M. I., 1993. Actinopterygian and acanthodian fishes from the Viséan of East Kirkton, West Lothian, Scotland. Transactions of the Royal Society of Edinburgh: Earth Sciences 84 (3-4), 317–327.

Coates, M. I., 1994. The origin of vertebrate limbs. Development Supplement, 169–180.

Coates, M. I., 2003. The evolution of paired fins. Theory in Biosciences 122, 266–287.

Coates, M. I., Jeffery, J. E., Ruta, M., 2002. Fins to limbs: What the fossils say. Evolution & Development 4 (5), 390–401.

Coates, M. I., Sequeira, S. E. K., 2001. A new stethacanthid chondrichthyan from the Lower Carboniferous of Bearsden, Scotland. Journal of Vertebrate Paleontology 21 (3), 438–459.

Cohn, M. J., Patel, K., Krumlauf, R., Wilkinsont, D. G., Clarke, J. D. W., Tickle, C., 1997. *Hox9* genes and vertebrate limb specification. Nature (387), 97–101.

Colbert, M. W., Rowe, T., 2008. Ontogenetic sequence analysis: Using parsimony to characterize developmental sequences and sequence polymorphism. Journal of Experimental Zoology Part B: Molecular and Developmental Evolution 310B (5), 398–416.

Cope, E. D., 1889. Synopsis of the families of Vertebrata. The American Naturalist 23 (274), 849–877.

Cosmidis, J., Benzerara, K., Gheerbrant, E., Estève, I., Bouya, B., Amaghzaz, M., 2013a. Nanometer-scale characterization of exceptionally preserved bacterial fossils in Paleocene phosphorites from Ouled Abdoun (Morocco). Geobiology 11 (2), 139–153.

Cosmidis, J., Benzerara, K., Menguy, N., Arning, E., 2013b. Microscopy evidence of bacterial microfossils in phosphorite crusts of the Peruvian shelf: Implications for phosphogenesis mechanisms. Chemical Geology 359, 10–22.

Cracraft, J., 2005. Phylogeny and evo-devo: Characters, homology, and the historical analysis of the evolution of development. Zoology 108, 345–356.

Cumbaa, S. L., Schultze, H.-P., 2002. An Early Devonian (Emsian) acanthodian from the Bear Rock Formation, Anderson River, Northwest Territories, Canada. Canadian Journal of Earth Sciences 39 (10), 1457–1465.

Cunningham, J. A., Rahman, I. A., Lautenschlager, S., Rayfield, E. J., Donoghue, P. C. J., 2014. A virtual world of paleontology. Trends in Ecology & Evolution 29 (6), 347–357.

Cunningham, J. A., Rücklin, M., Blom, H., Botella, H., Donoghue, P. C. J., 2012. Testing models of dental development in the earliest bony vertebrates, *Andreolepis* and *Lophosteus*. Biology Letters 8 (5), 833–837.

Damas, H., 1944. Recherches sur le développement de *Lampetra fluviatilis* L. Contribution à l'étude de la céphalogenèse des vertébrés. Archives de Biologie 55, 1–284.

Davis, S. P., 2002. Comparative anatomy and relationships in acanthodian fishes. Ph.D. thesis, London, UK.

Davis, S. P., Finarelli, J. A., Coates, M. I., 2012. *Acanthodes* and shark-like conditions in the last common ancestor of modern gnathostomes. Nature 486 (7402), 247–250.

de Jong, I. M. L., Colbert, M. W., Witte, F., Richardson, M. K., 2009. Polymorphism in developmental timing: Intraspecific heterochrony in a Lake Victoria cichlid. Evolution & Development 11 (6), 625–635.

de Ricqlès, A., Padian, K., 2009. Quelques apports à la théorie de l'Évolution, de la « Synthèse orthodoxe » à la « Super synthèse évo-dévo » 1970–2009 : un point de vue. Comptes Rendus Palevol 8 (2–3), 341–364.

Dean, M. N., Summers, A. P., 2006. Mineralized cartilage in the skeleton of chondrichthyan fishes. Zoology 109 (2), 164–168.

Delfino, M., Sánchez-Villagra, M. R., 2010. A survey of the rock record of reptilian ontogeny. Seminars in Cell & Developmental Biology 21 (4), 432–440.

Denison, R., 1978. Placodermi. In: Schultze, H.-P. (Ed.), Handbook of Paleoichthyology. Vol. 2. Gustav Fisher Verlag, Stuttgart, p. 128.

Denison, R., 1979. Acanthodii. In: Schultze, H.-P. (Ed.), Handbook of Paleoichthyology. Vol. 5. Gustav Fischer Verlag, New York, p. 59.

Denison, R. H., Lillian, A., 1960. Fishes of the Devonian Holland Quarry Shale of Ohio. Chicago: Natural History Museum.

Derycke, C., Chancogne-Weber, C., 1995. Histological discovery on acanthodian scales from the Famennian of Belgium. Geobios 28, Supple (19), 31–34.

Dineley, D. L., 1999. Mid- and Late Devonian fossil fishes sites of England and Wales. In: Dineley, D. L., Metcalf, S. J. (Eds.), Fossil fishes of Great britain. Joint Nature Conservation Comittee, United Kingdom, pp. 225–226.

Donoghue, P. C. J., 2002. Evolution of development of the vertebrate dermal and oral skeletons: Unraveling concepts, regulatory theories, and homologies. Paleobiology 28 (4), 474–507.

Donoghue, P. C. J., Forey, P. L., Aldridge, R. J., 2000. Conodont affinity and chordate phylogeny. Biological Reviews 75 (02), 191–251.

Donoghue, P. C. J., Keating, J. N., 2014. Early vertebrate evolution. Palaeontology 57 (5), 879–893.

Donoghue, P. C. J., Purnell, M. A., 2005. Genome duplication, extinction and vertebrate evolution. Trends in Ecology & Evolution 20 (6), 312–319.

Donoghue, P. C. J., Purnell, M. A., 2009. Distinguishing heat from light in debate over controversial fossils. BioEssays 31 (2), 178–189.

Donoghue, P. C. J., Sansom, I. J., 2002. Origin and early evolution of vertebrate skeletonization. Microscopy Research and Technique 59 (5), 352–372.

Donoghue, P. C. J., Smith, M. P., 2001. The anatomy of *Turinia pagei* (Powrie), and the phylogenetic status of the Thelodonti. Earth and Environmental Science Transactions of the Royal Society of Edinburgh 92 (01), 15–37.

Dorozhkin, S. V., Epple, M., 2002. Biological and medical significance of calcium phosphates. Angewandte Chemie International Edition 41 (17), 3130–3146.

Downs, J. P., Donoghue, P. C. J., 2009. Skeletal histology of *Bothriolepis canadensis* (Placodermi, Antiarchi) and evolution of the skeleton at the origin of jawed vertebrates. Journal of Morphology 270 (11), 1364–1380.

Dupret, V., 2004. The phylogenetic relationships between actinolepids (Placodermi: Arthrodira) and other arthrodires (phlyctaeniids and brachythoracids). Fossils and Strata 50, 44–55.

Dupret, V., Sanchez, S., Goujet, D., Tafforeau, P., Ahlberg, P. E., 2014. A primitive placoderm sheds light on the origin of the jawed vertebrate face. Nature 507 (7493), 500–503.

El Albani, A., Cloutier, R., Candilier, A.-M., 2002. Early diagenesis of the Upper Devonian Escuminac Formation in the Gaspé Peninsula, Québec: Sedimentological and geochemical evidence. Sedimentary Geology 146 (3–4), 209–223.

Elliott, D. K., Ilyes, R. R., 1996. New Early Devonian pteraspidids (Agnatha, Heterostraci) from Death Valley National Monument, Southeastern California. Journal of Paleontology 70 (01), 152–161.

Faustino, M., Power, D. M., 2001. Osteologic development of the viscerocranial skeleton in sea bream: Alternative ossification strategies in teleost fish. Journal of Fish Biology 58 (2), 537–572.

Fischer-Rousseau, L., Cloutier, R., Zelditch, M. L., 2009. Morphological integration and developmental progress during fish ontogeny in two contrasting habitats. Evolution & Development 11 (6), 740–753.

Fisher, J. P., Pearcy, W. G., 2005. Seasonal changes in growth of Coho salmon (*Oncorhynchus kisutch*) of Oregon and Washington and concurrent changes in the spacing of scale circuli. Fishery Bulletin 103 (1), 34–51.

Forey, P. L., 1995. Agnathans recent and fossil, and the origin of jawed vertebrates. Reviews in Fish Biology and Fisheries 5 (3), 267–303.

Forey, P. L., Ahlberg, P. E., Lukševičs, E., Zupinš, I., 2000. A new coelacanth from the Middle Devonian of Latvia. Journal of Vertebrate Paleontology 20 (2), 243–252.

Forey, P. L., Janvier, P., 1993. Agnathans and the origin of jawed vertebrates. Nature 361, 129–134.

Forey, P. L., Young, V. T., 1985. Acanthodian and coelacanth fish from the Dinantian of Foulden, Berwickshire, Scotland. Transactions of the Royal Society of Edinburgh: Earth Sciences 76, 53–59.

Francillon Vieillot, H., De Buffrénil, V., Castanet, J., Géraudie, J., Meunier, F. J., Sire, J. Y., Zylberberg, L., De Ricqlès, A., 1990. Microstructure and mineralization of vertebrate skeletal tissues. Skeletal biomineralization: patterns, processes and evolutionary trends, 175–234.

Franz-Odendaal, T. A., Vickaryous, M. K., 2006. Skeletal elements in the vertebrate eye and adnexa: Morphological and developmental perspectives. Developmental Dynamics 235 (5), 1244–1255.

Freitas, R., Zhang, G., Cohn, M. J., 2007. Biphasic *Hoxd* gene expression in shark paired fins reveals an ancient origin of the distal limb domain. PLoS ONE 2 (8), e754.

Friedman, M., Brazeau, M. D., 2010. A reappraisal of the origin and basal radiation of the Osteichthyes. Journal of Vertebrate Paleontology 30 (1), 36–56.

Friedman, M., Brazeau, M. D., 2013. Palaeontology: A jaw-dropping fossil fish. Nature 502 (7470), 175–177.

Friedman, M., Matt, F., 2007. *Styloichthys* as the oldest coelacanth: Implications for early osteichthyan relationships. Journal of Systematic Palaeontology 5 (3), 289–343.

Fritzsch, B., 1990. The evolution of metamorphosis in amphibians. Journal of Neurobiology 21 (7), 1011–1021.

Gabbott, S., Aldridge, R., Theron, J., 1995. A giant conodont with preserved muscle tissue from the Upper Ordovician of South Africa. Nature 374, 800–803.

Gagnier, P.-Y., 1996. Acanthodii. In: Schultze, H.-P., Cloutier, R. (Eds.), Devonian Fishes and Plants of Miguasha, Quebec, Canada. Verlag Dr. Friedrich Pfeil, München, Ch. 16, pp. 149–164.

Gagnier, P.-Y., Goujet, D., 1997. Nouveaux poissons acanthodiens du Dévonien du Spitsberg. Geodiversitas 19 (3), 505–513.

Gagnier, P.-Y., Wilson, M. V. H., 1996. Early Devonian acanthodians from Northern Canada. Palaeontology 39 (2), 241–258.

Gai, Z., Donoghue, P. C. J., Zhu, M., Janvier, P., Stampanoni, M., 2011. Fossil jawless fish from China foreshadows early jawed vertebrate anatomy. Nature 476 (7360), 324–327.

Gardiner, B. G., 1984. The relationships of the palaeoniscid fishes, a review based on new specimens of *Mimia* and *Moythomasia* from the Upper Devonian of Western Australia. Bulletin of the British Museum (Natural History) 37 (4), 173–428.

Gavaia, P. j., Sarasquete, C., Cancela, M. L., 2000. Detection of mineralized structures in early stages of development of marine Teleostei using a modified alcian blue-alizarin red double staining technique for bone and cartilage. Biotechnic & Histochemistry 75 (2), 79–84.

Geraudie, J., Meunier, F., 1982. Comparative fine structure of the osteichthyan dermotrichia. The Anatomical Record 202 (3), 325–328.

Gess, R. W., Coates, M. I., Rubidge, B. S., 2006. A lamprey from the Devonian period of South Africa. Nature 443 (7114), 981–984.

Ghysen, A., Dambly-Chaudière, C., 2004. Development of the zebrafish lateral line. Current Opinion in Neurobiology 14 (1), 67–73.

Giles, S., Coates, M. I., Garwood, R. J., Brazeau, M. D., Atwood, R., Johanson, Z., Friedman, M., 2015a. Endoskeletal structure in *Cheirolepis* (Osteichthyes, Actinopterygii), an early ray-finned fish. Palaeontology 58 (5), 849–870.

Giles, S., Friedman, M., Brazeau, M. D., 2015b. Osteichthyan-like cranial conditions in an Early Devonian stem gnathostome. Nature 520 (7545), 82–85.

Goodrich, E. S., 1958. Studies on the Structure and Development of Vertebrates. vol. 1. Dover Publications, New York.

Goujet, D., 2001. Placoderms and basal gnathostome apomorphies. In: Ahlberg, P. E. (Ed.), Major Events in Early Vertebrate Evolution. Taylor & Francis, Ch. 13, pp. 209–222.

Goujet, D., Young, G. C., 2004. Placoderm anatomy and phylogeny: New insights. In: Arratia, G., Wilson, M. V. H., Cloutier, R. (Eds.), Recent Advances in the Origin and Early Radiation of Vertebrates. Verlag Dr. Fiedrich Pfeil, München, pp. 109–126.

Gould, S. J., 1977. Ontogeny and Phylogeny. Belknap Press of Harvard University Press, USA.

Graham-Smith, W., 1935. *Scaumenella mesacanthi*, gen. et sp. n., a peculiar organism from the Upper Devonian of Scaumenac Bay, P.Q., Canada. Annals and Magazine of Natural History 16 (10), 473–476.

Grande, L., 2010. An empirical synthetic pattern study of gars (Lepisosteiformes) and closely related species, based mostly on skeletal anatomy. The resurrection of Holostei. Copeia 10 (2A), 1.

Grande, L., Bemis, W. E., 1998. A comprehensive phylogenetic study of amiid fishes (Amiidae) based on comparative skeletal anatomy. An empirical search for interconnected patterns of natural history. In: Fraser, N. C. (Ed.), Memoirs of the Society of Vertebrate Paleontology. Vol. 4. p. 690.

Green, S. A., Bronner, M. E., 2014. The lamprey: A jawless vertebrate model system for examining origin of the neural crest and other vertebrate traits. Differentiation 87 (1), 44–51.

Greeniaus, J. W., Wilson, M. V., 2003. Fossil juvenile Cyathaspididae (Heterostraci) reveal rapid cyclomorial development of the dermal skeleton. Journal of Vertebrate Paleontology 23 (2), 483–487.

Grogan, E. D., Lund, R., 2008. A basal elasmobranch, *Thrinacoselache gracia* n. gen. and sp. (Thrinacodontidae, new family) from the Bear Gulch Limestone, Serpukhovian of Montana, USA. Journal of Vertebrate Paleontology 28 (4), 970–988.

Gross, W., 1947. Die Agnathen und Acanthodier des obersilurischen Beyrichienkalks. Palaeontographica, Abt. A, Paläozoologie-Stratigraphie 96, 91–158.

Gross, W., 1957. Mundzähne und Hautzähne der Acanthodier und Arthrodiren. Palaeontographica, Abt. A, Paläozoologie-Stratigraphie 109, 1–40.

Gross, W., 1971. Downtonische und dittonische Acanthodier-reste des Ostseegebietes. Palaeontographica Abteilung A Palaeozoologie-Stratigraphie 136, 1–82.

Grotmol, S., Kryvi, H., Keynes, R., Krossøy, C., Nordvik, K., Totland, G. K., 2006. Stepwise enforcement of the notochord and its intersection with the myoseptum: An evolutionary path leading to development of the vertebra? Journal of Anatomy 209 (3), 339–357.

Grotmol, S., Kryvi, H., Nordvik, K., Totland, G., 2003. Notochord segmentation may lay down the pathway for the development of the vertebral bodies in the Atlantic salmon. Anatomy and Embryology 207 (4-5), 263–272.

Grünbaum, T., Cloutier, R., Dumont, P., 2003. Congruence between chondrification and ossification sequences during caudal skeleton development: A Moxostomatini case study. The Big Fish Bang, 161–176.

Grünbaum, T., Cloutier, R., Vincent, B., 2012. Dynamic skeletogenesis in fishes: Insight of exercise training on developmental plasticity. Developmental Dynamics 241 (10), 1507–1524.

Gupta, N. S., Cambra-Moo, O., Briggs, D. E. G., Love, G. D., Fregenal-Martinez, M. A., Summons, R. E., 2008. Molecular taphonomy of macrofossils from the Cretaceous Las Hoyas Formation, Spain. Cretaceous Research 29 (1), 1–8.

Haddon, C., Lewis, J., 1996. Early ear development in the embryo of the zebrafish, *Danio rerio*. Journal of Comparative Neurology 365 (1), 113–128.

Hall, B. K., 2002. Palaeontology and evolutionary developmental biology: A science of the nineteenth and twenty–first centuries. Palaeontology 45 (4), 647.

Hall, B. K., 2007. Homoplasy and homology: Dichotomy or continuum? Journal of Human Evolution 52 (5), 473–479.

Hall, T. E., 2008. Pattern Formation. In: Finn, R. N., Kapoor, B. G. (Eds.), Fish Larval Physiology. Science Publishers, Ch. 1, pp. 3–25.

Hanke, G. F., 2002. *Paucicanthus vanelsti* gen. et sp. nov., an Early Devonian (Lochkovian) acanthodian that lacks paired fin-spines. Canadian Journal of Earth Sciences 39 (7), 1071–1083.

Hanke, G. F., 2008. *Promesacanthus eppleri* n. gen., n. sp., a mesacanthid (Acanthodii, Acanthodiformes) from the Lower Devonian of northern Canada. Geodiversitas 30 (2), 287–302.

Hanke, G. F., Davis, S. P., 2008. Redescription of the acanthodian *Gladiobranchus probaton* Bernacsek & Dineley, 1977, and comments on diplacanthid relationships. Geodiversitas 30 (2), 303–330.

Hanke, G. F., Davis, S. P., 2012. A re-examination of *Lupopsyrus pygmaeus* Bernacsek & Dineley, 1977 (Pisces, Acanthodii). Geodiversitas 34 (3), 469–487.

Hanke, G. F., Davis, S. P., Wilson, M. V. H., 2001. New species of the acanthodian genus *Tetanopsyrus* from Northern Canada, and comments on related taxa. Journal of Vertebrate Paleontology 21 (4), 740–753.

Hanke, G. F., Wilson, M. V. H., 2004. New teleostome fishes and acanthodian systematics. In: Arratia, G., Wilson, M. V. H., Cloutier, R. (Eds.), Recent Advances in the Origin and Early Radiation of Vertebrates. Verlag Dr Friedrich Pfeil, München, pp. 189–216.

Hanke, G. F., Wilson, M. V. H., 2006. Anatomy of the Early Devonian acanthodian *Brochoadmones milesi* based on nearly complete body fossils, with comments on the evolution and development of paired fins. Journal of Vertebrate Paleontology 26 (3), 526–537.

Hanke, G. F., Wilson, M. V. H., 2010. The putative stem-group chondrichthyans *Kathemacanthus* and *Seretolepis* from the Lower Devonian MOTH locality, Mackenzie Mountains, Canada. In: Elliott, D. K., Maisey, J. G., Yu, X., Miao, D. (Eds.), Morphology, Phylogeny and Paleobiogeography of Fossil Fishes. Dr Friedrich Pfeil, München, pp. 159–182.

Hawthorn, J. R., Wilson, M. V. H., Falkenberg, A. B., 2008. Development of the dermoskeleton in *Superciliaspis gabrielsei* (Agnatha: Osteostraci). Journal of Vertebrate Paleontology 28 (4), 951–960.

Heidtke, U. H. J., 1990. Studien über *Acanthodes* (Pisces: Acanthodii) aus dem saarpfälzischen Rotliengend (?Ober-Karbon - Unter-Perm - SW-Deutschland). Pollichia 19, 1–86.

Heimberg, A. M., Cowper-Sal·lari, R., Sémon, M., Donoghue, P. C. J., Peterson, K. J., 2010. microRNAs reveal the interrelationships of hagfish, lampreys, and gnathostomes and the nature of the ancestral vertebrate. Proceedings of the National Academy of Sciences 107 (45), 19379–19383.

Holmgren, N., 1942. Studies on the head of fishes. An embryological, morphological and phylogenetic study. Part III: The phylogeny of elasmobranch fishes. Acta Zoologica 23, 1–88.

Horner, J. R., Goodwin, M. B., 2009. Extreme cranial ontogeny in the Upper Cretaceous dinosaur *Pachycephalosaurus*. PLoS ONE 4 (10), e7626.

Hutchinson, P., 1973. A revision of the redfieldiiform and perleidiform fishes from the Triassic of Bekker's Kraal (South Africa) and Brookville (New South Wales). Bulletin of the British Museum (Natural History), Geology 22, 233–354.

Ifrim, C., Stinnesbeck, W., Frey, E., 2007. Upper Cretaceous (Cenomanian-Turonian and Turonian-Coniacian) open marine plattenkalk deposits in NE Mexico. Neues Jahrbuch für Geologie und Paläontologie-Abhandlungen 245 (1), 71–81.

Janvier, P., 1993. Patterns of diversity in the skull of jawless fishes. In: Hanken, J., Hall, B. K. (Eds.), The skull. Vol. 2. The University of Chicago Press, Chicago, Ch. 4, pp. 131–188.

Janvier, P., 1996a. The dawn of the vertebrates: Characters versus common ascent in the rise of current vertebrate phylogenies. Palaeontology 39 (2), 259–287.

Janvier, P., 1996b. Early Vertebrates. Oxford University Press, United States.

Janvier, P., 2001. Ostracoderms and the shaping of the gnathostome characters. In: Ahlberg, P. E. (Ed.), Major Events in Early Vertebrate Evolution. Taylor & Francis, London New York, Ch. 11, pp. 172–186.

Janvier, P., 2003. Vertebrate characters and the Cambrian vertebrates. Comptes Rendus Palevol 2 (6–7), 523–531.

Janvier, P., 2007. Living primitive fishes and fishes from deep time. In: David J. McKenzie, A. P. F., Colin, J. B. (Eds.), Primitive Fishes. Vol. Volume 26. Academic Press, pp. 1–51.

Janvier, P., 2008. Early jawless vertebrates and cyclostome origins. Zoological Science 25 (10), 1045–1056.

Janvier, P., 2015. Facts and fancies about early fossil chordates and vertebrates. Nature 520 (7548), 483–489.

Janvier, P., Arsenault, M., 2002. Palaeobiology: Calcification of early vertebrate cartilage. Nature 417 (6889), 609.

Janvier, P., Arsenault, M., 2007. The anatomy of *Euphanerops longaevus* Woodward, 1900, an anaspid-like jawless vertebrate from the Upper Devonian of Miguasha, Quebec, Canada. Geodiversitas 29 (1), 143–216.

Janvier, P., Arsenault, M., Desbiens, S., 2004. Calcified cartilage in the paired fins of the osteostracan *Escuminaspis laticeps* (Traquair 1880), from the Late Devonian of Miguasha (Québec, Canada), with a consideration of the early evolution of the pectoral fin endoskeleton in vertebrates. Journal of Vertebrate Paleontology 24 (4), 773–779.

Jarvik, E., 1977. The systematic position of acanthodian fishes. In: Andrews, M. S., Miles, R. S., Walker, A. D. (Eds.), Problems in Vertebrate Evolution. Vol. 4. Academic Press for the Linnean Society of London, London, pp. 199–225.

Jarvik, E., 1980. Basic Structure and Evolution of Vertebrates. Vol. 1. Academic Press, London.

Jarvik, E., 1996. The evolutionary importance of *Eusthenopteron foordi* (Osteolepiformes). In: Schultze, H.-P., Cloutier, R. (Eds.), Devonian Fishes and Plants of Miguasha, Quebec, Canada. Verlag Dr. Friedrich Pfeil, München, Ch. 22, pp. 285–313.

Johanson, Z., 2010. Evolution of paired fins and the lateral somitic frontier. Journal of Experimental Zoology Part B: Molecular and Developmental Evolution 314 (5), 347–352.

Johanson, Z., Smith, M. M., Joss, J. M. P., 2007. Early scale development in *Heterodontus* (Heterodontiformes; Chondrichthyes): A novel chondrichthyan scale pattern. Acta Zoologica 88 (3), 249–256.

Johanson, Z., Tanaka, M., Chaplin, N., Smith, M., 2008. Early Palaeozoic dentine and patterned scales in the embryonic catshark tail. Biology Letters 4 (1), 87–90.

Johanson, Z., Trinajstic, K., 2014. Fossilized ontogenies: The contribution of placoderm ontogeny to our understanding of the evolution of early gnathostomes. Palaeontology 57 (3), 505–516.

Johanson, Z., Trinajstic, K., Carr, R., Ritchie, A., 2013. Evolution and development of the synarcual in early vertebrates. Zoomorphology 132 (1), 95–110.

Jollie, M., 1984a. Development of cranial and pectoral girdle bones of *Lepisosteus* with a note on scales. Copeia 2, 476–502.

Jollie, M., 1984b. Development of the head and pectoral skeleton of *Amia* with note on the scales. Gegenbaurs Morphologie Jahrbuch Leipzig 130 (2), 315–351.

Joss, J., Longhurst, T., 2001. Lungfish paired fins. In: Ahlberg, P. E. (Ed.), Major Events in Early Vertebrate Evolution. Taylor & Francis, London New York, Ch. 21, pp. 370–376.

Kalvoda, J., Novák, M., Bábek, O., Brzobohatý, R., Holá, M., Holoubek, I., Kanický, V., Škoda, R., 2009. Compositional changes in fish scale hydroxylapatite during early diagenesis; an example from an abandoned meander. Biogeochemistry 94 (3), 197–215.

Karatajute-Talimaa, V., Predtechenskyj, N., 1995. The distribution of the vertebrates in the Late Ordovician and Early Silurian palaeobasins of the Siberian Platform. Bulletin du Muséum National d'Histoire Naturelle. Section C, Sciences de la Terre, Paléontologie, Géologie, Minéralogie 17 (1-4), 39–55.

Karatajute-Talimaa, V. N., 1992. The early stage of the dermal skeleton formation in chondrichthyans. In: Mark-Kurik, E. (Ed.), Fossil Fishes as Living Animals. Academy of Sciences of Estonia, Tallinn, pp. 223–231.

Karatajute-Talimaa, V. N., 1998. Determination methods for the exoskeletal remains of early vertebrates. Fossil Record 1 (1), 21–51.

Karatajute-Talimaa, V. N., Smith, M. M., 2002. Early acanthodians from the Lower Silurian of Asia. Earth and Environmental Science Transactions of the Royal Society of Edinburgh 93 (3), 277–299.

Katz, H. R., Hale, M. E., 2016. A large-scale pattern of ontogenetic shape change in ray-finned fishes. PLoS ONE 11 (3), e0150841.

Keating, J. N., Donoghue, P. C. J., 2016. Histology and affinity of anaspids, and the early evolution of the vertebrate dermal skeleton. Proceedings of the Royal Society of London B: Biological Sciences 283 (1826).

Kemp, N. E., 1977. Banding pattern and fibrillogenesis of ceratotrichia in shark fins. Journal of Morphology 154 (2), 187–203.

Kemp, N. E., Westrin, S. K., 1979. Ultrastructure of calcified cartilage in the endoskeletal tesserae of sharks. Journal of Morphology 160 (1), 75–101.

Khoury, B. M., Bigelow, E. M. R., Smith, L. M., Schlecht, S. H., Scheller, E. L., Andarawis-Puri, N., Jepsen, K. J., 2015. The use of nano-computed tomography to enhance musculoskeletal research. Connective tissue research 56 (2), 106–119.

Kolodny, Y., Luz, B., Sander, M., Clemens, W., 1996. Dinosaur bones: Fossils or pseudomorphs? The pitfalls of physiology reconstruction from apatitic fossils. Palaeogeography, Palaeoclimatology, Palaeoecology 126 (1), 161–171.

Kowalewski, M., Dyreson, E., Marcot, J. D., Vargas, J. A., Flessa, K. W., Hallman, D. P., 1997. Phenetic discrimination of biometric simpletons: Paleobiological implications of morphospecies in the lingulide brachiopod *Glottidia*. Paleobiology 23 (04), 444–469.

Kuratani, S., Oisi, Y., Ota, K. G., 2016. Evolution of the vertebrate cranium: Viewed from hagfish developmental studies. Zoological Science 33 (3), 229–238.

Labs-Hochstein, J., MacFadden, B. J., 2006. Quantification of diagenesis in Cenozoic sharks: Elemental and mineralogical changes. Geochimica et Cosmochimica Acta 70 (19), 4921–4932.

Lehman, J.-P., 1957. Un problème non résolu : L'origine des vertébrés. La Nature (Science, progrès, découverte) 85, 174–177.

Levine, J. S., 1985. The vertebrate eye. In: Hildebrand, M., Bramble, D. M., Liem, K. F., Wake, D. B. (Eds.), Functional Vertebrate Morphology. Harvard University Press, Cambridge, MA, Ch. 16, pp. 317–337.

Lombardo, C., 1999. Sexual dimorphism in a new species of the actinopterygian *Peltopleurus* from the Triassic of Northern Italy. Palaeontology 42 (4), 741–760.

Long, J., Young, G., 1988. Acanthothoracid remains from the Early Devonian of New South Wales, including a complete sclerotic capsule and pelvic girdle. Memoirs of the Association of Australasian Palaeontologists 7, 65–80.

Long, J. A., 1983. A new diplacanthoid acanthodian from the Late Devonian of Victoria. Memoirs of the Association of Australasian Palaeontologists 1, 51–65.

Long, J. A., 1986. New ischnacanthid acanthodians from the Early Devonian of Australia, with comments on acanthodian interrelationships. Zoological Journal of the Linnean Society 87 (4), 321–339.

Long, J. A., Mark-Kurik, E., Johanson, Z., Lee, M. S. Y., Young, G. C., Min, Z., Ahlberg, P. E., Newman, M., Jones, R., den Blaauwen, J., Choo, B., Trinajstic, K., 2015. Copulation in antiarch placoderms and the origin of gnathostome internal fertilization. Nature 517 (7533), 196–199.

Long, J. A., Trinajstic, K., Johanson, Z., 2009. Devonian arthrodire embryos and the origin of internal fertilization in vertebrates. Nature 457 (7233), 1124–1127.

Lu, J., Giles, S., Friedman, M., den Blaauwen, J. L., Zhu, M., 2016. The oldest actinopterygian highlights the cryptic early history of the hyperdiverse ray-finned fishes. Current Biology.

Lund, R., 1985. The morphology of *Falcatus falcatus* (St. John and Worthen), a Mississippian stethacanthid chondrichthyan from the Bear Gulch Limestone of Montana. Journal of Vertebrate Paleontology 5 (1), 1–19.

Mabee, P. M., 2000. Developmental data and phylogenetic systematics: Evolution of the vertebrate limb. American Zoologist 40 (5), 789–800.

Mabee, P. M., Crotwell, P. L., Bird, N. C., Burke, A. C., 2002. Evolution of median fin modules in the axial skeleton of fishes. Journal of Experimental Zoology (Mol Dev Evol) 294 (2), 77–90.

MacFadden, B. J., Labs-Hochstein, J., Quitmyer, I., Jones, D. S., 2004. Incremental growth and diagenesis of skeletal parts of the lamnoid shark *Otodus obliquus* from the early Eocene (Ypresian) of Morocco. Palaeogeography, Palaeoclimatology, Palaeoecology 206 (3), 179–192.

Mahamid, J., Sharir, A., Addadi, L., Weiner, S., 2008. Amorphous calcium phosphate is a major component of the forming fin bones of zebrafish: Indications for an amorphous precursor phase. Proceedings of the National Academy of Sciences 105 (35), 12748–12753.

Maisano, J., 2002. The potential utility of postnatal skeletal developmental patterns in squamate phylogenetics. Zoological Journal of the Linnean Society 136 (2), 277–313.

Maisey, J. G., 1986. Heads and tails: A chordate phylogeny. Cladistics 2 (4), 201–256.

Maisey, J. G., 2001. A primitive chondrichthyan braincase from the Middle Devonian of Bolivia. In: Ahlberg, P. E. (Ed.), Major Events in Early Vertebrate Evolution. Taylor and Francis, Ch. 16, pp. 263–288.

Mallatt, J., 1996. Ventilation and the origin of jawed vertebrates: A new mouth. Zoological Journal of the Linnean Society 117 (4), 329–404.

Marinelli, W., Strenger, A., 1954. *Lampetra fluviatilis* L. In: Vergleichende Anatomie und Morphologie der Wirbeltiere. Franz Deuticke, Wien, pp. 1–80.

Märss, T., 2001. *Andreolepis* (Actinopterygii) in the Upper Silurian of Northern Eurasia. Proceedings of the Estonian Academy of Sciences Geology 50 (3), 174–189.

Märss, T., 2006. Exoskeletal ultrasculpture of early vertebrates. Journal of Vertebrate Paleontology 26 (2), 235–252.

Märss, T., 2011. A unique Late Silurian *Thelodus* squamation from Saaremaa (Estonia) and its ontogenetic development. Estonian Journal of Earth Sciences 60 (3), 137.

Märss, T., Ritchie, A., 1997. Articulated thelodonts (Agnatha) of Scotland. Transactions of the Royal Society of Edinburgh: Earth Sciences 88 (3), 143–195.

Matton, O., Cloutier, R., Stevenson, R., 2012. Apatite for destruction: Isotopic and geochemical analyses of bioapatites and sediments from the Upper Devonian Escuminac Formation (Miguasha, Québec). Palaeogeography, Palaeoclimatology, Palaeoecology 361–362, 73–83.

Maxwell, E. E., 2008. Ossification sequence of the avian order Anseriformes, with comparison to other precocial birds. Journal of morphology 269 (9), 1095–1113.

Mayr, E., 1993. What was the Evolutionary Synthesis? Trends in Ecology and Evolution 8 (1), 31–34.

McCoy, V. E., Saupe, E. E., Lamsdell, J. C., Tarhan, L. G., McMahon, S., Lidgard, S., Mayer, P., Whalen, C. D., Soriano, C., Finney, L., et al., 2016. The 'Tully monster'is a vertebrate. Nature 532, 496–499.

McCrimmon, H. R., Swee, U. B., 1967. Scale formation as related to growth and development of young carp, *Cyprinus carpio* L. Journal of the Fisheries Research Board of Canada 24 (1), 47–51.

Meunier, F., François, Y., Castanet, J., 1978. Etude histologique et microradiographique des écailles de quelques actinoptérygiens primitifs actuels. Bull. Soc. Zool. Fr 103, 309–318.

Meunier, F. J., 1981. 'Twisted plywood'structure and mineralization in the scales of a primitive living fish *Amia calva*. Tissue and Cell 13 (1), 165–171.

Mikulic, D. G., Briggs, D. E., Kluessendorf, J., 1985. A Silurian soft-bodied biota. Science 228 (4700), 715–717.

Miles, R. S., 1965. Some features in the cranial morphology of acanthodians and the relationships of the Acanthodii. Acta Zoologica 46, 233–255.

Miles, R. S., 1966. The acanthodian fishes of the Devonian Plattenkalk of the Paffrath Trough in the Rhineland. Arkiiv for Zoologi 18 (9), 147–194.

Miles, R. S., 1970. Remarks on the vertebral column and caudal fin of acanthodian fishes. Lethaia 3 (4), 343–362.

Miles, R. S., 1973a. Articulated acanthodian fishes from the Old Red Sandstone of England, with a review of the structure and evolution of the acanthodian shoulder-girdle. Bulletin of the British Museum of Natural History Geology 24 (2), 114–213.

Miles, R. S., 1973b. Relationships of acanthodians. In: Greenwood, P. H., Miles, R. S., Patterson, C. (Eds.), Interrelationships of Fishes. Vol. 53. Academic Press for the Linnean society of London, London, pp. 63–103.

Miller, R. F., Cloutier, R., Turner, S., 2003. The oldest articulated chondrichthyan from the Early Devonian period. Nature 425, 501–504.

Minelli, A., 2009. Phylo-evo-devo: Combining phylogenetics with evolutionary developmental biology. BMC Biology 7 (1), 1–3.

Morris, S. C., Caron, J.-B., 2012. *Pikaia gracilens* Walcott, a stem-group chordate from the Middle Cambrian of British Columbia. Biological Reviews 87 (2), 480–512.

Murdock, D. J. E., Gabbott, S. E., Mayer, G., Purnell, M. A., 2014. Decay of velvet worms (Onychophora), and bias in the fossil record of lobopodians. BMC Evolutionary Biology 14 (1), 222.

Murphy, C. D., Schaffrath, C., O'Hagan, D., 2003. Fluorinated natural products: The biosynthesis of fluoroacetate and 4-fluorothreonine in *Streptomyces cattleya*. Chemosphere 52 (2), 455–461.

Mütter, R. J., Richter, M., 2007. Acanthodian remains from the Middle-Late Permian of Brazil. Geological Journal 42 (2), 213–224.

Neave, F., 1936. The development of the scales of *Salmo*. Transactions of the Royal Society of Canada 30 (5).

Nemliher, J. G., Baturin, G. N., Kallaste, T. E., Murdmaa, I. O., 2004. Transformation of hydroxyapatite of bone phosphate from the ocean bottom during fossilization. Lithology and Mineral Resources 39 (5), 468–479.

Newman, M. J., 2002. A new naked jawless vertebrate from the middle Devonian of Scotland. Palaeontology 45 (5), 933–941.

Newman, M. J., Burrow, C. J., Den Blaauwen, J. L., Davidson, R. G., 2014. The Early Devonian acanthodian *Euthacanthus macnicoli* Powrie, 1864 from the Midland Valley of Scotland. Geodiversitas 36 (2), 321–348.

Newman, M. J., Davidson, R. G., Blaauwen, J. L. D., Burrow, C. J., 2012. The Early Devonian acanthodian *Uraniacanthus curtus* (Powrie, 1870) n. comb. from the Midland Valley of Scotland. Geodiversitas 34 (4), 739–759.

Newman, M. J., Trewin, N. H., 2001. A new jawless vertebrate from the Middle Devonian of Scotland. Palaeontology 44 (1), 43–51.

O'Hagan, D., Harper, D. B., 1999. Fluorine-containing natural products. Journal of Fluorine Chemistry 100 (1–2), 127–133.

Onimaru, K., Shoguchi, E., Kuratani, S., Tanaka, M., 2011. Development and evolution of the lateral plate mesoderm: Comparative analysis of amphioxus and lamprey with implications for the acquisition of paired fins. Developmental Biology 359 (1), 124–136.

Ørvig, T., 1967. Phylogeny of tooth tissues: Evolution of some calcified tissues in early vertebrates. Structural and chemical organization of teeth, 45–110.

Ørvig, T., 1977. A survey of odontodes ('dermal teeth') from developmental, structural, functional, and phyletic points of view. In: Andrews, S. M., Miles, R. S., Walker, A. D. (Eds.), Problems in Vertebrate Evolution. Vol. 4. Linnean Society Symposium Series, pp. 53–75.

Osse, J. W. M., Van den Boogaart, J. G. M., Van Snik, G. M. J., Van der Sluys, L., 1997. Priorities during early growth of fish larvae. Aquaculture 155 (1), 249–258.

Ota, K. G., Fujimoto, S., Oisi, Y., Kuratani, S., 2011. Identification of vertebra-like elements and their possible differentiation from sclerotomes in the hagfish. Nature Communications 2, 373–378.

Ota, K. G., Oisi, Y., Fujimoto, S., Kuratani, S., 2014. The origin of developmental mechanisms underlying vertebral elements: Implications from hagfish evo-devo. Zoology 117 (1), 77–80.

Ottaway, E. M., 1978. Rhythmic growth activity in fish scales. Journal of Fish Biology 12 (6), 615–623.

Parent, N., Cloutier, R., 1996. Distribution and preservation of fossils in the Escuminac Formation. In: Schultze, H.-P., Cloutier, R. (Eds.), Devonian Fishes and Plants of Miguasha, Quebec, Canada. Verlag Dr Friedrich Pfeil, München, Ch. 6, pp. 54–78.

Parker, W. K., 1883. On the skeleton of the marsipobranch fishes. Part II. *Petromyzon*. Philosophical Transactions of the Royal Society of London 174, 411–457.

Pasteris, J. D., Ding, D. Y., 2009. Experimental fluoridation of nanocrystalline apatite. American Mineralogist 94 (1), 53–63.

Patterson, C., 1982. Morphology and interrelationships of primitive actinopterygian fishes. American Zoologist 22 (2), 241–259.

Pernegre, V., 2006. A new pteraspidiform (Vertebrata, Heterostraci) from the Lower Devonian of Spitsbergen: New palaeo-ontogenetic data. Geodiversitas 28 (2), 239–248.

Pigliucci, M., 2007. Do we need an extended evolutionary synthesis? Evolution 61 (12), 2743–2749.

Piveteau, J., Lehman, J.-P., Dechaseaux, C., 1978. Précis de paléontologie des vertébrés. Masson.

Porro, L. B., Rayfield, E. J., Clack, J. A., 2015. Computed tomography, anatomical description and three-dimensional reconstruction of the lower jaw of *Eusthenopteron foordi* Whiteaves, 1881 from the Upper Devonian of Canada. Palaeontology 58 (6), 1031–1047.

Potthoff, T., 1984. Clearing and staining techniques. In: Moser, H. G., Richards, W. J., Cohen, D. M., P, F. M., Kendall, A. W., Richardson, S. L. (Eds.), Ontogeny and Systematics of Fishes. Vol. 1. American Society of Ichthyology and Herpetology Special Publication, pp. 35–37.

Potvin-Leduc, D., Cloutier, R., Landing, E., Vanaller Hernick, L., Mannolini, F., 2011. Fin spines and scales of the Middle Devonian shark *Wellerodus priscus*: Towards a chondrichthyan bauplan? In: 12th International Symposium on Early/Lower Vertebrates.

Prichonnet, G., Di Vergilio, M., Chidiac, Y., 1996. Stratigraphical, sedimentological and palaeontological context of the Escuminac Formation: Paleoenvironmental hypotheses. In: Schultze, H.-P., Cloutier, R. (Eds.), Devonian Fishes and Plants of Miguasha, Quebec, Canada. Verlag Dr Friedrich Pfeil, München, Ch. 3, pp. 23–36.

Pucéat, E., Reynard, B., Lécuyer, C., 2004. Can crystallinity be used to determine the degree of chemical alteration of biogenic apatites? Chemical Geology 205 (1–2), 83–97.

Qu, Q., Blom, H., Sanchez, S., Ahlberg, P., 2015. Three-dimensional virtual histology of Silurian osteostracan scales revealed by synchrotron radiation microtomography. Journal of Morphology 276 (8), 873–888.

Qu, Q., Sanchez, S., Zhu, M., Blom, H., Ahlberg, P. E., 2016. The origin of novel features by changes in developmental mechanisms: Ontogeny and three-dimensional microanatomy of polyodontode scales of two early osteichthyans. Biological Reviews.

Qu, Q., Zhu, M., Wang, W., 2013. Scales and dermal skeletal histology of an early bony fish *Psarolepis romeri* and their bearing on the evolution of rhombic scales and hard tissues. PLoS ONE 8 (4), e61485.

Reif, W.-E., 1979. Morphogenesis and histology of large scales of batoids (Elasmobranchii). Paläontologische Zeitschrift 53 (1-2), 26–37.

Reif, W.-E., 1982. Evolution of the dermal skeleton and dentition in vertebrates, the odontode regulation theory. Evolutionary Biology 15, 287–368.

Reif, W.-E., 1985. Squamation and ecology of sharks. Courier Forschungsinstitut Senckenberg 78, 1–255.

Renaud, C. B., 2011. Lampreys of the world. An annotated and illustrated catalogue of lamprey species known to date. FAO species catalogue for fisheries 5, 118.

Reynard, B., Balter, V., 2014. Trace elements and their isotopes in bones and teeth: Diet, environments, diagenesis, and dating of archeological and paleontological samples. Palaeogeography, Palaeoclimatology, Palaeoecology 416, 4–16.

Richardson, M. K., Admiraal, J., Wright, G. M., 2010. Developmental anatomy of lampreys. Biological Reviews 85 (1), 1–33.

Richter, M., Neis, P., Smith, M., 1999. Acanthodian and actinopterygian fish remains from the Itaituba Formation, Late Carboniferous of the Amazon Basin, Brazil, with a note on acanthodian ganoin. Neues Jahrbuch fur Geologie und Palaontologie-Monatshefte (12), 728–744.

Richter, M., Smith, M., 1995. A microstructural study of the ganoine tissue of selected lower vertebrates. Zoological Journal of the Linnean Society 114 (2), 173–212.

Riley, B. B., Moorman, S. J., 2000. Development of utricular otoliths, but not saccular otoliths, is necessary for vestibular function and survival in zebrafish. Journal of Neurobiology 43 (4), 329–337.

Ritchie, A., 1967. *Ateleaspis tessellata* Traquair, a non-cornuate cephalaspid from the Upper Silurian of Scotland. Journal of the Linnean Society of London, Zoology 47 (311), 69–81.

Ritchie, A., Gilbert-Tomlinson, J., 1977. First Ordovician vertebrates from the southern hemisphere. Alcheringa 1 (4), 351–368.

Rosen, D. E., Forey, P. L., Gardiner, B. G., Patterson, C., 1981. Lungfishes, tetrapods; paleontology, and plesiomorphy. Bulletin of the American Museum of Natural History 167 (4), 159–276.

Rücklin, M., Giles, S., Janvier, P., Donoghue, P. C. J., 2011. Teeth before jaws? Comparative analysis of the structure and development of the external and internal scales in the extinct jawless vertebrate *Loganellia scotica*. Evolution & Development 13 (6), 523–532.

Rude, P. D., Aller, R. C., 1991. Fluorine mobility during early diagenesis of carbonate sediment: An indicator of mineral transformations. Geochimica et Cosmochimica Acta 55 (9), 2491–2509.

Rutishauser, R., Moline, P., 2005. Evo-devo and the search for homology ("sameness") in biological systems. Theory in Biosciences 124, 213–241.

Sallan, L. C., 2012. Tetrapod-like axial regionalization in an early ray-finned fish. Proceedings of the Royal Society of London B: Biological Sciences 279 (1741), 3264–3271.

Sallan, L. C., Coates, M. I., 2014. The long-rostrumed elasmobranch *Bandringa* Zangerl, 1969, and taphonomy within a Carboniferous shark nursery. Journal of Vertebrate Paleontology 34 (1), 22–33.

Sanchez, S., Dupret, V., Tafforeau, P., Trinajstic, K. M., Ryll, B., Gouttenoire, P.-J., Wretman, L., Zylberberg, L., Peyrin, F., Ahlberg, P. E., 2013. 3D microstructural architecture of muscle attachments in extant and fossil vertebrates revealed by synchrotron microtomography. PLoS ONE 8 (2), e56992.

Sanchez, S., Tafforeau, P., Ahlberg, P. E., 2014. The humerus of *Eusthenopteron*: A puzzling organization presaging the establishment of tetrapod limb bone marrow. Proceedings of the Royal Society B: Biological Sciences 281 (1782).

Sánchez-Villagra, M. R., 2010. Developmental palaeontology in synapsids: The fossil record of ontogeny in mammals and their closest relatives. Proceedings of the Royal Society of London B: Biological Sciences, 1139 – 1147.

Sansom, R. S., 2014. Experimental decay of soft tissues. Paleontological Society Papers 20, 259–274.

Sansom, R. S., Freedman, K. I. M., Gabbott, S. E., Aldridge, R. J., Purnell, M. A., 2010. Taphonomy and affinity of an enigmatic Silurian vertebrate, *Jamoytius kerwoodi* White. Palaeontology 53 (6), 1393–1409.

Sansom, R. S., Gabbott, S. E., Purnell, M. A., 2011. Decay of vertebrate characters in hagfish and lamprey (Cyclostomata) and the implications for the vertebrate fossil record. Proceedings of the Royal Society B: Biological Sciences 278 (1709), 1150–1157.

Sansom, R. S., Gabbott, S. E., Purnell, M. A., 2013a. Atlas of vertebrate decay: A visual and taphonomic guide to fossil interpretation. Palaeontology 56 (3), 457–474.

Sansom, R. S., Gabbott, S. E., Purnell, M. A., 2013b. Unusual anal fin in a Devonian jawless vertebrate reveals complex origins of paired appendages. Biology Letters 9 (3), 1 – 5.

Sansom, R. S., Rodygin, S. A., Donoghue, P. C. J., 2008. The anatomy, affinity and phylogenetic significance of *Ilemoraspis kirkinskayae* (Osteostraci) from the Devonian of Siberia. Journal of Vertebrate Paleontology 28 (3), 613–625.

Sansom, R. S., Wills, M. A., 2013. Fossilization causes organisms to appear erroneously primitive by distorting evolutionary trees. Scientific Reports 3 (2545).

Schlosser, I. J., 1991. Stream fish ecology: A landscape perspective. BioScience 41 (10), 704–712.

Schoch, R. R., 2006. Skull ontogeny: Developmental patterns of fishes conserved across major tetrapod clades. Evolution & Development 8 (6), 524–536.

Schopf, J. M., 1975. Modes of fossil preservation. Review of Palaeobotany and Palynology 20 (1), 27–53.

Schultze, H.-P., 1966. Morphologische und histologische Untersuchungen an Schuppen mesozoischer Actinopterygier (Übergang von Ganoid-zu Rundschuppen). Neues Jahrbuch für Geologie und Paläontologie 126 (3), 232–314.

Schultze, H.-P., 1977. Ausgangsform und Entwicklung der rhombischen Schuppen der Osteichthyes (Pisces). Paläontologische Zeitschrift 51 (3-4), 152–168.

Schultze, H.-P., 1984. Juvenile specimens of *Eusthenopteron foordi* Whiteaves, 1881 (osteolepiform rhipidistian, Pisces) from the Late Devonian of Miguasha, Quebec, Canada. Journal of Vertebrate Paleontology 4 (1), 1–16.

Schultze, H.-P., 1988. Notes on the structure and phylogeny of vertebrate otoliths. Copeia 1988 (1), 257–259.

Schultze, H.-P., 1990. A new acanthodian from the Pennsylvanian of Utah, U.S.A., and the distribution of otoliths in gnathostomes. Journal of Vertebrate Paleontology 10 (1), 49–58.

Schultze, H.-P., 2015. Scales, enamel, cosmine, ganoine, and early osteichthyans. Comptes Rendus Palevol 15 (0), 83–102.

Schultze, H.-P., Bardack, D., 1987. Diversity and size changes in palaeonisciform fishes (Actinopterygii, Pisces) from the Pennsylvanian Mazon Creek fauna, Illinois, U.S.A. Journal of Vertebrate Paleontology 7 (1), 1–23.

Schultze, H.-P., Cumbaa, S. L., 2001. *Dialipina* and the characters of basal actinopterygians . In: Ahlberg, P. E. (Ed.), Major Events in Early Vertebrate Evolution. Taylor & Francis, London, Ch. 18, pp. 315–332.

Schweitzer, M. H., Avci, R., Collier, T., Goodwin, M. B., 2008. Microscopic, chemical and molecular methods for examining fossil preservation. Comptes Rendus Palevol 7 (2), 159–184.

Scotland, R. W., 2010. Deep homology: A view from systematics. BioEssays 32 (5), 438–449.

Shemesh, A., 1990. Crystallinity and diagenesis of sedimentary apatites. Geochimica et Cosmochimica Acta 54 (9), 2433–2438.

Shu, D. G., Morris, S. C., Han, J., Zhang, Z. F., Yasui, K., Janvier, P., Chen, L., Zhang, X. L., Liu, J. N., Li, Y., Liu, H. Q., 2003. Head and backbone of the Early Cambrian vertebrate *Haikouichthys*. Nature 421 (6922), 526.

Shubin, N., Tabin, C., 1997. Fossils, genes and the evolution of animal limbs. Nature 388 (6643), 639.

Shubin, N., Tabin, C., Carroll, S., 2009. Deep homology and the origins of evolutionary novelty. Nature 457 (7231), 818–823.

Simpson, G. G., 1961. Principles of animal taxonomy. No. 20. Columbia University Press.

Sire, J.-Y., 1989. Scales in young *Polypterus senegalus* are elasmoid: New phylogenetic implications. American Journal of Anatomy 186, 315–323.

Sire, J.-Y., 1994. Light and TEM study of nonregenerated and experimentally regenerated scales of *Lepisosteus oculatus* (Holostei) with particular attention to ganoine formation. The Anatomical Record 240 (2), 189–207.

Sire, J.-Y., 1995. Ganoine formation in the scales of primitive actinopterygian fishes, lepisosteids and polypterids. Connective Tissue Research 33 (1-3), 213–222.

Sire, J.-Y., 2001. Teeth outside the mouth in teleost fishes: How to benefit from a developmental accident. Evolution & Development 3 (2), 104–108.

Sire, J.-Y., Akimenko, M.-A., 2004. Scale development in fish: A review, with description of sonic hedgehog (*shh*) expression in the zebrafish (*Danio rerio*). International Journal of Developmental Biology 48, 233–247.

Sire, J.-Y., Allizard, F., Babiar, O., Bourguignon, J., Quilhac, A., 1997. Scale development in zebrafish (*Danio rerio*). Journal of Anatomy 190 (4), 545–561.

Sire, J.-Y., Arnulf, I., 1990. The development of squamation in four teleostean fishes with a survey of the literature. Japanese Journal of Ichthyology 37 (2), 133–143.

Sire, J.-Y., Donoghue, P. C. J., Vickaryous, M. K., 2009. Origin and evolution of the integumentary skeleton in non-tetrapod vertebrates. Journal of Anatomy 214 (4), 409–440.

Sire, J.-Y., Huysseune, A., 2003. Formation of dermal skeletal and dental tissues in fish: A comparative and evolutionary approach. Biological Reviews 78, 219–249.

Sire, Y., Géraudie, J., Meunter, F. J., Zylberberg, L., 1987. On the origin of ganoine: Histological and ultrastructural data on the experimental regeneration of the scales of *Calamolchthys calabaricus* (Osteichthyes, Brachyopterygii, Polypteridae). American Journal of Anatomy 180 (4), 391–402.

Soehn, K. L., Wilson, M. V., 1990. A complete, articulated heterostracan from Wenlockian (Silurian) beds of the Delorme Group, Mackenzie Mountains, Northwest territories, Canada. Journal of Vertebrate Paleontology 10 (4), 405–419.

Stensiö, E., 1964. Les Cyclostomes fossiles ou Ostracodermes. In: Piveteau, J. (Ed.), Traité de Paléontologie. Vol. 4. Masson, Paris, pp. 96–382.

Stensiö, E. A., 1962. Origine et nature des écailles placoïdes et des dents. In: Lehman, J.-P. (Ed.), Problèmes Actuels de Paléontologie : Evolution des Vertébrés. Vol. 104. Paris, pp. 75–85.

Summers, A. P., Ketcham, R. A., Rowe, T., 2004. Structure and function of the horn shark (*Heterodontus francisci*) cranium through ontogeny: Development of a hard prey specialist. Journal of Morphology 260 (1), 1–12.

Swofford, D., Sullivan, J., 2003. Phylogeny inference based on parsimony and other methods using PAUP. In: Salemi, M., Vandamme, A.-M. (Eds.), The Phylogenetic Handbook: A Practical Approach to DNA and Protein Phylogeny. Cambridge university press, Ch. 7, pp. 160–206.

Tanaka, G., Parker, A. R., Hasegawa, Y., Siveter, D. J., Yamamoto, R., Miyashita, K., Takahashi, Y., Ito, S., Wakamatsu, K., Mukuda, T., 2014. Mineralized rods and cones suggest colour vision in a 300 Myr-old fossil fish. Nature Communications 5 (5920), 1–6.

Tarlo, L. B., 1960. The invertebrate origins of the vertebrates. Vol. 22. Copenhagen.

Thomson, K., McCune, A., 1984. Scale structure as evidence of growth patterns in fossil semionotid fishes. Journal of Vertebrate Paleontology 4 (3), 422–429.

Trinajstic, K., 1999. New anatomical information on *Holonema* (Placodermi) based on material from the Frasnian Gogo Formation and the Givetian-Frasnian Gneudna Formation, Western Australia. Geodiversitas 21 (1), 69–84.

Trinajstic, K., 2001. Acanthodian microremains from the Frasnian Gneudna Formation, Western Australia. Records-Western Australian Museum 20 (2), 187–198.

Trinajstic, K., Boisvert, C., Long, J., Maksimenko, A., Johanson, Z., 2015. Pelvic and reproductive structures in placoderms (stem gnathostomes). Biological Reviews 90 (2), 467–501.

Trinajstic, K., Marshall, C., Long, J., Bifield, K., 2007. Exceptional preservation of nerve and muscle tissues in Late Devonian placoderm fish and their evolutionary implications. Biology Letters 3 (2), 197–200.

Trueman, C. N., Privat, K., Field, J., 2008. Why do crystallinity values fail to predict the extent of diagenetic alteration of bone mineral? Palaeogeography, Palaeoclimatology, Palaeoecology 266 (3–4), 160–167.

Trueman, C. N. G., Behrensmeyer, A. K., Tuross, N., Weiner, S., 2004. Mineralogical and compositional changes in bones exposed on soil surfaces in Amboseli National Park, Kenya: Diagenetic mechanisms and the role of sediment pore fluids. Journal of Archaeological Science 31 (6), 721–739.

Tulenko, F. J., Augustus, G. J., Massey, J. L., Sims, S. E., Mazan, S., Davis, M. C., 2016. *HoxD* expression in the fin-fold compartment of basal gnathostomes and implications for paired appendage evolution. Scientific Reports 6, 22720.

Tulenko, F. J., McCauley, D. W., MacKenzie, E. L., Mazan, S., Kuratani, S., Sugahara, F., Kusakabe, R., Burke, A. C., 2013. Body wall development in lamprey and a new perspective on the origin of vertebrate paired fins. Proceedings of the National Academy of Sciences 110 (29), 11899–11904.

Turner, S., 1992. Thelodont lifestyle. In: Mark-Kurik, E. (Ed.), Fossil Fishes as Living Animals. Academy of Sciences of Estonia, pp. 21–40.

Turner, S., 2004. Early vertebrates: Analysis from microfossil evidence. In: Arratia, G., Wilson, M. V. H., Cloutier, R. (Eds.), Recent Advances in the Origin and Early Radiation of Vertebrates. Verlag Dr Friedrich Pfeil, München, pp. 65–94.

Turner, S., Burrow, C. J., Schultze, H.-P., Blieck, A., Reif, E. R., Rexroad, C. B., Bultynck, P., Nowlan, G. S., 2010. False teeth: Conodont-vertebrate phylogenetic relationships revisited. Geodiversitas 32 (4), 545–594.

Upeniece, I., 1996. *Lodeacanthus gaujicus* n. g. et sp. (Acanthodii: Mesacanthidae) from the Late Devonian of Latvia. Modern Geology 20, 383–398.

Upeniece, I., 2001. The unique fossil assemblage from the Lode Quarry (Upper Devonian, Latvia). Mitt. Mus. Nat.kd. Berl. 4, 101–119.

Upeniece, I., 2011. Palaeoecology and juvenile individuals of the Devonian placoderm and acanthodian fishes from Lode site, Latvia. Ph.D. thesis, University of Latvia.

Upeniece, I., Beznosov, P., 2002. The squamation of mesacanthid *Lodeacanthus gaujicus* Upeniece. In: International Symposium "Geology of the Devonian System".

Urho, L., 2002. Characters of larvae–what are they? Folia Zoologica 51 (3), 161–186.

Valiukevičius, J., 1995. Acanthodian histology: Some significant aspects in taxonomical and phylogenetical research. Geobios 28, Supple, 157–159.

Valiukevičius, J., 2003. Devonian acanthodians from Severnaya Zemlya Archipelago (Russia). Geodiversitas 25 (1), 131–204.

Valiukevičius, J., Burrow, C., 2005. Diversity of tissues in acanthodians with *Nostolepis*-type histological structure. Acta Palaeontologica Polonica 50 (3), 635–649.

Wada, H., Hamaguchi, S., Sakaizumi, M., 2008. Development of diverse lateral line patterns on the teleost caudal fin. Developmental Dynamics 237 (10), 2889–2902.

Wagemans, F., Focant, B., Vandewalle, P., 1998. Early development of the cephalic skeleton in the turbot. Journal of Fish Biology 52 (1), 166–204.

Wang, X., Miao, D., Zhang, Y., 2005. Cannibalism in a semi-aquatic reptile from the Early Cretaceous of China. Chinese Science Bulletin 50 (3), 282–284.

Wang, Y., Von Euw, S., Fernandes, F. M., Cassaignon, S., Selmane, M., Laurent, G., Pehau-Arnaudet, G., Coelho, C., Bonhomme-Coury, L., Giraud-Guille, M.-M., Babonneau, F., Azaïs, T., Nassif, N., 2013. Water-mediated structuring of bone apatite. Nature Materials 12 (12), 1144–1153.

Warren, A., Currie, B. P., Burrow, C., Turner, S., 2000. A redescription and reinterpretation of *Gyracanthides murrayi* Woodward 1906 (Acanthodii, Gyracanthidae) from the Lower Carboniferous of the Mansfield Basin, Victoria, Australia. Journal of Vertebrate Paleontology 20 (2), 225–242.

Watson, D. M. S., 1937. The acanthodian fishes. Philosophical Transactions of the Royal Society of London. Series B, Biological Sciences 228 (549), 49–146.

Weiner, S., Bar-Yosef, O., 1990. States of preservation of bones from prehistoric sites in the Near East: A survey. Journal of Archaeological Science 17 (2), 187–196.

Welsch, U., 1968. Über den Feinbau der Chorda dorsalis von *Branchiostoma lanceolatum*. Zeitschrift für Zellforschung und mikroskopische Anatomie 87 (1), 69–81.

White, D. S., 1977. Early development and pattern of scale formation in the spotted sucker, *Minytrema melanops* (Catostomidae). Copeia 1977 (2), 400–403.

Whiteaves, J. F., 1887. Illustrations of the fossil fishes of the Devonian rocks of Canada. Transactions of the Royal Society of Canada 4 (4), 101–110.

Willmore, K. E., Young, N. M., Richtsmeier, J. T., 2007. Phenotypic variability: Its components, measurement and underlying developmental processes. Evolutionary Biology 34 (3-4), 99–120.

Wilson, L. A. B., 2013. The contribution of developmental palaeontology to extensions of evolutionary theory. Acta Zoologica 94, 254–260.

Wilson, L. B., Schradin, C., Mitgutsch, C., Galliari, F., Mess, A., Sánchez-Villagra, M., 2010. Skeletogenesis and sequence heterochrony in rodent evolution, with particular emphasis on the African striped mouse, *Rhabdomys pumilio* (Mammalia). Organisms Diversity & Evolution 10 (3), 243–258.

Wilson, M. V. H., Caldwell, M. W., 1998. The Furcacaudiformes: A new order of jawless vertebrates with thelodont scales, based on articulated Silurian and Devonian fossils from Northern Canada. Journal of Vertebrate Paleontology 18 (1), 10–29.

Wilson, M. V. H., Hanke, G. F., Märss, T., 2007. Paired fins and jawless vertebrates and their homologies accross the "agnathan" - gnathostome transition. In: Anderson, J. S., Sues, H.-D. (Eds.), Major Transitions in Vertebrate Evolution. Indiana University Press, USA, Ch. 3, pp. 122–149.

Witten, P. E., Huysseune, A., 2007. Mechanisms of chondrogenesis and osteogenesis in fins. In: Hall, B. K. (Ed.), Fins into limbs: Evolution, development and transformation. The University of Chicago Press, Chicago, Ch. 6, pp. 79–92.

Woodward, A. S., 1891. Catalogue of the Fossil Fishes in the British Museum (Natural History). Vol. II. London.

Woodward, A. S., 1900. On a new Ostracoderm (*Euphanerops longaevus*) from the Upper Devonian of Scaumenac Bay, Province of Quebec, Canada. Annals and Magazine of Natural History 7 (5), 416–419.

Wyffels, J., 2009. Embryonic development of chondrichthyan fishes—a review. Development of non-teleost fishes. Science Publishers, Enfield 301, 103.

Yang, Y., Niswander, L., 1995. Interaction between the signaling molecules (*Wnt7a*) and (*Shh*) during vertebrate limb development: Dorsal signals regulate anteroposterior patterning. Cell 80 (6), 939 – 947.

Yi, H., Balan, E., Gervais, C., Segalen, L., Fayon, F., Roche, D., Person, A., Morin, G., Guillaumet, M., Blanchard, M., 2013. A carbonate-fluoride defect model for carbonate-rich fluorapatite. American Mineralogist 98 (5-6), 1066–1069.

Yi, H., Balan, E., Gervais, C., Ségalen, L., Roche, D., Person, A., Fayon, F., Morin, G., Babonneau, F., 2014. Probing atomic scale transformation of fossil dental enamel using Fourier transform infrared and nuclear magnetic resonance spectroscopy: A case study from the Tugen Hills (Rift Gregory, Kenya). Acta Biomaterialia 10 (9), 3952–3958.

Young, G. C., 2010. Placoderms (armored fish): Dominant vertebrates of the Devonian period. Annual Review of Earth and Planetary Sciences 38, 523–550.

Young, G. C., Burrow, C. J., 2004. Diplacanthid acanthodians from the Aztec Siltstone (late Middle Devonian) of Southern Victoria Land, Antarctica. Fossils and Strata 50, 23–43.

Young, R. A., Brown, W. E., 1982. Structures of biological minerals. In: Nancollas, G. H. (Ed.), Biological Mineralization and Demineralization. Springer, pp. 101–141.

Young, V., 1995. Micro-remains from Early and Middle Devonian acanthodian fishes from the UK and their biostratigraphic possibilities. Ichthyolith Issues Special Publications 1, 65–68.

Zajic, J., 2005. Permian acanthodians of the Czech Republic. Czech Geological Survey Special Papers 18, 6–42.

Zangerl, R., 1981. Chondrichthyes 1 Paleozoic Elasmobranchii. In: Schultze, H.-P. (Ed.), Handbook of Paleoichthyology. Vol. 3A. Gustav Fischer, Stuttgart, p. 115.

Zhang, G., Boyle, D. L., Zhang, Y., Rogers, A. R., Conrad, G. W., 2012. Development and mineralization of embryonic avian scleral ossicles. Molecular vision 18, 348.

Zhu, M., Yu, X., 2002. A primitive fish close to the common ancestor of tetrapods and lungfish. Nature 418 (6899), 767–770.

Zhu, M., Yu, X., 2009. Stem sarcopterygians have primitive polybasal fin articulation. Biology Letters 5 (3), 372–375.

Zhu, M., Yu, X., Ahlberg, P. E., Choo, B., Lu, J., Qiao, T., Qu, Q., Zhao, W., Jia, L., Blom, H., Zhu, Y. a., 2013. A Silurian placoderm with osteichthyan-like marginal jaw bones. Nature 502 (7470), 188–193.

Zhu, M., Yu, X., Choo, B., Qu, Q., Jia, L., Zhao, W., Qiao, T., Lu, J., 2012a. Fossil fishes from China provide first evidence of dermal pelvic girdle in osteichthyans. PLoS ONE 7 (4), 1–9.

Zhu, M., Yu, X., Choo, B., Wang, J., Jia, L., 2012b. An antiarch placoderm shows that pelvic girdles arose at the root of jawed vertebrates. Biology Letters 8, 453–456.

Zhu, M., Yu, X., Janvier, P., 1999. A primitive fossil fish sheds light on the origin of bony fishes. Nature 397 (6720), 607–610.

Zhu, M., Zhao, W., Jia, L., Lu, J., Qiao, T., Qu, Q., 2009. The oldest articulated osteichthyan reveals mosaic gnathostome characters. Nature 458 (7237), 469–474.

Zidek, J., 1976. Kansas Hamilton Quarry (Upper Pennsylvanian) *Acanthodes*, with remarks on the previously reported North American occurrences of the genus. The University of Kansas Paleontological Contributions 83, 1–47.

Zidek, J., 1985. Growth in *Acanthodes* (Acanthodii: Pisces) data and implications. Paläontologische Zeitschrift 59 (1), 147–166.

Zylberberg, L., Meunier, F. J., Laurin, M., 2016. A microanatomical and histological study of the postcranial dermal skeleton of the devonian actinopterygian *Cheirolepis canadensis*. Acta Palaeontologica Polonica 61 (2), 363–376.